frontiers | Research Topics

Diagnostics and detection of african swine fever virus

Edited by
Yongtao Li, Luis G. Gimenez-Lirola, Bin Li and Wentao Li

Published in
Frontiers in Veterinary Science

ISSN 1664-8714
ISBN 978-2-8325-2320-9
DOI 10.3389/978-2-8325-2320-9

About Frontiers

Frontiers is more than just an open access publisher of scholarly articles: it is a pioneering approach to the world of academia, radically improving the way scholarly research is managed. The grand vision of Frontiers is a world where all people have an equal opportunity to seek, share and generate knowledge. Frontiers provides immediate and permanent online open access to all its publications, but this alone is not enough to realize our grand goals.

Frontiers journal series

The Frontiers journal series is a multi-tier and interdisciplinary set of open-access, online journals, promising a paradigm shift from the current review, selection and dissemination processes in academic publishing. All Frontiers journals are driven by researchers for researchers; therefore, they constitute a service to the scholarly community. At the same time, the *Frontiers journal series* operates on a revolutionary invention, the tiered publishing system, initially addressing specific communities of scholars, and gradually climbing up to broader public understanding, thus serving the interests of the lay society, too.

Dedication to quality

Each Frontiers article is a landmark of the highest quality, thanks to genuinely collaborative interactions between authors and review editors, who include some of the world's best academicians. Research must be certified by peers before entering a stream of knowledge that may eventually reach the public - and shape society; therefore, Frontiers only applies the most rigorous and unbiased reviews. Frontiers revolutionizes research publishing by freely delivering the most outstanding research, evaluated with no bias from both the academic and social point of view. By applying the most advanced information technologies, Frontiers is catapulting scholarly publishing into a new generation.

What are Frontiers Research Topics?

Frontiers Research Topics are very popular trademarks of the *Frontiers journals series*: they are collections of at least ten articles, all centered on a particular subject. With their unique mix of varied contributions from Original Research to Review Articles, Frontiers Research Topics unify the most influential researchers, the latest key findings and historical advances in a hot research area.

Find out more on how to host your own Frontiers Research Topic or contribute to one as an author by contacting the Frontiers editorial office: frontiersin.org/about/contact

Diagnostics and detection of african swine fever virus

Topic editors

Yongtao Li — Henan Agricultural University, China
Luis G. Gimenez-Lirola — Iowa State University, United States
Bin Li — Jiangsu Academy of Agricultural Sciences (JAAS), China
Wentao Li — Huazhong Agricultural University, China

Citation

Li, Y., Gimenez-Lirola, L. G., Li, B., Li, W., eds. (2023). *Diagnostics and detection of african swine fever virus*. Lausanne: Frontiers Media SA. doi: 10.3389/978-2-8325-2320-9

Table of contents

frontiers | Frontiers in Veterinary Science

TYPE Editorial
PUBLISHED 18 April 2023
DOI 10.3389/fvets.2023.1195138

OPEN ACCESS

EDITED AND REVIEWED BY
Salome Dürr,
University of Bern, Switzerland

*CORRESPONDENCE
Wentao Li
✉ wentao@mail.hzau.edu.cn
Yongtao Li
✉ yongtaole@126.com
Luis G. Gimenez-Lirola
✉ luisggl@iastate.edu
Bin Li
✉ libinana@126.com

RECEIVED 28 March 2023
ACCEPTED 05 April 2023
PUBLISHED 18 April 2023

CITATION
Zhang C, Li S, Zhang M, Li Y, Gimenez-Lirola LG, Li B and Li W (2023) Editorial: Diagnostics and detection of African swine fever virus. *Front. Vet. Sci.* 10:1195138. doi: 10.3389/fvets.2023.1195138

Editorial: Diagnostics and detection of African swine fever virus

Chengjun Zhang[1,2,3], Shuai Li[4], Mengjia Zhang[1,2,3], Yongtao Li[4]*, Luis G. Gimenez-Lirola[5]*, Bin Li[6]* and Wentao Li[1,2,3]*

[1]State Key Laboratory of Agricultural Microbiology, College of Veterinary Medicine, Huazhong Agricultural University, Wuhan, China, [2]Key Laboratory of Prevention & Control for African Swine Fever and Other Major Pig Diseases, Ministry of Agriculture and Rural Affairs, Wuhan, China, [3]Hubei Hongshan Laboratory, Wuhan, China, [4]College of Veterinary Medicine, Henan Agricultural University, Zhengzhou, China, [5]Department of Veterinary Diagnostic and Production Animal Medicine, College of Veterinary Medicine, Iowa State University, Ames, IA, United States, [6]Institute of Veterinary Medicine, Jiangsu Academy of Agricultural Sciences, Key Laboratory of Veterinary Biological Engineering and Technology Ministry of Agriculture, Jiangsu Key Laboratory for Food Quality and Safety-State Key Laboratory Cultivation Base of Ministry of Science and Technology, Nanjing, China

KEYWORDS

African swine fever virus, diagnosis, biomarkers, epidemiology, surveillance

Editorial on the Research Topic
Diagnostics and detection of African swine fever virus

African swine fever virus (ASFV) is a large, enveloped, double-stranded DNA virus that causes a contagious and lethal hemorrhagic disease. Since its first detected in the sub-Saharan Africa, were remains endemic, ASFV rapidly spread to numerous countries including Europe, Asia, and the Caribbean, causing substantial economic losses to the swine industry. Currently, in the absence of commercially available efficacious vaccine, the control of African swine fever (ASF) primarily relies on implementing strict biosecurity measures. One of the key measures is the early and accurate diagnosis of ASF. Therefore, the development of sensitive, rapid, and user-friendly detection methods is crucial. Despite the widespread use of commercialized quantitative real-time PCR (qPCR) and ELISA kits for ASFV detection, many clinical demands remain unmet.

This Research Topic, focused on novel diagnostic technologies for detecting ASFV, with the aim of encouraging new ideas that can improve the prevention and control strategies for ASF. This Research Topic included 13 articles, three of which presented novel ELISA detection methods, three were focused on qPCR methods, two utilized the CRISPR-Cas12a detection system, one evaluated both ELISA and qPCR methods, one article was related to animal experiments, while two discussed sample collection, and one introduced a new sequencing method.

Although there are many ELISA kits available on the market for detecting ASFV antibodies, they mainly target the p72, p30, and p54 proteins (1). However, the discovery of low-virulence, gene-deleted viruses has raised the demand for higher sensitivity and a more comprehensive set of detection targets for ASFV detection.

Jiang et al. developed an indirect ELISA method for identifying wild-type and CD2v-deleted ASFV strains using purified CD2v extracellular domain protein as detection antigen. This method showed excellent specificity to detect CD2v-deleted ASFV, with no cross-reaction with serum infected with other tested swine viruses, high sensitivity allowing identification of ASFV-infected clinical serum samples diluted up to 1:2,560.

Yang Y. et al. utilized the prokaryotic recombinant pB602L protein, a late non-structural protein that displayed strong antigenicity in ASFV, to develop an indirect ELISA method. The results showed that this method exhibited high specificity and sensitivity, with no cross-reactions with other antibodies from other tested swine viruses. This method was able to detect anti-ASFV antibody in serum samples diluted up to 1:6,400 times.

Using prokaryotic expression of proteins p22 and p30, Li J. et al. developed an indirect ELISA kit. Through their investigation, they discovered that optimal signal-to-noise ratios were achieved at various coating volume ratios. The ELISA method they established displayed high sensitivity and could detect positive serum samples at dilutions as high as 1:12,800 times, which was more effective than a commercial kit.

QPCR is the commonly used method for detecting ASFV, which typically employs primer pair and fluorescent probe targeting p72 gene as described in the WOAH Terrestrial Manual (2). Although this method is highly adaptable, it is quite time-consuming. In addition, the emergence of mutated low-virulent strains which induce intermittent detoxification in pigs, as well as the need for gene-deleted vaccine strain development and evaluation, has prompted the investigation of alternative detection techniques.

Hwang et al. developed a fast qPCR method for ASFV detection, which has the advantage of completing the process in just 50 min, a significant improvement compared to conventional PCR assays. The limit of detection (LOD) for genotype II ASFV is 6.91 genomic copies per reaction, while it ranges between 10 and 20 for other ASFV genotypes.

Qi et al. established a qPCR assay based on the ASFV MGF505-7R gene, which has recently been linked to ASFV virulence and could be a valuable target for vaccine development (3). This technique can detect ASFV-infected samples as early as 4 h post-infection, with the sensitivity of up to 10 copies/μL. Furthermore, this method has potential for use in "DIVA" (Differentiating Infected from Vaccinated Animals).

Yang H. et al. established a triplex qPCR method targeting the CD2v and MGF_360-14L and B646L gene of ASFV. The LOD of the method for B646L, MGF_360-14L, and CD2v were 78.9, 47.0, and 82.1 copies/μl, respectively. This technique has proven effective in detecting both genotype I and genotype II ASFV strains and holds potential for the identification of ASFV gene-deleted and wild-type strains.

Due to variations in sensitivity and specificity among different detection methods, it is difficult to confirm whether a sample with low viral load is positive or negative using only one method. Typically, the results are compared to a gold standard reference test. In the study by Schambow et al., a Bayesian latent class analysis (BLCA) model was used to utilized to assess the diagnostic performance of a novel indirect ELISA and a qPCR test for detecting ASFV during a cross-sectional field study in Vietnam. Paired serum and oral fluid (OF) samples were collected from pigs on 30 acutely ASF-affected farms, 37 chronically ASF-affected farms, and 20 unaffected farms, with both assays utilized. The findings indicate that qPCR exhibited superior sensitivity than ELISA for acutely affected pigs, while ELISA sensitivity was higher in the chronically affected pigs. Specificity was nearly 100% for all test/sample types. Additionally, the author compared five parallel testing schemes, which may provide valuable insight for selecting appropriate surveillance strategies.

The Cas12a detection system is a recently developed technology that has been applied to several pathogens. However, due to the limited sensitivity of Cas12a, it is necessary to first employ isothermal amplification methods, such as Recombinase Polymerase Amplification (RPA) or Loop-Mediated Isothermal Amplification (LAMP) amplification to amplify the target gene. The combined use of these methods greatly improves the detection sensitivity and specificity (4). Additionally, the system is cost-effective, does not require expensive amplification equipment, and provides easy-to-read results, which makes it more suitable for clinical applications.

Qin et al. integrated an isothermal LAMP/RPA and CRISPR/Cas12a-mediated cleavage detection system within a single reaction tube, enabling completion of the detection process within 40 min. The results can be visually observed, and the use of a single tube sealed with mineral oil reduces the risk of contamination. Utilizing LAMP as isothermal amplification method and with a reaction time of 60 min, the LOD is 5.8×10^2 copies/μL.

Wang et al. developed a method based on CRISPR-Cas12a combined with G-quadruplex allowing specific detection without the need of fluorescence probes. When paired with RPA amplification, the LOD of ASFV was 10^2 copies, and the LOD of PCV2 was 10^3 copies.

To examine blood parameters, viral loads and pathology of the first isolated ASFV in Vietnam, Oh et al. conducted an animal study. The research indicated that the sensitivity to the ASFV varies based on the individual predisposition of the host. The study found that each pig had a different viral load in the blood at the initial time of infection. Group I pigs, which died at 2–5 days post-viremia (dpv), had a higher viral load in the blood at the onset of viremia than Group II pigs, which died at 6–7 dpv. These findings reveal that more genetic and immunological investigations of ASFV-infected pigs are required to elucidate the dynamics of virus susceptibility.

Detecting viruses in water can be challenging due to their typically low concentrations, often falling below the detection limit of qPCR methods. To address this issue, Wu et al. developed a method for detecting ASFV in water by combining of $Fe(OH)_3$ modified diatomaceous earth and qPCR. The authors showed that this technique effectively enriched the virus in water samples, increasing LOD in 10 L of ASFV-contaminated water by 1×10^4 times without additional PEG treatment and further improvement with the addition of PEG. This method demonstrated greater sensitivity than the previously reported $Al(OH)_3$-modified EGM filter cartridge system and proved capable of detecting low levels of the virus in water samples that tested negative without enrichment.

Collecting samples from suspected ASFV-infected animals through necropsy in pig farms and the wild carries the risk of environmental contamination. Li X. et al. developed a non-invasive method for diagnosing ASFV infection in dead pigs. The authors reported that inguinal lymph node samples, collected using a minimally invasive sampler, contained more ASFV nucleic acids than swabs and constituted an ideal tissue

for diagnosing ASFV infection in dead pigs without the need for necropsy.

Genome sequencing is an essential tool for studying viral mutations and tracing their origins. However, traditional methods require the isolation of the virus and ultracentrifugation for enrichment, which can be time-consuming and must be conducted in ABSL-3 laboratory. Zhang et al. established a method for sequencing ASFV positive blood and serum samples without isolating virus. The authors improved C18 spacer MDA (Multiple Displacement Amplification) combined with host DNA exhaustion strategy to remove background DNA and fit Next generation sequencing (NGS) and Third generation sequencing (TGS). Furthermore, they developed a software that enables real-time analysis of TGS depth and coverage by utilizing cloud servers. Using this workflow, they successfully sequenced two uncultured ASFV positive samples in their study.

Author contributions

CZ, YL, and WL co-wrote the manuscript. All authors contributed to the article and approved the submitted version.

Funding

This project was funded by the National Key Research and Development Program of China (2021YFD1800101-2 and 2021YFD1801405) and Hubei Hongshan Laboratory (No. 2022hszd023).

Conflict of interest

The authors declare that the research was conducted in the absence of any commercial or financial relationships that could be construed as a potential conflict of interest.

Publisher's note

References

1. Yu X, Zhu X, Chen X, Li D, Xu Q, Yao L, et al. Establishment of a blocking ELISA detection method for against African swine fever virus p30 antibody. *Front Vet Sci.* (2021) 8:781373. doi: 10.3389/fvets.2021.781373

2. *Terrestrial Manual Online Access - WOAH - World Organisation for Animal Health*. Available online at: https://www.woah.org/en/what-we-do/standards/codes-and-manuals/terrestrial-manual-online-access/ (accessed April 04, 2023).

3. Ding M, Dang W, Liu H, Xu F, Huang H, Sunkang Y, et al. Combinational deletions of MGF360-9L and MGF505-7R attenuated highly virulent African swine fever virus and conferred protection against homologous challenge. *J Virol.* (2022) 96:e00329-22. doi: 10.1128/jvi.00329-22

4. Li C, Lin N, Feng Z, Lin M, Guan B, Chen K, et al. CRISPR/Cas12a based rapid molecular detection of acute hepatopancreatic necrosis disease in shrimp. *Front Vet Sci.* (2022) 8:819681. doi: 10.3389/fvets.2021.819681

frontiers | Frontiers in Veterinary Science

ORIGINAL RESEARCH
published: 18 July 2022
doi: 10.3389/fvets.2022.962438

One-Pot Visual Detection of African Swine Fever Virus Using CRISPR-Cas12a

Chao Qin[1], Jiajia Liu[1], Wenqi Zhu[1], Muchu Zeng[2], Ke Xu[1], Jinmei Ding[1], Hao Zhou[1], Jianshen Zhu[1], Yuqing Ke[2], Lai Yan Li[2], Gaoyuan Sheng[2], Zhuoru Li[2], Huaixi Luo[1], Shengyao Jiang[1], Kangchun Chen[1], Xianting Ding[2] and He Meng[1]**

[1] Shanghai Key Laboratory of Veterinary Biotechnology, Department of Animal Science, School of Agriculture and Biology, Shanghai Jiaotong University, Shanghai, China, [2] State Key Laboratory of Oncogenes and Related Genes, School of Biomedical Engineering, Institute for Personalized Medicine, Shanghai Jiaotong University, Shanghai, China

African swine fever virus (ASFV) is a leading cause of worldwide agricultural loss. ASFV is a highly contagious and lethal disease for both domestic and wild pigs, which has brought enormous economic losses to a number of countries. Conventional methods, such as general polymerase chain reaction and isothermal amplification, are time-consuming, instrument-dependent, and unsatisfactorily accurate. Therefore, rapid, sensitive, and field-deployable detection of ASFV is important for disease surveillance and control. Herein, we created a one-pot visual detection system for ASFV with CRISPR/Cas12a technology combined with LAMP or RPA. A mineral oil sealing strategy was adopted to mitigate sample cross-contamination between parallel vials during high-throughput testing. Furthermore, the blue fluorescence signal produced by ssDNA reporter could be observed by the naked eye without any dedicated instrument. For CRISPR-RPA system, detection could be completed within 40 min with advantageous sensitivity. While CRISPR-LAMP system could complete it within 60 min with a high sensitivity of 5.8×10^2 copies/μl. Furthermore, we verified such detection platforms display no cross-reactivity with other porcine DNA or RNA viruses. Both CRISPR-RPA and CRISPR-LAMP systems permit highly rapid, sensitive, specific, and low-cost Cas12a-mediated visual diagnostic of ASFV for point-of-care testing (POCT) applications.

Keywords: CRISPR/Cas12a, detection, African swine fever virus, RPA, LAMP

OPEN ACCESS

Edited by:
Bin Li,
Jiangsu Academy of Agricultural Sciences (JAAS), China

Reviewed by:
Qin Zhao,
Northwest A&F University, China
Yuan Wanzhe,
Agricultural University of Hebei, China

***Correspondence:**
Xianting Ding
dingxianting@sjtu.edu.cn
He Meng
menghe@sjtu.edu.cn

Specialty section:
This article was submitted to Veterinary Experimental and Diagnostic Pathology, a section of the journal Frontiers in Veterinary Science

Received: *06 June 2022*
Accepted: *23 June 2022*
Published: *18 July 2022*

Citation:
Qin C, Liu J, Zhu W, Zeng M, Xu K, Ding J, Zhou H, Zhu J, Ke Y, Li LY, Sheng G, Li Z, Luo H, Jiang S, Chen K, Ding X and Meng H (2022) One-Pot Visual Detection of African Swine Fever Virus Using CRISPR-Cas12a. Front. Vet. Sci. 9:962438. doi: 10.3389/fvets.2022.962438

INTRODUCTION

African swine fever (ASF) is a highly lethal and contagious disease in domestic pigs caused by the African swine fever virus (ASFV) and is a notifiable disease by the World Organization for Animal Health (OIE) (1). ASFV is a large and complex double-stranded DNA arbovirus that is the only member of *Asfivirus* genus (2). Based on the highly conserved gene *B646L* encoding the viral protein p72, ASFV is currently classified into 24 genotypes. In 2018, ASF began to spread in China, where the virus circulating was identified as genotype II (1, 3), an epidemic strain that was 100% consistent with that in Russia (4). Due to the absence of effective treatments or vaccines, ASF disease control mainly relies on culling pigs (2, 5). With high infectivity and mortality, ASFV has seriously affected animal husbandry.

The focus of prevention and control of ASF is currently still in the early diagnosis and outbreak control stages. Therefore, accurate and efficient laboratory diagnosis is of vital importance.

Quantitative PCR (qPCR) and conventional PCR, which are also recommended by OIE (6–8), are sensitive methods for the detection of ASFV. However, the dependence on expensive thermocyclers and skilled operators limits the application of these methods for point-of-care (POC) detection (9, 10). Isothermal amplification techniques, such as recombinase polymerase amplification (RPA) (11–13), loop-mediated isothermal amplification (LAMP) (14, 15), polymerase cross-linking spiral reaction (PCLSR) (16), and cross-priming amplification (CPA) (17), have been suggested for the detection of ASFV based on the highly conserved region of essential ASFV genes, such as *p72*. However, the reaction temperature close to room temperature can easily generate false-positive test results (18, 19). Therefore, it is necessary to develop a sensitive, specific, equipment-free, and visual method for the detection of ASFV.

Recently, clustered regularly interspaced short palindromic repeat (CRISPR)-associated endonuclease (CRISPR/Cas) systems have been developed to detect nucleic acid, including Cas13a (20–26), Cas12a (27–31), Cas9 (32–34), Cas12b (35), and Cas14 (36). Cas12a, an RNA-guided DNA endonuclease, recognizes a T nucleotide rich, such as 5′- (T) TTN-3′, protospacer-adjacent motif (PAM) with the help of CRISPR RNA (crRNA) (37). Then using a single RuvC catalytic domain (38–40), the Cas12a generates a 5′-overhang staggered cut on the target strand (TS) and the non-target strand (NTS). Both the crRNA-complementary ssDNA or dsDNA (the activator) activate the trans-cleavage to unleash the robust, non-specific ssDNA trans-cleavage activity of Cas12a. The Cas12a-based detection can be performed at physiological temperature or even at room temperature; meanwhile, the non-specific cleavage by these Cas12a enzymes occurs at a very high turnover rate (41–43), significantly simplifying the detection procedure and enabling the accurate detection of low-concentration targets. Combined with fluorophore quencher (FQ)–labeled reporter, the diagnostic technology based on CRISPR/cas12a has been successfully applied for the detection of the porcine reproductive and respiratory syndrome virus (PRRSV) (44), white spot syndrome virus (WSSV) (45), tobacco curly shoot virus (TCSV) (46), human papillomavirus 16 (HPV-16), parvovirus B19 (PB-19) (47), *Listeria monocytogenes* (48), foodborne bacteria (*Escherichia coli* and *Streptococcus aureus*) (49), and *Mycobacterium tuberculosis* (50).

To improve the convenience of existing tools and overcome the limitations of ASF diagnosis, a one-pot visual detection that integrates the CRISPR/Cas12a system with isothermal amplification has been developed in this study. The one-pot detection is sensitive, specific, low-cost, user-friendly, and ready to be used for on-site ASFV detection or other DNA-based pathogens.

MATERIALS AND METHODS

Preparation of Genomic DNA Samples

The 1941bp fragment (Genomic Sequence: NC_001659.2) of the ASFV *p72* gene (also known as *B646L*) was chemically synthesized and cloned into pUC57 plasmid (herein referred to as pUC57-p72 DNA) by Sangon Biotech (Shanghai). Co. Ltd. The pUC57-p72 DNA was used as the template for the optimization of the detection system, as well as for the determination of sensitivity, as standard ASFV plasmid was used in previous reports (16, 17). The DNA or cDNA of the pseudorabies virus (PRV), porcine reproductive and respiratory syndrome virus (PRRSV), porcine epidemic diarrhea virus (PEDV), and porcine deltacoronavirus (PDCoV) were obtained from the Shanghai Veterinary Research Institute (Chinese Academy of Agricultural Sciences), for the use as samples for specificity determination.

Oligonucleotide Primers for Amplification and crRNA Preparation

The most conserved region of the gene was subjected to design isothermal amplification primers. The RPA primers were designed using online software (Primer-blast) according to the TwistAmp assay. These forward and reverse primers formed a number of primer pairs, and the RPA products should be 100–200 bp. The LAMP primers were designed using PrimerExplorer V5 (http://primerexplorer.jp/e/), comprising of two outer primers F3 and B3, two inner primers FIP and BIP, and two loop primers LF and LB.

Using CHOPCHOP (https://chopchop.cbu.uib.no/), the 23nt crRNA targets were designed targeting the *p72* gene, which were also the targets of the RPA and LAMP. The primers and crRNAs sequences, listed in **Table 1**, were synthesized by Sangon Biotech.

RPA, LAMP Assays, and Cas12a/crRNA Nucleic Acid Detection

The RPA reaction was conducted using an RPA reaction mixture (TwistDx) containing 1.2 μl of primer RPA-F (10 μM), 1.2 μl of primer RPA-R (10 μM), 15 μl of primer-free rehydration buffer, 5.35 μl of ultrapure water, 1.25 μl of magnesium acetate (280 mM, MgOAc), and 1 μl of the template DNA or cDNA. The RPA reaction was incubated by PTC-200 thermocyclers (BIO-RAD) at a constant temperature of 37°C for 20 min.

The LAMP assay with the above designed LAMP primers was performed in a 25 μL reaction mixture containing 2.5 μl of 10× reaction buffer [200 mM Tris-HCl, 100 mM $(NH_4)_2SO_4$, 500 mM KCl, 80 mM $MgSO_4$, and 1% Tween 20], 2.5 μl of 10× LAMP primer mix [1.6 μM each of forward inner primer (FIP) and backward inner primer (BIP), 0.2 μM each of forward outer primer (F3) and backward outer primer (B3), 0.4 μM each of forward loop primer (FP) and backward loop primer (BP)], 3 μl of each dNTP (10mM), 4 μl of Betaine (5 M), 1 μl of Bst3.0 DNA polymerase (New England Biolabs), and 1 μl of the DNA or cDNA. The LAMP reaction was incubated by PTC-200 thermocyclers at a constant temperature of 65°C for 60 min.

The CRISPR/Cas12a-mediated cleavage assay (CRISPR reaction buffer) contained 2.5 μl of LbaCas12a (1 μM), 2.5 μl of crRNA (1 μM), 3 μl of ssDNA-FQ reporter (10 μM), 2 μl of RNase inhibitor (4U/μl), 4 μl of 10×NEBuffer, and 6 μl of ultrapure water. LbaCas12a, RNase inhibitor, and 10×NEBuffer were purchased from New England Biolabs, while the ssDNA-FQ reporter was synthesized with several nucleotides (5′-TTATT-3′) labeled with FAM at the 5′ end and a quencher at the 3′ end. The

TABLE 1 | Sequence of primers, crRNA, and FQ reporter in this study.

Name	Sequence (5′-3′)
RPA-F	CGCAAATTTTGCATCCCAGGGGATAAAATGACTG
RPA-R	GGATATTGTGAGAGTTCTCGGGAAAATGTTGTGA
LAMP-F3	CGCAAATTTTGCATCCCA
LAMP-B3	GGATATTGTGAGAGTTCTCGG
LAMP-FIP	GAGAGGGCCACTAGTTCCCTAAAATGACTGGATATAAGCACTT
LAMP-BIP	CAAGCCGCACCAAAGCAAACGAATTTCGGGTTGGTATGG
LAMP-LF	ACCGATACCTCCTGGCCGAC
LAMP-LB	TCTTACCGATGAAAATGATACGCAG
crRNA	UAAUUUCUACUAAGUGUAGAUCACAAGCCGCACCAAAGCAAACC
ssDNA reporter	6-FAM/TTATT/BHQ-1

reaction was incubated in PTC-200 thermocyclers for 40 min at 37 °C. In addition, the fluorescence signal of the ssDNA–FQ report was visualized by the 2500B transilluminator under blue light (Tanon).

Establishment and Optimization of the One-Pot Visual Detection System

One-pot detection combines isothermal pre-amplification and CRISPR/Cas12a-mediated cleavage detection in the same reaction tube. Briefly, the RPA or LAMP pre-amplification assays were added to an Eppendorf tube, and 35 μl of mineral oil was covered on the pre-amplification assay. After the RPA or LAMP reaction, 20 μl of CRISPR reaction buffer (pre-added inside the lid) was mixed with 25 μl of the amplification assay by hand shaking or spinning down in a minifuge for 5 s. The tube was put in PTC-200 thermocyclers at 37°C for 20 min, and the fluorescence signal after the CRISPR/Cas12a-mediated cleavage reaction was visualized using a transilluminator under blue light (**Figure 1**).

For the Cas12a-RPA one-pot detection system, a CRISPR reaction optimization experiment (incubated at 37°C for 5, 10, 20, and 30 min) was conducted to find an appropriate reaction time to shorten the one-pot detection. In addition, with a transfer step in between, the RPA and CRISPR reactions can be run sequentially. To optimize the one-pot detection, a single combined mixture of RPA and CRISPR reactions was carried out at the same reaction temperature (37 °C), which was "one-step" in one-pot detection. After 35 μl of mineral oil was used to cover the surface of the combined mixture, the reaction tube was put in PTC-200 thermocyclers at 37 °C for 20, 30, 40, and 50 min to optimize the detection system.

The reaction time of the CRISPR-LAMP one-pot detection system was optimized separately for different temperatures (65°C for LAMP and 37°C for CRISPR reaction). Briefly, LAMP pre-amplification was incubated at 65°C for 20, 30, 40, and 50 min, and CRISPR/Cas12a-mediated cleavage reaction was incubated at 37°C for 5, 10, 15, 20, 25, and 30 min after an optimized LAMP reaction time in one tube.

Evaluation of the One-Pot Visual Detection System

The specificity of the one-pot visual detection systems was determined by the optimized procedure, the genomic DNA or cDNA of PRV, PRRSV, PEDV, and PDCoV. Further, pUC57-p72 DNA and negative controls (ddH_2O) were also used, with the amount of genomic DNA or cDNA being 1 μl per reaction. In addition, all the genomic DNA or cDNA were used as templates for the PCR with their own specific primers (**Supplementary Table 1**) before evaluating the specificity of the one-pot visual detection system.

The analytic sensitivities of the newly developed one-pot visual detection systems were determined with the pUC57-p72 DNA ranging from 7×10^9 to 7×10^0 copies/μl using multiple dilution methods. The reaction mixtures were heated at 37 °C or 65 °C for an optimal amount of time. The ASFV *B646L* gene plasmid reference material [GBW(E) 091034], with high stability and uniformity, as well as an extended uncertainty of 0.9×10^3 copies/μl (K = 2), was used for further determination of the sensitivity of both the CRISPR-RPA and CRISPR-LAMP one-pot detection systems. The reference material was diluted, ranging from 5.8 × 104 to 5.8×10^0 copies/μl, and detected as previously described in the method section.

For further evaluation, diluted pUC57-p72 DNA was used as a template to compare the newly developed one-pot visual detection system with SYBR real-time qPCR. Briefly, 10 μl of 2 × ChamQ Universal SYBR qPCR Master Mix (Vazyme, Nanjing), 0.4 μl of primer F (10 μM), 0.4 μl of primer R (10 μM), 2 μl of DNA, and ddH_2O were included. The reactions were conducted in a 20 μl volume following the kit instructions. The reaction cycle parameters were set as denaturation at 95°C for 30 s, followed by 40 cycles of amplification, 95°C for 10 s and 60°C for 30 s in a CFX Connect fluorescence quantitative PCR detection system (BIO-RAD). The primers are listed in **Supplementary Table 1**, and the result was analyzed by GraphPad Prism 8.3.0.

RESULTS

Establishing the One-Pot Detection Assay

By adding isothermal pre-amplification and Cas12a-mediated cleavage reaction together in one tube, with mineral oil covering the surface of the LAMP/RPA amplification reagent, a one-tube visual detection system was assembled. For optimizing the CRISPR-RPA one-pot detection, the result (**Figure 2A**) showed that the fluorescence signal increased rapidly with time until it reached the peak value while the negative control remained no fluorescence signal. Moreover, the fluorescence signal was clear enough for the naked eye to detect at 20 min. Therefore, a total of 40 min (RPA for 20 min and CRISPR reaction for 20 min) reaction time were established for the CRISPR-RPA one-pot detection. Besides, after 40 min reaction time, the "one-step" in one-pot detection also showed an increased pattern

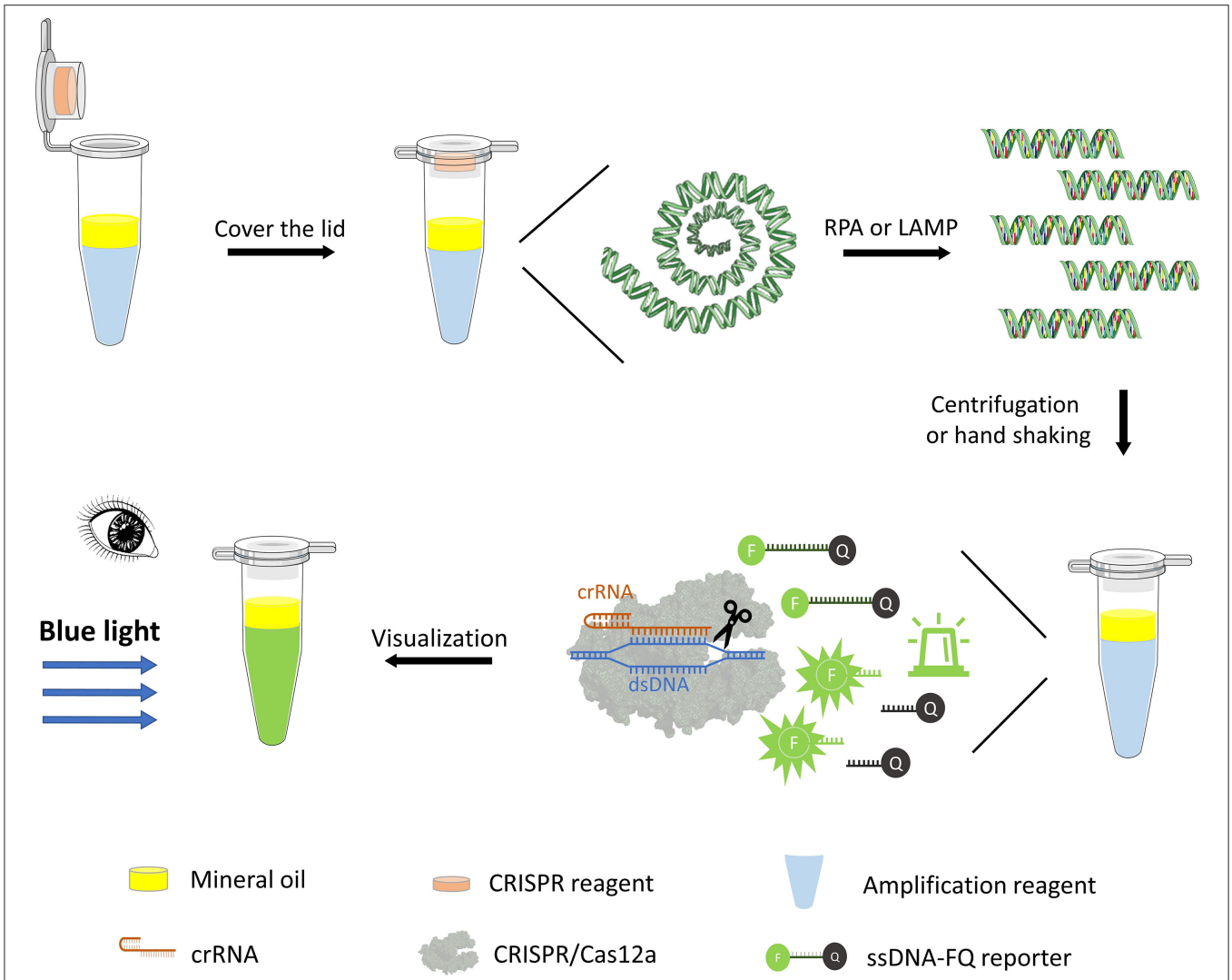

FIGURE 1 | One-pot visual detection system. One-pot visual detection system showing the process of DNA pre-amplification, Cas12a/crRNA cleavage reaction, and fluorescence visualization. RPA or LAMP reagent, crRNA, Cas12a enzyme, and ssDNA-FQ reporter are all in one tube, with mineral oil sealing. Target binding of Cas12a will unleash its ability to digest ssDNA-FQ reporter. The fluorophore FAM **(F)** is quenched by a quencher **(Q)** if intact and emits fluorescence when cleaved, which is visual under the blue light.

in the same fluorescence signal until reaching the peak value (**Supplementary Figure 1**).

For the CRISPR-LAMP one-pot detection system, the optimization was separated into two parts, LAMP optimization and CRISPR reaction optimization. After incubating at 65°C for different durations and a Cas12a-mediated reaction for 40 min, the result (**Figure 2B**) showed that 40 min is an appropriate pre-amplification time for LAMP. After LAMP pre-amplifying for the optimized time (40 min), a CRISPR reaction was conducted to adjust the time. The result (**Figure 2C**) showed that 20 min is an optimized time for CRISPR reaction. Eventually, a total of 60 min (40 min for LAMP and 20 min for CRISPR reaction) reaction time were established for CRISPR-LAMP one-pot detection.

Specificity of the One-Pot Visual Detection System

The specificity of the one-pot visual detection system was evaluated using pUC57-p72 DNA and other porcine viruses' genomic DNA or cDNA, including PRV, PRRSV, PEDV, and PDCoV. The specific of all the genomic DNA or cDNA were verified with PCR and the results of which are displayed in **Figure 3A**. For both the CRISPR-RPA and CRISPR-LAMP one-pot visual detections, after the template DNA was added and the tubes were incubated at a suitable temperature in the reaction order, the rapid reaction of pUC57-p72 DNA occurred and a strong fluorescence signal appeared while other genomic DNA or cDNA showed no signal (**Figures 3B,C**), which revealed there was no cross-reaction with other viruses. The results

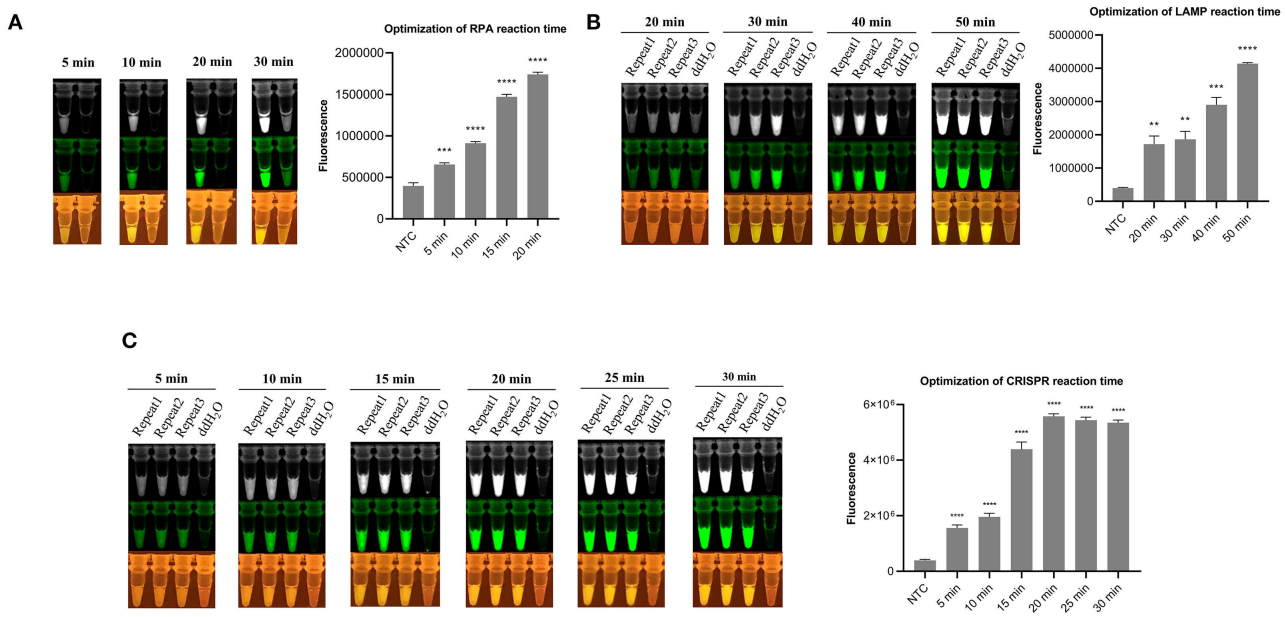

FIGURE 2 | Fluorescence signal image in optimization of detection system. **(A)** Optimization of RPA reaction time in CRISPR-RPA one-pot detection (5, 10, 15, and 20 min). **(B)** Optimization of LAMP reaction time in CRISPR-LAMP one-pot detection (20, 30, 40, and 50 min). **(C)** Optimization of CRISPR reaction time in CRISPR-LAMP one-pot detection (5, 10, 15, 20, 25, and 30 min). The fluorescence signal monochrome and pseudo green images were taken from Tanon 2000M camera, and the images at the bottom were taken behind the UV/blue light resistant observation window. Analysis of the value for the fluorescence image using the ImageJ software. Each measuring was run with three replicates ($n = 3$). $^{*}P < 0.05$, $^{**}P < 0.01$, $^{***}P < 0.001$, $^{****}P < 0.0001$, ns, not significant. Error bars represent the means ± s.d. from replicates. The unpaired two-tailed *t*-test was used to analyze the statistical significance.

demonstrated that both CRISPR-RPA and CRISPR-LAMP one-pot visual detection systems could be used for specific detection of ASFV.

While estimating the sensitivity and specificity of the one-pot visual detection system, it showed high specificity and accuracy, as well as low detection limit, particularly the limit of CRISPR-LAMP was much lower.

Sensitivity of the One-Pot Visual Detection System

On combining the RPA and CRISPR cleavage reactions, the sensitivity of the RPA-CRISPR reaction was determined with a 10-fold serial diluted template at a concentration of 7×10^9, 7×10^8, 7×10^7,7×10^6, 7×10^5, 7×10^4, 7×10^3, 7×10^2, 7×10^1, and 7×10^0 copies/μl of the pUC57-p72 DNA. The results showed that the developed RPA-CRISPR one-pot visual detection system can detect as low as 7×10^4 copies/μl of the dsDNA template (**Figure 4A**). The ASFV *B646L* gene plasmid reference material was diluted with a 10-fold serial at a concentration of 5.8×10^3, 5.8×10^2, 5.8×10^1, and 5.8×10^0 copies/μl to refine and accurate the limitation. The results showed that no significant fluorescence signal can be detected by the naked eye, meaning that the limit of the one-pot visual detection based on the RPA-CRISPR is 7×10^4 copies/μl within 40 min (**Figure 4B**). Besides, the sensitivity of "one-step" in one-pot detection is 7×10^8 copies/μl which is not an appropriate limit for virus detection (**Supplementary Figure 1**).

The limits of the LAMP-CRISPR detection system were determined using a 10-fold serial diluted pUC57-p72 DNA template, ranging from 7×10^9 to 7×10^0 copies/μl. The results showed that the developed LAMP-CRISPR one-pot visual detection system can detect as low as 7×10^2 copies/μl of the dsDNA template (**Figure 4C**). Using diluted ASFV *B646L* gene plasmid reference material as a template, the limit of one-pot visual detection system based on the LAMP-CRISPR was 5.8×10^2 copies/μl within 60 min, as shown in (**Figure 4D**).

Evaluating Consistency Between the One-Pot Visual Detection and qPCR

We further compared one-pot visual detection with the quantitative PCR (qPCR), the most commonly used detection method, as the gold standard. The same target on *p72* gene was used for the RPA and LAMP amplification to determine the analytical sensitivity of the qPCR. Serial dilutions were prepared from 10^9 to 10^0 copies/μl. The result showed that the limit of qPCR detection was 7×10^2 copies/μl (**Figure 3D**). Compared to qPCR detection, the limit of one-pot detection was similar and the CRISPR-LAMP could attain a sensitivity of 5.8×10^2 copies/μl. Moreover, both the CRISP-RPA and CRISPR-LAMP detection systems spent lesser detection time than the qPCR.

DISCUSSION

Since 2018, the rapid outbreak of ASF in China and in a number of other countries has resulted in tremendous economic losses

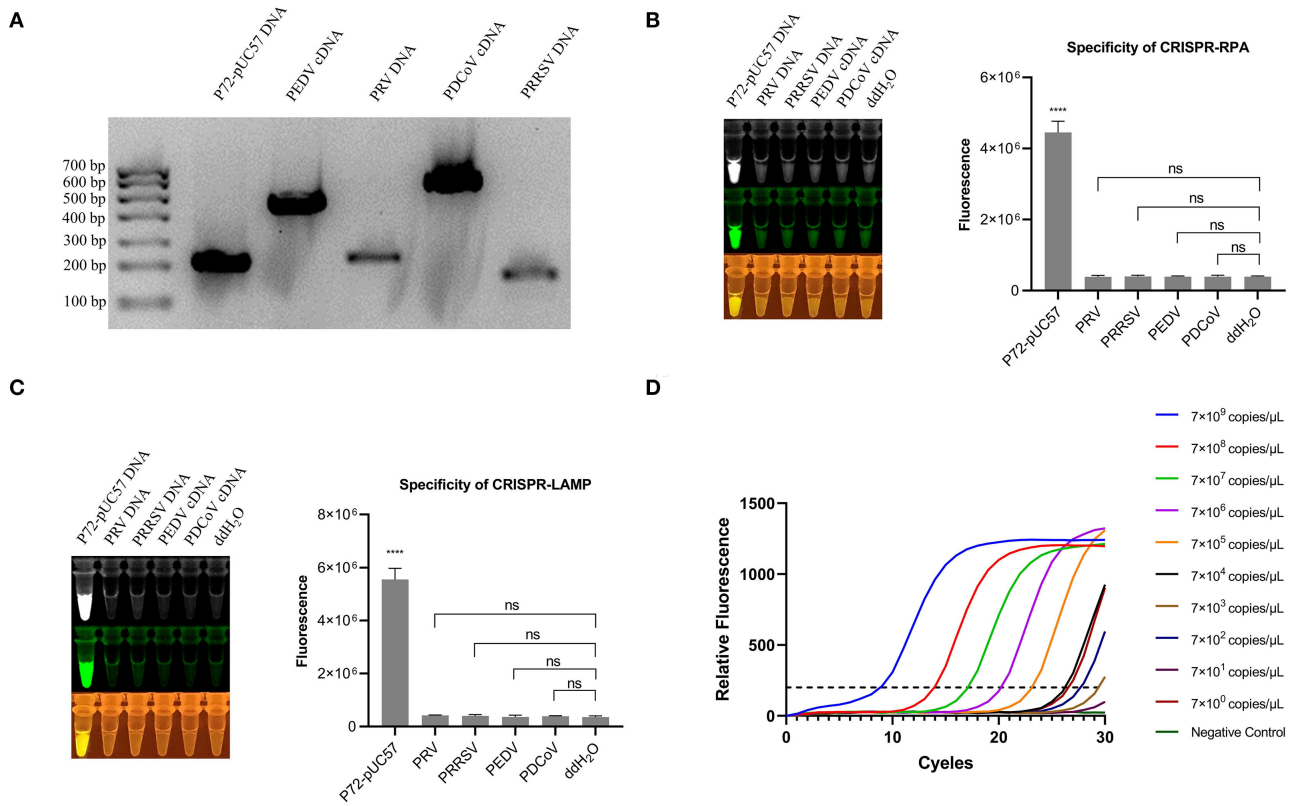

FIGURE 3 | Specificity of one-pot visual detection system and qPCR. **(A)** PCR amplification result of pUC57-p72 and porcine virus genomic DNA or cDNA. **(B)** Specificity of CRISPR-RPA one-pot detection with pUC57-p72 and porcine virus genomic DNA or cDNA. **(C)** Specificity of CRISPR-LAMP one-pot detection with pUC57-p72 and porcine virus genomic DNA or cDNA. **(D)** qPCR for 10-fold serial diluted pUC57-p72 DNA (qPCR was processed using GraphPad 8.0). Analysis of the value for the fluorescence image used the ImageJ software. Each measuring was run with three replicates ($n = 3$). $^{*}P < 0.05$, $^{**}P < 0.01$, $^{***}P < 0.001$, $^{****}P < 0.0001$, ns, not significant. Error bars represent the means ± s.d. from replicates. The unpaired two-tailed *t*-test was used to analyze the statistical significance.

(51). At present, molecular diagnostic techniques for detecting ASFV mainly rely on two OIE-recommended conventional and real-time qPCR technique methods. Although these techniques have been widely validated and are useful tools for detecting this disease, they remain inconvenient because of expensive instruments and professional operation systems. The CRISPR/Cas systems are revolutionary tools allowing for precise genome engineering, transcription regulation, and many other applications (52, 53). The Cas12a recognizes specific dsDNA sequences and then non-specifically cleaves the ssDNA, making it particularly suitable for detecting dsDNA viruses.

The cleavage site specificity of the Cas/crRNA complex is determined by the length of the crRNA and the sequence, number, location, and distribution of mismatch (54, 55). The 20nt or shorter nucleotide hybridizes with the dsDNA close to PAM region, which determines that CRISPR/Cas has high specificity (56). However, SNV in genome may cause off-target and false negatives when mutating on the target or the PAM (54, 57). The introduction of PAM through pre-amplification and multi-crRNA strategies may break the limitation caused by both PAM dependence and off-target, helping to improve the specificity of the detection system. The Cas12a enzyme itself has weak collateral cleavage activity; thus, it can only achieve low detection sensitivity without pre-amplification (27, 58). Therefore, in combination with isothermal amplification, such as RPA, LAMP, strand displacement amplification (SDA) (59–61), rolling circle amplification (RCA) (62, 63), exponential amplification reaction (EXPAR) (64, 65), and recombinase-aided amplification (RAA) (48, 66–68), we found that Cas12a was able to detect pathogens with high sensitivity and precision. In this study, we found that the CRISPR-RPA system is not highly sensitive, but it is faster than CRISPR-LAMP, which means that CRISPR-RPA is possible for rapid qualitative detection on the grassroots level.

Aerosol pollution, improper operation, and complex detection environment may unavoidably cause false positives in point-of-care testing (POCT), and two separate steps in CRISPR-based detection may make it more serious. However, one-pot detection could avoid false positives and high background positives caused by cross contamination (69–72). This means that template amplification, Cas-mediated enzyme cleavage reaction, and signal output are completed in one tube without opening or closing the cover (71, 73, 74). Moreover, to report the presence of target DNA, ssDNA probe linking a fluorophore (FAM in this study) and a quencher was used. After the

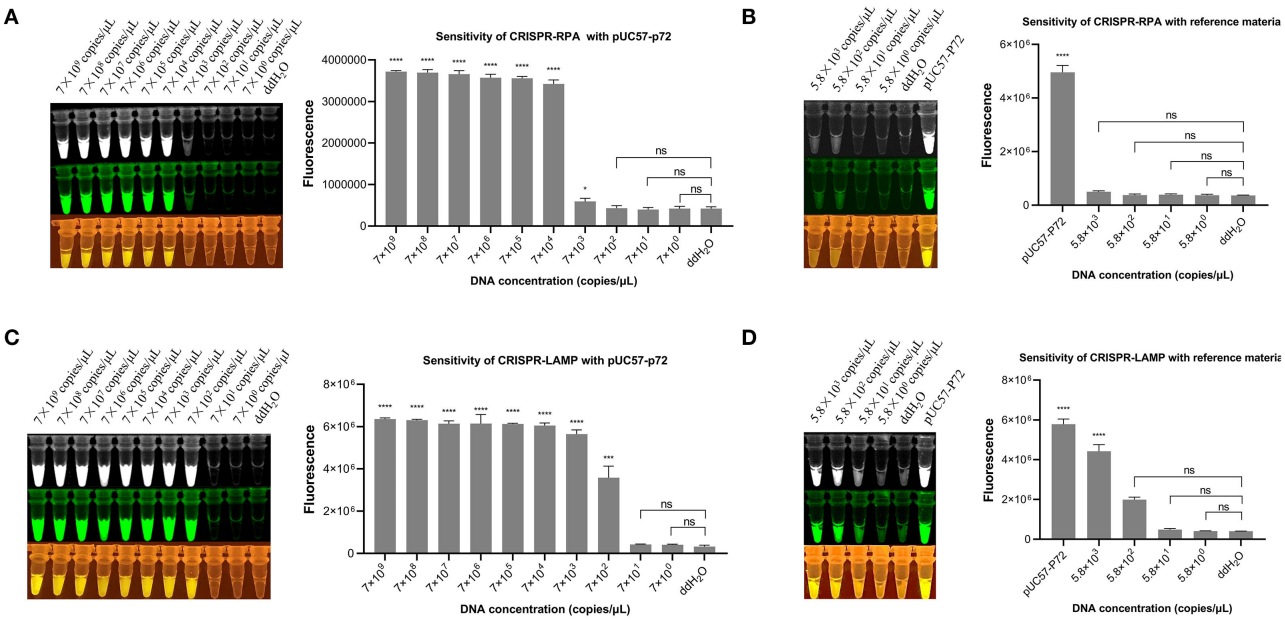

FIGURE 4 | Sensitivity of one-pot visual detection system. **(A)** The sensitivity of CRISPR-RPA one-pot detection with 10-fold serial diluted pUC57-p72 DNA. **(B)** The sensitivity of CRISPR-RPA one-pot detection with 10-fold serial diluted ASFV *B646L* gene plasmid reference material. **(C)** The sensitivity of CRISPR-LAMP one-pot detection with 10-fold serial diluted pUC57-p72 DNA. **(D)** The sensitivity of CRISPR-LAMP one-pot detection with 10-fold serial diluted ASFV *B646L* gene plasmid reference material. Analysis of the value for the fluorescence image using the ImageJ software. Each measuring was run with three replicates ($n = 3$). $^{*}P < 0.05$, $^{**}P < 0.01$, $^{***}P < 0.001$, $^{****}P < 0.0001$, ns, not significant. Error bars represent the means ± s.d. from replicates. The unpaired two-tailed *t*-test was used to analyze the statistical significance.

indiscriminate cleavage was triggered, the fluorophore on the ssDNA probe was released and detected by specific wavelength light, making it visible and suitable for POCT, thereby avoiding the problems described previously (74–76). The contradiction between sensitivity and specificity in the detection process is thus solved to a certain extent.

Depending on expensive thermocyclers and skilled operator, PCR as the gold standard is difficult to popularize in POCT. Therefore, lower cost and personnel requirement detection methods could be more advantageous and required. Strip-based lateral flow assay (LFA) is an option with low cost (20, 77, 78), but opening tube while inserting the strip makes it less suitable. Therefore, the CRISPR-isothermal amplification method used in this study shows more advantages in POCT. A hand warmer and water bath, which gets rid of thermocyclers, can satisfy the meet for pre-amplification. Besides, the fixed wavelength illuminant makes the results more intuitive, clear and reduces the dependency on skilled operators, which greatly reduces the cost of POCT.

In conclusion, a one-pot visual detection system was established and used for the rapid, sensitive, specific, and low-cost detection of ASFV. This integration has great potential for POCT detection of ASFV and other DNA-based pathogens, which could be an effective way for the timely monitoring of ASFV to prevent its occurrence and spread at an early stage.

DATA AVAILABILITY STATEMENT

The original contributions presented in the study are included in the article/**Supplementary Material**, further inquiries can be directed to the corresponding authors.

AUTHOR CONTRIBUTIONS

KX and MZ contributed to the conceptualization and biosensor design, fabrication, and manuscript preparation. CQ performed the experiments, data curation, and drafted the manuscript. JL, WZ, JD, HZ, JZ, YK, LL, GS, ZL, HL, SJ, and KC performed formal analysis, validation support, and manuscript proofreading. XD and HM reviewed, edited, and supervised this work. All authors have read and agreed to the published version of the manuscript.

FUNDING

This research was funded by the Agri-X Fund of Shanghai Jiao Tong University (Grant No. AF1500088/001/001).

SUPPLEMENTARY MATERIAL

The Supplementary Material for this article can be found online at: https://www.frontiersin.org/articles/10.3389/fvets.2022.962438/full#supplementary-material

REFERENCES

1. Sánchez-Vizcaíno J, Mur L, Sánchez M, Martínez-López B. African swine fever: New challenges and measures to prevent its spread. In: *Proceedings of the 82nd General Session World Assembly of Delegates of the World Organisation for Animal Health (OIE).* Paris (2014).
2. Galindo I, Alonso C. African swine fever virus: a review. *Viruses.* (2017) 9:103. doi: 10.3390/v9050103
3. Zhao D, Liu R, Zhang X, Li F, Wang J, Zhang J, et al. Replication and virulence in pigs of the first African swine fever virus isolated in China. *Emerg Microbes Infect.* (2019) 8:438–47. doi: 10.1080/22221751.2019.1590128
4. Zhou X, Li N, Luo Y, Liu Y, Miao F, Chen T, et al. Emergence of African swine fever in China, 2018. *Transbound Emerg Dis.* (2018) 65:1482–4. doi: 10.1111/tbed.12989
5. Revilla Y, Pérez-Núñez D, Richt JA. African swine fever virus biology and vaccine approaches. *Adv Virus Res.* (2018) 100:41–74. doi: 10.1016/bs.aivir.2017.10.002
6. Gallardo C, Nieto R, Soler A, Pelayo V, Fernández-Pinero J, Markowska-Daniel I, et al. Assessment of African swine fever diagnostic techniques as a response to the epidemic outbreaks in Eastern European union countries: how to improve surveillance and control programs. *J Clin Microbiol.* (2015) 53:2555–65. doi: 10.1128/JCM.00857-15
7. Luo Y, Atim SA, Shao L, Ayebazibwe C, Sun Y, Liu Y, et al. Development of an updated PCR assay for detection of African swine fever virus. *Arch Virol.* (2017) 162:191–9. doi: 10.1007/s00705-016-3069-3
8. Zsak L, Borca MV, Risatti GR, Zsak A, French RA, Lu Z, et al. Preclinical diagnosis of African swine fever in contact-exposed swine by a real-time PCR assay. *J Clin Microbiol.* (2005) 43:112–9. doi: 10.1128/JCM.43.1.112-119.2005
9. Daigle J, Onyilagha C, Truong T, Le VP, Nga BTT, Nguyen TL, et al. Rapid and highly sensitive portable detection of African swine fever virus. *Transbound Emerg Dis.* (2021) 68:952–9. doi: 10.1111/tbed.13770
10. Sastre P, Gallardo C, Monedero A, Ruiz T, Arias M, Sanz A, et al. Development of a novel lateral flow assay for detection of African swine fever in blood. *BMC Vet Res.* (2016) 12:206. doi: 10.1186/s12917-016-0831-4
11. Miao F, Zhang J, Li N, Chen T, Wang L, Zhang F, et al. Rapid and sensitive recombinase polymerase amplification combined with lateral flow strip for detecting African swine fever virus. *Front Microbiol.* (2019) 10:1004. doi: 10.3389/fmicb.2019.01004
12. Fan X, Li L, Zhao Y, Liu Y, Liu C, Wang Q, et al. Clinical validation of two recombinase-based isothermal amplification assays (RPA/RAA) for the rapid detection of African swine fever virus. *Front Microbiol.* (2020) 11:1696. doi: 10.3389/fmicb.2020.01696
13. Zhai Y, Ma P, Fu X, Zhang L, Cui P, Li H, et al. A recombinase polymerase amplification combined with lateral flow dipstick for rapid and specific detection of African swine fever virus. *J Virol Methods.* (2020) 285:113885. doi: 10.1016/j.jviromet.2020.113885
14. James HE, Ebert K, Mcgonigle R, Reid SM, Boonham N, Tomlinson JA, et al. Detection of African swine fever virus by loop-mediated isothermal amplification. *J Virol Methods.* (2010) 164:68–74. doi: 10.1016/j.jviromet.2009.11.034
15. Mee PT, Wong S, O'riley KJ, Da Conceição F, Bendita Da Costa Jong J, Phillips DE, et al. Field verification of an African swine fever virus loop-mediated isothermal amplification (LAMP) assay during an outbreak in timor-leste. *Viruses.* (2020) 12:1444. doi: 10.3390/v12121444
16. Wozniakowski G, Fraczyk M, Kowalczyk A, Pomorska-Mól M, Niemczuk K, Pejsak Z. Polymerase cross-linking spiral reaction (PCLSR) for detection of African swine fever virus (ASFV) in pigs and wild boars. *Sci Rep.* (2017) 7:42903. doi: 10.1038/srep42903
17. Fraczyk M, Wozniakowski G, Kowalczyk A, Niemczuk K, Pejsak Z. Development of cross-priming amplification for direct detection of the African swine fever virus, in pig and wild boar blood and sera samples. *Lett Appl Microbiol.* (2016) 62:386–91. doi: 10.1111/lam.12569
18. Tomita N, Mori Y, Kanda H, Notomi T. Loop-mediated isothermal amplification (LAMP) of gene sequences and simple visual detection of products. *Nat Protoc.* (2008) 3:877–82. doi: 10.1038/nprot.2008.57
19. Wang JC, Yuan WZ, Han QA, Wang JF, Liu LB. Reverse transcription recombinase polymerase amplification assay for the rapid detection of type 2 porcine reproductive and respiratory syndrome virus. *J Virol Methods.* (2017) 243:55–60. doi: 10.1016/j.jviromet.2017.01.017
20. Gootenberg JS, Abudayyeh OO, Lee JW, Essletzbichler P, Dy AJ, Joung J, et al. Nucleic acid detection with CRISPR-Cas13a/C2c2. *Science.* (2017) 356:438–42. doi: 10.1126/science.aam9321
21. Gootenberg JS, Abudayyeh OO, Kellner MJ, Joung J, Collins JJ, Zhang F. Multiplexed and portable nucleic acid detection platform with Cas13, Cas12a, and Csm6. *Science.* (2018) 360:439–44. doi: 10.1126/science.aaq0179
22. Myhrvold C, Freije CA, Gootenberg JS, Abudayyeh OO, Metsky HC, Durbin AF, et al. Field-deployable viral diagnostics using CRISPR-Cas13. *Science.* (2018) 360:444–8. doi: 10.1126/science.aas8836
23. Wu Y, Liu SX, Wang F, Zeng MS. Room temperature detection of plasma epstein-barr virus DNA with CRISPR-Cas13. *Clin Chem.* (2019) 65:591–2. doi: 10.1373/clinchem.2018.299347
24. Liu Y, Xu H, Liu C, Peng L, Khan H, Cui L, et al. CRISPR-Cas13a nanomachine based simple technology for avian influenza A (H7N9) virus on-site detection. *J Biomed Nanotechnol.* (2019) 15:790–8. doi: 10.1166/jbn.2019.2742
25. Qin P, Park M, Alfson KJ, Tamhankar M, Carrion R, Patterson JL, et al. Rapid and fully microfluidic ebola virus detection with CRISPR-Cas13a. *ACS Sens.* (2019) 4:1048–54. doi: 10.1021/acssensors.9b00239
26. Ke Y, Huang S, Ghalandari B, Li S, Warden AR, Dang J, et al. Hairpin-spacer crRNA-enhanced CRISPR/Cas13a system promotes the specificity of single nucleotide polymorphism (SNP) identification. *Adv Sci.* (2021) 8:2003611. doi: 10.1002/advs.202003611
27. Chen JS, Ma E, Harrington LB, Da Costa M, Tian X, Palefsky JM, et al. CRISPR-Cas12a target binding unleashes indiscriminate single-stranded DNase activity. *Science.* (2018) 360:436–9. doi: 10.1126/science.aar6245
28. Li SY, Cheng QX, Wang JM, Li XY, Zhang ZL, Gao S, et al. CRISPR-Cas12a-assisted nucleic acid detection. *Cell Discov.* (2018) 4:20. doi: 10.1038/s41421-018-0028-z
29. Li L, Li S, Wu N, Wu J, Wang G, Zhao G, et al. HOLMESv2: A CRISPR-Cas12b-assisted platform for nucleic acid detection and DNA methylation quantitation. *ACS Synth Biol.* (2019) 8:2228–37. doi: 10.1021/acssynbio.9b00209
30. Broughton JP, Deng X, Yu G, Fasching CL, Servellita V, Singh J, et al. CRISPR-Cas12-based detection of SARS-CoV-2. *Nat Biotechnol.* (2020) 38:870–4. doi: 10.1038/s41587-020-0513-4
31. Ke Y, Ghalandari B, Huang S, Li S, Huang C, Zhi X, et al. 2'-O-Methyl modified guide RNA promotes the single nucleotide polymorphism (SNP) discrimination ability of CRISPR-Cas12a systems. *Chem Sci.* (2022) 13:2050–61. doi: 10.1039/D1SC06832F
32. Pardee K, Green AA, Takahashi MK, Braff D, Lambert G, Lee JW, et al. Rapid, low-cost detection of zika virus using programmable biomolecular components. *Cell.* (2016) 165:1255–66. doi: 10.1016/j.cell.2016.04.059
33. Zhang Y, Qian L, Wei W, Wang Y, Wang B, Lin P, et al. Paired design of dCas9 as a systematic platform for the detection of featured nucleic acid sequences in pathogenic strains. *ACS Synth Biol.* (2017) 6:211–6. doi: 10.1021/acssynbio.6b00215
34. Hajian R, Balderston S, Tran T, Deboer T, Etienne J, Sandhu M, et al. Detection of unamplified target genes via CRISPR–Cas9 immobilized on a graphene field-effect transistor. *Nat Biomed Eng.* (2019) 3:427–37. doi: 10.1038/s41551-019-0371-x
35. Teng F, Guo L, Cui T, Wang XG, Xu K, Gao Q, et al. CDetection: CRISPR-Cas12b-based DNA detection with sub-attomolar sensitivity and single-base specificity. *Genome Biol.* (2019) 20:132. doi: 10.1186/s13059-019-1742-z
36. Harrington LB, Burstein D, Chen JS, Paez-Espino D, Ma E, Witte IP, et al. Programmed DNA destruction by miniature CRISPR-Cas14 enzymes. *Science.* (2018) 362:839–42. doi: 10.1126/science.aav4294
37. Shmakov S, Smargon A, Scott D, Cox D, Pyzocha N, Yan W, et al. Diversity and evolution of class 2 CRISPR-Cas systems. *Nat Rev Microbiol.* (2017) 15:169–82. doi: 10.1038/nrmicro.2016.184
38. Zetsche B, Gootenberg JS, Abudayyeh OO, Slaymaker IM, Makarova KS, Essletzbichler P, et al. Cpf1 is a single RNA-guided endonuclease of a class 2 CRISPR-Cas system. *Cell.* (2015) 163:759–71. doi: 10.1016/j.cell.2015.09.038

39. Dong D, Ren K, Qiu X, Zheng J, Guo M, Guan X, et al. The crystal structure of Cpf1 in complex with CRISPR RNA. *Nature.* (2016) 532:522–6. doi: 10.1038/nature17944
40. Stella S, Alcón P, Montoya G. Structure of the Cpf1 endonuclease R-loop complex after target DNA cleavage. *Nature.* (2017) 546:559–63. doi: 10.1038/nature22398
41. East-Seletsky A, O'Connell MR, Burstein D, Knott GJ, Doudna JA. RNA targeting by functionally orthogonal type VI-A CRISPR-Cas enzymes. *Mol Cell.* (2017) 66:373–83.e3. doi: 10.1016/j.molcel.2017.04.008
42. Kundert K, Lucas JE, Watters KE, Fellmann C, Ng AH, Heineike BM, et al. Controlling CRISPR-Cas9 with ligand-activated and ligand-deactivated sgRNAs. *Nat Commun.* (2019) 10:2127. doi: 10.1038/s41467-019-09985-2
43. Malzahn AA, Tang X, Lee K, Ren Q, Sretenovic S, Zhang Y, et al. Application of CRISPR-Cas12a temperature sensitivity for improved genome editing in rice, maize, and arabidopsis. *BMC Biol.* (2019) 17:9. doi: 10.1186/s12915-019-0629-5
44. Liu S, Tao D, Liao Y, Yang Y, Sun S, Zhao Y, et al. Highly sensitive CRISPR/Cas12a-based fluorescence detection of porcine reproductive and respiratory syndrome virus. *ACS Synth Biol.* (2021) 10:2499–507. doi: 10.1021/acssynbio.1c00103
45. Chaijarasphong T, Thammachai T, Itsathitphaisarn O, Sritunyalucksana K, Suebsing R. Potential application of CRISPR-Cas12a fluorescence assay coupled with rapid nucleic acid amplification for detection of white spot syndrome virus in shrimp. *Aquaculture.* (2019) 512. doi: 10.1016/j.aquaculture.2019.734340
46. Smith CW, Nandu N, Kachwala MJ, Chen Y-S, Uyar TB, Yigit MV. Probing CRISPR-Cas12a nuclease activity using double-stranded DNA-templated fluorescent substrates. *Biochemistry.* (2020) 59:1474–81. doi: 10.1021/acs.biochem.0c00140
47. Dai Y, Somoza RA, Wang L, Welter JF, Li Y, Caplan AI, et al. Exploring the trans-cleavage activity of CRISPR-Cas12a (cpf1) for the development of a universal electrochemical biosensor. *Angew Chem Int Ed Engl.* (2019) 58:17399–405. doi: 10.1002/anie.201910772
48. Li F, Ye Q, Chen M, Zhou B, Zhang J, Pang R, et al. An ultrasensitive CRISPR/Cas12a based electrochemical biosensor for Listeria monocytogenes detection. *Biosens Bioelectron.* (2021) 179:113073. doi: 10.1016/j.bios.2021.113073
49. Wang Y, Ke Y, Liu W, Sun Y, Ding X. A one-pot toolbox based on Cas12a/crRNA enables rapid foodborne pathogen detection at attomolar level. *ACS Sens.* (2020) 5:1427–35. doi: 10.1021/acssensors.0c00320
50. Ai JW, Zhou X, Xu T, Yang M, Chen Y, He GQ, et al. CRISPR-based rapid and ultra-sensitive diagnostic test for Mycobacterium tuberculosis. *Emerg Microbes Infect.* (2019) 8:1361–9. doi: 10.1080/22221751.2019.1664939
51. Wang N, Zhao D, Wang J, Zhang Y, Wang M, Gao Y, et al. Architecture of African swine fever virus and implications for viral assembly. *Science.* (2019) 366:640–4. doi: 10.1126/science.aaz1439
52. Dominguez AA, Lim WA, Qi LS. Beyond editing: repurposing CRISPR-Cas9 for precision genome regulation and interrogation. *Nat Rev Mol Cell Biol.* (2016) 17:5–15. doi: 10.1038/nrm.2015.2
53. Yin H, Xue W, Anderson DG. CRISPR-Cas: a tool for cancer research and therapeutics. *Nat Rev Clin Oncol.* (2019) 16:281–95. doi: 10.1038/s41571-019-0166-8
54. Yang L, Grishin D, Wang G, Aach J, Zhang CZ, Chari R, et al. Targeted and genome-wide sequencing reveal single nucleotide variations impacting specificity of Cas9 in human stem cells. *Nat Commun.* (2014) 5:5507. doi: 10.1038/ncomms6507
55. Fu Y, Sander JD, Reyon D, Cascio VM, Joung JK. Improving CRISPR-Cas nuclease specificity using truncated guide RNAs. *Nat Biotechnol.* (2014) 32:279–84. doi: 10.1038/nbt.2808
56. Li Y, Liu L, Liu G. CRISPR/Cas multiplexed biosensing: a challenge or an insurmountable obstacle? *Trends Biotechnol.* (2019) 37:792–5. doi: 10.1016/j.tibtech.2019.04.012
57. Scott DA, Zhang F. Implications of human genetic variation in CRISPR-based therapeutic genome editing. *Nat Med.* (2017) 23:1095–101. doi: 10.1038/nm.4377
58. Mustafa Mujahed I, Makhawi Abdelrafie M, Kraft Colleen S. SHERLOCK and DETECTR: CRISPR-cas systems as potential rapid diagnostic tools for emerging infectious diseases. *J Clin Microbiol.* (2021) 59:e00745–20. doi: 10.1128/JCM.00745-20
59. Zhou W, Hu L, Ying L, Zhao Z, Chu PK, Yu XF. A CRISPR-Cas9-triggered strand displacement amplification method for ultrasensitive DNA detection. *Nat Commun.* (2018) 9:5012. doi: 10.1038/s41467-018-07324-5
60. Gong S, Zhang S, Wang X, Li J, Pan W, Li N, et al. Strand displacement amplification assisted CRISPR-Cas12a strategy for colorimetric analysis of viral nucleic acid. *Anal Chem.* (2021) 93:15216–23. doi: 10.1021/acs.analchem.1c04133
61. Chen X, Deng Y, Cao G, Xiong Y, Huo D, Hou C. Ultra-sensitive MicroRNA-21 detection based on multiple cascaded strand displacement amplification and CRISPR/Cpf1 (MC-SDA/CRISPR/Cpf1). *Chem Commun.* (2021) 57:6129–32. doi: 10.1039/D1CC01938D
62. Tian B, Minero GAS, Fock J, Dufva M, Hansen MF. CRISPR-Cas12a based internal negative control for nonspecific products of exponential rolling circle amplification. *Nucleic Acids Res.* (2020) 48:e30. doi: 10.1093/nar/gkaa017
63. Xu L, Dai Q, Shi Z, Liu X, Gao L, Wang Z, et al. Accurate MRSA identification through dual-functional aptamer and CRISPR-Cas12a assisted rolling circle amplification. *J Microbiol Methods.* (2020) 173:105917. doi: 10.1016/j.mimet.2020.105917
64. Huang M, Zhou X, Wang H, Xing D. Clustered regularly interspaced short palindromic repeats/Cas9 triggered isothermal amplification for site-specific nucleic acid detection. *Anal Chem.* (2018) 90:2193–200. doi: 10.1021/acs.analchem.7b04542
65. Wang X, Chen X, Chu C, Deng Y, Yang M, Huo D, et al. Naked-eye detection of site-specific ssRNA and ssDNA using PAMmer-assisted CRISPR/Cas9 coupling with exponential amplification reaction. *Talanta.* (2021) 233:122554. doi: 10.1016/j.talanta.2021.122554
66. Wang X, Ji P, Fan H, Dang L, Wan W, Liu S, et al. CRISPR/Cas12a technology combined with immunochromatographic strips for portable detection of African swine fever virus. *Commun Biol.* (2020) 3:62. doi: 10.1038/s42003-020-0796-5
67. Ma QN, Wang M, Zheng LB, Lin ZQ, Ehsan M, Xiao XX, et al. RAA-Cas12a-Tg: a nucleic acid detection system for toxoplasma gondii based on CRISPR-Cas12a combined with recombinase-aided amplification (RAA). *Microorganisms.* (2021) 9:1644. doi: 10.3390/microorganisms9081644
68. Chen Y, Mei Y, Zhao X, Jiang X. Reagents-loaded, automated assay that integrates recombinase-aided amplification and Cas12a nucleic acid detection for a point-of-care test. *Anal Chem.* (2020) 92:14846–52. doi: 10.1021/acs.analchem.0c03883
69. Pang B, Xu J, Liu Y, Peng H, Feng W, Cao Y, et al. Isothermal amplification and ambient visualization in a single tube for the detection of SARS-CoV-2 using loop-mediated amplification and CRISPR technology. *Anal Chem.* (2020) 92:16204–12. doi: 10.1021/acs.analchem.0c04047
70. Chen Y, Shi Y, Chen Y, Yang Z, Wu H, Zhou Z, et al. Contamination-free visual detection of SARS-CoV-2 with CRISPR/Cas12a: a promising method in the point-of-care detection. *Biosens Bioelectron.* (2020) 169:112642. doi: 10.1016/j.bios.2020.112642
71. Ding X, Yin K, Li Z, Lalla RV, Ballesteros E, Sfeir MM, et al. Ultrasensitive and visual detection of SARS-CoV-2 using all-in-one dual CRISPR-Cas12a assay. *Nat Commun.* (2020) 11. doi: 10.1038/s41467-020-18575-6
72. Wang R, Qian C, Pang Y, Li M, Yang Y, Ma H, et al. opvCRISPR: One-pot visual RT-LAMP-CRISPR platform for SARS-CoV-2 detection. *Biosens Bioelectron.* (2021) 172:112766. doi: 10.1016/j.bios.2020.112766
73. Wang X, Zhong M, Liu Y, Ma P, Dang L, Meng Q, et al. Rapid and sensitive detection of COVID-19 using CRISPR/Cas12a-based detection with naked eye readout, CRISPR/Cas12a-NER. *Sci Bull.* (2020) 65:1436–9. doi: 10.1016/j.scib.2020.04.041
74. Wang B, Wang R, Wang D, Wu J, Li J, Wang J, et al. Cas12aVDet: a CRISPR/Cas12a-based platform for rapid and visual nucleic acid detection. *Anal Chem.* (2019) 91:12156–61. doi: 10.1021/acs.analchem.9b01526
75. He Q, Yu D, Bao M, Korensky G, Chen J, Shin M, et al. High-throughput and all-solution phase African swine fever virus (ASFV) detection using CRISPR-Cas12a and fluorescence based point-of-care system. *Biosens Bioelectron.* (2020) 154:112068. doi: 10.1016/j.bios.2020.112068
76. Cheng M, Xiong E, Tian T, Zhu D, Ju HQ, Zhou X. A CRISPR-driven colorimetric code platform for highly accurate telomerase activity

assay. *Biosens Bioelectron.* (2021) 172:112749. doi: 10.1016/j.bios.2020.112749
77. Takahashi MK, Tan X, Dy AJ, Braff D, Akana RT, Furuta Y, et al. A low-cost paper-based synthetic biology platform for analyzing gut microbiota and host biomarkers. *Nat Commun.* (2018) 9:3347. doi: 10.1038/s41467-018-05864-4
78. Fozouni P, Son S, Díaz De León Derby M, Knott GJ, Gray CN, D'ambrosio MV, et al. Amplification-free detection of SARS-CoV-2 with CRISPR-Cas13a and mobile phone microscopy. *Cell.* (2021) 184:323–33.e9. doi: 10.1016/j.cell.2020.12.001

Conflict of Interest: The authors declare that the research was conducted in the absence of any commercial or financial relationships that could be construed as a potential conflict of interest.

Publisher's Note: All claims expressed in this article are solely those of the authors and do not necessarily represent those of their affiliated organizations, or those of the publisher, the editors and the reviewers. Any product that may be evaluated in this article, or claim that may be made by its manufacturer, is not guaranteed or endorsed by the publisher.

frontiers | Frontiers in Veterinary Science

TYPE Original Research
PUBLISHED 08 September 2022
DOI 10.3389/fvets.2022.1006895

OPEN ACCESS

EDITED BY
Wentao Li,
Huazhong Agricultural University, China

REVIEWED BY
Fangfeng Yuan,
University of Illinois at Urbana-Champaign, United States
Yifei Lang,
Sichuan Agricultural University, China

*CORRESPONDENCE
Pengchao Ji
tiankonglan246@163.com
Gaiping Zhang
zhanggaiping2003@163.com

†These authors have contributed equally to this work

SPECIALTY SECTION
This article was submitted to Veterinary Experimental and Diagnostic Pathology, a section of the journal Frontiers in Veterinary Science

RECEIVED 29 July 2022
ACCEPTED 22 August 2022
PUBLISHED 08 September 2022

CITATION
Jiang W, Jiang D, Li L, Wan B, Wang J, Wang P, Shi X, Zhao Q, Song J, Zhu Z, Ji P and Zhang G (2022) Development of an indirect ELISA for the identification of African swine fever virus wild-type strains and CD2v-deleted strains. *Front. Vet. Sci.* 9:1006895. doi: 10.3389/fvets.2022.1006895

Development of an indirect ELISA for the identification of African swine fever virus wild-type strains and CD2v-deleted strains

Wenting Jiang[1,2†], Dawei Jiang[1,2,3†], Lu Li[1,2], Bo Wan[1,2,4], Jiabin Wang[1,2], Panpan Wang[1,2], Xuejian Shi[1,2], Qi Zhao[1,2], Jinxing Song[1,2], Zixiang Zhu[5,6], Pengchao Ji[1,2,4*] and Gaiping Zhang[1,2,3,4*]

[1]College of Veterinary Medicine, Henan Agricultural University, Zhengzhou, China, [2]International Joint Research Center of National Animal Immunology, College of Veterinary Medicine, Henan Agricultural University, Zhengzhou, China, [3]Longhu Laboratory, Zhengzhou, China, [4]Henan Engineering Laboratory of Animal Biological Products, College of Veterinary Medicine, Henan Agricultural University, Zhengzhou, China, [5]State Key Laboratory of Veterinary Etiological Biology, Lanzhou Veterinary Research Institute, College of Veterinary Medicine, Lanzhou University, Chinese Academy of Agricultural Sciences, Lanzhou, China, [6]African Swine Fever Regional Laboratory of China, Lanzhou Veterinary Research Institute, Chinese Academy of Agricultural Sciences, Lanzhou, China

African swine fever (ASF) is a potent infectious disease with detrimental effects on the global swine industry and no currently vaccine available. The emergence of low-virulence CD2v-deleted mutants manifested as non-hemadsorption (non-HAD) strains represents a significant challenge to the prevention and control of ASF. In this study, we aimed to establish an indirect ELISA (IELISA) method for the identification of ASFV wild-type and CD2v-deleted strains. We integrated the CD2v protein extracellular domain sequence (CD2v-Ex, 1–588 bp) of the highly pathogenic strain China/2018/AnhuiXCGQ into the genome of suspension culture-adapted Chinese hamster Ovary-S (CHO-S) cells using lentivirus vectors (LVs). By screening, we identified a monoclonal CHO-S cell line that stably expressed secretory CD2v-Ex Protein. We then used the purified CD2v-Ex Protein as the detection antigen to establish an indirect ELISA method (CD2v-IELISA) for identification of the ASFV wild-type and CD2v-Deleted ($CD2v^{-}$) strains. The CD2v-IELISA method showed excellent specificity with no cross-reaction with serum samples infected with ASFV ($CD2v^{-}$), porcine reproductive and respiratory syndrome virus (PRRSV), classical swine fever virus (CSFV), porcine circovirus (PCV), porcine pseudorabies virus (PRV), swine foot and mouth disease virus (FMDV) and porcine epidemic diarrhea virus (PEDV). Furthermore, this method showed high sensitivity, allowing identification of ASFV-infected clinical serum samples up to a dilution of 1:2,560. The coefficient of variation both in and between

10.3389/fvets.2022.1006895

batches was <10% with good reproducibility and a high compliance rate of 99.4%. This CD2v-IELISA method developed here is of great significance for the prevention, control and purification of ASFV.

KEYWORDS

ASFV, CD2v extracellular fragment, CHO cell line, indirect ELISA, identification, CD2v-deleted

Introduction

African swine fever (ASF) is an acute and severe infectious disease caused by African swine fever virus (ASFV), which can infect domestic pigs and wild boars of all ages and cause up to 100% mortality (1). ASFV is the only currently known insect-borne DNA virus with a genome size of 170–193 kb, encoding more than 150 kinds of proteins although the functions of more than half of these proteins remain to be clarified (2–4). There are currently 24 known genotypes of ASFV based on genetic differences in the protein 72 (p72) capsid protein, and eight serotypes based on hemadsorption inhibition assays (HAI) using ASFV reference immune antisera (5). No effective commercial vaccine is currently available; therefore, effective and accurate methods for laboratory diagnosis are of great significance for the prevention and control of ASFV infection (6, 7).

ASFV was first reported in China in 2018 in an ASF outbreak causing huge economic losses. This strain was identified as p72 genotype II and CD2v serogroup 8, homologous to the highly pathogenic Georgia/2007 strain (8). However, recent studies have shown that ASFV strains with different deletions or mutations of the *EP402R* gene are now spreading. These variant strains show non-hemadsorption (non-HAD) and certain differences in virulence and pathogenicity (reduced pathogenicity but still obvious residues, longer incubation period which can cause persistent infection and chronic disease course, high transmission ability, and marked variation in the clinical manifestations and morbidity between individuals) compared with the earliest isolated highly pathogenic HLJ/2018 strain (9). Consequently, the early diagnosis and monitoring of ASFV has become more difficult. A variety of methods for ASFV antibody detection have been published. Almost all of these methods were used to detect ASFV infection only, but were not able to distinguish infection by ASFV wild-type and CD2v-deleted strains.

ASFV has a complex icosahedral structure (∼260–300 nm in diameter) composed of a central nucleoid, core shell, inner membrane, capsid and outer membrane (10). The CD2v protein, encoded by the *EP402R* gene, is a characteristic glycoprotein located in the outer capsule membrane of ASFV. It consists of intracellular, transmembrane and extracellular regions, and it is actively expressed in the late stage of the viral infection process (11, 12). The structure of the CD2v extracellular region is homologous to that of the CD2 protein on the surface of host T cells and natural killer cells. CD2v expression can cause lymphocyte damage, which contributes to the immune escape of the virus. In addition, CD2v binds specifically to CD2 receptors on the surface of porcine red blood cells, leading to a blood adsorption phenomenon and participating in the transport of the virus in the infectious animal (13, 14).

The CD2v protein is an important structural surface antigen of wild-type ASFV. Infection with wild-type ASFV induces the production of specific antibodies that recognize the CD2v protein. Therefore, we used CHO cells to express CD2v as an extracellular protein, which we then used as a detection antigen to establish an iELISA for rapid detection of CD2v antibodies. This assay can be used to distinguish infection by ASFV wild-type strains (HAD) and CD2v-deleted strains (non-HAD) and might be of great importance in epidemiological investigation and normalized monitoring of ASFV.

Materials and methods

Plasmid construction and LV production

The CD2v protein extracellular region (GenBank: MK128995.1, CD2v-ex, 1–588 bp) gene sequence was optimized according to the CHO expression system and a 6× His-tag was introduced at the carboxyl terminus. The recombinant CD2v-ex gene sequence was then cloned into the pTRIP-Pure vector, pTRIP-Pure-CD2v-ex (GenScript, Nanjing, China). Adherent human embryonic kidney (HEK) 293T (ATCC, Manassas, VA, USA) cells were maintained in high glucose Dulbecco's modified Eagle's medium (DMEM; Solarbio, Beijing, China). At 40–50% confluence, HEK 293T cells were seeded in 6-well plates and co-transfected with pTRIP-Pure-CD2v-ex (0.65 μg), psPAX (0.9 μg) and pMDG.2 (0.5 μg) using Lipofectamine 2000 (Invitrogen, Carlsbad, CA, USA); a blank pTRIP-puro vector was used as a control 6–8 h after transfection, the medium was replaced with maintenance medium (DMEM containing 2% FBS). Supernatant containing the pseudotyped LVs was collected at 72 h post-transfection, centrifuged at 4,000 rpm for 10 min at 4°C and filtered through a 0.22 μm filter. The

supernatant was then used fresh in experiments or stored at −80°C as previously described (15).

Establishment of a stable CD2v-ex protein expressing cell clone

CHO-S cells (Thermo Fisher Scientific,Waltham, MA, USA) were passaged in 125-mL vent-cap cell shaker flasks (NEST, Wuxi, China) containing 25 mL ExpiCHO Expression Medium (Gibco, Grand Island, NY, USA) on an orbital shaker platform (100 rpm). When the cell viability exceeded 95%, 2×10^6 cells were mixed with the LV suspension at a ratio of 1:1 (16) in the presence of 5 μg/mL polybrene (Beyotime, Shanghai, China). After 24 h of culture in an orbital shaker at 37°C, the cells were collected by centrifugation at 500 rpm for 10 min at 25°C and resuspended in fresh ExpiCHO culture medium containing puromycin (Beyotime).

The process for screening of a stable cell clone was proceed as follows. Briefly, the transfected CHO-S cells were passaged at a density of 0.5×10^6 viable cells/mL in ExpiCHO culture medium containing 7.5 μg/mL puromycin. When the cell viability exceeded 90%, a second round of screening was performed in ExpiCHO Stable Production Medium (Gibco) containing 22.5 μg/mL puromycin. After 12 h, expression of CD2v-ex by cell clones was evaluated by western blot analysis. Briefly, cell culture supernatants and cell fragmentation supernatants were denatured at 98°C for 10 minand proteins were separated by 7.5% SDS-PAGE before transfer to a polyvinylidene fluoride (PVDF) membrane (Merck Millipore, Billerica, MA, Germany). After blocking for 1 h with 5% skimmed milk (m/v, SM) in tris buffered saline containing 0.05% Tween-20 (TBST, v/v), the membrane was incubated at room temperature (RT) for 1 h with anti-His-tag antibody (1:5,000 in 5% SM, Proteintech, catlog number 66005-1-Ig, Wuhan, China) or standard ASFV-positive serum (1:2,000 in 5% SM, CVCC, Beijing, China). After washing with TBST, the membrane was incubated at 37°C for 1 h with the corresponding secondary antibodies [HRP-conjugated goat anti-mouse IgG (1:5,000 in 5% SM, Proteintech, catlog number SA00001-2) or mouse anti-pig IgG (1:5000 in 5% SM, Immunoway, catlog number RS030232, Plano, TX, USA)]. The antibody-reactive bands were detected using beyoECL star solution (Beyotime) and visualized with a multifunctional imaging system (GE Amersham Imager 600, Boston, Massachusetts, USA).

After two rounds of drug screening, stably transduced cell lines were generated by limiting dilution cloning. The cells were seeded in 96-well plates (0.5 cell per well) with ExpiCHO Expression Medium containing 6 mM L-glutamine (Gibco) and statically incubated at 37°C. Clones expressing high levels of the transfected protein were screened in 24-well and 6-well plates. Finally, the clones expressing the highest levels of the transfected protein was selected in fed-batch culture in 125-mL flasks by feeding with 5, 10, 15 g/L glucose (Gibco) and 2% (v/v) GluMAX-1 (100×, Gibco) on days 3, 5, 7 at 37°C. Dot blot and western blot analysis were used to selecting the high-expressing clones (17).

Genomic verification and protein purification

CHO-CD2v cell lines were verified by measurement of genomic DNA and RNA expression. For DNA verification, genomic DNA was extracted from 1×10^7 stably transduced monoclonal cells using the DNAiso Reagent (Takara, Tokyo, Japan) and identified by PCR amplification. The identification primers were designed based on the optimized gene sequence (CD2v-ex-F: 5'-ATGATCATCCTGATCTTCCTGATC-3', CD2v-ex-R: 5'-TCAGCTGGACAGTGTCAGGTA-3', Tsingke, Beijing, China). The PCR mixture (final volume 20 μL) contained 10 μL 2× PrimeSTAR MAX Premix (Takara), 1 μL genomic DNA, 1 μL of each primer (10 μM), and 7 μL ddH_2O. The PCR conditions were set as follows: 98°C pre-denaturation for 30 s; 30 cycles of denaturation at 98°C for 10 s, annealing of 58.5°C for 30 s and extension at 72°C for 30 s; final extension at 72°C for 8 min. The PCR products were identified by 1% (m/v) agarose and sequenced by Beijing Tsingke (Tsingke). For RNA identification, total RNA was isolated using RNAiso Plus (Takara) and cDNA was obtained by reverse transcription using HiScript II One Step qRT-PCR Probe Kit (Vazyme, Shanghai, China). The following PCR operations were the same as the above mentioned.

To prepare purified CD2v-ex protein for subsequent tests, the selected CHO-CD2v cell line was cultured for 7–10 days in a shaking incubator (100 rpm) and fed with 5 g/L glucose (Gibco) and 2% (v/v) GlutaMax-1 (100×, Gibco) every 2 days. After centrifugation with 12,000 ×*g* for 10 min, the supernatant was collected and CD2v-ex protein was purified from the cell culture supernatant using HisTrap excel (Cytiva, Sweden). The purified protein was analyzed by SDS-PAGE.

Indirect ELISA method development

CD2v-ex protein was diluted with carbonate bicarbonate buffer (CBS buffer, pH 9.6) and used to coat 96-well plates (Beaver, Suzhou, China) at 4°C overnight. The plates were then washed five times with TBST and patted dry. After the plates were blocked for 1 h at RT with 5% SM (in TBST) and washed as above, serum samples were diluted with 1% bovine serum albumin (1% BSA, m/v) in 1× phosphate buffered saline (PBS) and then added to plates (100 μL/well) and incubated for 30 min at 37°C. Subsequently, the plates were washed as above and incubated with HRP-conjected monoclonal mouse

anti-pig IgG (Immunoway) diluted to 1:10,000 with 5% SM. After incubation for 40 min at 37°C and washing, the plates were incubated with 3,3′,5,5′-tetramethylbenzidine (TMB, Solarbio) at RT. The reactions were stopped after 10 min by adding 2 mol/L H_2SO_4 (50 μL/well). The optical density (OD) of each well was measured at 450 nm (OD_{450}) using a Multimode Microplate Reader (Tecan 10M, Switzerland).

The antigen and serum concentrations were optimized by checkerboard titration. Briefly, 96-well plates were coated with the recombinant antigen titrated to concentrations of 0.5–4 μg/mL (50–400 ng/well). ASFV-positive ($ASFV^+$) and ASFV-negative ($ASFV^-$) standard sera were serially diluted 1:10–1:320. Every combination was evaluated in duplicate.

The CD2v-iELISA reaction conditions were optimized according to the optimal antigen coating concentration and serum dilution determined as previously described. The optimal assay conditions were identified as those that yielded the highest OD_{450} ratio between the $ASFV^+$ and $ASFV^-$ serum samples (P/N value) as previously described (18). Every sample was evaluated in triplicate.

The status of 82 swine $ASFV^-$ serum samples stored in our laboratory was first confirmed using the P30-iELISA kit (Kernal, US) according to the manufacturer's instructions. These 82 serum samples were then analyzed using the optimized CD2v-iELISA method. The cut-off value was defined as the mean OD_{450} value + 3 × the standard deviation (SD), and samples above this cut-off value were considered to be $ASFV^+$ (19).

Determination of the specificity, sensitivity, reproducibility, and compliance rate

The specificity of the established CD2v-iELISA method was determined against the following serum samples: $ASFV^+$ (positive control), $ASFV^+$ with CD2v deleted ($CD2v^-$), porcine reproductive and respiratory syndrome virus positive ($PRRSV^+$), classical swine fever virus positive ($CSFV^+$), porcine circovirus positive (PCV^+), porcine pseudorabies virus positive (PRV^+), swine foot and mouth disease virus positive ($FMDV^+$) and porcine epidemic diarrhea virus positive ($PEDV^+$). The OD_{450} of each pathogenic serum sample was compared with the cut-off value and samples above this cut-off value indicated a cross-reaction.

The sensitivity of the CD2v-iELISA was evaluated using three clinical $ASFV^+$ and three $ASFV^-$ serum samples diluted from 1:160 to 1:5,120. The assay sensitivity correlated with the highest dilution of serum detectable according to the cut-off value.

Eight $ASFV^+$ positive and/or $ASFV^-$ serum samples were randomly selected. Triplicate samples were assayed in one batch to evaluate intra-assay variation and in three different batches were assayed separately to evaluate inter-assay variation expressed as the coefficient of variation (CV).

A total of 179 clinical swine $ASFV^+$ (n = 18), $ASFV^-$ (n = 112) and $ASFV^+$ ($CD2v^-$) (n = 49) serum samples determined by real-time quantitative PCR (qPCR) and HAD tests were kindly provided by Lanzhou Veterinary Research Institute and analyzed using the established CD2v-ex-iELISA method to determine the compliance rate.

Statistical analysis

All statistical analysis was conducted using GraphPad Prism 8.2 software (Graph Pad Prism Inc., California, USA). Data were presented as the mean + SD. Significant differences between samples were assessed using Student's t-test. $P < 0.05$ was set as the threshold for statistical significance.

Results

Establishment of a stable CD2v-ex protein expressing cell clone

To establish a stable CD2v-ex protein expressing CHO-S cell line, CHO-S cells were first transduced with packaged LV suspensions to generate CHO-S cells expressing CD2v-ex (CD2v-ex) and CD2v-ex expression was verified by western blot analysis. A specific diffuse band (70–95 kD) was detected in CHO-CD2v cell culture supernatant (Figures 1A,B), consistent with eukaryotic expressed glycosylated proteins' characteristics (16, 20), suggesting that CHO-CD2v cells successfully secreted express glycosylated CD2v-ex. Furthermore, the protein was recognized by anti-His-tag antibody and $ASFV^+$ serum. To select a stable CD2v-expressing CHO cell line, monoclonal cells were obtained by limiting dilution cloning and then successively selected and expanded from 96-well plates (n = 92), to 24-well plates (n = 26) and finally, to 6-well plates (n = 8, 1C6, 2D2, 3B3, 3G4, 4D12, 5C5, 6E4, 7B5). Three high-expression CHO-CD2v cell clones (1C6, 6E4, 7B5) were then selected (Figure 1C), and the highest expression monoclonal cell line in fed-batch culture was identified as 1C6 by western blot analysis (Figure 1D). In addition, viable cells monitoring revealed that 1C6 showed a comparable growth curve compared with blank CHO-S cells in fed-batch culture (Figure 1E), suggesting that 1C6 was a high-expressing CHO-CD2v clone with growth characteristics similar to those of the parent line.

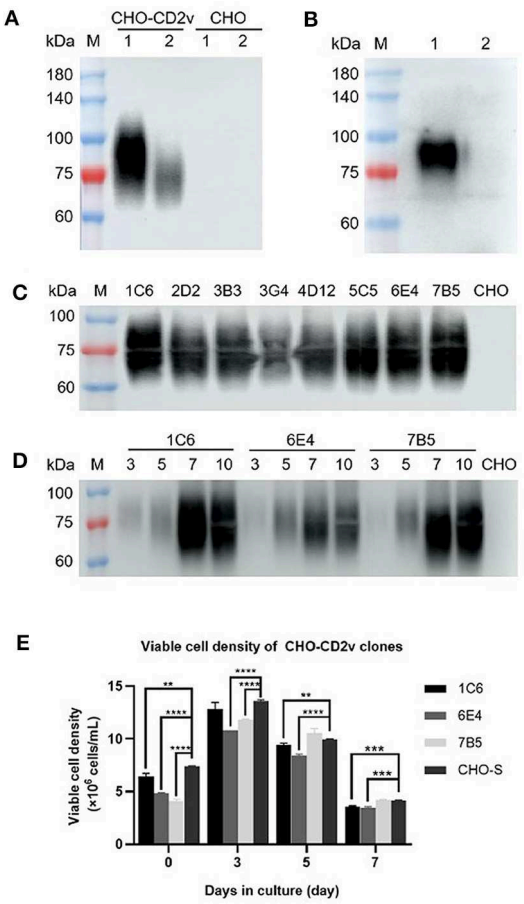

FIGURE 1
Establishment of a stable CD2v-ex protein expressing cell clone. Western blot detection of CD2v-ex protein expression after transduction of CHO-S cells using an anti-His-tag antibody: Lane 1: cell culture supernatant, Lane 2: cell fragmentation supernatant **(A)**. Western blot detection of CD2v-ex protein expression using standard ASFV^{+} serum **(B)**. Western blot comparison of expression levels of CHO-CD2v monoclonal cell lines (1C6, 2D2, 3B3, 3G4, 4D12, 5C5, 6E4, 7B5) after culture for 5 days in a 6-well plate **(C)**. Western blot detection of CD2v-ex protein in culture supernatants of three high-expression cell clones (1C6, 6E4, 7B5) collected on days 3, 5, 7, 10 **(D)**. Viable cell density of three high-expression CHO-CD2v clones after 3, 5, 7, 10 days in culture. $^{**}p < 0.01$, $^{***}p < 0.0001$, and $^{****}p < 0.00001$ **(E)**. Blank CHO-S cells were treated as a negative control; M: Protein marker 2,510.

Genomic verification and protein purification

For further verification of the selected CHO-CD2v clone (1C6), we extracted its genomic DNA and RNA, respectively. Integration of the CD2v-ex gene sequence into CHO-S cell genomic DNA was confirmed by PCR and transcription into mRNA for protein expression was verified by RT-PCR, as evidenced by detection of a specific band of the expected size (588 bp) (Figures 2A,B), and the sequencing results were correct. The CD2v-ex protein was purified from cell culture supernatant using HisTrap excel (Cytiva) in binding buffer (20 mM Tris-HCl,300 mM NaCl, pH 8.0) to purified it from cell culture supernatant. CD2v-ex was eluted from the column with the same binding buffer supplemented with 75 mM imidazole and SDS-PAGE confirmed the presence of the purified CD2v-ex protein (Figure 2C).

Determination of the CD2v-IELISA reaction conditions

To determine the optimal reaction conditions of CD2v-iELISA, we first identified the optimal coating antigen concentration and serum dilution factor by checkerboard titration, with the coating antigen concentration at 0.5–4 μg/mL and serum dilution at 1:10–1:320. The maximum positive/negative (P/N) value was obtained when the concentration of CD2v-ex protein was 2 μg/mL (200 ng/well) and the serum dilution was 1:160 (Table 1). Using the same criterion of the conditions that yield the maximum P/N value, the remaining reaction conditions were successfully optimized (Figures 3A–J) as described in Table 2. The cut-off value was determined using the optimal CD2v-iELISA method to analyze 82 ASFV^{-} serum samples. The mean OD_{450} value was 0.1017 and the SD was 0.0616 (Figure 3K), resulting in a cut-off value of 0.2865 (0.287, mean + 3 × SD). Therefore, only samples with OD_{450} values ≥0.287 were considered to be ASFV^{+}; all others were classified as ASFV^{-}. negative.

Determination of the CD2v-IELISA specificity, sensitivity, reproducibility, and compliance rate

To determine the CD2v-iELISA method specificity, we analyzed ASFV^{+}(CD2v^{-}), PRRSV^{+}, CSFV^{+}, PCV^{+}, PRV^{+}, FMDV^{+} and PEDV^{+} serum samples; ASFV^{+} was used as the positive control. All pathogen positive sera tested negative with the exception of the ASFV^{+} control (Figure 4A), indicating excellent assay specificity.

To determine the CD2v-iELISA sensitivity, we analyzed three clinical ASFV^{+} and three ASFV^{-} serum samples (diluted from 1:160 to 1:5,120) using the determined cut-off value. The highest dilution of the ASFV^{+} sample that was detected in the assay was 1:2,560 (Figure 4B), indicating an assay sensitivity up to 1:2,560.

The reproducibility of the CD2v-iELISA was determined based on intra- and inter-assay CV values calculated by analyzing eight randomly selected ASFV^{+} and/or ASFV^{-} serum samples in a single batch and three different batches,

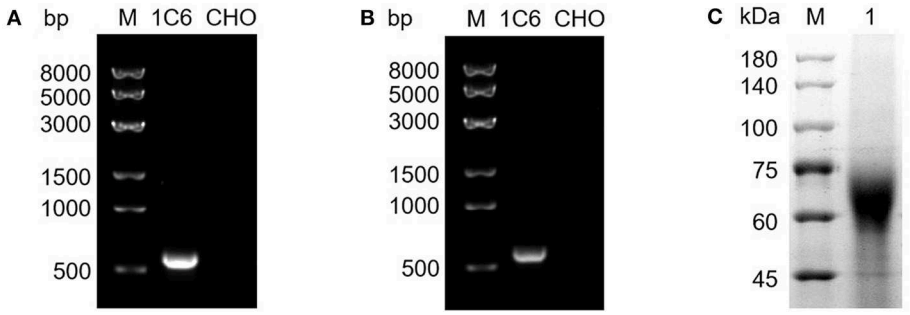

FIGURE 2
Genomic verification and protein purification of a high-expression CHO-CD2v cell line. The total genomic DNA and RNA of 1C6 cell line were extracted from the 1C6 cell line and the presence of the CD2v-ex at the genomic DNA and mRNA levels confirmed by PCR **(A)** and RT-PCR **(B)** analyses, respectively; blank CHO-S cells were treated as a negative control. SDS-PAGE analysis of purified CD2v-ex protein **(C)**.

TABLE 1 Determination of the optimal reaction conditions of the CD2v-iELISA.

Antigen concentration (μg/mL)		Serum dilution					
		1:10	1:20	1:40	1:80	1:160	1:320
4	P[a]	2.740	2.673	2.635	2.580	2.549	2.455
	N[a]	0.942	0.588	0.328	0.209	0.177	0.192
	P/N[b]	2.910	4.547	8.041	12.347	14.429	12.805
2	P	2.736	2.561	2.584	2.553	2.524	2.335
	N	1.119	0.666	0.346	0.167	0.113	0.119
	P/N	2.445	3.844	7.465	15.266	22.429	19.665
1	P	2.646	2.599	2.606	2.507	2.456	2.256
	N	1.220	0.729	0.307	0.213	0.140	0.145
	P/N	2.169	3.564	8.491	11.777	17.485	15.611
0.5	P	2.337	2.318	2.392	2.300	1.403	1.102
	N	1.282	0.775	0.401	0.222	0.144	0.137
	P/N	1.823	2.993	5.966	10.354	9.729	8.046

[a]Each data point represents the mean of two replicates. [b]P/N value data represent the ratios of positive mean value (P) to negative mean value (*N*).

respectively. As shown in Table 3, the intra- and inter-assay values were both <10%, suggesting a high repeatability and low variability.

To determine the CD2v-iELISA compliance, was analyzed ASFV$^+$ (n = 18), ASFV$^-$ (n = 112), and ASFV$^+$ (CD2v$^-$) (n = 49) serum samples. The assay showed 100% sensitivity and specificity in identification of ASFV$^+$ and ASFV$^+$ (CD2v$^-$) serum samples, and the total compliance rate was 99.4% (Figure 4C).

Discussion

ASFV was first reported in Kenya in 1921 (21) and reached Europe in the 1950s, where it persisted and became endemic (22–24). China was the first country in Asia to report the occurrence of ASF, which subsequently spread to 16 Asian countries including Korea, Japan, and Vietnam by 2021. Since 2005, ASF has been reported in 73 countries around the world according to the World Organization for Animal Health (OIE), resulting in huge economic losses to the pig industry. Laboratory assays are designed primarily to detect nucleic acids, antigens and antibodies. The ASFV detection tests recommended by the OIE include virus isolation, fluorescent antibody testing (FAT), and real-time and routine PCR testing, which is the most widely used technique at the EU National Reference Laboratory (NRL) level (25). Although the ELISA method is not as sensitive as PCR, it has important application value due to its ease of operation and potential for analysis of large-scale samples (26).

The CHO cell expression system is widely used in recombinant protein expression because of its ability to

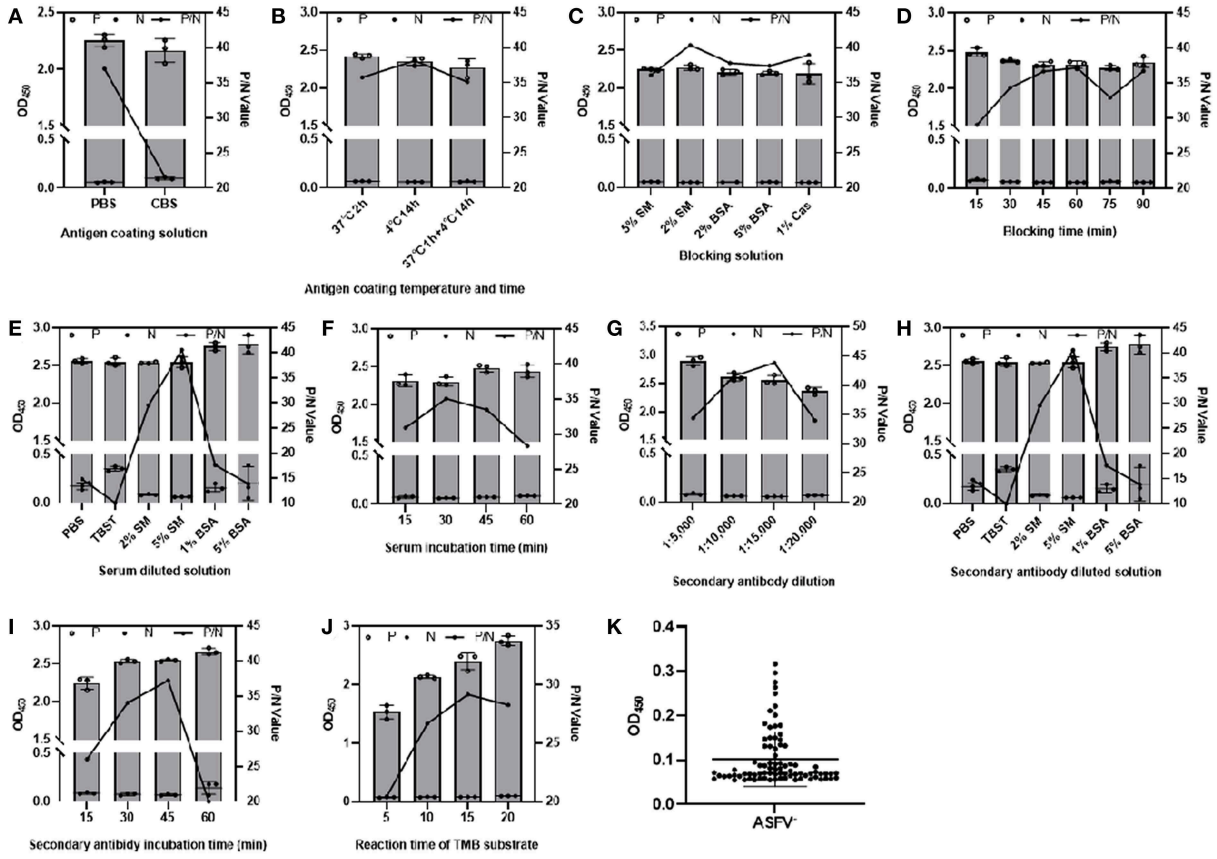

FIGURE 3
Optimization of CD2v-iELISA conditions. The CD2v-iELISA method was optimized by changing the following parameters: antigen coating solutions **(A)**, antigen coating temperature and time **(B)**, blocking solution **(C)**, blocking time **(D)**, serum dilution **(E)**, incubation time **(F)**; secondary antibody dilutions **(G)**, secondary antibody dilution factor **(H)**, secondary antibody incubation time **(I)**, TMB substrate incubation time **(J)**. P and N value data represent mean ± SD and P/N value data represent the ratios of positive mean value (P) to negative mean value (N). A total of 82 negative sera were analyzed to determine the cut-off value **(K)**.

TABLE 2 Optimized conditions of the CD2v-iELISA.

Reaction conditions	Evaluation options	Optimized results
Antigen coating solution	PBS (pH 7.2), CBS (pH 9.6)	PBS (pH 7.2)
Coating temperature and time	37°C 2 h, 4°C overnight, 37°C 1 h and then 4°C overnight	4°C overnight
Blocking solutions	2% SM, 5% SM, 2% BSA, 5% BSA, 1% casein (Cas)	2% SM
Blocking time	30, 45, 60, 75 and 90 min	60 min
Serum diluent	PBS, TBST, 2% SM, 5% SM, 1% BSA and 5% BSA	1% BSA
Serum incubation time	15, 30, 45 and 60 min	30 min
Secondary antibody dilution	PBS, TBST, 2% SM, 5% SM, 1% BSA and 5% BSA	5% SM
Secondary antibody dilution factor	1:5000, 1:10,000, 1:15,000 and 1:20,000	1:15,000
Secondary antibody incubation time	15, 30, 45 and 60 min	45 min
TMB substrate reaction time	5, 10, 15 and 20 min	15 min

SM was diluted in TBST (m/v), BSA and Cas was diluted in PBS (m/v), FBS was diluted in PBS (v/v).

maintain appropriate post-translational modifications, and glycosylation in particular (27). Furthermore, recombinant protein expression can be improved by integrating the target gene into the host genome to generate a stable cell line (28). CHO cells are used most widely used in mammalian expression systems involved in the production

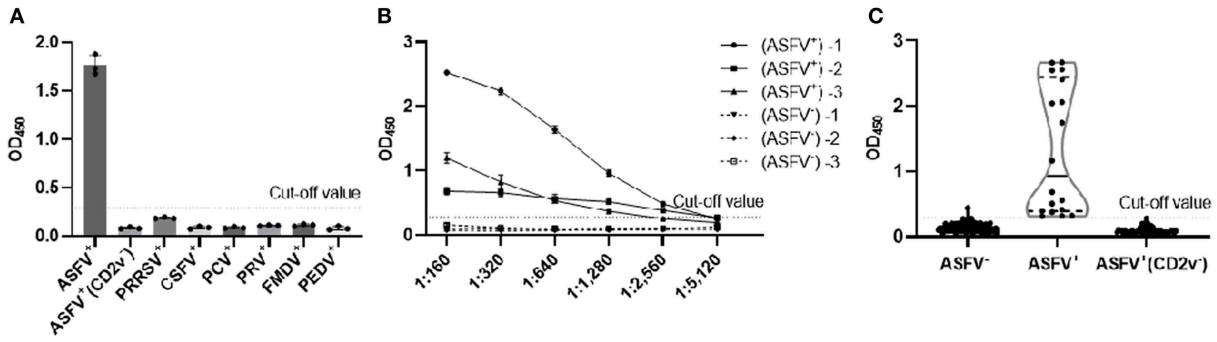

FIGURE 4
Determination of the specificity, sensitivity, and compliance rate of the CD2v-iELISA. The CD2v-iELISA did not detect ASFV$^+$(CD2V$^-$), PRRSV$^+$, CSFV$^+$, PCV$^+$, PRV$^+$, FMDV$^+$ and PEDV$^+$ serum samples at 1:160 dilution **(A)**. Three clinical ASFV$^+$ and three ASFV$^-$ serum samples were diluted from 1:160 to 1:5,120 to determine the highest dilution of serum detected in the assay according to the cut-off value **(B)**. The CD2v-iELISA was used to detect ASFV$^+$ ($n = 18$), ASFV$^-$ ($n = 112$), ASFV$^+$ (CD2v$^-$) ($n = 49$) serum samples to determine the assay compliance rate of the assay according to the cut-off value **(C)**.

TABLE 3 CD2v-ex-iELISA repeatability.

Sample number	Intra-assay repeatability		Inter-assay repeatability	
	Mean ± SD[a]	CV[b]	Mean ± SD[a]	CV[b]
1	0.686 ± 0.040	5.80	1.372 ± 0.023	1.67
2	0.876 ± 0.035	3.94	1.148 ± 0.041	3.56
3	1.865 ± 0.039	2.07	2.325 ± 0.068	2.91
4	0.089 ± 0.006	6.37	0.076 ± 0.004	5.20
5	0.087 ± 0.005	5.21	0.111 ± 0.009	8.38
6	0.183 ± 0.011	6.11	0.250 ± 0.021	8.29
7	0.076 ± 0.007	9.62	0.103 ± 0.009	8.89
8	0.103 ± 0.008	8.14	0.115 ± 0.010	9.00

[a]Each data point represents the mean of three replicates. [b]CV (coefficient of variation) = SD/Mean × 100%.

of >70% of recombinant biopharmaceutical proteins (29). After genetic modification and domestication, several modified CHO cell lines, such as CHO-K1, CHO-S, and CHO-DG44, have been modified to generate genetically stable systems for the production of a variety of different types of proteins (30). The CHO-S cell line was adapted to suspension culture and use in large-scale production of recombinant proteins.

Blocking ELISA (bELISA) and iELISA methods are used for the detection of ASFV-specific antibodies generated against important structural antigens such as protein 30 (p30), protein 54 (p54) and p72 (31, 32). Among the commercial ASFV ELISA kits currently available, the Ingenasa-bELISA is based on p72 (Ingenasa, Spain), while the IDvet-iELISA is based on protein 32 (p32), protein 62 (p62) and p72 (ID-vet, France), and the Svanovir-iELISA is based on p30 (Svanovir, Sweden).

With the prevalence of low-force ASFV CD2v mutants, a detection method that can be used to distinguish wild-type ASFV from CD2v-deleted strains of ASFV is urgently required for effective monitoring. In previous research, a specific quantum dot-based immunochromatographic assay was developed using CD2v as the diagnostic antigen to detect ASFV antibodies with a titer of $1{:}5.12 \times 10^5$ and a compliance rate of 85.92% (33). A triplex real-time PCR assay that was also successfully established to identify pigs infected with wild-type ASFV strains and an ASFV double-gene deletion strain (MGF360-505R and/or CD2v), was completely consistent with the OIE-recommended assay (34). In this study, the CD2v protein was truncated and the extracellular domain was selected for expression with a signal peptide without an intracellular cell-penetrating peptide (CPP), which not only retained the key domain involved in blood adsorption, but also improved protein secretion and expression (35). The CHO-CD2v stable cell line established in this study not only expressed a protein that was similar to the natural conformation, but also ensured stable and high-level expression of the protein of interest. Compared with transient transfection, this approach is significantly more cost-effective. The recombinant CD2v-ex protein was used as a coating antigen to establish and optimize the ASFV CD2v specific antibodies detection method, showing a pretty high concordance rate of 99.4 (178/179), and it was more applicable to the detection of large-scale samples than the PCR method.

In this study, we established an iELISA method using CD2v-ex protein as a coating protein for rapid, specific and sensitive diagnosis of ASFV CD2v antibodies. Compared with commercial ELISA kits coated with conserved ASFV

antigens (such as p30, p54, p72), this CD2v-iELISA provides a method for specific identification of ASFV wild-type and CD2v-deleted strain infections. Therefore, we propose that the application this CD2v-iELISA with the traditional ASFV detection method will have more effective diagnostic value because of its negative results of $ASFV^{+}(CD2v^{-})$ serum samples.

Data availability statement

The original contributions presented in the study are included in the article/supplementary material, further inquiries can be directed to the corresponding author/s.

Author contributions

WJ and DJ contributed to design and perform the majority of experiments. WJ draft the manuscript. LL and BW carried out the western blot and dot blot analysis. JW, PW, and XS was responsible for PCR and RT-PCR identifications. QZ, JS, and ZZ analyzed data. PJ contributed to revising the work critically for important intellectual content. PJ and ZZ provided approval for publication of the content and agreed to be accountable for all aspects of the work in ensuring that questions related to the accuracy or integrity of any part of the work are appropriately investigated and resolved. All authors read, contributed to, and approved the final manuscript.

Funding

This study was funded by the National Natural Science Foundation of China (grant number: 31941001) and the Key Scientific Research Project of Colleges and Universities of Henan Province (grant numbers: 22B230006 and 21A230010).

Acknowledgments

We thank Lanzhou Veterinary Research Institute, Chinese Academy of Agricultural Sciences for providing serum samples.

Conflict of interest

The authors declare that the research was conducted in the absence of any commercial or financial relationships that could be construed as a potential conflict of interest.

Publisher's note

References

1. Wang G, Xie M, Wu W, Chen Z. Structures and functional diversities of ASFV proteins. *Viruses.* (2021) 13:2014. doi: 10.3390/v13112124

2. Chen XL, Wang JH, Zhao W, Shi CW, Yang KD, Niu TM, et al. Lactobacillus plantarum surface-displayed ASFV (P54) with porcine IL-21 generally stimulates protective immune responses in mice. *AMB Express.* (2021) 11:114. doi: 10.1186/s13568-021-01275-9

3. Dixon LK, Chapman D, Netherton CL, Upton CJVR. African swine fever virus replication and genomics. *Virus Res.* (2013) 173:3–14. doi: 10.1016/j.virusres.2012.10.020

4. Yang J, Li S, Feng T, Zhang X, Yang F, Cao W, et al. African swine fever virus F317l protein inhibits NF-κB activation to evade host immune response and promote viral replication. *mSphere.* (2021) 6:e0065821. doi: 10.1128/mSphere.00658-21

5. Malogolovkin A, Burmakina G, Titov I, Sereda A, Gogin A, Baryshnikova E, et al. Comparative analysis of African swine fever virus genotypes and serogroups. *Emerg Infect Dis.* (2015) 21:312–5. doi: 10.3201/eid2102.140649

6. Gaudreault NN, Madden DW, Wilson WC, Trujillo JD, Richt JA. African swine fever virus: an emerging DNA arbovirus. *Front Vet Sci.* (2020) 7:215. doi: 10.3389/fvets.2020.00215

7. He Q, Yu D, Bao M, Korensky G, Chen J, Shin M, et al. High-throughput and all-solution phase African swine fever virus (ASFV) detection using CRISPR-Cas12a and fluorescence based point-of-care system. *Biosens Bioelectron.* (2020) 154:112068. doi: 10.1016/j.bios.2020.112068

8. Ge S, Li J, Fan X, Liu F, Li L, Wang Q, et al. Molecular characterization of African swine fever virus, China, 2018. *Emerg Infect Dis.* (2018) 24:2131–3. doi: 10.3201/eid2411.181274

9. Sun E, Zhang Z, Wang Z, He X, Zhang X, Wang L, et al. Emergence and prevalence of naturally occurring lower virulent African swine fever viruses in domestic pigs in China in 2020. *Sci China Life Sci.* (2021) 64:752–65. doi: 10.1007/s11427-021-1904-4

10. Wang N, Zhao D, Wang J, Zhang Y, Wang M, Gao Y, et al. Architecture of African swine fever virus and implications for viral assembly. *Science.* (2019) 366:640–4. doi: 10.1126/science.aaz1439

11. Dixon LK, Abrams CC, Bowick G, Goatley LC, Kay-Jackson PC, Chapman D, et al. African swine fever virus proteins involved in evading host defence systems. *Vet Immunol Immunopathol.* (2004) 100:117–34. doi: 10.1016/j.vetimm.2004.04.002

12. Goatley LC, Dixon LK. Processing and localization of the African swine fever virus CD2v transmembrane protein. *J Virol.* (2011) 85:3294–305. doi: 10.1128/JVI.01994-10

13. Borca MV, Kutish GF, Afonso CL, Irusta P, Carrillo C, Brun A, et al. An African swine fever virus gene with similarity to the T-lymphocyte surface antigen CD2 mediates hemadsorption. *Virology.* (1994) 199:463–8. doi: 10.1006/viro.1994.1146

14. Malogolovkin A, Burmakina G, Tulman ER, Delhon G, Diel DG, Salnikov N, et al. African swine fever virus CD2v and C-type lectin gene loci mediate serological specificity. *J Gen Virol.* (2015) 96:866–73. doi: 10.1099/jgv.0.000024

15. Broussau S, Jabbour N, Lachapelle G, Durocher Y, Tom R, Transfiguracion J, et al. Inducible packaging cells for large-scale production of lentiviral vectors in serum-free suspension culture. *Mol Ther.* (2008) 16:500–7. doi: 10.1038/sj.mt.6300383

16. Niu Y, Wang A, Zhou J, Liu H, Chen Y, Ding P, et al. Development of an indirect ELISA kit for rapid detection of varicella-zoster virus antibody by glycoprotein E. *Front Microbiol.* (2022) 13:897752. doi: 10.3389/fmicb.2022.897752

17. Yuan Y, Zong H, Bai J, Han L, Wang L, Zhang X, et al. Bioprocess development of a stable Fut8(-/-)-CHO cell line to produce defucosylated anti-HER2 antibody. *Bioprocess Biosyst Eng.* (2019) 42:1263–71. doi: 10.1007/s00449-019-02124-7

18. Zhong K, Zhu M, Yuan Q, Deng Z, Feng S, Liu D, et al. Development of an indirect ELISA to detect African swine fever virus pp62 protein-specific antibodies. *Front Vet Sci.* (2021) 8:798559. doi: 10.3389/fvets.2021.798559

19. Gao Z, Shao JJ, Zhang GL, Ge SD, Chang YY, Xiao L, et al. Development of an indirect ELISA to specifically detect antibodies against African swine fever virus: bioinformatics approaches. *Virol J.* (2021) 18:97. doi: 10.1186/s12985-021-01568-2

20. Li JG, Chen C, Liu-Chen LYJB. N-Glycosylation of the human kappa opioid receptor enhances its stability but slows its trafficking along the biosynthesis pathway. *Biochemistry.* (2007) 46:10960–70. doi: 10.1021/bi700443j

21. Montgomery ER. On a form of swine fever occurring in British East Africa (Kenya Colony). *J Comp Pathol Ther.* (1921) 34:159–91. doi: 10.1016/S0368-1742(21)80031-4

22. Galindo I, Alonso C. African swine fever virus: a review. *Viruses.* (2017) 9:103. doi: 10.3390/v9050103

23. Sanchez-Cordon PJ, Montoya M, Reis AL, Dixon LK. African swine fever: a re-emerging viral disease threatening the global pig industry. *Vet J.* (2018) 233:41–8. doi: 10.1016/j.tvjl.2017.12.025

24. Sánchez-Vizcaíno JM, Mur L, Martínez-López B. African swine fever (ASF): five years around Europe. *Vet Microbiol.* (2013) 165:45–50. doi: 10.1016/j.vetmic.2012.11.030

25. Gallardo C, Nieto R, Soler A, Pelayo V, Fernandez-Pinero J, Markowska-Daniel I, et al. Assessment of African swine fever diagnostic techniques as a response to the epidemic outbreaks in eastern European union countries: how to improve surveillance and control programs. *J Clin Microbiol.* (2015) 53:2555–65. doi: 10.1128/Jcm.00857-15

26. Oura C, Edwards L, Batten CA. Virological diagnosis of African swine fever–comparative study of available tests. *Virus Res.* (2013) 173:150–8. doi: 10.1016/j.virusres.2012.10.022

27. Tihanyi B, Nyitray L. Recent advances in CHO cell line development for recombinant protein production. *Drug discov today Techno.* (2020) 38:25–34. doi: 10.1016/j.ddtec.2021.02.003

28. Kim JY, Kim YG, Lee GM, CHO. cells in biotechnology for production of pecombinant proteins: current state and further potential. *Appl Microbiol Biotechnol.* (2012) 93:917–30. doi: 10.1007/s00253-011-3758-5

29. Walsh G. Biopharmaceutical benchmarks 2014. *Nat Biotechnol.* (2014) 32:992–1000. doi: 10.1038/nbt.3040

30. Lalonde ME, Durocher Y. Therapeutic glycoprotein production in mammalian cells. *J biotechno.* (2017) 251:128–40. doi: 10.1016/j.jbiotec.2017.04.028

31. Gimenez-Lirola LG, Mur L, Rivera B, Mogler M, Sun Y, Lizano S, et al. Detection of African swine fever virus antibodies in serum and oral fluid specimens using a recombinant protein 30 (p30) dual matrix indirect ELISA. *PLoS One.* (2016) 11:e0161230. doi: 10.1371/journal.pone.0161230

32. Yuan F, Petrovan V, Gimenez-Lirola LG, Zimmerman JJ, Rowland RRR, Fang Y. Development of a blocking enzyme-linked immunosorbent assay for detection of antibodies against African swine fever virus. *Pathogens.* (2021) 10:10060760. doi: 10.3390/pathogens10060760

33. Niu Y, Zhang G, Zhou J, Liu H, Chen Y, Ding P, et al. Differential diagnosis of the infection caused by wild-type or CD2v-deleted ASFV strains by quantum dots-based immunochromatographic assay. *Lett Appl Microbiol.* (2022) 74:1001–7. doi: 10.1111/lam.13691

34. Lin Y, Cao C, Shi W, Huang C, Zeng S, Sun J, et al. Development of a triplex real-time PCR assay for detection and differentiation of gene-deleted and wild-type African swine fever virus. *J Virol Methods.* (2020) 280:113875. doi: 10.1016/j.jviromet.2020.113875

35. Yang S, Zhang X, Cao Y, Li S, Shao J, Sun S, et al. Identification of a new cell-penetrating peptide derived from the African swine fever virus CD2v protein. *Drug Deliv.* (2021) 28:957–62. doi: 10.1080/10717544.2021.1909178

frontiers | Frontiers in Veterinary Science

TYPE Original Research
PUBLISHED 08 September 2022
DOI 10.3389/fvets.2022.978398

OPEN ACCESS

EDITED BY
Yongtao Li,
Henan Agricultural University, China

REVIEWED BY
Elisabetta Razzuoli,
Experimental Zooprophylactic Institute for Piedmont, Liguria and Valle d'Aosta (IZSTO), Italy
Jean Nepomuscene Hakizimana,
Sokoine University of Agriculture, Tanzania
Ilya Titov,
Federal Research Center of Virology and Microbiology, Russia

*CORRESPONDENCE
Bumseok Kim
bskims@jbnu.ac.kr
Sang-Ik Oh
ohsangik@korea.kr
Hu Suk Lee
h.s.lee@cgiar.org

†These authors have contributed equally to this work

SPECIALTY SECTION
This article was submitted to Veterinary Experimental and Diagnostic Pathology, a section of the journal Frontiers in Veterinary Science

RECEIVED 26 June 2022
ACCEPTED 01 August 2022
PUBLISHED 08 September 2022

CITATION
Oh S-I, Nguyen TTH, Yang M-S, Nga BTT, Bui VN, Le VP, Yi S-W, Kim E, Hur T-Y, Lee HS and Kim B (2022) Blood parameters and pathological lesions in pigs experimentally infected with Vietnam's first isolated African swine fever virus.
Front. Vet. Sci. 9:978398.
doi: 10.3389/fvets.2022.978398

Blood parameters and pathological lesions in pigs experimentally infected with Vietnam's first isolated African swine fever virus

Sang-Ik Oh[1,2*†], Thi Thu Huyen Nguyen[3,4†], Myeon-Sik Yang[2†], Bui Thi To Nga[4], Vuong Nghia Bui[5], Van Phan Le[4], Seung-Won Yi[1], Eunju Kim[1], Tai-Young Hur[1], Hu Suk Lee[6,7*] and Bumseok Kim[2*]

[1]National Institute of Animal Science, Rural Development Administration, Wanju, South Korea, [2]College of Veterinary Medicine, Jeonbuk National University, Iksan, South Korea, [3]Bac Giang Agriculture and Forestry University, Hanoi, Vietnam, [4]College of Veterinary Medicine, Vietnam National University of Agriculture, Hanoi, Vietnam, [5]Virology Department, National Institute of Veterinary Research, Hanoi, Vietnam, [6]International Livestock Research Institute, Hanoi, Vietnam, [7]College of Veterinary Medicine, Chungnam National University, Daejeon, South Korea

African swine fever virus (ASFV) is a notable virus and one of the most serious global threats to the pig industry. Improving awareness about host–virus interactions could facilitate the understanding of the disease pathogenesis. Therefore, we investigated changes in blood parameters, viral loads, and pathological changes in ASFV-inoculated pigs according to the time of death after the onset of viremia. For the analyses, the ASFV-infected pigs ($n = 10$) were divided into two groups (five pigs/group) according to their time of death after the onset of viremia. The blood cell count dynamics and serum biochemistry profiles were similar between the groups; however, viral load distribution was different. A comparison of the histopathological changes and immunohistochemistry results between the two groups indicated that the lymphoid system, particularly the spleen, was more damaged in the early stage of the disease than in the last stage. Additionally, the virus-induced lesions in other organs (liver and kidney) were more severe in the late stage than in the early stage. Our findings provide invaluable information on the characteristics of blood parameters and pathological lesions in pigs infected with the Asia-epidemic ASFV strain and the course of ASF, targeting internal organs in pigs. Overall, this study characterizes the host-pathogen interaction in ASFV infection, offering insight for the establishment of ASF control strategies.

KEYWORDS

African swine fever virus, pathology, blood count, biochemical parameter, histopathology, viral load, pathobiology

Introduction

African swine fever (ASF) is a serious infectious disease in domestic pigs caused by the African swine fever virus (ASFV), which has a fatality rate approaching 100%. ASFV is a large, double-stranded DNA virus (170–193 kbp) that belongs to the *Asfivirus* genus of the family *Asfarviridae* (1, 2). To date, eight ASFV serotypes have been established based on the viral hemagglutinin CD2-like protein (CD2v) and C-type lectin 24 genotypes with different levels of virulence are known (2, 3). In 2007, genotype II ASFV was introduced into Georgia, which spread to neighboring European countries, finally reaching China in August 2018; the first outbreak of ASF in East and South-East Asia was reported in Liaoning (4). In February 2019, ASFV (VUNA/HY/Vietnam) was detected in a backyard pig farm in northern Vietnam, located ∼250 km from the Chinese border (5). This Asian strain has the characteristics of the intergenic region II variant of genotype II, with an additional tandem-repeat sequence (5′-GGAATATATA-3′) between the 173R and 1329L genes (6–8).

Since no treatment is available for ASF, several studies have attempted to develop ASF vaccines (9–11). However, currently, there are no commercially available vaccines to prevent ASF in pigs (12, 13). Therefore, the control of ASF outbreaks depends on rapid and accurate diagnosis by veterinarians and monitoring of healthy pigs (14). ASFV-infected pigs usually develop viremia at 4–8 days post-inoculation (dpi). Considering the absence of fully neutralizing antibodies, viremia could persist for weeks or months (15). The lymph node macrophages and monocytes nearest the point of entry are the primary cells for ASFV replication (15, 16). The replicated virus spreads through the blood and lymphatic system to all organs, including the spleen, other lymph nodes, tonsils, lungs, liver, and kidneys (15). Subsequently, ASFV-infected domestic pigs develop severe clinical signs (e.g., fever, cough, difficulty breathing, decreased appetite, and hemorrhagic skin, and finally die within 7–13 days, with various histopathological features, including splenomegaly, hemorrhagic lymph nodes, severe pulmonary edema, and petechial hemorrhage in the kidneys (17, 18).

Understanding ASF pathogenesis may help predict the course of the disease, laying the groundwork for developing vaccines and therapies (15). Understanding pathology is crucial for understanding pathogenesis and may complement other approaches to better understand host–virus interactions (17). Pathological lesions and clinical signs in ASFV-infected pigs vary depending on the virulence of the virus strains, host characteristics, dose, and route of infection (19). Several studies have reported the clinical signs, pathological changes, and blood parameters in pigs experimentally infected with European strains of ASFV (20–22). However, there have been few pathophysiological studies on the comprehensive changes in pigs which inoculated with the Asian-epidemic strain (4). In Vietnam, some studies and case reports on the molecular profile, pathogenicity, transmission, and pathology of ASF have been published (8, 23–25), including our study that showed that the VUNA/HY/Vietnam strain in the peracute/acute phase led to the death of pigs at 7.0 ± 1.2 dpi, with a short incubation time (3.7 ± 0.5 dpi) (24). However, these results are insufficient to understand the host–virus interactions of the Vietnamese strain.

To better understand these host–virus interactions, we investigated changes in the blood parameters, viral loads, and pathological lesions in pigs experimentally infected with the VUNA/HY/Vietnam ASFV strain, which were grouped according to the time of death after the onset of viremia. The findings provide invaluable information on the biochemical parameters and pathological lesions in pigs experimentally infected with the Asian ASFV strain (peracute to acute form) and thus will help determine the course of ASF in the internal organs of domestic pigs.

Materials and methods

Virus strain

In this study, domestic pigs were experimentally infected with ASFV, VNUA/HY/Vietnam strain (GenBank accession number: MK554698). The virus was isolated from the spleens of naturally infected pigs during the first outbreak in Hung Yen Province, north of Hanoi, Vietnam, in February 2019 (5). The virus was propagated in porcine alveolar macrophages using Dulbecco's modified Eagle's medium supplemented with 5% fetal bovine serum and stored at −80°C. A hemadsorption assay was used to titrate the virus, as previously described (26). The isolated virus was added to 96-well plates containing primary porcine alveolar cells in triplicate. Ten-fold serial dilutions were performed. The 50% hemadsorbing dose per milliliter (HAD_{50}/ml) was calculated for 7 dpi. Virus titers were calculated using the method described by Reed and Muench (27).

Experimental design

We used 15 healthy 7–8-week-old pigs (Yorkshire × Landrace × Duroc) obtained from two sows in the same herd at a commercial pig farm. All pigs were confirmed to be seronegative for the endemic pathogens in pigs from Vietnam: ASFV, porcine circovirus 2, foot-and-mouth disease, classical swine fever virus, and porcine reproductive and respiratory

Abbreviations: ASFV, African swine fever virus; ASF, African swine fever; dpi, days post-inoculation; dpv, days post-viremia; HAD_{50}/ml, 50% hemadsorbing dose per milliliter; EDTA, ethylene diamine tetra-acetic acid; WBCs, white blood cells; RBCs, red blood cells; AST, aspartate aminotransferase; ALT, alanine aminotransferase.

syndrome virus. All pigs were carefully monitored daily for seven days before ASFV inoculation. The detailed experimental procedure has been described previously (24). Ten pigs were intramuscularly inoculated with 1 ml of ASFV at a titer of $10^{3.5}$ HAD_{50}/ml per pig (ASFV-infected group), and five pigs were not inoculated (negative control group). The ASFV-infected group was assigned to an animal biosafety level 2 facility at the National Institute of Veterinary Research, Hanoi, Vietnam. The study was conducted according to the guidelines of the National Institute of Veterinary Research, Vietnam, and approved by the Institutional Animal Care and Use Committee of the National Institute of Animal Science, Republic of Korea (approval number: NIAS 2020-463). Whole blood was collected daily from the 10 ASFV-infected pigs after experimental inoculation with ASFV. DNA was extracted, and the presence of ASFV was assessed using a VDx ASFV qPCR kit (Median Diagnostics, Chuncheon, Korea) following the manufacturer's instructions. The onset of viremia in each pig was determined as the day when the cycle threshold value of the collected blood sample was <40. ASFV-infected pigs were divided into two groups according to the time of natural death after the onset of viremia. Group I contained five pigs that died 2–5 days post-viremia (dpv), and Group II comprised five additional pigs that died at 6–7 dpv.

Blood count analysis

Blood samples were collected daily from the jugular vein of each pig before feeding in the morning. Blood samples were placed into BD Vacutainer K2 ethylene diamine tetra-acetic acid (EDTA) tubes (BD Biosciences, Franklin Lakes, NJ, USA) containing 2 ml anticoagulant solution (EDTA). An automated hematology analyzer (Mindray BC-2800 Vet; Mindray Bio-Medical Electronics Co., Ltd., Shenzhen, China) was used to perform a complete blood cell count [white blood cells (WBCs), red blood cells (RBCs), hemoglobin levels, and platelet counts] (22). Results were compared to the calibrated Mindray references for pigs.

Serum and biochemical parameters

Blood samples were collected daily from the jugular vein of each pig before feeding in the morning and placed in plain (5 ml) BD Vacutainer tubes (BD Biosciences, Franklin Lakes, NJ, USA). Serum was separated by centrifugation at 1,800 $\times$ *g* for 10 min and stored at −20°C. Biochemical analyses were performed using a semi-automatic biochemical analyzer (Mindray BA-88A; Mindray, Shenzhen, China). Measurements of aspartate aminotransferase (AST), alanine aminotransferase (ALT), creatinine, and urea were used to diagnose organ damage, especially to the liver and kidneys. All procedures for the analysis of biochemical parameters were performed at the Viet Pet Clinic in Hanoi, Vietnam.

Gross pathology and tissue collection

Complete necropsies were performed on all pigs according to the standardized macroscopic lesion guidelines for ASFV infection in pigs (28). Gross lesions were observed in ten organs, including the spleen; submandibular, mesenteric, and inguinal lymph nodes; liver, lungs, kidneys, tonsils, heart, and colon. During necropsy, tissue samples of the ten organs were collected from four pigs according to their time of death [Group I ($n = 2$, died at 3–4 dpv); Group II ($n = 2$, died at 6–7 dpv)].

Viremia and viral gene (p72) detection in tissue samples

To detect viremia, DNA was extracted from whole blood using a nucleic acid extraction kit (DNeasy Blood & Tissue Kit; Qiagen, Hilden, Germany). A total of 100 tissue samples (~1 g each) from ten necropsied pigs were homogenized in 3 ml of sterile phosphate-buffered saline. DNA was extracted from 100 µl aliquots of each homogenized tissue sample according to manufacturer instructions (DNA Mini Kit; Qiagen, Hilden, Germany). The extracted DNA was analyzed for the presence of ASFV DNA using a VDx ASFV qPCR kit (Median Diagnostics). Briefly, 5 µl DNA was placed in a tube containing 10 µl 2× master mix and 5 µl 4× oligo mix. A quantitative polymerase chain reaction was performed using the IQ5 Multicolor Real-Time PCR Detection System (Bio-Rad Laboratories Ltd., Hercules, CA, USA). The reaction conditions used have been described previously (24). Blood samples with a cycle threshold value of <40 were considered positive for ASFV. Copy numbers were calculated based on the standard samples provided by the manufacturer.

Histopathology and immunohistochemistry

Tissue samples (spleen; submandibular, mesenteric, and inguinal lymph nodes; liver; lungs; kidneys; tonsils; heart; and colon) were collected from four pigs (#54, #48, #60, and #43) among the experimental 10 pigs and immersed in 10% neutral buffered formalin. Pigs #54 and #48 were included in Group I, and pigs #60 and #43 were in Group II. Representative sections of each tissue sample were cut and embedded in paraffin. Paraffin-embedded tissues were sectioned at a thickness of 3–4 µm and then subjected to hematoxylin and eosin staining for histopathological examination. Histopathological changes were categorized according to the protocols of Galindo-Cardiel

et al. (28) and Sehl et al. (21), as follows: normal (0), mild (1), moderate (2), and severe (3).

For ASFV immunohistochemistry, a monoclonal antibody against the p72 major capsid protein (clone 1BC11; Ingensa, Madrid, Spain) was used as the primary antibody. The Simple Stain MAX PO method with Histofine Simple Stain MAX PO (MULTI; Nichirei Biosciences, Tokyo, Japan) was used as the secondary antibody. Briefly, tissue sections were deparaffinized and immersed in 3% hydrogen peroxide and methanol to block endogenous peroxidase. The tissue sections were rinsed with Tris-buffered saline containing 5% Tween 20 (TBS-T) before antigen retrieval by heating the slides in citrate buffer (pH 6.0; 0.05% Tween 20) at 120°C for 10 min. The tissue sections were incubated with 10% normal goat serum at 25°C for 15 min prior to primary antibody incubation overnight at 4°C. The primary antibody was diluted 1:300 in TBS containing 1% bovine serum albumin. As negative controls, duplicate sections were incubated with 1% bovine serum albumin in TBS instead of the primary antibody. The tissue sections were thoroughly rinsed with TBS-T and incubated with the secondary antibody, Universal Immuno-enzyme Polymer (Simple Stain MAX PO), for 30 min. After rinsing the tissue sections with TBS-T, 3,3′-diaminobenzidine (Dako, Tokyo, Japan) was used as the chromogen. Finally, the tissue sections were rinsed with tap water and counterstained with Mayer's hematoxylin. ASFV antigen detection using the immunohistochemical method was scored according to the proportion of positively stained mononuclear cells or macrophages in three fields under ×400 magnification, as follows: no positive cells (0), 1–10 positive cells (1), 11–20 positive cells (2), 21–30 positive cells (3), 31–40 positive cells (4), and ≥ 41 positive cells (5).

Statistical analyses

All statistical analyses were conducted using SPSS (version 26.0; IBM Corp., Armonk, NY, USA). Biochemical parameters and mean viral copies in blood for Group I, Group II, and the negative control group were analyzed using one-way analysis of variance and Duncan's test. The viral load in the 10 collected tissue samples was analyzed by Student's *t*-test between Groups I and II. A p-value < 0.05 was considered statistically significant.

Results

Viral detection in blood

A rapid increase in virus titers was observed in both groups of ASFV-infected pigs (Figure 1). Notably, Group I (died at 2–5 dpv) pigs had an ~10^3-fold higher copy number of the ASFV than Group II (died at 6–7 dpv) pigs ($8.5 \times 10^5 \pm 8.2 \times 10^5$ vs. $7.0 \times 10^2 \pm 6.5 \times 10^2$ copies/μl, respectively; $p = 0.336$). Virus titers markedly increased 1 day after the onset of viremia. Pigs started dying when the copy number exceeded 4.3×10^6 copies/μl in Group I and 6.0×10^6 copies/μl in Group II. The mean viral load in the blood of dead pigs in Group I was significantly higher than that in the blood of dead pigs in Group II at 1 dpv ($p = 0.011$), 2 dpv ($p = 0.032$), and 3 dpv ($p = 0.021$). The mean ASFV copy number dramatically increased between 0 ($8.5 \times 10^8 \pm 6.9 \times 10^8$ copies/μl) and 1 dpv ($3.3 \times 10^6 \pm 5.2 \times 10^8$ copies/μl) in Group I, and between 0 dpv ($6.9 \times 10^2 \pm 6.5 \times 10^2$ copies/μl) and 2 dpv ($2.3 \times 10^6 \pm 7.5 \times 10^8$ copies/μl) in Group II. The viral load subsequently increased until all pigs died [Group I: 5 dpv (1.1×10^7 copies/μl); Group II: 6 dpv ($1.1 \times 10^7 \pm 2.4 \times 10^6$ copies/μl)]. The detailed results of the viral detection in blood samples from each pig are shown in Supplementary Table 1.

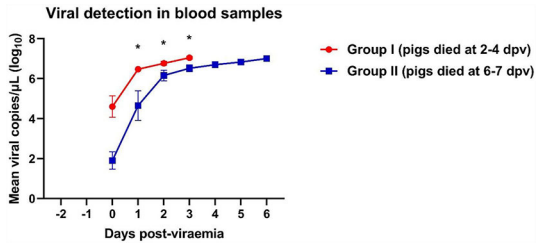

FIGURE 1
Viral load in pigs experimentally infected with African swine fever virus. Mean viral copy number per microliter in two groups divided by the number of days between the onset of viremia and death. *$p < 0.05$. dpv, days post-viremia.

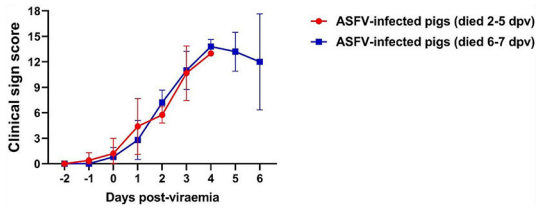

FIGURE 2
Clinical sign scores in two groups. The red line (Group I) represents the pigs that died at 2–5 days post-viremia (dpv), and the blue line (Group II) represents the pigs that died at 6–7 dpv.

Clinical sign score

The clinical signs exhibited by each pig were scored according to a method described in our previous study (24). The average onset time of clinical symptoms (over 3 scores) was 1.4 ± 0.6 dpv (Group I: 1.2 ± 0.7 dpv; Group II: 1.6 ± 0.5 dpv). The dynamics of the clinical sign scores in both groups were similar (Figure 2).

Blood counts

White blood cell (WBC) counts varied according to the stage of ASFV infection. WBC counts rapidly increased at 0–1 dpv in both ASFV-infected groups and sharply declined at 2–4 dpv in Group I and 4–6 dpv in Group II (Figure 3). Leukocytosis occurred mainly during the first few days after the onset of viremia in eight ASFV-infected pigs [Group I (4/5) and Group II (4/5)]. Leukocytopenia was observed during the last few days of life in one pig in Group I; however, a tendency toward leucopenia was notable in Groups I and II. The WBC count in Group II was significantly higher than that in the control group at 4 dpv ($p = 0.040$) and 5 dpv ($p = 0.001$). Erythrocytopenia was observed during the last few days of life in five pigs [Group I (4/5) and Group II (2/5)]. The lowest number of red blood cells (RBCs) was detected in pig #40 in Group I (3.1×10^{12} RBCs/L on the last day of life), which also presented with erythrocytopenia one day before death (3.6×10^{12} RBCs/L). A significant decrease in RBC count was recorded at 3 dpv ($p < 0.001$) in Group I and at 4 dpv ($p < 0.001$), 5 dpv ($p = 0.037$), and 6 dpv ($p = 0.035$) in Group II, compared with the control group. A strong tendency toward reduction in hemoglobin levels was identified. Four pigs [Group I (2/5) and Group II (2/5)] developed anemia during the last few days of life. There was a significant difference between Group II and the control group at 4 dpv ($p = 0.020$). The analysis performed 6 days after the onset of viremia showed a marked tendency toward decreased platelet count in the two ASFV-infected groups compared with that in the control group. Only two pigs presented thrombocytopenia before they died [Group I (1/5) and Group II (1/5)]. The platelet count was significantly lower in Group I than in the control group at 1 dpv ($p < 0.001$), 2 dpv ($p < 0.001$), and 3 dpv ($p = 0.003$), and in Group II than in the control group at 2 dpv ($p < 0.001$), 3 dpv ($p = 0.003$), 5 ($p = 0.018$), and 6 dpv ($p = 0.048$).

Biochemical parameters

Although the ALT levels of all ASFV-infected pigs were included in the reference range, ALT levels gradually increased after 2 dpv (Figure 4). ALT levels in Group I pigs significantly differed from those in Group II and control pigs. A different pattern was observed in the levels of AST. AST levels peaked shortly after the onset of viremia (1 and 2 dpv in Groups I and II, respectively), followed by a reduction (below the reference range) during the last few days of life [Group I (2/5) and Group II (5/5)]. AST levels were significantly lower in Group II than in the control group at 5 dpv ($p < 0.001$) and 6 dpv ($p = 0.008$). The ALT/AST ratio dramatically increased in both ASFV-infected groups at 2 dpv. ALT/AST ratios in the ASFV-infected groups were significantly higher than that in the control group at 4 dpv ($p = 0.013$) and 5 dpv ($p = 0.040$).

A strong tendency toward increased creatinine levels was observed in Group II pigs during the last few days of life. The creatinine levels in Group I were significantly higher than those in Group II and the control group at 3 dpv ($p = 0.029$). The creatinine levels in Group II were significantly higher than those in the control group at 5 dpv ($p = 0.008$) and 6 dpv ($p < 0.001$). High urea levels (above the reference range) were observed in Group I pigs on the last day of life. Although urea levels were included in the reference range, they tended to increase in ASFV-infected pigs after the onset of viremia.

Gross lesions

Post-mortem examinations were performed on all pigs according to a previous study (26). ASFV-infected pigs had hemorrhagic lymphadenitis in the submandibular, mesenteric, and inguinal lymph nodes (Table 1). Although splenomegaly was common in both ASFV-infected groups, Group I pigs had more severe lesions (necrosis and hemorrhage) in the spleen than Group II pigs, whereas more macroscopic lesions were observed in the various organs of Group II pigs than in the tissues of Group I pigs: pericardial fluid [Group I (2/5) and Group II (5/5)], severe pneumonia [Group II only (1/5)], petechial hemorrhages in the kidneys [Group II only (1/5)], and hemorrhage in the colon [Group I (1/5) and Group II (2/5)].

Organ viral loads

ASFV DNA was detected in all 10 organs evaluated in ASFV-infected pigs (Figure 5). In the spleen, the mean viral load was significantly higher in Group I pigs than in Group II pigs ($9.6 \times 10^5 \pm 1.3 \times 10^5$ *vs.* $3.4 \times 10^5 \pm 9.0 \times 10^4$ copies/μl, respectively; $p = 0.013$). Moreover, the mean viral load in the spleen tended to decrease from the early to the late stage of infection (death at 2, 3, 4, 5, 6, and 7 dpv: 1.4×10^6, 1.3×10^6, 7.2×10^5, 6.7×10^5, 3.7×10^5, and 3.1×10^5 copies/μl, respectively). Detailed information for each pig regarding the onset of viral detection in blood and time of death is shown in Supplementary Table 1. The mean viral load in submandibular and mesenteric lymph nodes, lung, and tonsil exhibited minimal difference between the two groups. Although the mean values from the inguinal lymph node, liver, kidney, heart, and colon between pigs from Group I and II were different, which could have been caused by one or two pigs having particularly high virus titers, the median values of viral titer in the spleen, mesenteric lymph node, and tonsil were higher in Group I than in II, whereas those in the lung were higher in Group II than in Group I. Overall, according to the analyses based on median viral titer values, there were no differences between the two groups.

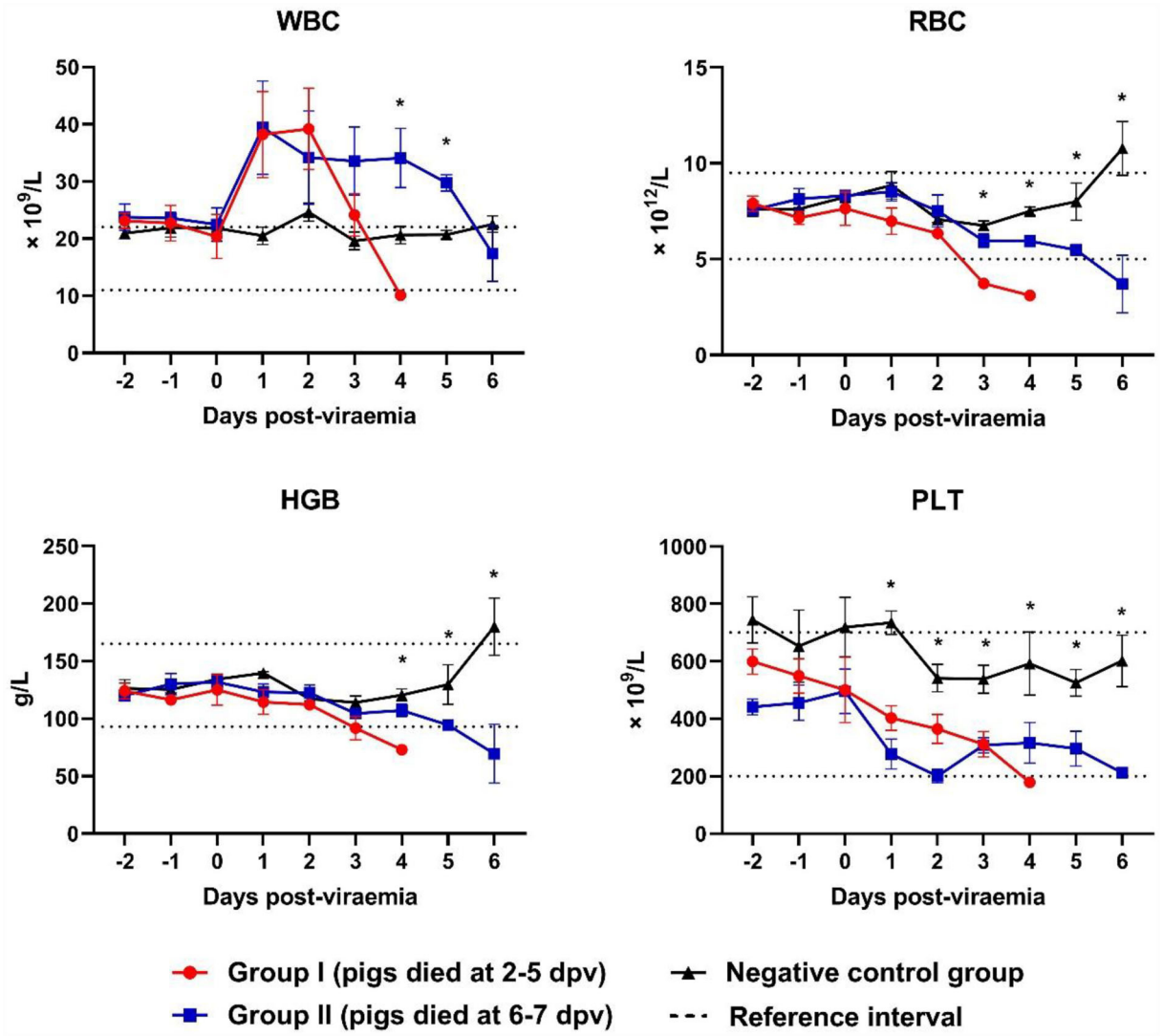

FIGURE 3
Blood counts during infection. *$p < 0.05$. WBC, white blood cell, RBC, red blood cell; HGB, hemoglobin; PLT, platelet. The reference intervals of each blood parameter are represented as dotted lines.

Histopathology

Hematoxylin and eosin-stained spleen; submandibular, mesenteric, and inguinal lymph node; liver, lung, kidney, tonsil, heart, and colon sections from four ASFV-infected pigs [Group I (#54 and #48) and Group II (#60 and #43)] were examined and scored semi-quantitatively based on previous reports (21, 28). Supplementary Table 2 presents the histopathological lesion scores for the four pigs. Figure 6 presents the histopathological findings of various tissues in the ASFV-infected pigs in this study.

Mild-to-severe vascular damage was observed in the spleen of all necropsied pigs. In Group I pigs, moderate lymphocytolytic lesions were present; however, in Group II pigs, the lesions were mild. Lymphoid depletion was moderate-to-severe in Group I, whereas it was mild-to-moderate in Group II pigs. Necrosis of lymphocytes was moderate-to-severe in Group I pigs and mild in Group II pigs.

Moderate-to-severe vascular congestion was also observed in the submandibular lymph nodes of Group I pigs, whereas mild congestion was observed in Group II pigs. Lymphocyte apoptosis (lymphocytolysis) was detected in the lymphoid follicles of one pig in Group I (#54) that died soon after the onset of viremia. Mild-to-moderate necrosis of endothelial cells was detected in Group I pigs, whereas severe necrotic lesions were observed in Group II pigs.

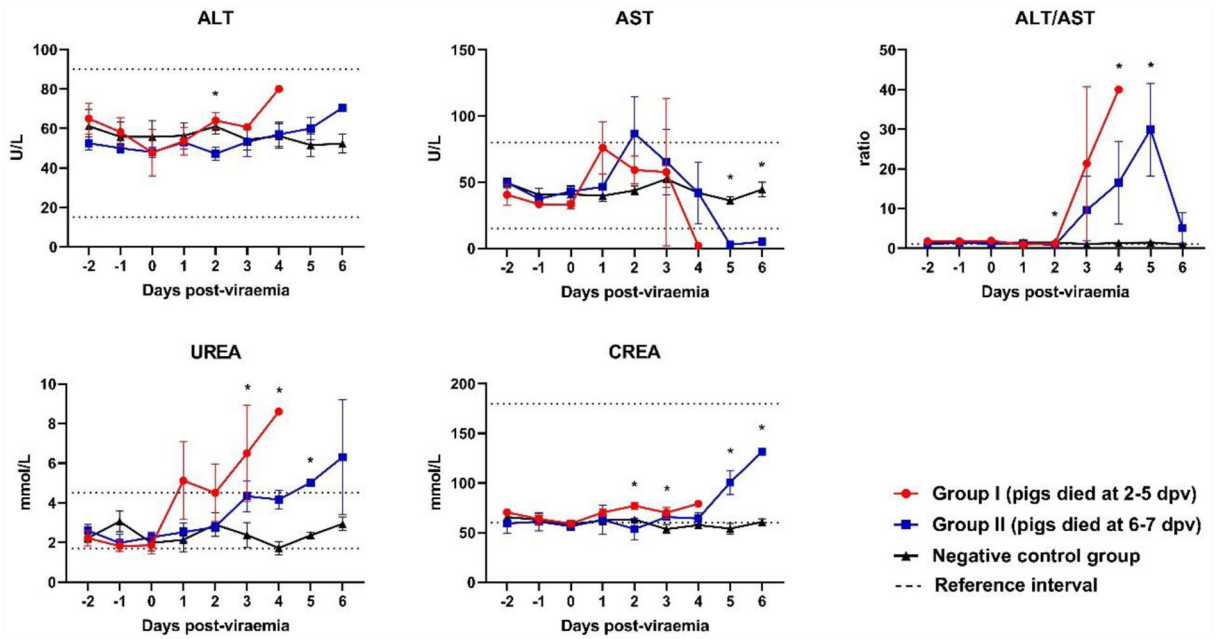

FIGURE 4
Biochemical parameters of the liver and kidneys. *$p < 0.05$. ALT, alanine aminotransferase; AST, aspartate aminotransferase; CREA, creatinine; UREA, urea. The reference intervals of each blood parameter are represented as dotted lines.

In the liver, diffuse congestion and hemorrhage were observed in one pig in Group I (#48) and both pigs in Group II (#60 and #43). In pig #54, which died at 3 dpv, mild congestion and hemorrhage were observed in the absence of hepatocyte necrosis. Histopathology showed lymphoid infiltrates, mainly in the hepatic sinus. The extent of the lesion gradually increased from mild (pig #54, which died at 3 dpv) to severe (pig #43, which died 7 at dpv).

Histopathological analysis of the lungs showed moderate-to-severe pulmonary congestion in all necropsied pigs in this study. Hemorrhagic lesions were observed in one pig in each of the two groups (#54 and #60, respectively). These pigs also exhibited moderate-to-severe pulmonary edema and interstitial lung inflammation. Mild alveolar edema and interstitial pneumonia were detected in pigs without lung hemorrhagic lesions (#48 and #43).

Hemorrhagic lesions were observed in only one pig by examining gross renal lesions. However, histopathological examination detected mild-to-severe kidney vasculopathy in all ASFV-infected pigs. Group II pigs also had moderate-to-severe interstitial nephritis, which was not observed in Group I pigs. Accordingly, the mean total histopathological score in Group II was considerably higher than that in Group I (8.0 vs. 3.5, respectively).

Immunohistochemistry

The immunohistochemical analysis detected numerous p72-positive cells in the spleens of three pigs that died at 3 dpv (#54), 4 dpv (#48), and 6 dpv (#43), respectively (score, 4–5; Figure 7A). A relative reduction was observed in pig #43, which died at 7 dpv (score 3). Compared to the other three pigs, pig #54, which died at 3 dpv, had fewer p72-positive cells in the submandibular lymph nodes. A higher proportion of ASFV antigen-positive cells was observed in the submandibular lymph nodes of Group II pigs (score 4; Figure 7B). Few p72-positive cells were observed in the liver of pig #54 (score 2). Conversely, abundant p72-positive cells were observed in the livers of the other three pigs (score 4; Figure 7C). In the lungs, viral antigens were detected multifocally in the mononuclear cells of all ASFV-infected pigs (score $\geq$3; Figure 7D). A particularly high proportion of p72-positive cells was detected in the lungs of pig #43, which died at 7 dpv (score 5). In the kidneys, the proportion of p72-positive cells was smaller in Group I (average score 2) than in Group II (average score 3.5), which exhibited a similar trend to that in the histopathological analysis (Figure 7E). The immunohistochemical scores of the mesenteric and inguinal lymph nodes, tonsils, heart, and colon of ASFV-infected pigs are shown in Supplementary Table 3.

TABLE 1 Gross organ lesions.

Organ	Gross lesion†	Number of pigs (%)‡		
		Group I	Group II	Control
Spleen	Swelling	2/5 (40%)	5/5 (100%)	0/5 (0%)
	Congestion	4/5 (80%)	4/5 (80%)	0/5 (0%)
	Hemorrhage	1/5 (20%)	0/5 (0%)	0/5 (0%)
	Necrosis	1/5 (20%)	0/5 (0%)	0/5 (0%)
Lymph nodes§	Swelling	5/5 (100%)	5/5 (100%)	0/5 (0%)
	Hemorrhage	5/5 (100%)	5/5 (100%)	0/5 (0%)
Tonsils	Swelling	5/5 (100%)	5/5 (100%)	0/5 (0%)
	Hemorrhage	5/5 (100%)	5/5 (100%)	0/5 (0%)
Liver	Swelling	5/5 (100%)	5/5 (100%)	0/5 (0%)
	Hemorrhage	1/5 (20%)	0/5 (0%)	0/5 (0%)
Lungs	Swelling	4/5 (80%)	4/5 (80%)	0/5 (0%)
	Hemorrhage	4/5 (80%)	4/5 (80%)	0/5 (0%)
	Pneumonia	0/5 (0%)	1/5 (20%)	0/5 (0%)
Kidneys	Swelling	4/5 (80%)	4/5 (80%)	0/5 (0%)
	Hemorrhage	0/5 (0%)	1/5 (20%)	0/5 (0%)
Heart	Pericardial fluid	2/5 (40%)	5/5 (100%)	0/5 (0%)
Colon	Hemorrhage	1/5 (20%)	2/5 (40%)	0/5 (0%)

† Macroscopic lesions were analyzed according to a previously published guideline (26).
‡ Group I, ASFV-inoculated pigs (died 2–5 dpv); Group II, ASFV-inoculated pigs (died 6–7 dpv); Control, negative control group (not inoculated with ASFV).
§ Submandibular, mesenteric, and inguinal lymph nodes.
ASFV, African swine fever virus; dpv, days post-viremia.

Discussion

The diagnosis of ASF in pigs may be complicated if pigs are infected with an ASFV strain that has not yet been characterized. Moreover, ASFV can cause death in the host within a short period after infection. Therefore, a complicated diagnosis can lead to delayed identification of a novel ASF outbreak. After experimentally infecting pigs with the highly virulent VNUA/HY/Vietnam ASFV strain, we analyzed blood counts and serum chemistry in blood samples from the inoculated pigs. In addition, we observed the pathological changes and host–virus interactions in pigs that died naturally of viral infection.

Numerous studies have shown that the development of clinical signs and the onset of death after ASFV infection depend on the virulence of the virus strain, the dose of the virus, routes of infection, and individual predisposition of pigs (11, 29–31). In this study, we determined the onset of viremia and viral loads in pigs infected with the same ASFV strain (VNUA/HY/Vietnam) using identical doses and routes of infection. A recent study revealed that the 50% pig lethal dose (PLD_{50}) was 1 ml of ASFV at a titer of $10^{1.7}$ HAD_{50}/ml. Hence, a dose of $1.0 \times 10^{3.5}$ HAD_{50}/ml virus (1 ml) was used in this study to observe a sufficient pathophysiological changes by ASFV infection in the virus inoculated pigs (32). In addition, a frequently selected age (7–8-week-old) of animal for ASFV inoculation experiment was chosen to compare the pathophysiological changes between pigs infected with Vietnam's first isolated ASFV and those with virus from other countries (11, 32–34). Ten ASFV-infected pigs were divided into two groups, according to the time of natural death after the onset of viremia. Interestingly, Group I pigs, which died at 2–5 dpv, had a higher viral load in the blood at the onset of viremia than Group II pigs, which died at 6–7 dpv. These results were similar to those of previous studies which reported that pigs infected with a higher dose of ASFV showed a higher viral load in the blood and earlier time of death than those infected with a lower dose (32, 35). Our study also showed that Group I pigs had a markedly higher viral load in the blood at 1–3 dpv, compared to Group II pigs. Although all pigs in this study were inoculated with same dose of ASFV, a different viral load in the blood was observed in each individual pig at the initial time of infection. The discrepancy of the viral susceptibility in each pig may explain these findings, because the severity of ASFV is known to differ based on the individual predisposition of the host (29, 30). Overall, these findings suggest that the initial viral load in the blood of ASFV-infected pigs is an important factor in determining the severity of the clinical course and time of natural death. In addition, each pig had a distinct level of susceptibility to ASFV infection, which implied that the timing of natural death would vary among individuals even though the pigs were infected with the same amount of virus. Further genetic and immunological studies of ASFV-infected pigs are needed to elucidate the dynamics of virus susceptibility.

Macrophages and monocytes are the primary target cells for the replication of ASFV. Therefore, the virus induces the activation and destruction of monocytes and macrophages (36). The infected monocyte–macrophage system secretes proinflammatory cytokines such as interleukin-1/6 and tumor necrosis factor-alpha, which strongly induce lymphocyte apoptosis (37). Severe leucopenia is considered the result of the abovementioned immunological processes (22, 36, 37). Recent studies of European strains of ASFV showed that WBC counts in ASFV-infected pigs gradually decreased after the onset of viremia (22, 35). However, a sharp increase in WBC counts was observed in this study early after the onset of viremia (until 1–2 dpv) in both groups, resulting in leukocytosis in ASFV-infected pigs up until the last day of life. A previous study of an atypical strain from Armenia in 2011 reported that this strain (a more chronic form) showed moderate leukocytosis with a slight left shift (38). Hühr et al. (39), in contrast, reported that leukocytosis was observed in ASFV-infected wild boars but was not detected in domestic pigs. These results suggest that, compared to the European strains, the Vietnamese strain exhibits different patterns of changes in WBC counts (inflammatory processes). ASFV infection in pigs also increases vascular permeability, leading to hemorrhage

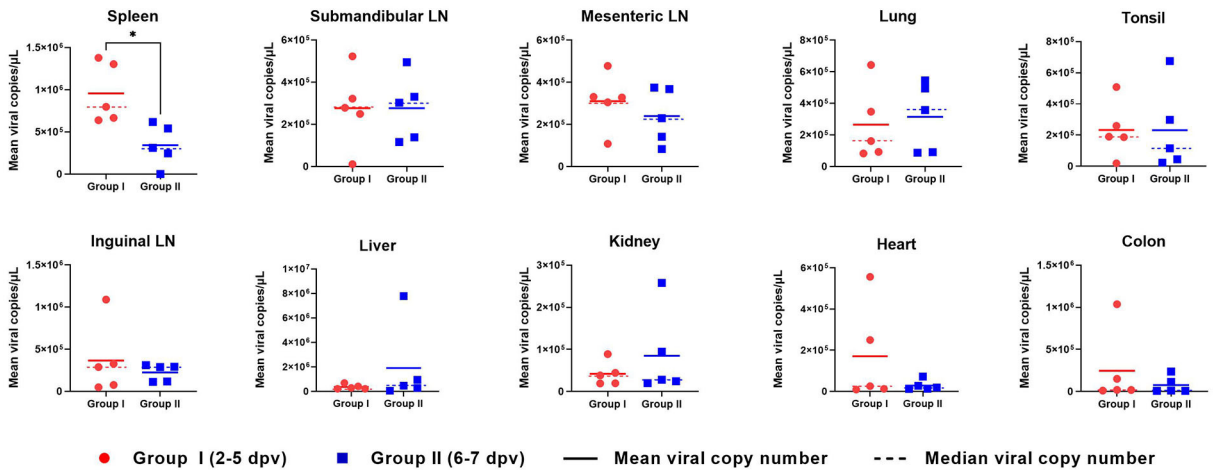

FIGURE 5
Organ viral load in pigs experimentally infected with African swine fever virus. The mean (solid lines) and median (dotted lines) viral copy number per microliter in two groups divided by the number of days between the onset of viremia and death are shown. *$p < 0.05$. dpv, days post-viremia; LN, lymph node.

and organ devastation (36). This may result in a reduction in RBC counts and hemoglobin levels, which are consistent with the findings of this study. Erythrocytopenia was observed in all ASFV-infected pigs (Groups I and II) from 2 days before death, similar to the results of a previous study on pigs infected with high-dose ASFV from Poland (22). The platelet count was significantly lower in the two ASFV-infected groups than in the control group and markedly decreased after the onset of viremia. These results were concordant with those of previous studies of other European strains (22, 35). The tendency toward thrombocytopenia may be caused by disseminated intravascular coagulation, as well as the apoptosis of megakaryocytes (36).

Serum biochemical profiles were examined to determine ASFV-induced damage to internal organs (especially the liver and kidneys) and to determine the clinical course of ASF. In the case of ALT, a marked increase was observed in all ASFV-infected pigs during the last 2–3 days of life, which is consistent with the findings of a previous study by Semerjyan et al. (40) on the Georgia strain in 2007. We also observed a marked increase in AST levels [Group I (1 dpv) and Group II (2 dpv)], which was consistent with the findings of a previous study by Walczak et al. (18). After 2 dpv, the AST levels decreased markedly until the last day of life. The high ALT and near-absent AST levels (range, 1–3 U/L) in ASFV-infected pigs during the last 1–2 days of life suggest that liver function was almost completely lost before death. The ALT/AST ratio was used to measure viral hepatitis. The ALT/AST ratio rapidly increased in Group I compared to Group II. Urea levels tended to increase more gradually in Groups I and II, as they had previously (22). However, a sudden increase in creatinine levels during the last 2–3 days of life was observed in Group II pigs, which was not detected in Group I pigs. This suggests that kidney failure was more severe in the later stages [Group II (died at 6–7 dpv)] than in the early stages [Group I (died at 2–5 dpv)] of infection.

Previous studies have reported a sharp increase in the number of macrophages in ASFV target organs, which is associated with the presence of the virus (36). We hypothesized a time-based relationship between the presence of ASFV in various internal organs and the time of death in ASFV-infected pigs. ASFV replicates mainly in mononuclear phagocytic cells in the tonsils or submandibular lymph nodes and then spreads to various internal organs through the blood and lymphatic system (36). In this study, the viral load in the tonsils and lymph nodes did not differ significantly between the two groups. However, it is noteworthy that a significantly higher viral load was detected in the spleens of Group I pigs than in those of Group II pigs ($p = 0.013$), suggesting that the spleen may be more severely affected by ASFV in the early stages of infection. These findings are similar to those reported in a 2014 study of a moderately virulent ASFV strain in Estonia (21). Although the mean values for the lungs, liver, kidney, and colon showed no significant difference, the median value for the lungs was markedly higher in Group II than in Group I. These findings are inconsistent with those of another study on the Estonian strain, which showed that pigs sacrificed at 4 dpi had a higher viral load than those sacrificed at 7 or 10 dpi (21). Differences in the virulence of the ASFV strains may explain the discrepancy in the results between the two studies. Moreover, the tissue samples in our study were collected from pigs that died naturally from the infection, whereas the previous study collected samples from sacrificed pigs (21). Further studies examining the viral loads

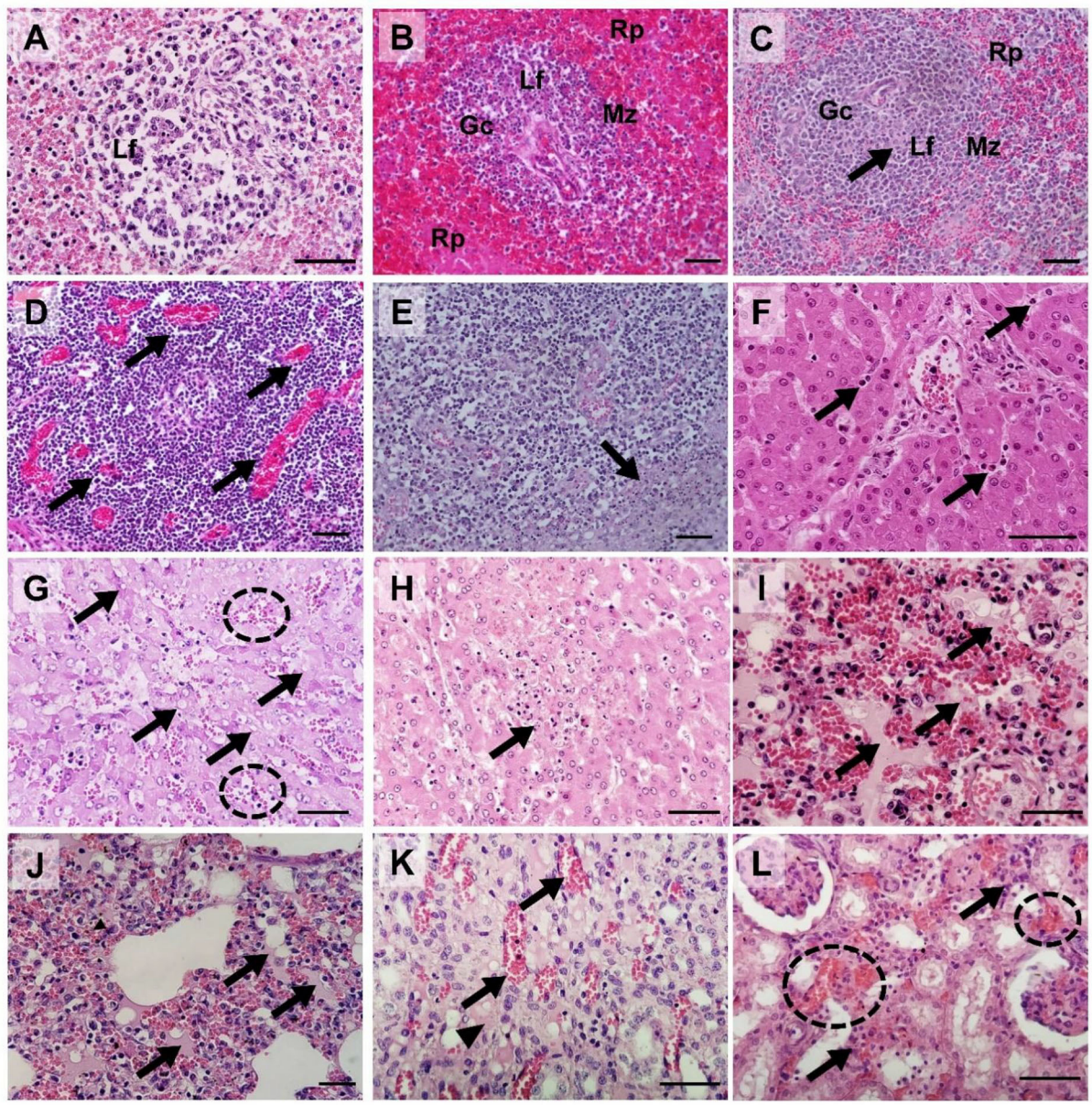

FIGURE 6
Histopathological findings in pigs experimentally infected with African swine fever virus. **(A)** Spleen [pig #54: died at 3 dpv [(Group I)]: Severe lymphoid depletion with the presence of pyknosis and karyorrhexis in the lymphoid follicle (Lf); **(B)** Spleen [pig #60: died at 6 dpv (Group II)]: Mild lymphocytic depletion in germinal center (Gc), The marginal zone (Mz) infiltrated by erythrocytes, severe and diffuse engorgement in the red pulp (Rp); **(C)** Spleen [pig #48: died at 4 dpv (Group I)]: Necrosis of lymphocytes (arrow) within the lymphoid follicle (Lf); **(D)** Submandibular lymph nodes (pig #54): Severe congestion (arrows); **(E)** Submandibular lymph nodes (pig #60): Focal necrosis (arrow); **(F)** Liver (pig #54): Neutrophils (arrows) in sinusoids. **(G)** Liver (pig #60): Multifocal congestions (dash circle) and the cytoplasmic vacuoles (arrows); **(H)** Liver (pig #43: died at 7 dpv [Group II]): Vacuolar degeneration with necrotic hepatocytes (arrow); **(I)** Lungs (pig #54): Pulmonary hemorrhages with edema (arrows); **(J)** Lungs (pig #60): Moderate pulmonary hemorrhages with edema fluids (arrows) and interstitial pneumonia; **(K)** Kidney (pig #48): Congestion (arrows) and interstitial edema (arrowhead) in the renal medulla.; **(L)** Kidney (pig #60): Multifocal hemorrhage (dash circles) and mononuclear cell infiltration in the renal interstitium (arrows). Hematoxylin and eosin stain (×400 magnification; scale bar, 50 μm). dpv, days post-viremia; Gc, germinal center; Lf, lymphoid follicle; Mz, marginal zone; Rp, red pulp.

in organs from a large number of sacrificed pigs per day are required to elucidate the mechanism of ASFV spread in the organs of ASFV-infected pigs.

To determine which internal organs were most affected by ASFV in the early and late stages of infection, we examined the histopathological lesions and viral antigen distributions in

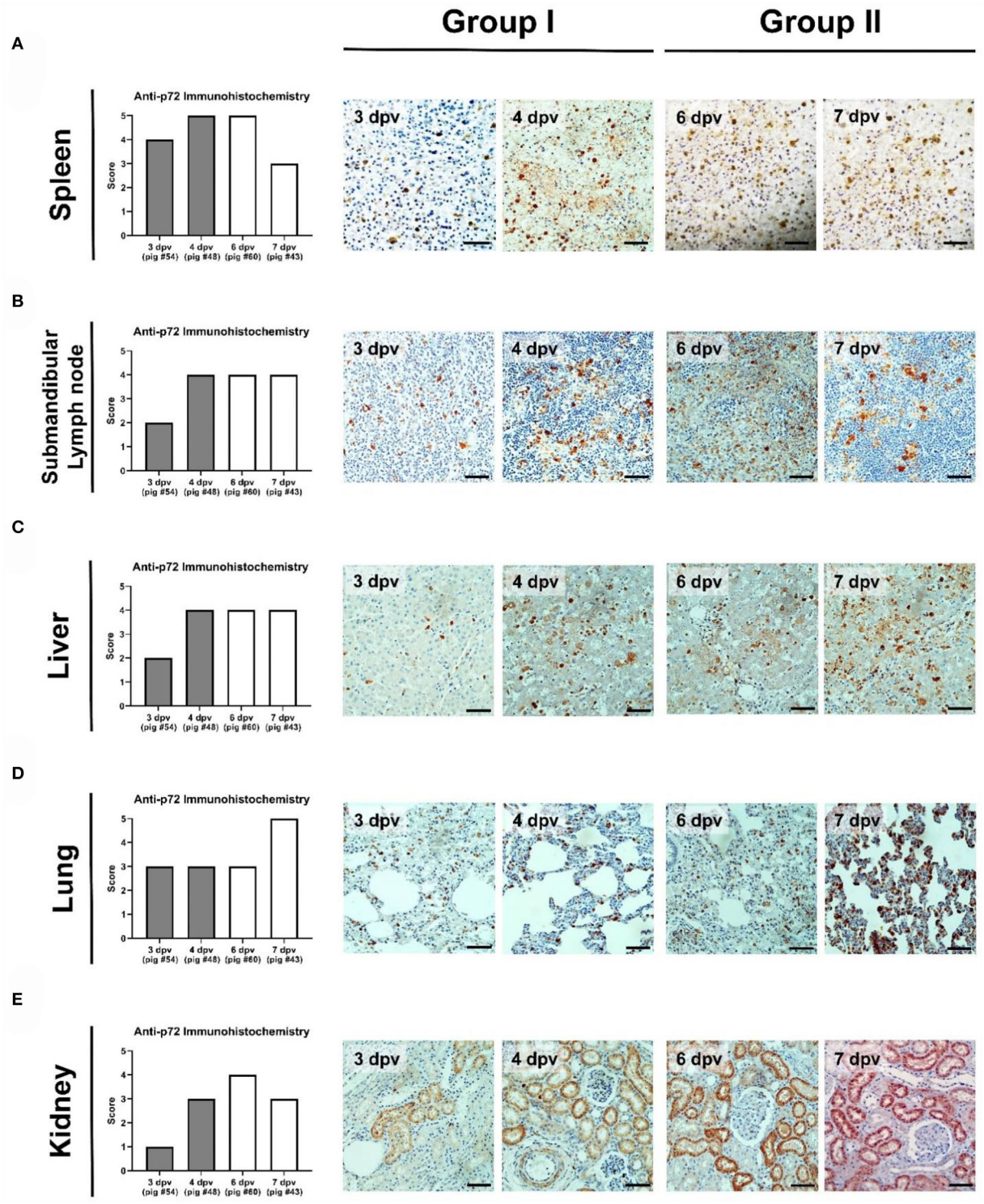

FIGURE 7
Immunohistochemical analysis of p72 in the organs of pigs experimentally infected with African swine fever virus. **(A)** Spleen, **(B)** submandibular lymph nodes, **(C)** liver, **(D)** lungs, and **(E)** kidneys scored according to the proportion of positively stained mononuclear cells or macrophages in three fields under ×400 magnification. No positive cells (0), 1–10 positive cells (1), 11–20 positive cells (2), 21–30 positive cells (3), 31–40 positive cells (4), ≥41 positive cells (5). Scale bar, 50 μm.

various organ tissues of four ASFV-infected pigs [Group I: died at 3 dpv (#54) and 4 dpv (#48); Group II: died at 6 dpv (#60) and 7 dpv (#43)]. Group I pigs had more diverse and severe histopathological lesions in the spleen compared to Group II pigs. Apoptotic or necrotic lymphocytes were more prevalent in the spleen of Group I pigs than in Group II pigs. The severity of histopathological lesions in the spleen was seemingly related to the number of immunolabelled cells. Immunohistochemical analysis revealed fewer ASFV antigen-labeled mononuclear cells or macrophages in the splenic red pulp of pigs that died at 7 dpv than in those that died before 7 dpv, suggesting that the spleen could be more severely damaged within ∼1 week after the onset of viremia. These results are consistent with those of a previous study (21). Regarding the submandibular lymph nodes [known to be the first site of virus replication (15)], congestion and hemorrhage gradually decreased with a delay in time to death in individual pigs. In contrast, severe necrotic lesions in the lymphoid follicles were observed more frequently in Group II pigs than in Group I pigs, and apoptosis was only observed in the submandibular lymph nodes of pig #54, which died at 3 dpv. Massive destruction of lymphoid organs and tissues by ASFV infection is attributed to necrotic lymph nodes (41). Similar histopathological lesions were observed in the tonsils and mesenteric and inguinal lymph nodes (Supplementary Table 2). Overall, the results suggest that histopathological lesions of the lymphoid system are more severe in the early stages (Group I) than in the later stages (Group II) of infection. The findings of a previous study support the hypothesis that the apoptosis or necrosis of myelomonocytic cells in spleen tissue peaks at 7 dpi and then decreases at 10 dpi (21).

In the liver, mild-to-moderate and moderate-to-severe lymphocytic infiltrates were present in the sinus of pigs that died in the early (Group I) and late (Group II) stages of infection, respectively. Sinusoidal inflammatory infiltrates are commonly observed in pigs infected with other strains of ASFV (including genotype II in Europe and genotype X in Africa) (17, 42). Notably, pig #54, which died at 3 dpv, showed mild vasculopathy, whereas the other three pigs had severe hemorrhagic lesions. The results were similar to those of a histopathological study of an ASF outbreak at a swine farm in Vietnam (23). The p72 antigen was more pronounced in Group II than in Group I, implying that the liver was more damaged in the later stages than in the early stages of infection. In the lungs, the histopathological changes differed according to the above findings in organs such as the spleen, lymph nodes, and liver. There was no consistent relationship between the lesions in ASFV-infected lungs and the time of death after the onset of viremia. In particular, pig #54 had severe lesions in all categories, including pneumonia, indicating that this pig died from severe pulmonary failure. These results were also evident when immunohistochemistry and polymerase chain reaction were used to evaluate the viral antigen distribution. The effect of ASFV on the lungs depends on the characteristics of the host. Further studies are needed to analyze the host factors that could influence the susceptibility of the lungs to ASFV. In contrast, all ASFV-infected pigs had moderate-to-severe congestion in the liver, which was inconsistent with the findings of a previous case study of pig farms in Vietnam (23). Group II pigs presented more severe kidney lesions than Group I pigs. Hyperemia and bleeding were observed in all pigs, whereas necrosis and interstitial nephritis were only observed in Group II pigs. Although there were no significant differences in immunohistochemical findings or virus titers, the results showed that ASFV could cause serious renal lesions in the later stages of infection. ASFV antigen-labeled cells were detected in the renal tubular epithelium of all pigs in this study, a finding consistent with that in a previous report (23).

Through this pathological study, we aimed to elucidate the course of ASFV infection and the cause of mortality by comparing various organ tissue lesions in pigs that naturally died at 3, 4, 6, and 7 dpv. Our findings provide insights into the mechanism and viral course of systemic infection with ASFV in domestic pigs. However, our study has some limitations with respect to the elucidation of host–virus interactions. As we investigated the pathological findings in only two pigs in each group, no statistical significance could be observed in this study. Consequently, the present findings could not definitively conclude the detailed viral course of ASFV infection in pigs. Additionally, the current data were obtained from pigs that died naturally from ASFV infection; data were not collected from pigs sacrificed daily. Despite close monitoring, the pigs died before reaching the predetermined humane endpoints of the study, which could have affected sample quality. Future studies with large numbers of daily sacrificed pigs could provide a more scientific basis for the pathogenesis of ASFV infection.

Conclusions

In this study, we investigated the ability of the ASFV strain (VNUA/HY/Vietnam), the first ASFV isolated in Vietnam, to develop pathological processes in infected pigs. Changes in the patterns of complete blood counts and serum biochemical profiles were similar between Group I (pigs that died at 2–5 dpv) and Group II (pigs that died at 6–7 dpv), according to the time of natural death after the onset of viremia. Group I pigs showed more rapid and severe changes in the biochemical parameters of ASFV infection than Group II pigs. Moreover, the mean number of viral copies in the blood of Group I pigs was significantly higher than that in Group II at the onset of viremia, suggesting that individual viral susceptibility was major factor in the timing of death. The viral load of the spleens in Group I was significantly higher than that of the spleens in Group II, indicating that the spleen may be most severely affected during the early stages of ASFV infection. Histopathology and immunohistochemistry also revealed that the spleens and lymph nodes of Group I pigs were more severely affected by ASFV than

those of Group II pigs, whereas the liver and kidneys of Group I pigs were less severely affected than those of Group II pigs. These results suggest that the virus could affect the lymphoid system in the early stages of infection and then spread to various internal organs *via* the blood and lymphatic system. However, our study has several limitations with respect to the number of necropsied pigs and the lack of evidence for elucidating the host characteristics according to the time of natural death after the onset of viremia. Therefore, further studies are required to examine pathological lesions in large numbers of sacrificed pigs per day.

Data availability statement

The original contributions presented in the study are included in the article/Supplementary material, further inquiries can be directed to the corresponding authors.

Ethics statement

The animal study was reviewed and approved by Institutional Animal Care and Use Committee of the National Institute of Animal Science, the Republic of Korea (approval number: NIAS 2020-463, 2020.2.20.).

Author contributions

S-IO and HSL made substantial contributions to the conception and design of the work. S-IO, M-SY, BTTN, and BK were responsible for the acquisition and interpretation of pathological data. S-IO, TTHN, VNB, VPL, and HSL were responsible for laboratory analyses. S-IO, S-WY, EK, and T-YH were responsible for the interpretation of the analyzed data. S-IO was a major contributor in writing the manuscript. S-IO, TTHN, and M-SY wrote the original draft. S-IO, HSL, and BK revised the manuscript prior to the submission. All authors read and approved the final manuscript.

Funding

This work was carried out with the support of the Cooperative Research Program for Agriculture Science and Technology Development (Project title: Analysis and monitoring of clinical and epidemiological features of African swine fever, Project No. PJ01484301), Rural Development Administration, Republic of Korea.

Acknowledgments

The authors thank the National Institute of Veterinary Research, Ministry of Agriculture and Rural Development, Vietnam.

Conflict of interest

The authors declare that the research was conducted in the absence of any commercial or financial relationships that could be construed as a potential conflict of interest.

Publisher's note

All claims expressed in this article are solely those of the authors and do not necessarily represent those of their affiliated organizations, or those of the publisher, the editors and the reviewers. Any product that may be evaluated in this article, or claim that may be made by its manufacturer, is not guaranteed or endorsed by the publisher.

Supplementary material

The Supplementary Material for this article can be found online at: https://www.frontiersin.org/articles/10.3389/fvets.2022.978398/full#supplementary-material

References

1. Dixon LK, Chapman DA, Netherton CL, Upton C. African swine fever virus replication and genomics. *Virus Res.* (2013) 173:3–14. doi: 10.1016/j.virusres.2012.10.020

2. Galindo I, Alonso C. African swine fever virus: a review. *Viruses.* (2017) 9:103. doi: 10.3390/v9050103

3. Malogolovkin A, Sereda A. African swine fever virus hemadsorption inhibition assay. In: Netherton CL, editor. *African Swine Fever Virus. Methods in Molecular Biology*. Berlin: Springer Protocols (2022), p. 2503. doi: 10.1007/978-1-0716-2333-6_11

4. Zhou X, Li N, Luo Y, Liu Y, Miao F, Chen T, et al. Emergence of African swine fever in China, 2018. *Transbound Emerg Dis.* (2018) 65:1482–4. doi: 10.1111/tbed.12989

5. Le VP, Jeong DG, Yoon SW, Kwon HM, Trinh TBN, Nguyen TL, et al. Outbreak of African swine fever, Vietnam, 2019. *Emerg Infect Dis.* (2019) 25:1433–5. doi: 10.3201/eid2507.190303

6. Ge S, Li J, Fan X, Liu F, Li L, Wang Q, et al. Molecular characterization of African swine fever virus, China, 2018. *Emerg Infect Dis.* (2018) 24:2131–3. doi: 10.3201/eid2411.181274

7. Kim HJ, Cho KH, Lee SK, Kim DY, Nah JJ, Kim HJ, et al. Outbreak of African swine fever in South Korea, 2019. *Transbound Emerg Dis.* (2020) 67:473–5. doi: 10.1111/tbed.13483

8. Mai NTA, Vu XD, Nguyen TTH, Nguyen VT, Trinh TBN, Kim YJ, et al. Molecular profile of African swine fever virus (ASFV) circulating in Vietnam during 2019–2020 outbreaks. *Arch Virol.* (2021) 166:885–90. doi: 10.1007/s00705-020-04936-5

9. Borca MV, Ramirez-Medina E, Silva E, Vuono E, Rai A, Pruitt S, et al. Development of a highly effective African swine fever virus vaccine by deletion of the I177L gene results in sterile immunity against the current epidemic Eurasia strain. *J Virol.* (2020) 94:e02017–9. doi: 10.1128/JVI.02017-19

10. Borca MV, Rai A, Ramirez-Medina E, Silva E, Velazquez-Salinas L, Vuono E, et al. A cell culture-adapted vaccine virus against the current African swine fever virus pandemic strain. *J Virol.* (2021) 95:e0012321. doi: 10.1128/JVI.00123-21

11. Chen W, Zhao D, He X, Liu R, Wang Z, Zhang X, et al. A seven-gene-deleted African swine fever virus is safe and effective as a live attenuated vaccine in pigs. *Sci China Life Sci.* (2020) 63:623–34. doi: 10.1007/s11427-020-1657-9

12. Muñoz-Pérez C, Jurado C, Sánchez-Vizcaíno JM. African swine fever vaccine: Turning a dream into reality. *Transbound Emerg Dis.* (2021) 68:2657–68. doi: 10.1111/tbed.14191

13. Wu K, Liu J, Wang L, Fan S, Li Z, Li Y, et al. Current state of global African swine fever vaccine development under the prevalence and transmission of ASF in China. *Vaccines.* (2020) 8:531. doi: 10.3390/vaccines8030531

14. Gallardo C, Fernández-Pinero J, Arias M. African swine fever (ASF) diagnosis, an essential tool in the epidemiological investigation. *Virus Res.* (2019) 271:197676. doi: 10.1016/j.virusres.2019.197676

15. Sánchez-Vizcaíno JM, Laddomada A, Arias ML. African swine fever virus. In: Zimmerman JJ, Karriker LA, Ramirez A, Schwartz KJ, Stevenson GW, Zhang J, editors. *Diseases of Swine*. Hoboken, NJ: John Wiley & Sons, Inc. (2019), p. 44352. doi: 10.1002/9781119350927.ch25

16. OIE. Technical disease card of African swine fever. (2019). Available online at: https://www.oie.int/fileadmin/Home/eng/Animal_Health_in_the_World/docs/pdf/Disease_cards/AFRICAN_SWINE_FEVER.pdf (accessed 16 June 2019).

17. Sánchez-Cordón PJ, Floyd T, Hicks D, Crooke HR, McCleary S, McCarthy RR, et al. Evaluation of lesions and viral antigen distribution in domestic pigs inoculated intranasally with African swine fever virus Ken05/Tk1 (Genotype X). *Pathogens.* (2021) 10:768. doi: 10.3390/pathogens10060768

18. Pikalo J, Zani L, Hühr J, Beer M, Blome S. Pathogenesis of African swine fever in domestic pigs and European wild boar - lessons learned from recent animal trials. *Virus Res.* (2019) 271:197614. doi: 10.1016/j.virusres.2019.04.001

19. Sánchez-Vizcaíno JM, Mur L, Gomez-Villamandos JC, Carrasco L. An update on the epidemiology and pathology of African swine fever. *J Comp Pathol.* (2015) 152:9–21. doi: 10.1016/j.jcpa.2014.09.003

20. Davies K, Goatley LC, Guinat C, Netherton CL, Gubbins S, Dixon LK, et al. Survival of African swine fever virus in excretions from pigs experimentally infected with the Georgia 2007/1 isolate. *Transbound Emerg Dis.* (2017) 64:425–31. doi: 10.1111/tbed.12381

21. Sehl J, Pikalo J, Schäfer A, Franzke K, Pannhorst K, Elnagar A, et al. Comparative pathology of domestic pigs and wild boar infected with the moderately virulent African swine fever virus strain "Estonia 2014". *Pathogens.* (2020) 9:662. doi: 10.3390/pathogens9080662

22. Walczak M, Wasiak M, Dudek K, Kycko A, Szacawa E, Olech M, et al. Blood counts, biochemical parameters, inflammatory, and immune responses in pigs infected experimentally with the African swine fever virus isolate Pol18_28298_O111. *Viruses.* (2021) 13:521. doi: 10.3390/v13030521

23. Izzati UZ, Inanaga M, Hoa NT, Nueangphuet P, Myint O, Truong QL, et al. Pathological investigation and viral antigen distribution of emerging African swine fever in Vietnam. *Transbound Emerg Dis.* (2021) 68:2039–50. doi: 10.1111/tbed.13851

24. Lee HS, Bui VN, Dao DT, Bui NA, Le TD, Kieu MA, et al. Pathogenicity of an African swine fever virus strain isolated in Vietnam and alternative diagnostic specimens for early detection of viral infection. *Porcine Health Manag.* (2021) 7:36. doi: 10.1186/s40813-021-00215-0

25. Nga BTT, Tran Anh Dao B, Nguyen Thi L, Osaki M, Kawashima K, Song D, et al. Clinical and pathological study of the first outbreak cases of African swine fever in Vietnam, 2019. *Front Vet Sci.* (2020) 7:392. doi: 10.3389/fvets.2020.00392

26. Malmquist WA, Hay D. Hemadsorption and cytopathic effect produced by African swine fever virus in swine bone marrow and buffy coat cultures. *Am J Vet Res.* (1960) 21:104–8.

27. Reed LJ, Muench HA, A. simple method of estimating fifty per cent endpoints. *Am J Epidemiol.* (1938) 27:493–7. doi: 10.1093/oxfordjournals.aje.a118408

28. Galindo-Cardiel I, Ballester M, Solanes D, Nofrarías M, López-Soria S, Argilaguet JM, et al. Standardization of pathological investigations in the framework of experimental ASFV infections. *Virus Res.* (2013) 173:180–90. doi: 10.1016/j.virusres.2012.12.018

29. Pietschmann J, Guinat C, Beer M, Pronin V, Tauscher K, Petrov A, et al. Course and transmission characteristics of oral low-dose infection of domestic pigs and European wild boar with a Caucasian African swine fever virus isolate. *Arch Virol.* (2015) 160:1657–67. doi: 10.1007/s00705-015-2430-2

30. Karalova E, Zakaryan H, Voskanyan H, Arzumanyan H, Hakobyan A, Nersisyan N, et al. Clinical and post-mortem investigations of genotype II induced African swine fever. *Porcine Res.* (2015) 5:1–11. Available online at: https://porc.bioflux.com.ro/docs/2015.1-11.pdf

31. Walczak M, Zmudzki J, Mazur-Panasiuk N, Juszkiewicz M, Wozniakowski G. Analysis of the clinical course of experimental infection with highly pathogenic African swine fever strain, isolated from an outbreak in Poland. Aspects related to the disease suspicion at the farm level. *Pathogens.* (2020) 9:237. doi: 10.3390/pathogens9030237

32. Zhao D, Liu R, Zhang X, Li F, Wang J, Zhang J, et al. Replication and virulence in pigs of the first African swine fever virus isolated in China. *Emerg Microbes Infect.* (2019) 8:438–47. doi: 10.1080/22221751.2019.1590128

33. González-Juarreo M, Lunney JK, Sánchez-Vizcaino JM, Mebus C. Modulation of splenic macrophages, and swine leukocyte antigen (SLA) and viral antigen expression following African swine fever virus (ASFV) inoculation. *Arch Virol.* (1992) 123:145–56. doi: 10.1007/BF01317145

34. Yamada M, Masujin K, Kameyama KI, Yamazoe R, Kubo T, Iwata K, et al. Expreimental infection of pigs with different doses of the African swine fever virus Armenia 07 strain by intramuscular injection and direct contact. *J Vet Med Sci.* (2020) 82:1835–45. doi: 10.1292/jvms.20-0378

35. Post J, Weesendorp E, Montoya M, Loeffen WL. Influence of age and dose of African swine fever virus infections on clinical outcome and blood parameters in pigs. *Viral Immunol.* (2017) 30:58–69. doi: 10.1089/vim.2016.0121

36. Gómez-Villamandos JC, Bautista MJ, Sánchez-Cordón PJ, Carrasco L. Pathology of African swine fever: the role of monocyte-macrophage. *Virus Res.* (2013) 173:140–9. doi: 10.1016/j.virusres.2013.01.017

37. Wang S, Zhang J, Zhang Y, Yang J, Wang L, Qi Y, et al. Cytokine storm in domestic pigs induced by infection of virulent African swine fever virus. *Front Vet Sci.* (2020) 7:601641. doi: 10.3389/fvets.2020.601641

38. Sargsyan MA, Voskanyan HE, Karalova EM, Hakobyan LH, Karalyan ZA. Third wave of African swine fever infection in Armenia: Virus demonstrates the reduction of pathogenicity. *Vet World.* (2018) 11:5–9. doi: 10.14202/vetworld.2018.5-9

39. Hühr J, Schäfer A, Schwaiger T, Zani L, Sehl J, Mettenleiter TC, et al. Impaired T-cell responses in domestic pigs and wild boar upon infection with a highly virulent African swine fever virus strain. *Transbound Emerg Dis.* (2020) 67:3016–32. doi: 10.1111/tbed.13678

40. Semerjyan AB, Tatoyan MR. Karalyan, NY, Nersisyan, NH, Hakobyan, LH, Arzumanyan, HH, et al. Cardiopathology in acute African swine fever. *Ann Parasitol.* (2018) 64:253–8. doi: 10.17420/ap6403.161

41. Sierra MA, Quezada M, Fernandez A, Carrasco L, Gomez-Villamandos JC, Martin de las Mulas JM, et al. Experimental African swine fever: evidence of the virus in interstitial tissues of the kidney. *Vet Pathol.* (1989) 26:173–6. doi: 10.1177/030098588902600211

42. Sánchez-Cordón PJ, Vidaña B, Neimanis A, Núñez A, Wikström E, Gavier-Widén D. Pathology of African swine fever. In: Iacolina L, Penrith ML, Bellini S, Chenais E, Jori F, Montoya M, et al., editors. *Understanding and Combatting African Swine Fever: A European Perspective*. Wageningen: Wageningen Academic Publishers (2021), p. 87–139. doi: 10.3920/978-90-8686-910-7_4

frontiers | Frontiers in Veterinary Science

TYPE Original Research
PUBLISHED 15 September 2022
DOI 10.3389/fvets.2022.943099

OPEN ACCESS

EDITED BY
Bin Li,
Jiangsu Academy of Agricultural Sciences (JAAS), China

REVIEWED BY
Bin Zhou,
Nanjing Agricultural University, China
Changjiang Weng,
Harbin Veterinary Research Institute (CAAS), China

*CORRESPONDENCE
Bin Wu
wub@mail.hzau.edu.cn

SPECIALTY SECTION
This article was submitted to Veterinary Experimental and Diagnostic Pathology, a section of the journal Frontiers in Veterinary Science

RECEIVED 13 May 2022
ACCEPTED 29 August 2022
PUBLISHED 15 September 2022

CITATION
Yang H, Peng Z, Song W, Zhang C, Fan J, Chen H, Hua L, Pei J, Tang X, Chen H and Wu B (2022) A triplex real-time PCR method to detect African swine fever virus gene-deleted and wild type strains. *Front. Vet. Sci.* 9:943099. doi: 10.3389/fvets.2022.943099

A triplex real-time PCR method to detect African swine fever virus gene-deleted and wild type strains

Hao Yang[1,2], Zhong Peng[1,2], Wenbo Song[1,2], Chen Zhang[1,2], Jie Fan[1,2], Hongjian Chen[1,2], Lin Hua[1,2], Jie Pei[1,2,3], Xibiao Tang[2], Huanchun Chen[1,2] and Bin Wu[1,2]*

[1]State Key Laboratory of Agricultural Microbiology, College of Veterinary Medicine, Huazhong Agricultural University, Wuhan, China, [2]Diagnostic Center for Animal Diseases, The Cooperative Innovation Center for Sustainable Pig Production, Wuhan, China, [3]Hubei Provincial Center for Animal Disease Prevention and Control, Wuhan, China

Currently there is still no effective vaccines and drugs available for African swine fever virus (ASFV), a life-threatening virus to domestic pigs and wild boars. Therefore, accurate diagnosis is important for the prevention and control of the virus. In this study, we developed a triplex real-time PCR method to detect and differentiate ASFV gene-deleted and wild type strains based on three viral genes B646L, MGF_360-14L gene, and CD2v. Standard curves plotted showed that there was a strong linear correlation ($R^2 > 0.99$) between *Ct* values and the corresponding copy numbers of synthesized standard plasmids. The detection limits of the method for B646L, MGF_360-14L, and CD2v were 78.9, 47.0, and 82.1 copies/μl, respectively. Detection results of different types of swine viruses showed that the method only gave amplification curves to ASFV. Finally, we found the triplex real-time PCR method developed in this study displayed better results on detecting the laboratory sample mocks, and it could be used as a supplemental method to detect ASFV genotype I strains. These findings suggest that the triplex real-time PCR method developed in this study have good specificity and sensitivity. This triplex real-time PCR method might also represent an effective tool for the detection of ASFV gene-deleted and wild type strains.

KEYWORDS

B646L, CD2v, MGF_360-14L, African swine fever virus, triplex real-time PCR method, gene-deleted and wild type strains

Introduction

Since its report for the first time in Kenya in Africa in 1914 (1), African swine fever (ASF) has been a life-threatening disease to global domestic pigs and wild boars with up to 100% case mortality rate (2). ASF is caused by a double-stranded DNA virus belonging to the *Asfarviridae* family, called African swine fever virus (ASFV), which possesses a genome containing ~150–167 protein encoding genes for virus replication and pathogenesis (3). Among these genes, the capsid protein P72 encoding gene B646L

is a conserved region for all ASFV strains (including the wild-type and gene-deleted vaccines) and is a common genetic marker for the virus genotyping (4, 5). Based on this gene, ASF strains are divided into 24 different genotypes (genotypes I to XXIV) (4). For the other genes, CD2v and the multigene family (MGF) 360-505R (including MGF_360-14L), are important virulence-associated genes and their deleting strains have become one of the most promising ASF attenuated vaccine candidates (6–10).

In August 2018, the first case of ASF outbreak in China was reported (11). Just <1 year passed by, ASF has been spread in almost all parts of this largest pork producer of the world. Initially, only ASFV genotype II wild-type strains have been isolated in China (11, 12). However, a recent study has found heterogeneous types of ASFV strains, including those with mutations, deletions, insertions, or short-fragment replacement compared with the earliest isolate (Pig/HLJ/2018) in China (12). Compared to the pigs infected by wild-type strains, pigs infected with ASFV variant strains display a prolonged incubation period and mild manifestations; meanwhile, there is a lower amount of detoxification in ASFV variant strain infected pigs than in wild type strain infected pigs; viral strains are always detoxified intermittently in those pigs infected with ASFV variant strains; these characteristics make the ASFV variant strains more difficult to be detected than the wild type strains (13). More seriously, the isolation of two ASFV genotype I field strains (HeN-ZZ-P1-21 and SD/DY-I-21) were reported in 2021, and these two Chinese genotype I isolates lack 10 open reading frames (ORFs), including the MGF_110, MGF_360 and MGF_505 families, compared to the genome sequences of the highly pathogenic genotype I strains L60 and Benin 97/1 (14). These findings suggest a worrisome and complex condition of ASFV prevalence in pig industry in China. Considering there are currently no effective vaccines and/or drugs available, accurate diagnosis is important for the prevention and control of the disease (15). Since real-time PCR method is one of the most-commonly used method and also the recommended method for ASF detection in China (16), we explored the possibility of developing a triplex real-time PCR method targeting the CD2v and MGF_360-14L genes together with B646L for the detection and differentiation of ASFV gene-deleted and wild type strains in this study.

Materials and methods

Analysis on the genome sequences of ASFV isolates from China

A total of 14 complete genome sequences of ASFV isolates from China were downloaded from GenBank (https://www.ncbi.nlm.nih.gov/genome/browse/#!/viruses/10302/). Apart from two belonged to ASFV genotype I isolates (HeN/ZZ-P1/2021, Gen-Bank accession no. MZ945536; SD/DY-I/2021, GenBank accession no. MZ945537) (14), the remaining sequences belonged to the genotype II isolates (Supplementary Table S1). Sequence alignments were performed and visualized using BLAST Ring Image Generator (BRIG) (17).

Standard plasmid construction, primer- and probe-design

Primers and probes targeting B646L, CD2v, and MGF_360-14L were designed using the SnapGene software (version 5.3; https://www.snapgene.com/) and Primer Premier 5 program (18). The probe for B646L was labeled with the 5'-reported dye 6-carboxyfluorescein (FAM) and the 3'-quencher BHQ1, the probe for MGF_360-14L was labeled with the 5'-reported dye Cy5 and the 3'-quencher BHQ2, and the probe for CD2v was labeled with the dye VIC and the 3'-quencher BHQ1 (Table 1). The partial length of B646L (616 bp, base pairs 1,026–1,641), MGF_360-14L gene (541 bp, base pairs 54–594), and CD2v gene (559 bp, base pairs 525–1,083) from the whole genome sequence of ASFV genotype II strain Pig/HLJ/2018 (GenBank accession no. MK333180) were synthesized and cloned into the pUC57 plasmid to generate the recombinant standard plasmids ASFV-B646L-pUC57 (280.70 ng/μl; 7.89×10^{10} copies/μl), ASFV-MGF_360-14L-pUC57 (163.34 ng/μl; 4.70×10^{10} copies/μl), and ASFV-CD2v-pUC57 (288.03 ng/μl; 8.21×10^{10} copies/μl), respectively. A recombinant standard plasmid pUC57-I-B646L-CD2v-MGF_360-14L (100.00 ng/μl) carrying B646L, CD2v, MGF_360-14L from the genotype I strain Benin 97/1 (GenBank accession no. AM712239) was also synthesized.

PCR reaction volume and optimization of amplification conditions

Genomic DNA was extracted using a Vazyme DNA/RNA Extraction Kit (Cat NO. RM-201-02; Nanjing, China) following the manufactory instructions. The triplex real-time PCR assay was performed in a 25-μl reaction volume, which contains template DNA 5-μl, AceQ® Uniwersal U+ Probe Master Mix (Vazyme, Nanjing, China) 12.5-μl, each of the forward and reverse primers (0.12, 0.16, 0.20, 0.24, 0.28, or 0.32 μM), each of the TaqMan probes (0.12, 0.16, 0.20, 0.24, 0.28, or 0.32 μM), and nuclease-free water up to 25-μl. PCR assay was performed on an CFX96 Touch Real-Time PCR Detection System (Bio-Rad, Hercules, CA) with the following conditions: 95°C for 5 min, followed by 40 cycles of 95°C for 15 s, annealing at different temperatures (55–60°C) for 45 s. Fluorescence was recorded at 59°C. Copy number was calculated using the formula (Copy number = $[(6.02 \times 10^{23}) \times ([ng/\mu l] \times 10^{-9})]/[$DNA length ×

TABLE 1 Primers and probe sequences used in this study.

Primer/probe	Sequence (5'-3')	Targe gene	Size (bp)
P72-F	CTACCTGGAACATCTCCGATCA	B646L	106
P72-R	CTTATCTCTGCGTGGTGAGT		
P72-P	6-FAM-CTCATCAACACCGAGATTGGCACAAG-BHQ-1		
MGF-F	TTGGGGCGCAAATCCTGAAT	MGF_360-14L	86
MGF-R	GCGTTAAGCCTCCCAGTTC		
MGF-P	Cy5-ACACAGCCGCTTTAGATACACGGCA-BHQ-2		
CD2v-F	CCACCACCTGAATCTAATGAAGAAG	CD2v	111
CD2v-R	CTGATAACGACTGTAAGGCTTAGG		
CD2v-P	VIC-ACAATGTCAGCATGATGACACCACTTCC-BHQ-1		

660]) described previously (19). In addition, plasmids (ASFV-B646L-pUC57, ASFV-MGF_360-14L-pUC57, and ASFV-CD2v-pUC57) with a series of 10-fold dilution (10^{-2}-10^{-11}) were used as the templates to validate the method.

Construction of standard curves

To generate standard curves, a series of 10-fold dilutions (10^{-2}-10^{-9}) were given to the three synthesized standard plasmids (ASFV- B646L-pUC57, ASFV-MGF_360-14L-pUC57, and ASFV-CD2v-pUC57), which were used as the template DNA to perform the triplex real-time PCR assays. Standard curves were generated based on the cycle threshold (*Ct*) values and the copy numbers (lg values) of the template DNA. Coefficients of determination (R^2) were calculated using GraphPad Prism v. 8.0.1 (https://www.graphpad.com/scientific-software/prism/).

Validation of specificity and sensitivity

To test the stability of the generated triplex real-time PCR method, separated assays were performed to detect the recombinant standard plasmids at different concentrations and compared the Ct values. The specificity and sensitivity of the generated triplex real-time PCR method was validated using the genomic DNA extracted from the other viruses, including pseudorabies virus (PRV), porcine reproductive and respiratory syndrome virus (PRRSV), Japanese encephalitis virus (JEV), porcine parvovirus (PPV), and porcine circovirus type 2 (PCV2). In addition, the synthesized plasmids pUC57-ΔMGF_360-14L, pUC57-ΔCD2v, pUC57-ΔMGF_360-14L/CD2v, and pUC57-MGF_360-14L/CD2v were also used as the template DNA to validate the method. We also compared the detection results of the triplex real-time PCR method developed in this study (hereinafter referred to as the "tr-PCR") to those of a reported triplex real-time PCR method (hereinafter referred to as the "r-PCR") (5), and a recommended real-time PCR method in China (hereinafter referred to as the "gb-PCR") (16). DNA extracted from different types of samples (soil, water, pig anticoagulant blood, pig feces, environmental swabs, pig tissues) mixed ASFV genomic DNA (extracted from positive field samples) were detected by the three real-time PCR methods.

Evaluation of the possible application of the triplex real-time PCR method to detect ASFV genotype I strains

To assess the possible application of the triplex real-time PCR method to detect ASFV genotype I strains, the synthesized plasmid pUC57-I-B646L-CD2v-MGF_360-14L (10^5 copy/μl) was used as the template for PCR detection. The triplex real-time PCR assay was performed in a 25-μl reaction volume, which contains template DNA 5-μl, AceQ® Uniwersal U+ Probe Master Mix (Vazyme, Nanjing, China) 12.5-μl, each of the forward and reverse primers (0.20 μM), each of the TaqMan probes (0.20 μM), and nuclease-free water up to 25-μl. PCR assay was performed on an CFX96 Touch Real-Time PCR Detection System (Bio-Rad, Hercules, CA) with the following conditions: 95°C for 5 min, followed by 40 cycles of 95°C for 15 s, annealing at different temperatures (59°C) for 45 s.

Specific statements

The inactivation of an ASFV strain used for the simulation of virus-containing samples was performed in Huazhong Agricultural University Animal Biosafety Level-3 Laboratory (ABSL-3, <city>Wuhan</city>, China) following the requirements of the Ministry of Agriculture and Rural Affairs (MARA) of the People's Republic of China (MARA General Office Document no. [2019] 12).

Results

Sequence analysis indicates the condition of application

Sequence comparisons of the primer-target regions of B646L, CD2v, and MGF_360-14L from different ASFV strains demonstrated that B646L was highly conserved, not only between ASFV strains belonging to the same genotype, but also between the genotype I and genotype II strains (Figure 1). Although MGF_360-14L was conserved among the eleven Chinese genotype II strains and the two genotype I strains L60 and Benin 97/1, this gene was missing in the genome sequences of the two genotype I strains HeNZZ (GenBank accession no. MZ945536) and SDDY (GenBank accession no. MZ945537) from China (Figure 1; Supplementary Figure S1). For CD2v, sequence alignments revealed that this gene was conserved among the Chinese genotype II strains, but it was various between the Chinese genotype II strains and the genotype I strains (Figure 1). Based on the above findings, it may conclude that the primer-target area of B646L in this study was a proper marker for the detection of presence of ASFV; while the primer-target area of MGF_360-14L could be used to differentiated MGF_360-14L-deletion strains from the wild type strains; and the primer-target area of CD2v was applicable for differentiating CD2v-deletion strains from the wild type strains, or differentiating genotype II wild type strains from genotype I wild type strains.

Optimization of the amplification conditions

We next investigated the optimal concentrations of the primers and probes. To achieve this, we detected 10^4 copies/μl of plasmids with different concentrations of primers and probes (0.12, 0.16, 0.20, 0.24, 0.28, or 0.32 μM) at the annealing temperature of 59.0°C. The results revealed that an optimal amplification condition occurred when the concentrations were set as 0.20 μM (Supplementary Figure S2A). To explore the optimal annealing temperature for tr-PCR, we detected the plasmids with 0.20 μM of primers and probes at 55.0, 56.0, 57.0 58.0, 59.0, and 60.0°C. The results revealed that the tr-PCR assay displayed the optimal amplification conditions at the annealing temperature of 59.0°C (Supplementary Figure S2B).

Detection limit and standard curves

To test the detection limit of tr-PCR, a series of 10-fold dilutions were given to ASFV-B646L-pUC57 (from 7.89×10^{10} to 78.9 copies/μl), ASFV-MGF_360-14L-pUC57 (from 4.70×10^{10} to 47.0 copies/μl), and ASFV-CD2v-pUC57 (from 8.21×10^{10} to 82.1 copies/μl). Plasmids with different copy numbers were then detected using tr-PCR. The results revealed that the detection limits for B646L, MGF_360-14L, and CD2v were 78.9, 47.0, and 82.1 copies/μl, respectively (Figures 2A–C). Standard curves plotted using GraphPad Prism software v. 8.0.1 showed that there was a strong linear correlation ($R^2 > 0.99$) between Ct values and the corresponding copy numbers of ASFV-B646L-pUC57, ASFV-MGF_360-14L-pUC57, and ASFV-CD2v-pUC57. The standard curves of the three standard plasmids were plotted with slopes of −3.903, −4.037, and −3.969, respectively (Figures 2D–F).

Stability, specificity, and sensitivity of the triplex real-time PCR method

We chose different standard plasmids at $\sim 10^2$ copies/μl or $\sim 10^6$ copies/μl as the DNA templates to test the coefficient of variation (*C.V.*) values of the method. The results showed that *C.V.* values determined within different detection groups and between different detection groups were lower than 1.5% (Table 2), indicating the developed method possesses a good stability. Specificity tests revealed that only DNA samples from ASFV showed positive amplification curves for the three fluorescence channels of FAM, Cy5 and VIC; while those from PRV, PRRSV, JEV, PPV, and PCV2 did not show amplification curves (Figures 3A–C).

Next, we used the synthesized plasmids pUC57-ΔMGF_360-14L, pUC57-ΔCD2v, pUC57-ΔMGF_360-14L/CD2v, and pUC57-MGF_360-14L/CD2v as the template DNA to validate the method. The results revealed that the method could differentiate the three types of gene-deletion plasmids as well as the gene-completeness plasmid, suggesting the method is able to differentiate ASFV wild type and gene-deletion strains (Figure 4).

Comparison of the detection results of different real-time PCR methods

To evaluate the accuracy of tr-PCR, inactivated ASFV strains were mixed with soil samples ($n = 6$), water samples ($n = 6$), pig anticoagulant blood samples ($n = 6$), pig fecal samples ($n = 6$), table and floor swabs (spraying on the surfaces of tables and/or floors then collecting the swabs), and/or pig tissue samples ($n = 6$). Genomic DNA were extracted from these samples and were detected using tr-PCR, r-PCR (5), and gb-PCR (16). The results revealed that 17 samples, 17 samples, and 16 samples were detected to be positive by using these three methods, respectively, indicating that tr-PCR showed a similar result of detection to r-PCR (Figure 5; Supplementary Table S2).

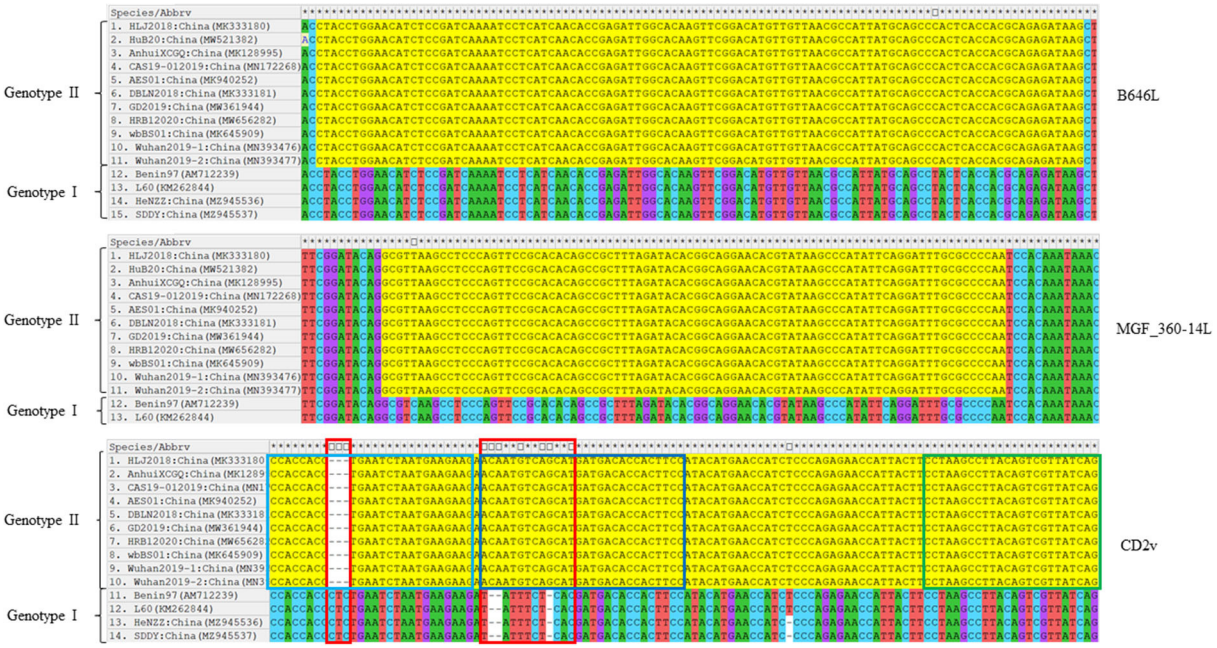

FIGURE 1
Nucleotide sequence comparisons of the primer-target regions of B646L, CD2v, and MGF_360-14L from different ASFV strains. The primer-target regions of B646L, CD2v, and MGF_360-14L are heighted in yellow. In CD2v gene, different regions between the genotype I strains and genotype II strains are shown in red boxes; CD2v forward primer, probe, and reverse primer are shown in light blue, dark blue, and green boxes.

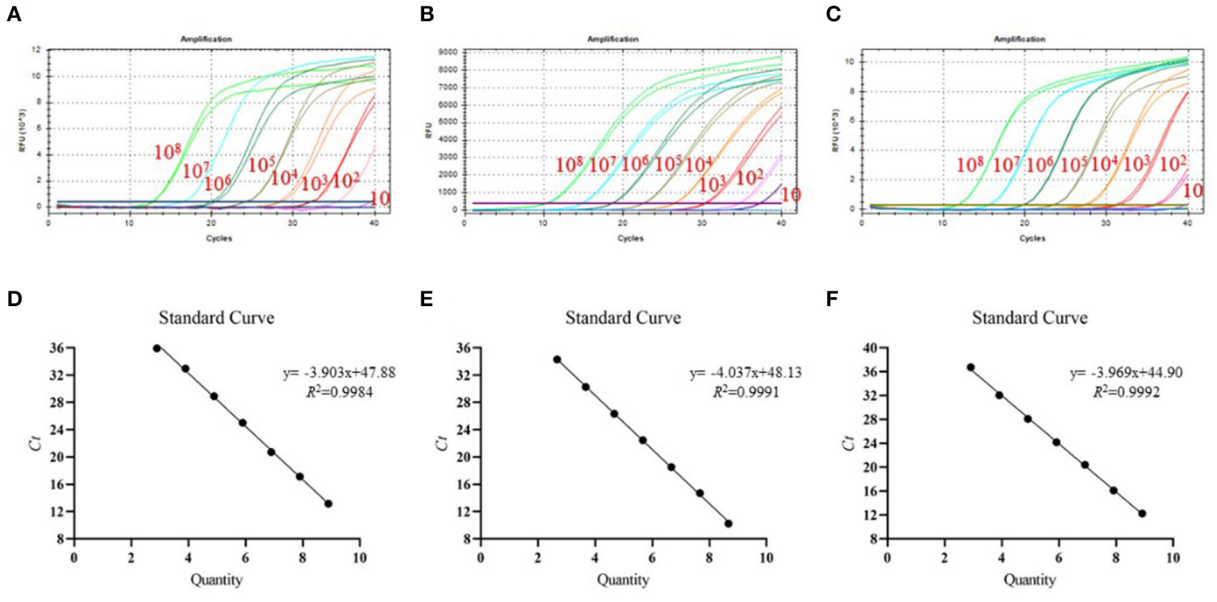

FIGURE 2
Detection limit and standard curves of the triplex real-time PCR method developed in this study. **(A)** Detection limit for B646L; **(B)** Detection limit for MGF_360-14L; **(C)** Detection limit for CD2v; **(D)** Plasmid DNA standard curve for B646L, $y = -3.903x + 47.88$, $R^2 = 0.9984$; **(E)** Plasmid DNA standard curve for MGF_360-14L, $y = -4.037x + 48.13$, $R^2 = 0.9991$; **(F)** Plasmid DNA standard curve for CD2v gene, $y = -3.969x + 44.90$, $R^2 = 0.9992$.

TABLE 2 Validation of the Detection repeatability of the developed triplex real-time PCR method.

Genes	DNA (copies/μL)	Rounds of testing	*Ct* mean[a]	*Ct* Standard deviation	*C.V.*[a]	*C.V.* between groups
B646L	7.89×10^2	1	33.34	0.24	0.73%	0.74%
		2	32.99	0.26	0.79%	
		3	33.47	0.42	1.25%	
	7.89×10^3	1	29.53	0.11	0.37%	0.49%
		2	29.33	0.16	0.54%	
		3	29.60	0.21	0.70%	
	7.89×10^4	1	26.68	0.09	0.33%	0.17%
		2	26.59	0.08	0.29%	
		3	26.63	0.05	0.19%	
	7.89×10^5	1	23.14	0.12	0.54%	0.19%
		2	23.16	0.09	0.40%	
		3	23.07	0.02	0.11%	
	7.89×10^6	1	19.15	0.13	0.67%	0.54%
		2	18.95	0.15	0.77%	
		3	19.02	0.09	0.46%	
MGF_360-14L	4.70×10^2	1	35.29	0.66	1.86%	1.35%
		2	34.41	1.40	4.06%	
		3	34.58	0.20	0.56%	
	4.70×10^3	1	30.53	0.06	0.18%	0.36%
		2	30.62	0.05	0.16%	
		3	30.41	0.09	0.30%	
	4.70×10^4	1	26.06	0.19	0.71%	0.28%
		2	25.96	0.23	0.90%	
		3	26.10	0.06	0.24%	
	4.70×10^5	1	22.46	0.04	0.16%	0.56%
		2	22.49	0.09	0.41%	
		3	22.69	0.18	0.78%	
	4.70×10^6	1	18.49	0.05	0.28%	0.14%
		2	18.44	0.13	0.72%	
		3	18.48	0.05	0.28%	
CD2v	8.21×10^2	1	32.18	0.16	0.51%	0.29%
		2	32.03	0.20	0.63%	
		3	32.01	0.36	1.11%	
	8.21×10^3	1	29.40	0.07	0.25%	0.31%
		2	29.39	0.05	0.17%	
		3	29.55	0.11	0.36%	
	8.21×10^4	1	26.48	0.17	0.64%	0.23%
		2	26.43	0.30	1.15%	
		3	26.36	0.42	1.61%	
	8.21×10^5	1	23.78	0.06	0.27%	0.01%
		2	23.78	0.04	0.19%	
		3	23.78	0.06	0.25%	
	8.21×10^6	1	19.76	0.07	0.35%	0.18%
		2	19.69	0.02	0.10%	
		3	19.75	0.10	0.53%	

[a]Ct, cycle threshold; C.V., coefficient of variation.

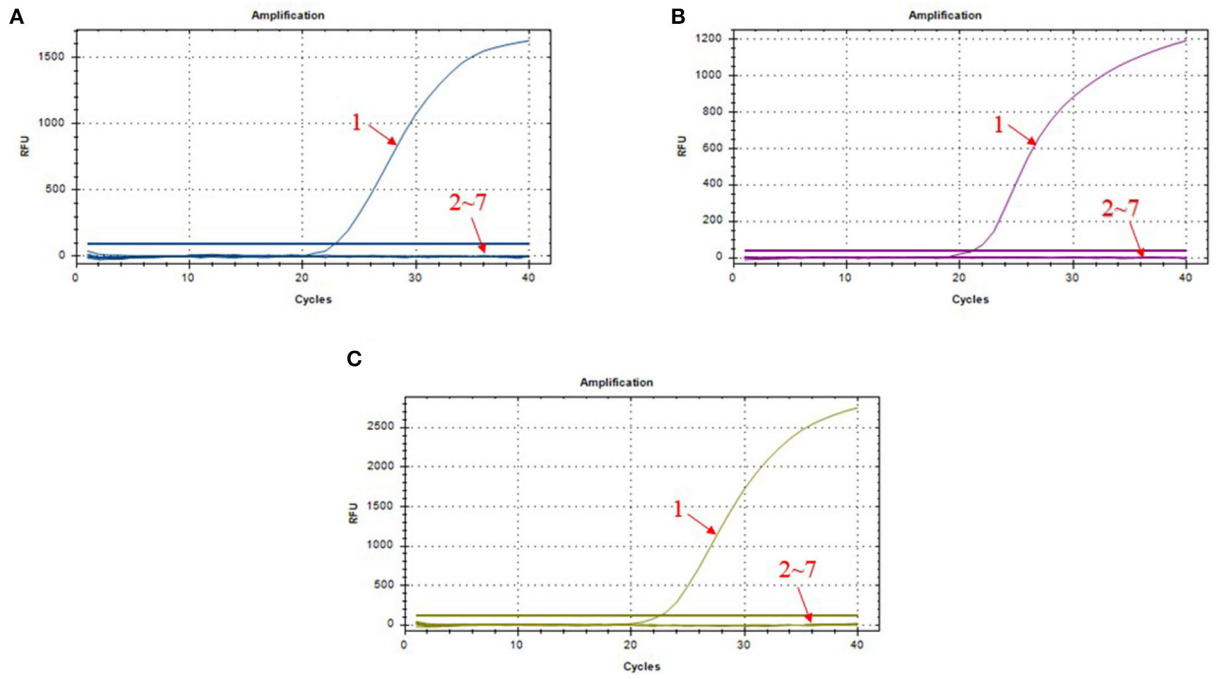

FIGURE 3
Amplification curves in the specificity test of triplex real-time PCR assay. **(A)** amplification curves of B646L; **(B)** amplification curves of MGF_360-14L; **(C)** amplification curves of CD2v; 1: ASFV; 2–7: PRV, PRRSV, JEV, PPV, PCV2, and DNA-free water.

The possible application of the triplex real-time PCR method to detect ASFV genotype I strains

Our above sequence alignment results revealed that the genotype I strains reported in China (HeNZZ and SDDY) lacked the MGF_360-14L gene, and the CD2v gene was different between the genotype I and genotype II strains (Figure 1; Supplementary Figure S1). Therefore, the triplex real-time PCR method developed in this study might have a possible use in detecting ASFV strains. To explore this, the synthesized plasmid pUC57-I-B646L-CD2v-MGF_360-14L was used as the template to perform the PCR assays. The results revealed that the triplex real-time PCR method was able to give amplifying curves of the B646L and MGF_360-14L of ASFV genotype I strains but it did not give the amplifying curve of CD2v (Figure 6).

Discussion

ASF is a World Organization for Animal Health (WOAH) listed animal infectious disease and one of the most severe threats to global pig industry. Despite of ~107 years of research, there is still no effective vaccines and/or drugs available for the treatment of the disease (20). Therefore, accurate detection is important for the control and prevention of ASF (15, 21). Since real-time PCR method is one of the most-commonly used method and also the recommended method for ASF detection in China (16), we therefore constructed a triplex real-time PCR method in this study.

The triplex real-time PCR method in this study was developed based on three genes B646L, CD2v (EP402R), and MGF_360-14L. Among them, B646L is a conserved gene among different ASFV strains and is commonly used for the detection and genotyping of ASFV (5, 16, 22, 23). According to the published data, only ASFV genotype II and genotype I strains have been reported in China until recently (12–14), and genotype II is the epidemic genotype in the field (12, 24, 25). The three genes we selected for developing the real-time PCR method were conserved among the wild type. Particularly, recent studies have reported the prevalence of CD2v/MGF360-deleted ASFV strains in pig farms in China (12, 14). Therefore, the triplex real-time PCR method developed based on these three genes might have a potential use for the detection of ASFV gene deletion strains and wild type strains. It is worthy of note that both CD2v (EP402R) and MGF_360-14L are important genes most-frequently deleted for vaccine study (6–10). While no approved commercial vaccine is currently available to protect pigs from the virus in China, the triplex real-time PCR method may also represent a potential choice to differentiate ASFV vaccines strains and wild type strains in the future if there are associated vaccines approved. However, considering many other

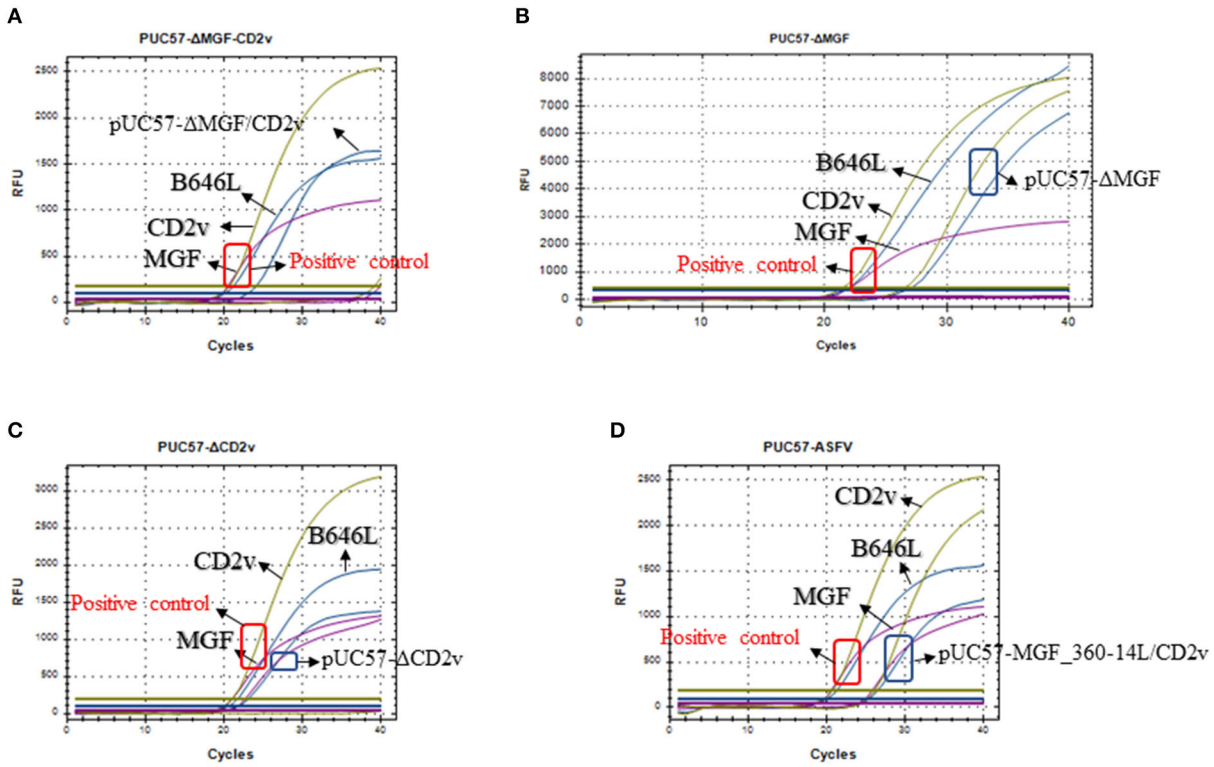

FIGURE 4
Detection of the triplex real-time PCR methods developed in this study on the mocks with different gene deletions. **(A)** Detection of the MGF_360-14L/CD2v double deletion plasmid pUC57-ΔMGF_360-14L/CD2v; **(B)** Detection of the MGF_360-14L deletion plasmid pUC57-ΔMGF_360-14L; **(C)** Detection of the CD2v deletion plasmid pUC57-ΔCD2v; **(D)** Detection of the wild type plasmid pUC57-MGF_360-14L/CD2v; curves in blue represents the amplification curves of B646L; curves in purple represents the amplification curves of MGF_360-14L; curves in glode represents the amplification curves of CD2v. In all panels, a plasmid containing all three genes was used a positive control template gene and the amplification results are shown in red box; while the detection results based on different types of plasmids are shown in blue box.

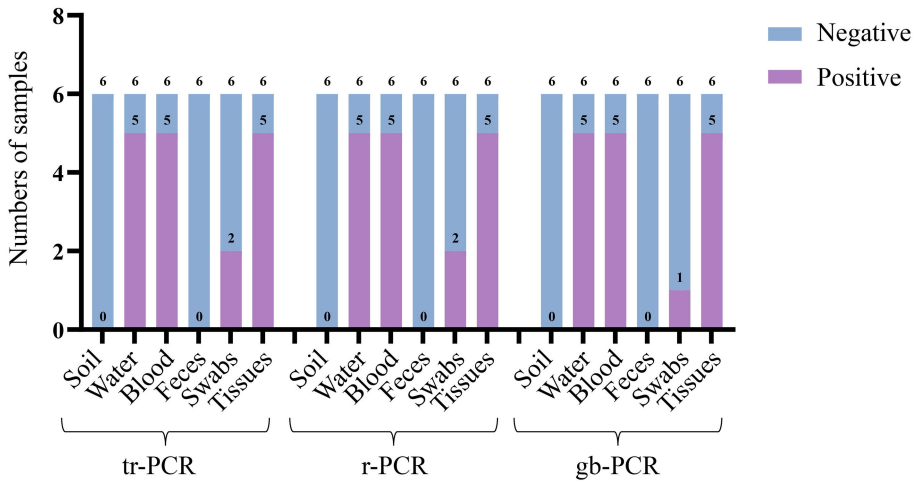

FIGURE 5
Detection of different real-time PCR methods on different laboratory sample mocks.

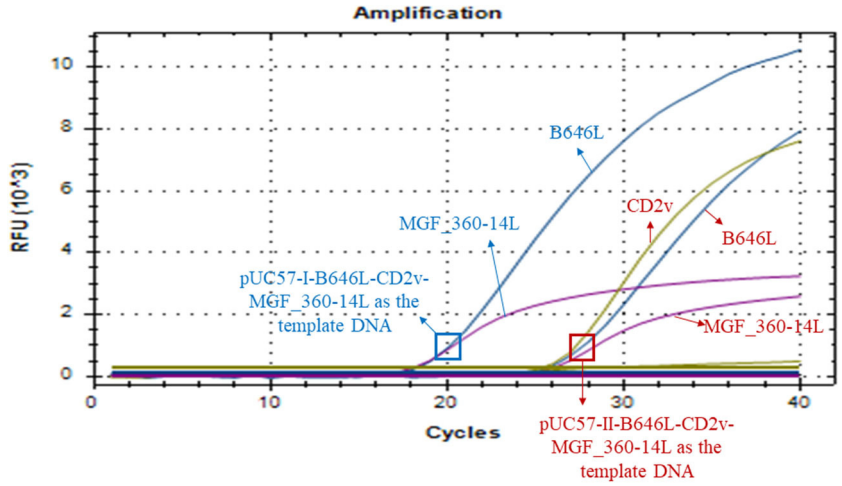

FIGURE 6
Amplification curves of triplex real-time PCR assay on detecting B646L, CD2v, and MGF_360-14L from ASFV genotype I strains. The result of the method using a plasmid containing B646L, CD2v, and MGF_360-14L (pUC57-I-B646L-CD2v-MGF_360-14L) from ASFV genotype I strains is shown in blue, while result of the method using a plasmid containing B646L, CD2v, and MGF_360-14L (pUC57-II-B646L-CD2v-MGF_360-14L) from ASFV genotype II strains is shown in red.

genes, e.g., A137R (26), I177L (27), E184L (28), etc., have been also demonstrated as suitable targets for deletion to develop vaccine candidates, these genes should be also included for the development of proper multiplex real-time PCR methods for the differentiation of ASFV vaccines strains and wild type strains in future.

Our whole genome sequence alignments also found B646L and CD2v (EP402R) were relatively conserved between ASFV genotype II and genotype I strains, but the two genotype I strains recently isolated from China lacked the MGF_360-14L gene. These findings are in agreement with the recent study reporting the isolation of these two genotype I strains (14). Therefore, the triplex real-time PCR method developed in this study may also have a potential use to detect the recent emerging genotype I strains in China.

Specificity and sensitivity are important measures of the diagnostic accuracy of a test (29). In this study, we conducted different assays to validate the specificity and sensitivity of the developed triplex real-time PCR method. Detection results of different types of swine viruses (ASFV, PRV, PRRSV, JEV, PPV, and PCV2) showed that the method only gave amplification curves to ASFV, and the detection limits of the for B646L, MGF_360-14L, and CD2v were 78.9, 47.0, and 82.1 copies/μl, respectively. These results are in agreement with the recent reported triplex real-time PCR method (5). Moreover, the triplex real-time PCR method developed in this study displayed better results on detecting the laboratory sample mocks. These findings suggest that the triplex real-time PCR method developed in this study have good specificity and sensitivity.

A noteworthy point is that a target gene of the triplex real-time PCR method developed in this study is MGF_360-14L. While ASFV genotype II strains lacking this gene has been reported in China (12), ASFV genotype I strains (HeNZZ and SDDY) reported in China also do not contain this gene (14). In this regard, the triplex real-time PCR method developed in this study could either detect ASFV genotype II MGF_360-14L-deletion strains or detect ASFV genotype I strains. In addition, the triplex real-time PCR method developed in this study did not give the amplifying curve of the CD2v gene of ASFV genotype I strains. Considering a few cases report the isolation of ASFV genotype I strains, the triplex real-time PCR method developed in this study could be used as a supplemental method to detect ASFV genotype I strains.

In summary, we developed a triplex real-time PCR method to detect ASFV gene-deleted and wild type strains. This method was found to be specific and sensitive, and it exhibited better results on detecting both laboratory sample mocks than the other used real-time PCR methods. Most importantly, the triplex real-time PCR method also demonstrated a potential to initially detect ASFV genotype I strains. It might also represent an effective tool for the detection of ASFV gene-deleted and wild type strains.

Data availability statement

The original contributions presented in the study are included in the article/Supplementary material, further inquiries can be directed to the corresponding author/s.

Author contributions

HY, ZP, and BW: conceptualization. HY, WS, CZ, JF, HoC, LH, JP, and XT: methodology, formal analysis, and investigation. HY and ZP: writing—original draft preparation. HuC, ZP, and BW: writing—review and editing. BW: funding acquisition. ZP and BW: supervision. All authors contributed to the article and approved the submitted version.

Funding

This work was supported in part by the National Natural Science Foundation of China (grant no. U20A2059) and Hubei Provincial Key Research and Development Program (grant no. 2021BBA085).

Conflict of interest

The authors declare that the research was conducted in the absence of any commercial or financial relationships that could be construed as a potential conflict of interest.

Publisher's note

Supplementary material

The Supplementary Material for this article can be found online at: https://www.frontiersin.org/articles/10.3389/fvets.2022.943099/full#supplementary-material

SUPPLEMENTARY FIGURE S1
Sequence comparison of ASFV isolates from China.

SUPPLEMENTARY FIGURE S2
Results of the optimizations of the primer/probe concentrations **(A)** and annealing temperatures **(B)**.

SUPPLEMENTARY TABLE S1
The genome sequences of ASFV Chinese isolates used in this study.

SUPPLEMENTARY TABLE S2
Results of three real-time PCR methods detecting the laboratory sample mocks.

References

1. Blasco R, Agüero M, Almendral JM, Viñuela E. Variable and constant regions in African swine fever virus DNA. *Virology.* (1989) 168:330–8. doi: 10.1016/0042-6822(89)90273-0

2. Galindo I, Alonso C. African swine fever virus: a review. *Viruses.* (2017) 9:103. doi: 10.3390/v9050103

3. Dixon LK, Chapman DA, Netherton CL, Upton C. African swine fever virus replication and genomics. *Virus Res.* (2013) 173:3–14. doi: 10.1016/j.virusres.2012.10.020

4. Gallardo C, Fernández-Pinero J, Pelayo V, Gazaev I, Markowska-Daniel I, Pridotkas G, et al. Genetic variation among african swine fever genotype II viruses, Eastern and Central Europe. *Emerg Infect Dis.* (2014) 20:1544–7. doi: 10.3201/eid2009.140554

5. Lin Y, Cao C, Shi W, Huang C, Zeng S, Sun J, et al. Development of a triplex real-time pcr assay for detection and differentiation of gene-deleted and wild-type African swine fever virus. *J Virol Methods.* (2020) 280:113875. doi: 10.1016/j.jviromet.2020.113875

6. Chen W, Zhao D, He X, Liu R, Wang Z, Zhang X, et al. A seven-gene-deleted african swine fever virus is safe and effective as a live attenuated vaccine in pigs. *Sci China Life Sci.* (2020) 63:623–34. doi: 10.1007/s11427-020-1657-9

7. Reis AL, Abrams CC, Goatley LC, Netherton C, Chapman DG, Sanchez-Cordon P, et al. Deletion of African swine fever virus interferon inhibitors from the genome of a virulent isolate reduces virulence in domestic pigs and induces a protective response. *Vaccine.* (2016) 34:4698–705. doi: 10.1016/j.vaccine.2016.08.011

8. Monteagudo PL, Lacasta A, López E, Bosch L, Collado J, Pina-Pedrero S, et al. Ba71δcd2: a new recombinant live attenuated African swine fever virus with cross-protective capabilities. *J Virol.* (2017) 91:e01058–17. doi: 10.1128/JVI.01058-17

9. Sánchez-Cordón PJ, Jabbar T, Berrezaie M, Chapman D, Reis A, Sastre P, et al. Evaluation of protection induced by immunisation of domestic pigs with deletion mutant African swine fever virus beninδmgf by different doses and routes. *Vaccine.* (2018) 36:707–15. doi: 10.1016/j.vaccine.2017.12.030

10. Gladue DP, O'Donnell V, Ramirez-Medina E, Rai A, Pruitt S, Vuono EA, et al. Deletion of Cd2-Like (Cd2v) and C-Type Lectin-Like (Ep153r) Genes from African swine fever virus Georgia-Δ9gl abrogates its effectiveness as an experimental vaccine. *Viruses.* (2020) 12:1185. doi: 10.3390/v12101185

11. Zhou X, Li N, Luo Y, Liu Y, Miao F, Chen T, et al. Emergence of African swine fever in China, 2018. *Transbound Emerg Dis.* (2018) 65:1482–4. doi: 10.1111/tbed.12989

12. Sun E, Zhang Z, Wang Z, He X, Zhang X, Wang L, et al. Emergence and prevalence of naturally occurring lower virulent African swine fever viruses in domestic pigs in China in 2020. *Sci China Life Sci.* (2021) 64:752–65. doi: 10.1007/s11427-021-1904-4

13. Laboratory. NASFR. *Technical Guidelines for Monitoring African Swine Fever Variant Strains in Pig Farms.* (2021). Available online at: www.moa.gov.cn/govpublic/xmsyj/202103/t20210322_6364254.htm (accessed March 22, 2021).

14. Sun E, Huang L, Zhang X, Zhang J, Shen D, Zhang Z, et al. Genotype I African swine fever viruses emerged in domestic pigs in China and caused chronic infection. *Emerg Microbes Infect.* (2021) 10:2183–93. doi: 10.1080/22221751.2021.1999779

15. Gallardo C, Fernández-Pinero J, Arias M. African swine fever (Asf) diagnosis, an essential tool in the epidemiological investigation. *Virus Res.* (2019) 271:197676. doi: 10.1016/j.virusres.2019.197676

16. Wu X, Li L, Hu Y, Fan X, Zou Y, Ren W, et al. *Diagnostic Techniques for African Swine Fever. National Standard GB/T 18648-2020* Beijing: Standardization Administration. (2020).

17. Alikhan NF, Petty NK, Ben Zakour NL, Beatson SA. Blast ring image generator (Brig): simple prokaryote genome comparisons. *BMC Genom.* (2011) 12:402. doi: 10.1186/1471-2164-12-402

18. Lalitha S. Primer Premier 5. *Biotech Softw Int Rep.* (2004) 1:270–2. doi: 10.1089/152791600459894

19. Wang R, Zhang W, Ye R, Pan Z, Li G, Su S. One-step multiplex taqman probe-based method for real-time pcr detection of four canine

diarrhea viruses. *Mol Cell Probes.* (2020) 53:101618. doi: 10.1016/j.mcp.2020.101618

20. Bosch-Camós L, López E, Rodriguez F. African swine fever vaccines: a promising work still in progress. *Porcine Health Manag.* (2020) 6:17. doi: 10.1186/s40813-020-00154-2

21. Li Z, Wei J, Di D, Wang X, Li C, Li B, et al. Rapid and accurate detection of African swine fever virus by DNA endonuclease-targeted crispr trans reporter assay. *Acta Biochim Biophys Sin.* (2020) 52:1413–9. doi: 10.1093/abbs/gmaa135

22. Bisimwa PN, Ongus JR, Tiambo CK, Machuka EM, Bisimwa EB, Steinaa L, et al. First Detection of African Swine Fever (Asf) Virus Genotype X and Serogroup 7 in Symptomatic Pigs in the Democratic Republic of Congo. *Virol J.* (2020) 17:135. doi: 10.1186/s12985-020-01398-8

23. Achenbach JE, Gallardo C, Nieto-Pelegrín E, Rivera-Arroyo B, Degefa-Negi T, Arias M, et al. Identification of a new genotype of African swine fever virus in domestic pigs from Ethiopia. *Transbound Emerg Dis.* (2017) 64:1393–404. doi: 10.1111/tbed.12511

24. Ge S, Li J, Fan X, Liu F, Li L, Wang Q, et al. Molecular characterization of African swine fever virus, China, 2018. *Emerg Infect Dis.* (2018) 24:2131–3. doi: 10.3201/eid2411.181274

25. Teklue T, Sun Y, Abid M, Luo Y, Qiu HJ. Current status and evolving approaches to African swine fever vaccine development. *Transbound Emerg Dis.* (2020) 67:529–42. doi: 10.1111/tbed.13364

26. Gladue DP, Ramirez-Medina E, Vuono E, Silva E, Rai A, Pruitt S, et al. Deletion of the A137r gene from the pandemic strain of African Swine fever virus attenuates the strain and offers protection against the virulent pandemic virus. *J Virol.* (2021) 95:e0113921. doi: 10.1128/JVI.01139-21

27. Borca MV, Ramirez-Medina E, Silva E, Vuono E, Rai A, Pruitt S, et al. Development of a highly effective african swine fever virus vaccine by deletion of the I177l gene results in sterile immunity against the current epidemic Eurasia Strain. *J Virol.* (2020) 94:e02017–19. doi: 10.1128/JVI.02017-19

28. Ramirez-Medina E, Vuono E, Rai A, Pruitt S, Espinoza N, Velazquez-Salinas L, et al. Deletion of E184l, a putative diva target from the pandemic strain of African swine fever virus, produces a reduction in virulence and protection against virulent challenge. *J Virol.* (2022) 96:e0141921. doi: 10.1128/JVI.01419-21

29. Zhu W, Zeng N, Wang N. Sensitivity, specificity, accuracy, associated confidence interval and roc analysis with practical sas implementations. *NESUG Proc Health Care Life Sci.* (2010) 19:67. Available online at: https://www.lexjansen.com/nesug/nesug10/hl/hl07.pdf

frontiers | Frontiers in Veterinary Science

TYPE Original Research
PUBLISHED 20 September 2022
DOI 10.3389/fvets.2022.936781

OPEN ACCESS

EDITED BY
Luis G. Gimenez-Lirola,
Iowa State University, United States

REVIEWED BY
Gaurav Kumar Sharma,
Indian Veterinary Research Institute (IVRI), India
Jessie Trujillo,
Kansas State University, United States

*CORRESPONDENCE
Fangzhou Chen
chenfz@mail.hzau.edu.cn
Qigai He
he628@mail.hzau.edu.cn

†These authors have contributed equally to this work and share first authorship

SPECIALTY SECTION
This article was submitted to Veterinary Experimental and Diagnostic Pathology, a section of the journal Frontiers in Veterinary Science

RECEIVED 05 May 2022
ACCEPTED 03 August 2022
PUBLISHED 20 September 2022

CITATION
Zhang C, Cheng T, Li D, Yu X, Chen F and He Q (2022) Low-host double MDA workflow for uncultured ASFV positive blood and serum sample sequencing. *Front. Vet. Sci.* 9:936781. doi: 10.3389/fvets.2022.936781

Low-host double MDA workflow for uncultured ASFV positive blood and serum sample sequencing

Chengjun Zhang[1,2†], Tangyu Cheng[1,2†], Dongfan Li[2,3], Xuexiang Yu[2,3], Fangzhou Chen[1,2,3*] and Qigai He[1,2,3*]

[1]State Key Laboratory of Agricultural Microbiology, Huazhong Agricultural University, Wuhan, China, [2]College of Veterinary Medicine, Huazhong Agricultural University, Wuhan, China, [3]The Cooperative Innovation Center for Sustainable Pig Production, Huazhong Agricultural University, Wuhan, China

African swine fever (ASF) is a highly lethal and contagious disease caused by African swine fever virus (ASFV). Whole-genome sequencing of ASFV is necessary to study its mutation, recombination, and trace its transmission. Uncultured samples have a considerable amount of background DNA, which causes waste of sequencing throughput, storage space, and computing resources. Sequencing methods attempted for uncultured samples have various drawbacks. In this study, we improved C18 spacer MDA (Multiple Displacement Amplification)-combined host DNA exhaustion strategy to remove background DNA and fit NGS and TGS sequencing. Using this workflow, we successfully sequenced two uncultured ASFV positive samples. The results show that this method can significantly reduce the percentage of background DNA. We also developed software that can perform real-time base call and analyses in set intervals of ASFV TGS sequencing reads on a cloud server.

KEYWORDS

African swine fever, next generation sequencing (NGS), genome sequencing, nanopore sequencing, workflow

Introduction

The African swine fever virus (ASFV) is the only member of the Asfarviridae family that causes contagious and lethal diseases. The first case of ASF was reported in Kenya in 1921 (1), while it was first documented in 2018 in China (2). Since then, 14 countries reported an ASFV outbreak between 2018 and 2021 in Southeast Asia (3). The disease has caused significant economic loss to the pig industry worldwide. So far, there have been no commercially effective vaccines, although inactivated, subunit, DNA, and gene-deleted vaccines that could offer at least partial protection against ASF exist (4, 5). A few gene-deletion vaccines and poxvirus vector-based vaccines have shown promising results in animals (6, 7), but further research is needed before their commercialization. Until now, ASFV has still been considered the most threatening virus for the pig industry.

ASFV is a double-stranded DNA virus of about 180–220-nm long. Its genome size is around 170–190 kb and encodes 150 proteins. Based on the 3'-term of the B464L gene, ASFV can be divided into 24 genotypes (8). However, previous studies have indicated that B464L is a relatively conserved gene. Research has been conducted to study different isolates, and it has been concluded that even those with the same genotype can have different phenotypes. A study showed several recombination possibilities between different strains (9). Experiments confirmed that some gene deletion viruses show widely varying virulence (6, 10, 11). Whole genome sequencing is considered necessary to better analyze this variation.

The first research on the ASFV genome using Sanger sequencing was published in 1995 (12). Nowadays, we can easily use high throughput sequencing platforms like MGI, Illumina, and Ion torrent to perform NGS sequencing. However, unlike the human or bacterial genome, the ASFV genome is small, and the uncultured clinical tissue and blood samples have a considerable amount of background DNA from the host, causing the ASFV reads to occupy between 0.01 and 0.1% of the total DNA (13, 14). Sequencing that can reach a hundred times the sequencing depth of the ASFV genome is usually needed to obtain a high-quality genome, implying that about 20–200 G of data is required to obtain the ASFV genome. This process, including the analysis and storage of data, can be very costly. Many attempts are being made to obtain the ASFV genome with low-cost techniques. Some experiments were conducted based on un-methylated DNA enrichment in sequencing. This implies removing the highly methylated host DNA (13, 15). Other trials were based on bait hybridization and used 11,958 biotinylated RNA-baits and Streptavidin beads to bait the DNA library that can hybridize with these baits (16). Long amplicon sequencing can also be applied, where only 40% of the region of the ASFV genome is focused on by using 6 pairs of primers to cover those regions (17). We compare these methods in Table 1 and conclude that researchers either faced difficulties with biased results, limited application, or the need to synthesize an extensive bait library.

Unlike the NGS sequencing method based on terminal end fluorescent-labeled dNTP and optical signal reader, TGS sequencing technology is developed on nanopore and electrical signal analysis. In this case, the sequencing equipment is smaller and can respond to real-time analysis. It can also generate longer reads and is not affected by GC bias. Long reads simplify the appraisal of deletions, insertions, translocations, and other genome-wide changes (18). They can also help cross high complex and repeated regions of the ASFV genome in the assembling stage (14). A study was conducted to sequence the ASFV genome using the Nanopore sequencing method and obtained 0.15% of the reads mapped to the ASFV genome (19). TGS needs high quality and a sufficient amount of long DNA to ensure it can successfully build the library and obtain satisfactory sequencing efficiency. Compared with NGS, which involves parallel sequencing of millions of reads, TGS has only 512 (the MinION and GridION flow cell) and 2,675 (the PromethION flow cell) nanopores to perform sequencing at the same time, implying that it is more sensitive to background DNA when sequencing an impure sample. Furthermore, the chip's life is highly affected by accumulated sequencing time and background DNA, indicating a need for longer sequencing time and higher cost.

After removing background DNA, the DNA concentration is usually $<$ 200 pg/ul, making it challenging to build the TGS library for sequencing. MDA (multiple displacement amplification) is a method for DNA amplification that is widely used in genome amplification. MDA is based on a DNA polymerase called phi29 found in the Bacillus subtilis phage. This DNA polymerase is low biased and, compared to other DNA polymerases, has advantageous features, such as high fidelity, strong strand displacement, and ongoing isothermal amplification. DNA can be amplified a thousand times in a typical overnight reaction, and DNA larger than 10 Kb can be yielded, making it optimum for TGS sequencing. However, MDA is unsuitable for ultra-low DNA input ($<$10 ng), which is the starting material obtained after treatment with our nuclease digestion strategy. This is due to the high percentage of junk DNA generated by template-independent amplification (20, 21). Researchers found that using a 5′ end block with a C18 spacer random primer can eliminate template-independent amplification (22). However, as the stand procedure of Oxford nanopore protocol requires the adaptor and barcode to ligate to 5′ ends of DNA, it is assumed that the 5′ end block with a spacer can avoid DNA ligation with adaptor and nanopore sequencing. Moreover, hyper-branched DNA, the final form of MDA product, will also block the nanopore, resulting in low sequencing efficiency and potential death of the nanopore. These issues need to be solved so that nanopores can be used to sequence ASFV samples.

In this study, we combine nuclease enzyme mix digestion and double MDA to generate low host percentage and enough long DNA for NGS and TGS library building (Figure 1). We successfully used our LHDM workflow to sequence two uncultured ASFV positive samples. Because of the significant reduction of background DNA percentage, we were able to obtain the genome of ASFV from the uncultured sample at low costs in the sequencing throughput, smaller storage space, and computing resources. TGS can provide an early estimate of samples before NGS and help in the assembly because of its flexibility and its ability to sequence long reads. Using the LHDM TGS software we developed, real-time analysis can be done for ASFV TGS sequencing on the cloud server.

TABLE 1 Sequencing strategy for an uncultured sample compared with LHDM.

	Required sequencing data	Bias	Cost	Fit with third generation sequencing
Directly sequencing	Very high	Low	High (sequencing cost)	Yes, but not recommended
Hybrid capture method	Low	Relatively high	High (library)	No
Long distance PCR method	Low	High(can get full genome)	Low	Contrived
Un-methylated DNA enrichment	Relatively high	Low	Relatively high (sequencing cost)	Yes
LHDM (workflow in this research)	Relatively low	Low	Low	Yes

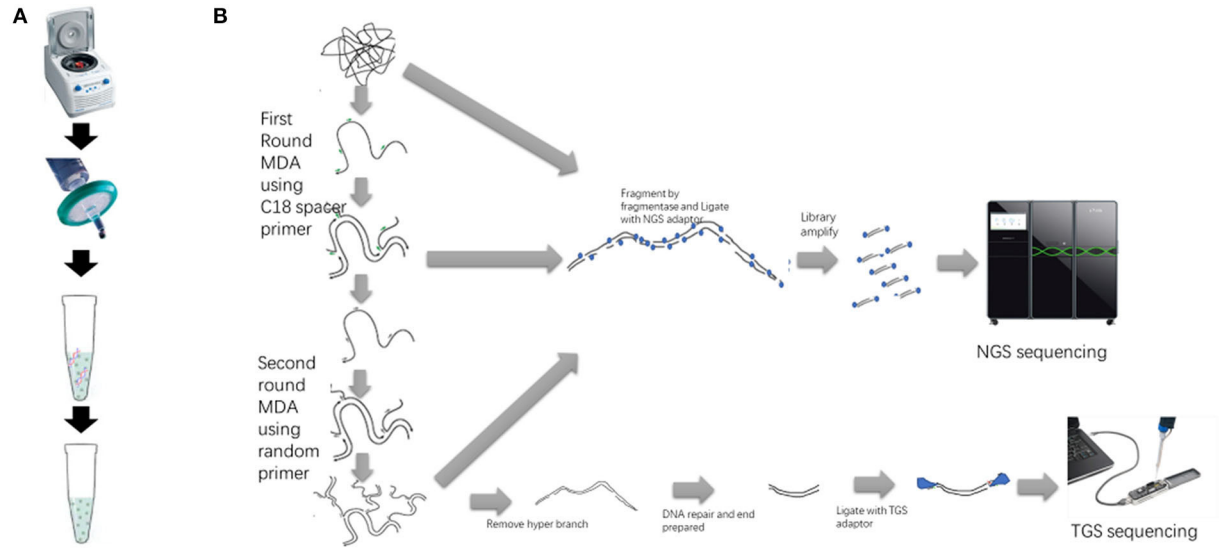

FIGURE 1
Sample preparation, double MDA, and library preparation workflow of NGS and TGS. **(A)** The sample preparation procedure includes centrifugation, filtration, and digestion with DNase mix. **(B)** The sequencing library preparation procedure. The first-round MDA product and the second-round MDA product can also be used to build the NGS library.

Materials and methods

Sample collection and preparation

Blood samples were collected from suspected ASF-infected pigs, Sample 1 being a serum sample and Sample 2 an anti-agglutinated blood sample. Two cycles of freezing and thawing were carried out to induce cell rupture. The samples were centrifuged at 8,000 × g for 10 min and then filtered using a 0.45-μm filter. A 100-μl sample was diluted to 200 μl to obtain a solution of 15-mM Tris-HCL, 30-mM $MgCl_2$, 2× anti-anti (Thermofisher15240062). Approximately, 11 μl of enzyme mix [5-μl DNase I (Takara 2270A), 5-ul Turbo DNAse (ThermofisherAM2239), 1-μl ultranuclease (Hzymes HBP000107)] were added, and the sample was placed in an incubator at 37°C for 1 h. After adding 15-ul 0.5-M EDTA, DNases were inactivated by Qiagen buffer AL and Proteinase K at 60°C for 20 min, and the DNA was extracted using the Qiagen DNA mini kit (51304).

DMDA amplification

Approximately 10.6-μl DNA and a 5-μl 100-μM 5'end block with a C18 spacer random primer were denaturalized

at 95°C for 5 min. Approximately, a 2-μl 10 × Phi29DNA polymerase buffer, 0.4-μl BSA, 1-μl 10-mM DNTP, and 10-U Phi29DNA polymerase were added to each sample, and then incubated under 28°C for 15 h. The sample was purified using the Monarch PCR & DNA cleanup kit (NEB T1030S). A volume of 10.6-μl purified DNA, and a 5-μl 100-μM random primer were used, and the first round of reaction repeated at an incubation temperature of 30°C for 6 h. The Equalbit 1 × dsDNA HS Assay Kit (Vazyme EQ121-011) was used to qualify DNA concentration. Approximately, 10-U S1 Nuclease (Takara 2410A) for 1-ug double-strand DNA was added to the DNA to remove hyper-branched parts of DNA. After digestion at 23°C for 20 min, the sample was purified using the Monarch PCR & DNA cleanup kit (NEB T1030S).

TGS library preparation

A TGS library was prepared using the Oxford nanopore technology Native barcoding amplicons (with EXP-NBD104, EXP-NBD114, and SQK-LSK109) protocol. Approximately, 600-ng DNA was used as starting material. The Monarch PCR & DNA cleanup kit (NEB T1030S) was used to purify the samples rather than AMPure XP beads after the DNA repair and end preparing step. In the last step, the beads were washed using SFB (Short Fragment Buffer).

NGS library preparation

An NGS library was constructed using VAHTS Universal Plus DNA Library Prep Kit (Vazyme, NDM617). Approximately, 10-ul DNA was added to FEA reaction and incubated at 37°C for 17 min for fragmentation. Approximately, 1:20 diluted DNA Adapters for MGI (vazyme, NM108) was used in Adapter Ligation. Approximately, 17 PCR cycles were used in the library amplification stage. Size selection was then carried out using 68 ul in the first round and 20 ul in the second round. For samples not treated by DNase mix, 1:10- and 1:2-diluted DNA Adapters were used, separately.

TGS sequencing

Sequencing was performed on an R9.4.1 flowcell with a Minion device (Oxford nanopore technology). The Minokow software was used to collect the raw signal on a laptop. Approximately, 4,000 reads were set for a fast5 file. Basecalling in Minokow was disabled. Using our software, raw fast5 files were uploaded to a cloud computer with 2080ti GPU to perform real-time basecall and coverage analysis.

Results

NGS sequencing result

NGS sequencing was performed on the MGI T7 platform. Approximately, 15.17-M and 31.94-M reads from Samples 1 and 2 were obtained, respectively. After removing adaptors and the low-quality base, Sample 1 maintained 13.66-M high-quality reads, and Sample 2 maintained 29.36-M high-quality reads. By mapping to reference, both paired reads were considered as Mapped reads. Approximately, 1.4% of reads from Sample 1 were mapped to the ASFV genome, and Sample 2 had 44.9% reads mapped to the ASFV genome. Compared with the sample not treated by DNase mix, the ASFV reads had been raised 46 and 112 times, respectively. Detailed results are shown in Table 2.

TGS sequencing result

After 8-h run, sequencing was stopped, and the R9.4 flow cell was washed. Base-calling and barcoding were performed. A total of 1.97-G data and 1.5-M reads were obtained. The longest read was 325,663 bp, which was not ASFV nuclear acid. After mapping to the Pig/HLJ/2018 strain, the mapping rate was 3.62 and 0.02%. Details of sequencing are shown in Table 3. Read length and quality are shown in Figure 2.

Real-time analysis by TGS

Our set in Minokow was generating one fast5 for every 4,000 reads. Our software (Figure 3) was set to upload new files to cloud GPU in the 1st hour after 5 new fast5 had been generated. This takes about 5 min. Based on real-time analysis by our software, the first ASFV reads were detected for Sample 2 and Sample 1 after 5 and 10 min, respectively. Approximately, 30-x depth is the requirement for the assembly in most assembled software. Genome coverage of Sample 2 reached 81% within the first 5 min, 92% within 10 min, and 99% within 40 min. Position with 30-x depth reached 90% in 2.5 h and 99% in 7.7 h. Detailed results are shown in Figure 4 below. The dataflow and the interface of LHDM-ASFV-TGS software are shown in Figure 3.

Metagenomic analysis of NGS and TGS data

Because of the low-mapping rate of Sample 1, and reads mapped ratio difference between TGS and NGS, a metagenomic analysis was performed using Kraken2 and the minusb database, which contains all the virus genomes. Results (Figure 5) showed

TABLE 2 NGS sequencing data information and the mapping rate to ASFV genome.

	Raw reads	Raw base	Reads after filter by fastp	Base After filter by fastp	Q30 base after filter	Mapped readsand mapping rate to ASFV genome
Sample 1-untreated	30.93 M	4.63 G	30.91 M	4.51 G	4.32 G	11.25 K (0.03%)
Sample 1	15.17 M	2.28 G	13.66 M	1.94 G	1.73 G	0.19 M (1.4%)
Sample 2-untreated	37.89 M	5.68 G	37.87 M	5.46 G	5.16 G	157.60 K (0.4%)
Sample 2	31.94 M	4.79 G	29.36 M	4.12 G	3.65 G	13.20 M (44.9%)

TABLE 3 TGS sequencing data information and the mapping rate to ASFV genome.

	Reads	Reads N50	Longest read length	Total base	Reads mapped rate to ASFV genome	Mapped reads N50	Longest read length
Sample 1	658,546	2,264	325,663	0.90 G	126 (0.02%)	4,113	12,714
Sample 2	925,609	2,175	30,327	1.17 G	33,482 (3.62%)	2,464	27,106

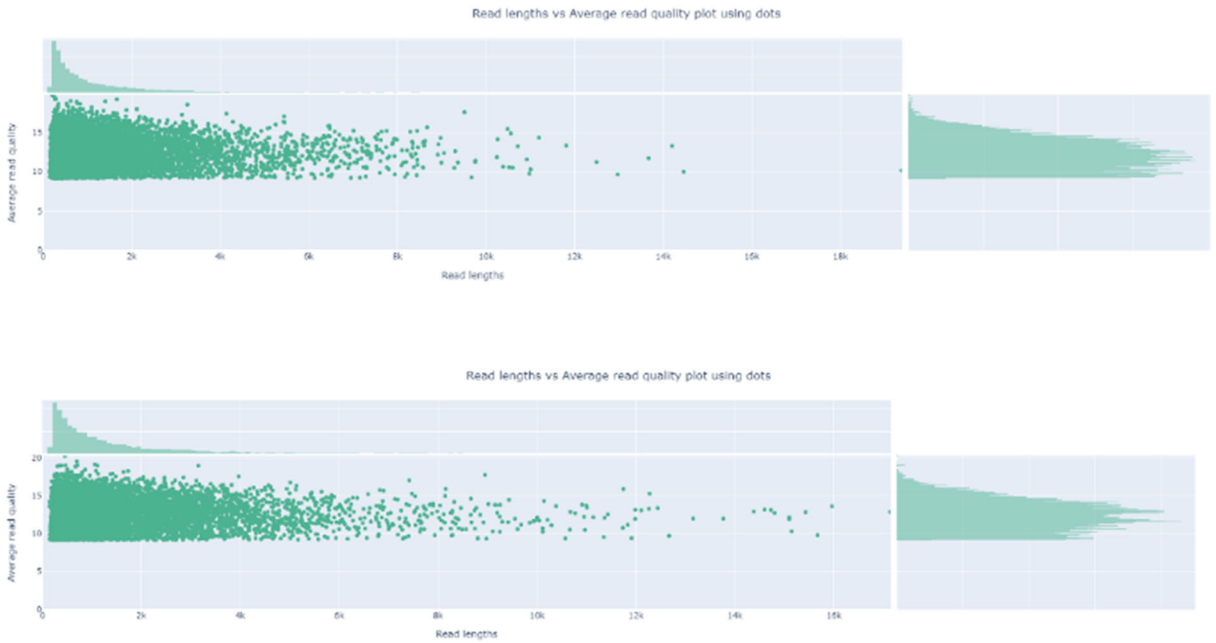

FIGURE 2
Read Length and the average read quality plot. The read length and quality were visualized by nanoplot.

that Torque teno sus virus (42% in Sample 1 and 53% in Sample 2), a single-stranded circular DNA virus, occupied most reads in the TGS result.

There was no Sus Scrofa genome in the kraken2 database. Hence, bowtie2 was used to map unclassified reads to the sus scrofa genome. The mapping rates were 61.84 and 72.37% for Sample 1 and Sample 2, respectively, implying that most of the unhit reads belonged to unknown species in our sample.

Assembled genome information

Considering that not all the background DNA belongs to pig and that a high percentage of reads belonged to unknown species, we chose to map all the reads to the ASFV genome before assembly. Because of the high depth, NGS Assembly was relatively easy. TGS reads of Sample 1 were insufficient for assembly. Hence, no TGS

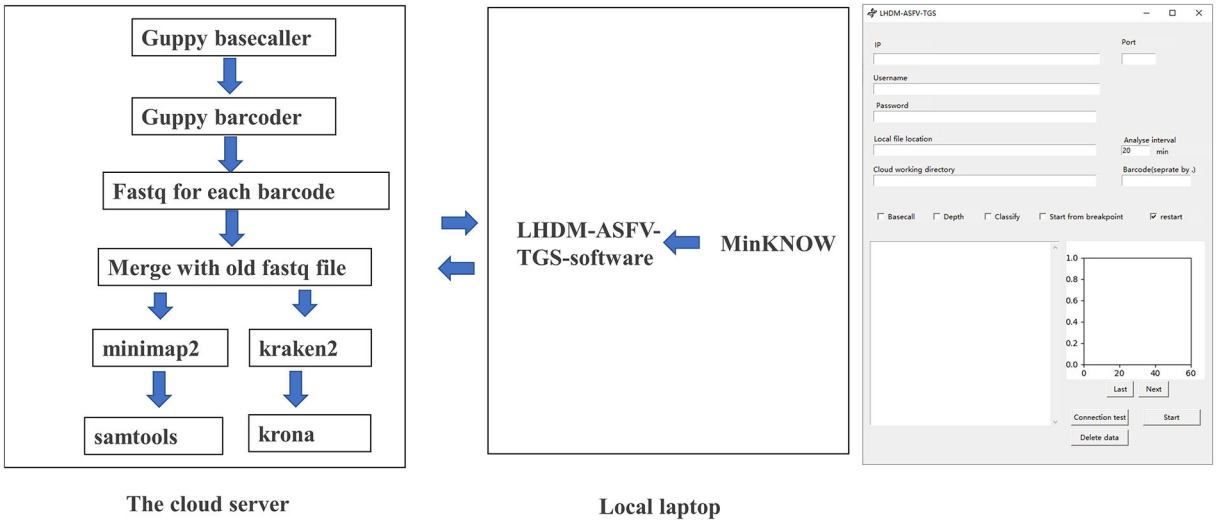

FIGURE 3
The analysis dataflow and the interface of LHDM-ASFV-TGS software.

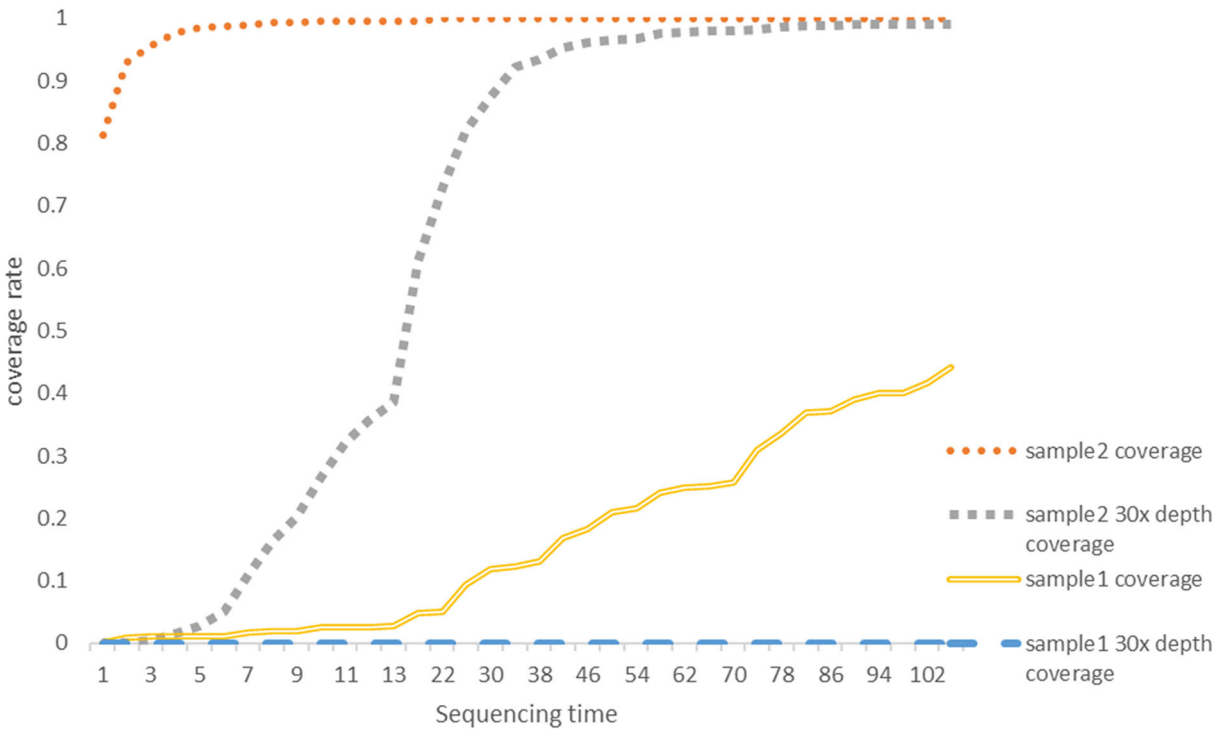

FIGURE 4
The genome coverage rate with a sequencing time graph. The coverage data were generated by LHDM-ASFV-TGS software. The units of the X axis are 5 min; the vertical axis represents the coverage rate; 30-x depth means for a specific site in the genome of ASFV was sequencing at least 30 times. Each curve represents the coverage and the 30-x coverage rate of Sample 1 and Sample 2 on the graph.

contig of Sample 1 was generated. Assembly was done by canu and Flye, respectively. NGS and TGS contigs were connected by ragtag and hand. Medak polished TGS scaffold. The final genomes of Sample 1-NGS, Sample 2-NGS, and Sample 2-TGS were 187,984, 188,050, and 186,575, respectively.

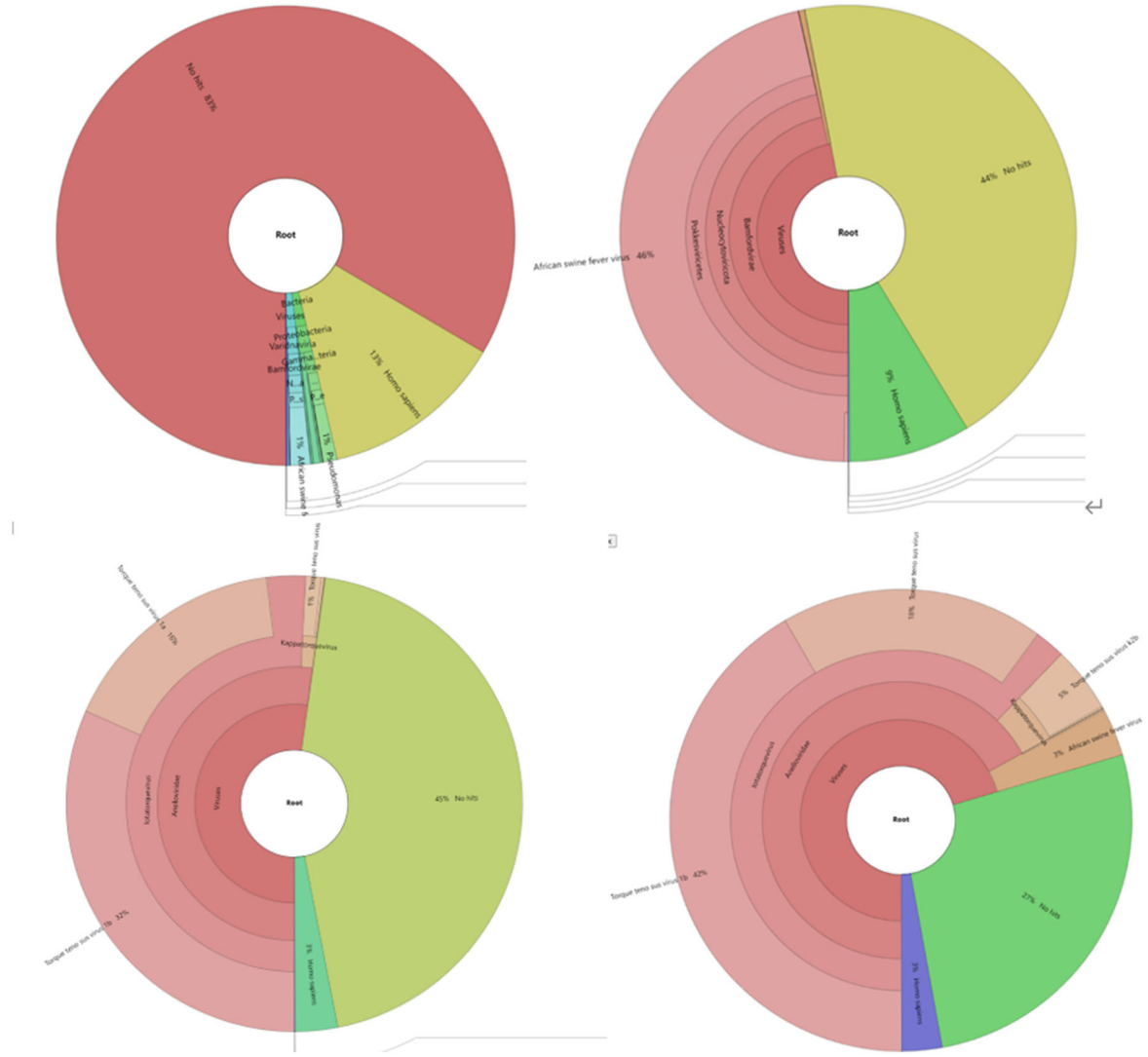

FIGURE 5
Metagenomic analysis of sequencing data with the Minisub database and kraken2. Different species are shown in different colors. (1) Metagenomic classification results of Sample1 NGS sequencing results; results for ASFV shown in blue. (2) Metagenomic classification results of Sample 1 NGS sequencing results, results for ASFV shown in pink. (3) Metagenomic classification results of Sample 1 TGS sequencing results, results for ASFV not shown due to low-percentage reads. (4) Metagenomic classification results of Sample 2 TGS sequencing results, results for ASFV shown in light brown color.

Genome phylogenetic and mutation analysis

Based on the genome phylogenetic tree in Figure 6, it was deduced that the two isolates of Sample 1 and Sample 2 were closest to ASFV-SY18 and HRB/2020 isolates, respectively. The two isolates might be the Offspring of the first reported isolate PIGHLJ/2018 in China. Full genomes offer more information for virus evolution and traceability.

Compared to PIG/HLJ/2018, Sample 1 had 5 single sites in genes MGF_110-3L, MGF_360-6L, A240L and C475L, and Sample 2 had 8 single-site mutations in genes MGF_300-1L, MGF_505-2R, MGF360-15R, F1055L, CP530R, NP1450L, and I215L. Sample 1 had 3 single nucleic acid deletions in genes MGF 300-2L, MGF 110-7L, and MGF 110-14L and 1 partial deletion in gene MGF 110-114L. Sample 2 had 1 single site deletion in gene I11L, 2 single-site insertions in gene MGF110-7L and gene D1133L, and 2 partial deletions in gene ASFV_G_ACD_00350 and MGF_110-13L. There was no gene-wide gene deletion in the two isolates. Detailed information can be found in Supplementary Tables S1, S2.

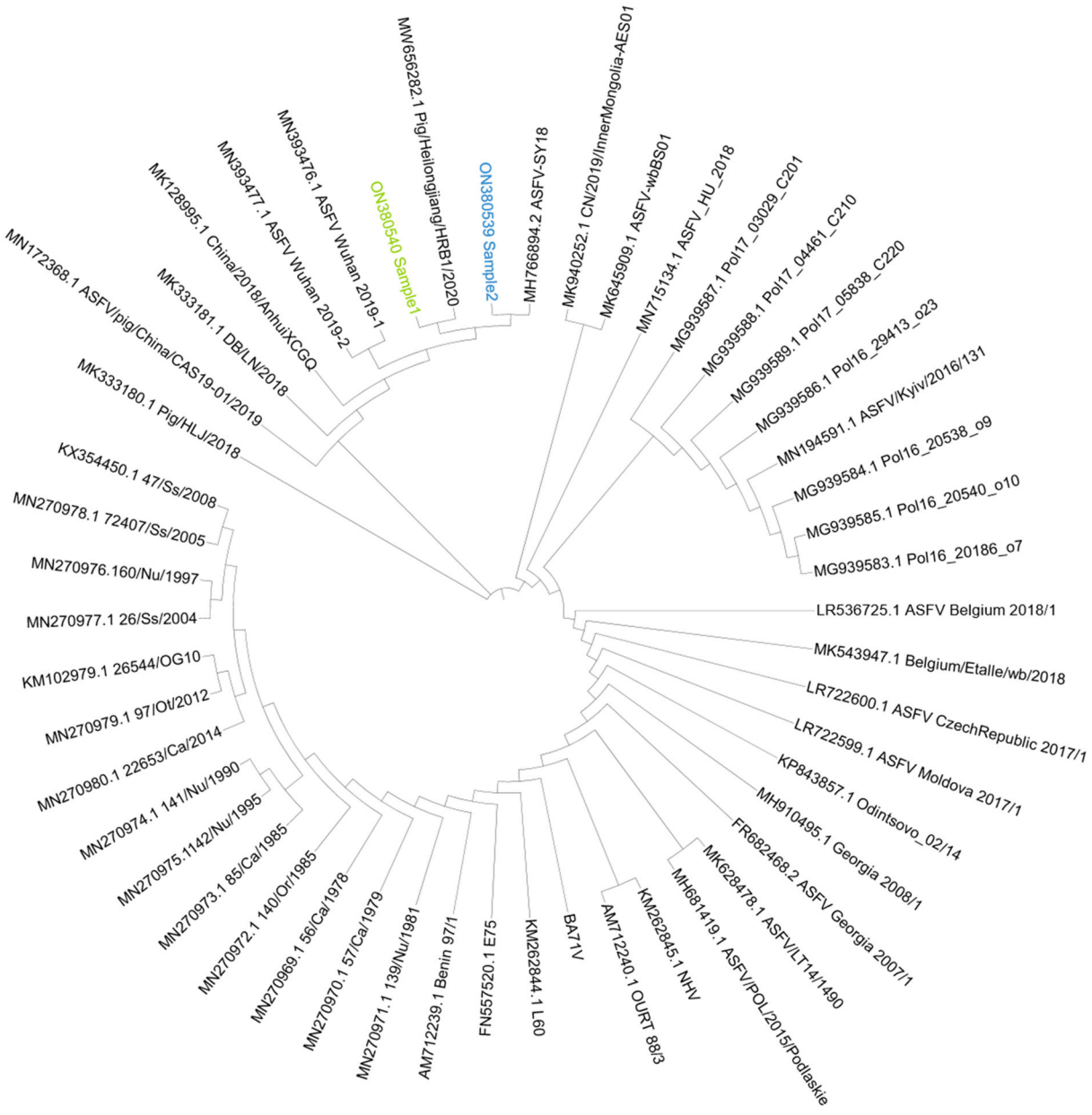

FIGURE 6
The genome phylogenetic tree. The phylogenetic tree was constructed by iqtree and visualized by ITOL. Sample 1 was marked as green, and Sample 2 was marked as blue.

Comparison between TGS assemble and NGS assemble

Compared to the NGS assemble, the TGS assemble has 110 indel sites, out of which 14 were insertion sites, all being in the poly region. Approximately, 96 nucleotides were deleted, out of which 44 were from the poly region, 1 from the non-poly region, and 51 from the segment deletion. There is no SNP site when comparing TGS with the NGS assemble. All the indel information can be found in Supplementary Table S3.

Discussion

It is possible to obtain low-host DNA with a high percentage of the ASFV genome using our enzyme mix and buffer settings.

ASFV occupied 1.4 and 44% of the total reads in the two NGS samples, which is a significant improvement compared to the untreated sample. However, the elimination of background DNA depends on digesting cell-free nucleic acids and requires complete unbroken virion. The DNA of inactivate virus can also be digested, depending on how the virus was inactivated. This workflow needs a sample with a lived virus, implying that it needs to be processed in an ABSL-3 laboratory and might limit its usage.

It was observed that the concentration of Mg^{2+} in the buffer depended on the common sample type. Mg^{2+} is also critical to enzymatic activity. Since most blood samples were collected using the EDTA anticoagulation tube, a reaction buffer with a final concentration of 30-mM Mg^{2+} and 15 mM of Tris-HCL was used in this study. NGS data show that the ASFV DNA percentage was at the same level as the host, showing that the enzyme was used at its optimum efficiency in our experiment.

It is also important to consider that this workflow sequences all DNA viruses, including bacteriophages. If the sample was contaminated, bacteria and bacteriophages could replicate very fast. Phages cannot be removed using this workflow, so it is crucial to ensure that an unspoiled sample is used.

TGS can generate very long reads, and we obtained the longest read of 27 Kb, covering 14% of the ASFV genome. The long reads can help us easily cross repeated regions when assembling and quickly find the indel gene.

The TGS sequencing base call requires a high-performance GPU. Most laptops might not be able to carry out this process effectively due to the need for long hours of continuous work, increasing the risk of overheating. This partly limits the usage of nanopore technology. In this study, we wrote the script to automatically upload the sequencing data and analyses to other Linux GPU servers, which is the most accessible solution to this issue.

More than 24–30 h was needed to finalize the NGS PE150 sequencing, especially for the sequencing of a low host sample that only needs a very low output yield. In this case, a large amount of samples is necessary for one run. TGS sequencing can be stopped at any time, and the chip reused, making the sequencing process more flexible. Our software can help decide when to stop sequencing. Sample 1 of TGS showed a low percentage of ASFV reads. We did not keep sequencing to get enough ASFV depth. At this stage, sequencing follows the Bernoulli process. Its sensitivity depends on the target-sample background ratio. Only increasing the sequencing output has a limited effect (23). Our software can be downloaded on the following link https://github.com/chauncyzhang/LHdMDAsoftware.

Running the NGS equipment whenever needed is neither practical nor cost-effective in most cases and laboratories. It usually takes more than 3 weeks to get NGS data from commercial companies on the market, especially considering the low data requirements for each sample. We can use TGS to decide whether the sample should be sequenced and how much data are suitable for the sample.

Because the DNA input is usually lower than all commercial kit ranges, it may fail when building the NGS library. We successfully built the NGS library using our protocol because a junk DNA phenomenon is prevented by the C18 spacer random primer. The output of Step 1 MDA or Step 2 can also be used as the starting material to build the NGS library.

According to our TGS results, the torque teno sus virus (42% reads in Sample 1 and 53% reads in Sample 2) has a single-stranded circular DNA, occupying a considerable percentage of total reads. Single-stranded circular DNA cannot be built into the NGS library using our method but can be amplified by the TGS workflow. Meanwhile, all double-strand DNA can be built into the TGS Library, the same as NGS. Because of high-background DNA and amplification of ssDNA and circle DNA, the sequencing results are unacceptable, so we did not perform TGS on the untreated sample by DNAse mix. Considering the high positive rate of this virus in pigs (40–100%) (24, 25), AMPure XP Beads or high molecular weight DNA extract kits (e.g., Qiagen 12462 or NEB T3060L) can be used to remove the TTSV DNA from the virus for further experimentation. These kits can assist in the removal of small circular DNA and increase the input DNA length.

Growth of ASFV in PAM cells and ultracentrifuge can also be used to obtain low-host high amount of ASFV DNA but requires the use of an ABSL-3 lab for virus isolation and passage. However, there is no ultracentrifuge equipment in some ABSL-3 laboratories. It has been reported that ASFV may lose some genes in the MGF region in the passage in 293T cells (26). Nevertheless, according to our results, there are only a few mutations in these two isolates, and other isolates sequenced by some research also only have a few mutations (19, 27). Considering that ASFV may mutate during the passage, it might be a better strategy to carry out sequencing before virus isolation.

Compared to the NGS assemble, we found that most false sequencing occurs in repeat poly regions by TGS, which is one of the drawbacks of TGS. We still need NGS data to polish the TGS genome at this time, but the quality of the TGS assemble is high and can also provide a certain amount of information. With the release of the R10 flow cell and Q20+ reagent, it is possible to obtain higher-quality TGS sequencing data.

Data availability statement

The datasets presented in this study can be found in online repositories. The names of the repository/repositories and accession number(s) can be found below:

https://www.ncbi.nlm.nih.gov/genbank/, ON380539; https://www.ncbi.nlm.nih.gov/genbank/, ON380540.

Author contributions

CZ, FC, and QH contributed to the conception or design of the work and drafted the manuscript. CZ and TC completed the most experiments and data analysis. DL and XY had contribution on sample obtain process and other experiments. QH managed the whole project. FC and QH applied the fundings. All authors have reviewed and edited the manuscript, contributed to the article, and approved the submitted version.

Funding

This project was funded by the Epidemiological Characteristics and Evolution of African Swine Fever Virus and Early Detection Technology (31941004), Young Scientists Fund of the National Natural Science Foundation of China (Grant No. 31902300), and the Research and Application of Key Technology Against African Swine Fever (2019ABA089).

Conflict of interest

The authors declare that the research was conducted in the absence of any commercial or financial relationships that could be construed as a potential conflict of interest.

Publisher's note

Supplementary material

The Supplementary Material for this article can be found online at: https://www.frontiersin.org/articles/10.3389/fvets.2022.936781/full#supplementary-material

References

1. Gogin A, Gerasimov V, Malogolovkin A, Kolbasov D. African swine fever in the north caucasus region and the Russian Federation in years 2007–2012. *Virus Res.* (2013) 173:198–203. doi: 10.1016/j.virusres.2012.12.007

2. Ge S, Li J, Fan X, Liu F, Li L, Wang Q, et al. Molecular characterization of african swine fever virus, China, 2018. *Emerging Infect Dis.* (2018) 24:2131. doi: 10.3201/eid2411.181274

3. Tran XH, Le TTP, Nguyen QH, Do TT, Nguyen VD, Gay CG, et al. African swine fever virus vaccine candidate Asfv-G-Δi177l efficiently protects european and native pig breeds against circulating vietnamese field strain. *Transboundary Emerging Dis.* (2021) 69:e497–504. doi: 10.1111/tbed.14329

4. Argilaguet JM, Pérez-Martín E, Nofrarías M, Gallardo C, Accensi F, Lacasta A, et al. DNA vaccination partially protects against african swine fever virus lethal challenge in the absence of antibodies. *PLoS ONE.* (2012) 7:e40942. doi: 10.1371/journal.pone.0040942

5. Gaudreault NN, Richt JA. Subunit vaccine approaches for african swine fever virus. *Vaccines.* (2019) 7:56. doi: 10.3390/vaccines7020056

6. Chen W, Zhao D, He X, Liu R, Wang Z, Zhang X, et al. A seven-gene-deleted african swine fever virus is safe and effective as a live attenuated vaccine in pigs. *Sci China Life Sci.* (2020) 63:623–34. doi: 10.1007/s11427-020-1657-9

7. Lopera-Madrid J, Medina-Magües LG, Gladue DP, Borca MV, Osorio JE. Optimization in the expression of asfv proteins for the development of subunit vaccines using poxviruses as delivery vectors. *Sci Rep.* (2021) 11:1–12. doi: 10.1038/s41598-021-02949-x

8. Arias M, Jurado C, Gallardo C, Fernández-Pinero J, Sánchez-Vizcaíno J. Gaps in African swine fever: analysis and priorities. *Transboundary Emerging Dis.* (2018) 65:235–47. doi: 10.1111/tbed.12695

9. Zhu Z, Xiao C-T, Fan Y, Cai Z, Lu C, Zhang G, et al. Homologous recombination shapes the genetic diversity of african swine fever viruses. *Vet Microbiol.* (2019) 236:108380. doi: 10.1016/j.vetmic.2019.08.003

10. Ramirez-Medina E, Vuono EA, Rai A, Pruitt S, Silva E, Velazquez-Salinas L, et al. Evaluation in swine of a recombinant african swine fever virus lacking the MGF-360-1l gene. *Viruses.* (2020) 12:1193. doi: 10.3390/v12101193

11. Li D, Liu Y, Qi X, Wen Y, Li P, Ma Z, et al. African swine fever virus mgf-110-9l-deficient mutant has attenuated virulence in pigs. *Virologica Sinica.* (2021) 36:187–95. doi: 10.1007/s12250-021-00350-6

12. Yanez RJ, Rodriguez JM, Nogal ML, Yuste L, Enriquez C, Rodriguez JF, et al. Analysis of the complete nucleotide sequence of african swine fever virus. *Virology.* (1995) 208:249–78. doi: 10.1006/viro.1995.1149

13. De Oliveira RP, Lucas P, Chastagner A, De Boisseson C, Vial L, Le Potier M-F, et al. Evaluation of un-methylated DNA enrichment in sequencing of African swine fever virus complete genome. *J Virol Methods.* (2020) 285:113959. doi: 10.1016/j.jviromet.2020.113959

14. Forth JH, Forth LF, Blome S, Höper D, Beer M. African swine fever whole-genome sequencing—quantity wanted but quality needed. *PLoS Pathogens.* (2020) 16:e1008779. doi: 10.1371/journal.ppat.1008779

15. Ndlovu S, Williamson A-L, Malesa R, Van Heerden J, Boshoff CI, Bastos AD, et al. Genome sequences of three African swine fever viruses of genotypes I, Iii, and Xxii from South Africa and Zambia, isolated from ornithodoros soft ticks. *Microbiol Resource Announcements.* (2020) 9:e01376–19. doi: 10.1128/MRA.01376-19

16. Forth JH, Forth LF, King J, Groza O, Hübner A, Olesen AS, et al. A deep-sequencing workflow for the fast and efficient generation of high-quality african swine fever virus whole-genome sequences. *Viruses.* (2019) 11:846. doi: 10.3390/v11090846

17. Meekins DA, Trujillo JD, Gaudreault NN, Morozov I, Pérez-Núñez D, Revilla Y, et al. Long amplicon sequencing for improved genetic characterization of african swine fever virus. *J Virol Methods.* (2020) 285:113946. doi: 10.1016/j.jviromet.2020.113946

18. Athanasopoulou K, Boti MA, Adamopoulos PG, Skourou PC, Scorilas A. Third-generation sequencing: the spearhead towards the radical transformation of modern genomics. *Life.* (2021) 12:30. doi: 10.3390/life12010030

19. Jia L, Jiang M, Wu K, Hu J, Wang Y, Quan W, et al. Nanopore sequencing of African swine fever virus. *Sci China Life Sci.* (2020) 63:160–4. doi: 10.1007/s11427-019-9828-1

20. Nelson JR. Random-Primed, Phi29 DNA polymerase-based whole genome amplification. *Curr Protocols Mol Biol.* (2014) 105:15.3. 1-.3. 6. doi: 10.1002/0471142727.mb1513s105

21. Pan X, Durrett RE, Zhu H, Tanaka Y, Li Y, Zi X, et al. Two methods for full-length rna sequencing for low quantities of cells and single cells. *Proc Natl Acad Sci.* (2013) 110:594–9. doi: 10.1073/pnas.1217322109

22. Wang W, Ren Y, Lu Y, Xu Y, Crosby SD, Di Bisceglie AM, et al. Template-dependent multiple displacement amplification for profiling human circulating RNA. *Biotechniques.* (2017) 63:21–7. doi: 10.2144/000114566

23. Ebinger A, Fischer S, Höper D. A theoretical and generalized approach for the assessment of the sample-specific limit of detection for clinical metagenomics. *Comput Struct Biotechnol J.* (2021) 19:732–42. doi: 10.1016/j.csbj.2020.12.040

24. Aramouni M, Segalés J, Cortey M, Kekarainen T. Age-related tissue distribution of swine torque teno sus virus 1 and 2. *Vet Microbiol.* (2010) 146:350–3. doi: 10.1016/j.vetmic.2010.05.036

25. Xiao C-T, Giménez-Lirola L, Huang Y-w, Meng X-J, Halbur PG, Opriessnig T. The prevalence of torque teno sus virus (TTSUV) is common and increases with the age of growing pigs in the United States. *J Virol Methods.* (2012) 183:40–4. doi: 10.1016/j.jviromet.2012.03.026

26. Wang T, Wang L, Han Y, Pan L, Yang J, Sun M, et al. Adaptation of African swine fever virus to Hek293t cells. *Transboundary Emerging Dis.* (2021) 68:2853–66. doi: 10.1111/tbed.14242

27. Sun E, Zhang Z, Wang Z, He X, Zhang X, Wang L, et al. Emergence and prevalence of naturally occurring lower virulent African swine fever viruses in domestic pigs in China in 2020. *Sci China Life Sci.* (2021) 64:752–65. doi: 10.1007/s11427-021-1904-4

frontiers | Frontiers in Veterinary Science

TYPE Original Research
PUBLISHED 23 September 2022
DOI 10.3389/fvets.2022.971841

OPEN ACCESS

EDITED BY
Wentao Li,
Huazhong Agricultural University, China

REVIEWED BY
Gaurav Kumar Sharma,
Indian Veterinary Research Institute (IVRI), India
Baochao Fan,
Jiangsu Academy of Agricultural Sciences (JAAS), China

*CORRESPONDENCE
Jianchao Wei
jianchaowei@shvri.ac.cn
Zhiyong Ma
zhiyongma@shvri.ac.cn

SPECIALTY SECTION
This article was submitted to Veterinary Experimental and Diagnostic Pathology, a section of the journal Frontiers in Veterinary Science

RECEIVED 17 June 2022
ACCEPTED 05 September 2022
PUBLISHED 23 September 2022

CITATION
Yang Y, Xia Q, Sun Q, Zhang Y, Li Y, Ma X, Guan Z, Zhang J, Li Z, Liu K, Li B, Shao D, Qiu Y, Ma Z and Wei J (2022) Detection of African swine fever virus antibodies in serum using a pB602L protein-based indirect ELISA. *Front. Vet. Sci.* 9:971841. doi: 10.3389/fvets.2022.971841

Detection of African swine fever virus antibodies in serum using a pB602L protein-based indirect ELISA

Yang Yang[1], Qiqi Xia[1], Qin Sun[1,2], Yan Zhang[1,2], Yuhao Li[1], Xiaochun Ma[1], Zhixin Guan[1], Junjie Zhang[1], Zongjie Li[1], Ke Liu[1], Beibei Li[1], Donghua Shao[1], Yafeng Qiu[1], Zhiyong Ma[1]* and Jianchao Wei[1]*

[1]Shanghai Veterinary Research Institute, Chinese Academy of Agricultural Sciences, Shanghai, China, [2]College of Animal Science, Yangtze University, Jingzhou, China

African Swine Fever (ASF) is an acute, highly contagious and deadly infectious disease that has a huge impact on the swine industry. It is caused by the African swine fever virus (ASFV). The most acute forms of ASF in domestic pigs have mortality rates of up to 100%. The lack of a commercial vaccine and effective therapeutic drugs has brought great challenges to the prevention and control of ASF. Current, the African swine fever virus requires a huge amount of detection, so there is a need for more sensitive and accurate detection technology. The protein pB602L, as a late non-structural protein, has a high corresponding antibody titer and strong antigenicity in infected swine. In this research, the B602L gene was constructed into the pColdI prokaryotic expression vector, and prokaryotic expression of the soluble pB602L protein was induced by IPTG. Western blot analysis demonstrated that the protein had strong immunogenicity. We established an indirect ELISA method for the detection of anti-ASFV using purified recombinant pB602L protein as antigen. The detection method showed excellent specificity without cross-reactions with antibodies against PRRSV, CSFV, JEV, and GETV. The method could detect anti-ASFV in serum samples that were diluted up to 6,400 times, showing high sensitivity. The coefficients of variation of the intra-assay and inter-assay were both <10%. The assays had excellent specificity, sensitivity, and repeatability. In summary, we developed an accurate, rapid, and economical method for the detection of anti-ASFV in pig serum samples with great potential for ASF monitoring and epidemic control.

KEYWORDS

African swine fever virus, indirect ELISA, B602L, prokaryotic expression system, antibodies in serum

Introduction

African swine fever (ASF) is a highly contagious hemorrhagic and transboundary viral disease of swine for which currently no preventive vaccine is available (1). It is a devastating disease with mortality rates close to 100% in young herds, causing severe socioeconomic losses. Since it was first reported in Kenya in 1921 (2), ASF has become endemic in many African countries (3). Recently, ASF emerged in Asian countries, including China (4), where it spread rapidly to many parts of the country (5). At present, ASF continues to place a huge burden on the pig industry in the affected areas (6).

Current approaches to control and prevent ASF include early diagnosis, rapid elimination of infectious sources, and interruption of transmission routes. Therefore, the development of rapid, sensitive, and field-deployable African swine fever virus (ASFV) assays are important for disease surveillance and control (7, 8). Currently, there are several early diagnostic techniques available to detect ASFV, including PCR, loop-mediated isothermal amplification, fluorescence quantitative PCR, colloidal gold rapid strip, hemadsorption, enzyme-linked immunosorbent assay (ELISA), and other serological tests (9). Serological testing is been widely used in ASF eradication and control programs; since no vaccine is available, the presence of ASF antibodies implies previous infection. Therefore, serology is suitable for detecting potential virus-carrying animals in epidemic situations. ELISA is the most commonly used serological test, so it can be widely used for screening purposes (10).

ASFV is the sole member of the genus Asfarvirus within the family Asfarviridae and is a unique and genetically complex virus (11). ASFV is a large, double-stranded, linear DNA virus with a complex structure. The genome size is about 170–190 kb. ASFV encodes more than 150 proteins, of which more than 50 are structural proteins (12). ASFV can be divided into 23 different genotypes according to the ASFV B646L gene encoding the p72 major capsid protein (13). Morphologically, ASFV has a icosahedral shape and a complex structural architecture composed of several concentric layers (14, 15). ASFV infects mononuclear macrophages mainly through megalocytosis and clathrin-mediated endocytosis (1). pB602L is a nonstructural protein that functions as a molecular chaperone of the major structural protein p72, forming aberrant "zipper-like" structures instead of icosahedral virus particles in the absence of pB602L (16). B602L contains a central variable region (CVR) that allows frequently subgenotyping of ASFV isolates based on this region (17). The central variable region (CVR) within the B602L gene of the African swine fever virus (ASFV) is highly polymorphic within the ASFV genotypes defined by sequencing of the C-terminal end of the p72 locus (17, 18). Previous studies have shown that pB602L is strongly antigenic and can be used to develop diagnostic tools for ASFV. Previously, a pB602L-based ELISA assay was employed to detect serum antibodies against ASFV, and the test results were mostly consistent with those obtained using the gold standard, western blot assays (16). B Gutiérrez-Castañeda et al. showed that pB602L is recognized by hyperimmune antisera from domestic pigs and bushpigs at late time points after infection, suggesting it may be useful diagnostically to distinguish animals persistently infected with virus (17). pB602L may be a suitable target for the development of diagnostic tools to assess the humoral immune responses to these vaccines, as antibodies against pB602L are only produced after this protein is expressed in host cells (1, 17).

In this study, we successfully expressed and purified the ASFV pB602L protein and established an indirect ELISA method for the detection of anti-ASFV using purified pB602L as a diagnostic antigen, laying the foundation for the development of early diagnosis kits for ASFV and functional research of the pB602L protein.

Materials and methods

Serum samples

ASFV (SY-18) infection inactivated sera ($n = 30$) were obtained from the China Animal Health & Epidemiology Center (Qingdao, China). All positive sera were tested by gold standard. And all positive sera were tested by the Svanova ASFV p30 antibody detection kit and the Ingenasa ASFV p72 ELISA kit.

Positive sera against pathogenic Japanese encephalitis virus (JEV), classical swine fever virus (CSFV), Getah virus (GETV), Porcine circovirus 2 (PCV2), Porcine parvovirus (PPV)-, and Pseudorabies virus (PRV) were prepared in our laboratory.

All 120 negative serum samples were collected before the outbreak of ASFV in China from 2016 to 2017 and were confirmed to be negative by the Svanova ASFV p30 antibody detection kit and the Ingenasa ASFV p72 ELISA kit.

Cloning and expression of pB602L

The transmembrane region of pB602L protein was predicted through TMHMM-2.0 (Denmark, http://www.cbs.dtu.dk/services/TMHMM/). The full-length B602L coding region of ASFV SY-18 (GenBank accession, MH766894.1) was synthesized by Tsingke Biotechnology (Shanghai, China) and amplified using primers. F (5′-CTCGGTACCCTCGAGGGATCCATGGCAGAATTTAATATTGA-3′) and R (5′-GACTGCAGGTCGACAAGCTTCTACAATTCTGCTTTTGTAT-3′).

The recombinant expression plasmid was constructed by ligating the PCR product of the B602L gene into the vector pCold I. The ligation product was transformed into *E.coli* DH5α, and the recombinant plasmid was successfully constructed by sequencing. Next, the constructed plasmids were transformed

into *E.coli* BL21, and then protein expression was induced for 14–16 h with 0.5 mM IPTG at 16°C. The recombinant pB602L protein was purified by Ni^{+} affinity chromatography and identified by SDS-PAGE and western blots. ASFV-positive pig serum (dilution of 1:5,000) and anti-His (dilution of 1:5,000) were used as the primary antibodies for the western blot assays.

Establishment of an indirect ELISA antibody detection method for ASFV pB602L protein

Square titration

The working concentration of pB602L protein antigen and serum dilution were optimized using square titration. In short, the antigen pB602L was coated on plates at concentrations of 0.625, 0.32, 0.16, 0.08, and 0.04 μg/mL. Anti-ASFV positive and negative standard sera were diluted at 1:50, 1:100, 1:200, and 1:400. The condition with the highest OD450 ratio of positive and negative sera (P/N value) and an OD450 value of positive sera close to 1.0 was selected as the best working condition.

Working conditions for pB602L-ELISA

In addition to optimal pB602L protein coating concentration and serum dilution, different blocking solutions (5% skim milk, 1% gelatin, and 2% BSA) and reaction times of various materials were also explored, and the optimal reaction time of serum was also tested. The optimal concentration and reaction time of HRP-conjugated anti-pig antibody were tested using the following dilutions: 1:2,500, 1:5,000 and 1:10,000. Furthermore, the TMB response time was optimized. The OD450 and P/N values of these groups were compared to determine the best working conditions.

Cut-off value for pB602L-ELISA

The optimal cutoff value for iELISA was determined using a total of 64 negative serum samples from ASFV-uninfected swnie. The OD450 values were measured, and statistical analysis was performed to calculate the average value (AV) and standard deviation (SD) of the OD450 values. The cut-off value was determined as AV + 3SD (19, 20).

Specificity and sensitivity of pB602L-ELISA

The constructed pB602L-ELISA method was applied against porcine reproductive and respiratory syndrome virus (PRRSV)-, Japanese encephalitis virus (JEV)-, classical swine fever virus (CSFV)-, Getah virus (GETV)-, Porcine circovirus 2 (PCV2)-, Porcine parvovirus (PPV)-, and Pseudorabies virus (PRV)-positive sera,ASFV-positive and -negative sera. We diluted ASFV-positive serum from 1:100 to 1:204,800 to determine the highest dilution of serum. We diluted ASFV-positive serum from 1:100 to 1:204,800 to determine the highest dilution of serum. Based on the critical value, the sensitivity of the constructed ELISA method was appraised. Statistical analysis Coefficient of Variation.

Reproducibility of pB602L-ELISA

Six random serum samples were randomly selected, and the established pB602L-ELISA assay was used to conduct intra-assays repeatability tests on three different ELISA plates coated in the same batch. In addition, three different batches of coated ELISA plates were randomly selected for inter-assay repeatability experiments. Statistical analysis was performed to calculate intra- and inter-assays variation [coefficient of variation (CV)] between runs.

Comparison of pB602L-ELISA with commercial kits

All 150 clinical serum samples were tested applying the pB602L-ELISA methed. The results were compared with the results of a commercial ELISA kit for anti-ASFV detection to evaluate the performance of pB602L-ELISA by calculating the concordance rate as follows: [(true positive + true negative) / (true positive + true negative + true negative + false positive) × 100%].

Statistical analysis

All data were analyzed using Prism 5 software (GraphPad Software, La Jolla, CA, USA). All data were analyzed using a two-tailed Student's *t*-test. $P < 0.05$ was considered statistically significant.

Results

Expression and purification of pB602L protein

The pB602L protein had no transmembrane region (Figure 1A). In this study, we expressed the full length of pB602L protein (Figure 1B). The 65-kDa ASFV pB602L protein was successfully expressed. It was detected in the soluble supernatant fraction by WB analysis applying anti-His and ASFV-positive pig serum (Figure 1C).

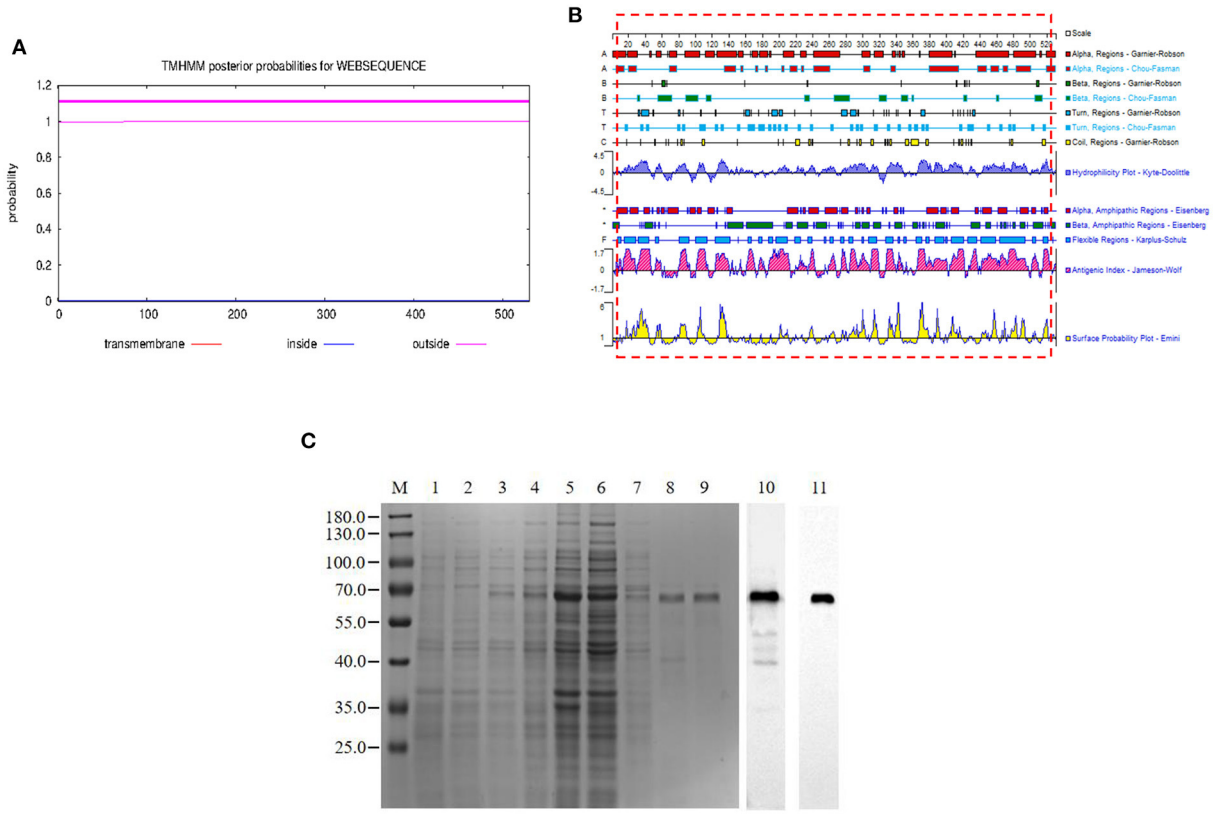

FIGURE 1
Expression and purification of the pB602L protein. **(A)** Prediction of the full-length transmembrane region of pB602L protein **(B)** Expression of pB602L protein in vector pCold I. **(C)** Protein marker, 1- transformed cells of BL21/pCold after IPTG induction for 16 h, 2- whole bacteria without induction, 3- BL21/pCold-B602L whole bacteria after IPTG induction for 16 h, 4-BL21/pCold-B602L supernatant after induction at 16°C, 5-BL21/pCold-B602L precipitation after IPTG induction for 16 h, 6-Purification of recombinant pB602L protein flow-through by Ni^+ spin column affinity chromatography, 7-Ni^+ spin column affinity chromatography purification of recombinant protein pB602L 40mM imidazole washing solution, 8, 9-purified recombinant pB602L protein by affinity chromatography of Ni^+ spin column, 10-Western blot analysis of p602L protein using ASFV-positive pig serum, 11-Western blot analysis of p602L protein using anti-His. A prominent band with the expected size 65 kDa appeared after incubation.

Establishment of the pB602L-ELISA method

The working concentration of pB602L protein antigen and serum dilution were optimized using square titration. The experimental results show that the optimal coating concentration of antigen for the pB602L-ELISA method is 0.04 μg/mL, the optimal dilution of serum is 1:100 (Table 1). In addition, other conditions of the pB602L-ELISA method were improved. In brief, the best blocking solution is 2% BSA in PBST, and optimal blocking incubation is 2 h at 37°C (Figure 2A). The optimal reaction time for serum was 1 h at 37°C (Figure 2B). The optimal dilution of HRP-conjugated anti-pig was 1:5,000, and the optimal reaction condition was 1 h at 37°C (Table 2). Finally, the optimal reaction time for TMB solution was 15 min at 37°C (Figure 2C).

Optimization of the cut-off value

The average OD450 value of negative sera ($n = 64$) was 0.192, and the SD was 0.049, so the cut-off value of the pB602L-ELISA method was AV + 3SD = 0.340 (Figure 3A). Therefore, samples with an OD450 value of the tested serum of ≥0.340 are considered positive. Conversely, samples with an OD450 value of <0.340 are considered negative.

Diagnostic specificity of pB602L-ELISA

The established pB602L-ELISA method was used to test anti-PRRSV-, anti-JEV-, anti-GETV-, anti-CSFV-, anti-PCV2-, anti-PPV-, and anti-PRV-positive pig serum. Except for the ASFV-positive control, all sera were negative (OD450 < 0.340), which

TABLE 1 P/N values at different conditions.

Serum dilution		Antigen coating concentration (μg/mL)				
		0.625	0.320	0.160	0.080	0.040
1:50	P	3.585	3.209	2.715	2.424	2.363
	N	0.086	0.105	0.086	0.08	0.088
	P/N	41.686	30.562	31.570	30.300	26.852
1:100	P	3.095	2.410	1.775	1.555	1.483
	N	0.093	0.120	0.088	0.066	0.080
	P/N	33.279	20.083	20.170	23.561	18.538
1:200	P	2.359	1.764	1.211	1.116	1.056
	N	0.076	0.078	0.08	0.084	0.073
	P/N	31.039	22.615	15.138	13.286	14.466
1:400	P	1.599	1.240	0.951	0.740	0.769
	N	0.077	0.080	0.072	0.066	0.055
	P/N	20.766	15.500	13.208	11.212	13.982

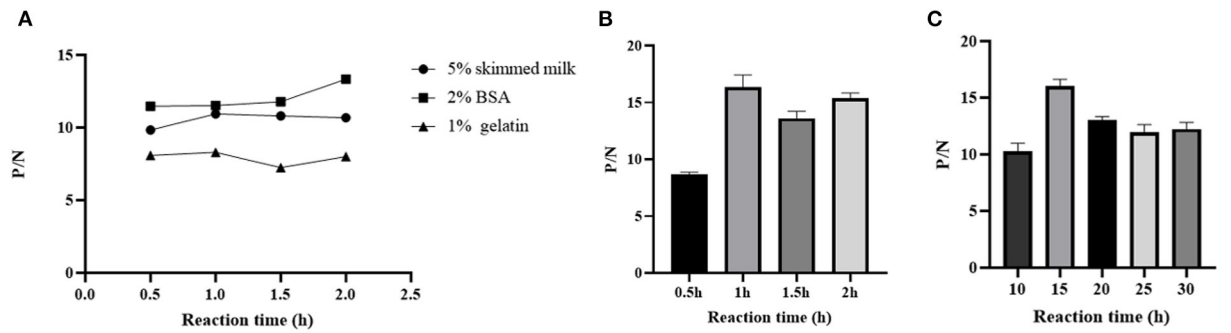

FIGURE 2
Optimization of pB602l-ELISA method conditions. **(A)** Optimization of the type of pB602L-ELISA blocking solution and working conditions. The best blocking solution was 2% BSA in PBST, and optimal blocking conditions are 2 h at 37°C. **(B)** Determination of serum action conditions. The optimal reaction time for serum was 1 h at 37 °C. **(C)** Determination of TMB solution action conditions. The optimal reaction time for TMB solution was 15 min at 37°C.

TABLE 2 HRP-conjugated anti-pig working conditions.

HRP anti-pig antibody dilution		HRP anti-pig antibody action conditions			
		37°C 0.5 h	37°C 1 h	37°C 1.5 h	37°C 2 h
1:2,500	P	1.082	1.268	1.263	1.464
	N	0.300	0.255	0.233	0.268
	P/N	3.607	4.973	5.421	5.463
1:5,000	P	0.774	1.048	1.192	1.248
	N	0.183	0.163	0.195	0.203
	P/N	4.230	6.429	5.519	6.148
1:10,000	P	0.526	0.784	1.003	1.065
	N	0.169	0.175	0.234	0.176
	P/N	3.112	4.480	4.286	6.051

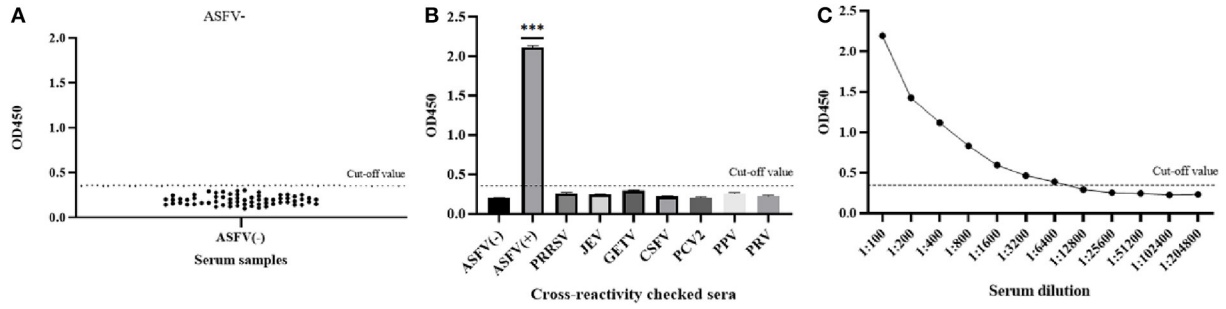

FIGURE 3
Sensitivity and specificity of the pB602L-ELISA method. **(A)** Determination of the cut-off value of pB602L-ELISA (OD450 = 0.340). Distributions of OD values determined for ASFV-negative ($n = 64$) serum samples using pB602L-ELISA. The average value (AV) of the negative sera was calculated, and the cutoff value was set at 0.340 (AV+3×SD). **(B)** The specificity test of the pB602L-ELISA method. ASFV-positive serum, ASFV-negative serum and PRRSV, JEV, GETV, CSFV, PCV2, PPV, PRV antibody-positive swine serum were measured using the pB602L-ELISA, and the OD450 values with all antisera except the ASFV-positive serum were lower than the cutoff value (0.340). **(C)** Sensitivity of the pB602L-ELISA method. Two-fold serial dilutions from 1:100 to 1:204,800 of ASFV-positive serum were tested by pB620L-ELISA method, and the highest dilution that could be detected using the cutoff value (0.340) was found to be 1:6,400, ***$p < 0.001$. Each dot represents a serum sample, and the dashed line indicates the cutoff value of the pB602L-ELISA.

indicated that the established ELISA method has good specificity (Figure 3B).

Diagnostic sensitivity of pB602L-ELISA

The ASFV-positive serum was diluted according to different dilutions. The results showed that the maximum dilution of serum that still had an OD450 value above the cutoff value of 0.340 was 1:6,400, so the sensitivity of the established pB620L-ELISA method was 1:6,400 (Figure 3C), indicating that the established indirect ELISA method is extremely sensitive.

Repeatability of the pB602L-ELISA method

Intra-assay variation and inter-assay variation were calculated to verify the repeatability of the pB602L-ELISA method. The maximum CV of the intra-assay repeatability test was 4.27% (Table 3), and the maximum CV of the inter-assay repeatability test was 5.82% (Table 3), both <10%. These results indicate that the established ELISA method has good repeatability.

Comparison of the pB602L-ELISA method to commercial kits

The performance of the pB602L-ELISA method was compared with that of a commercial ELISA kit (ID Screen® African Swine Fever Competition) for anti-ASFV detection in terms of specificity and accuracy. The results are shown in Table 4. The concordance rate of the detection results of these two methods is 97.33%.

Discussion

ASF is a devastating and economically significant disease that can affect domestic and wild swine (7, 8). It was introduced in China in 2018, and because of its high fatality rate, disease prevention and control has become extremely important for the Chinese pig industry (4). At present, the control of the disease mainly relies on rapid diagnosis and culling of infected pigs and those in close contact with them. ASFV has caused huge economic losses to the global swine industry (21).

ASFV is complex, and its genome encodes many proteins related to immune evasion. There is currently no safe and effective vaccine available (3132). Consequently, it is very significant to develop a method that can quickly and accurately detect ASFV. At present, serological detection techniques and molecular diagnostic methods are still regarded as the main means of identifying infected animals and preventing and controlling ASF (12, 22). There are many methods for detecting viral DNA, including real-time quantitative PCR and *in situ* hybridization with nucleic acid probes (23). Although these methods have high sensitivity, they also have high requirements on experimental operation technology and the experimental environment (23, 24). Serological diagnosis based on ELISA is not only stable detection means, but it also has good specificity, high sensitivity, simple operation, and low cost, so it is appropriate for the detection of large batches of samples, and hence it is widely used in practice (22). Therefore, the

TABLE 3 The results of the repeating test.

Sample number	The result of intra			The result of inter		
	Average value	Standard deviation	Coefficient variation	Average value	Standard deviation	Coefficient variation
1	2.062	0.088	4.27%	2.674	0.099	3.73%
2	1.809	0.012	0.68%	2.512	0.057	2.25%
3	1.754	0.045	2.56%	1.218	0.049	4.09%
4	2.160	0.044	2.05%	2.541	0.078	3.08%
5	3.064	0.047	1.55%	0.877	0.051	5.82%
6	0.805	0.017	2.05%	1.129	0.033	2.95%

TABLE 4 Comparison of the pB602L-ELISA method and a commercial ELISA kit.

Detection method		Commercial ASFV ELISA antibody kit		
		Positive	Negative	Total
pB602L-ELISA	Positive	29	3	32
	Negative	1	117	118
	Total	30	120	150
Relative sensitivity			96.66%	
Relative specificity			97.50%	
Compliance rate			97.33%	

OIE considered ELISA as the first serological method for the diagnosis of ASF (23). Most commercial ELISA assays have been developed based on recombinant ASFV structural proteins such as p72, p54, and p30, and these assays have been used for clinical diagnosis of porcine ASFV infection (25). At present, studies have shown that in addition to the structural proteins of ASFV, such as p72, p54, and p30, its non-structural proteins, such as pK205R and pB602L, also have good immunogenicity, so an effective ELISA method could be established based on these proteins (17, 23).

The pB602L protein of ASFV is encoded by the B602L gene, which contains a central variable region and is frequently used for subgenotyping of ASFV isolates (26). One of the proven markers to characterize this virus is the central variable region (CVR) within the B602L gene (17, 27). pB602L is an important nonstructural protein and a molecular chaperone of the major structural protein p72, which is required for the formation of the icosahedral capsid structure of ASFV (16). The B602L gene contains a central variable region, so the amino acid sequence alignment analysis of the B602L protein of different genotypes of ASFV strains was carried out. The results are shown in of the Supplementary Figures 1, 2. The B602L protein of the strain has only a few amino acid differences, and the B602L protein has a high homology in different genotype. We also performed an amino acid sequence alignment analysis of the B602L protein of the genotype II ASFV strain prevalent in China. The results are shown in of the Supplementary Figure 3. The alignment results show that the B602L protein of the known prevalent strains in China is not different. In conclusion, the overall antigenicity of ASFV B602L protein is relatively high, and there is only genotype II ASFV strain in China, so the selection of B602L protein has high sensitivity. Previous studies have shown that pB602L has good antigenicity and immunogenicity; the protein can be recognized by domestic pig and wild boar immune sera, and it may serve as a candidate antigen for the development of diagnostic methods for ASFV (28). Consistently high serological responses against pB602L were observed at time points later in infection than responses against the structural proteins in domestic pigs and bushpigs infected with a range of different viral isolates (29, 30). B Gutiérrez-Castañeda et al. show that ASFV B602L protein can be applied to antibody kinetics (17). Consistently high serological responses against pB602L was observed at time points later in infection than responses against the structural proteins in domestic pigs and bushpigs infected with a range of different viral isolates (17). So Gutiérrez-Castañeda et al. (17) suggests that an ELISA against these proteins may be of use in distinguishing animals persistently infected with virus from animals immunized with vaccines incorporating virus structural proteins (17). This suggests that an ELISA against these proteins may be of use in distinguishing animals persistently infected with virus from animals immunized with vaccines incorporating virus structural proteins. Previously, a pB602L-based ELISA assay was used to detect ASFV serum antibodies, which also distinguished pigs persistently infected with native ASFV strains from pigs immunized with subunit vaccines of structural proteins (16). Compared with eukaryotic expression systems, prokaryotic expression systems have lower production costs, simple operation, stable protein preparation, and easy purification and are suitable for large-scale production (31, 32). Therefore, in this study, a prokaryotic expression system was used to express the ASFV pB602L protein. The results revealed that the obtained B602L protein was soluble

and strong antigenicity, and the B602L protein could be served as an ELISA antigen to create and improve an indirect ELISA detection assay.

The indirect ELISA antibody detection method established in this study has a sensitivity of up to 1:6,400. The established method does not cross-react with antibodies against other related swine viruses such as PRRSV, JEV, CSFV, GETV, PCV2, PPV, and PRV. The CV in not only intra-batch but also inter-batch repeatability tests were <10%, which indicated that the pB602L-ELISA method constructed in this research has favorable repeatability. The concordance rate with a commercial ELISA kit (ID Screen® African Swine Fever Competition) for anti-ASFV detection was 97.33%. In conclusion, the recombinant ASFV pB602L protein prepared in this study has good antigenicity, and the established indirect ELISA antibody detection method has good sensitivity, good specificity, and high efficiency, and hence it is suitable for the on-site detection of anti-ASFV. This will provide an experimental basis for the detection of ASFV and the specific diagnosis of the disease. It has the potential to become an effective tool for evaluating the humoral immune response in pigs and the protective effects of live attenuated vaccines. Similarly, the construction of ELISA detection method is of great implication for the prevention and treatment of ASF.

Conclusion

In this study, the pB602L-ELISA method for indirect ASFV detection was successfully established. It has good reproducibility and specificity, and production and operation are simple. This study lays the foundation for the development of a kit for large-scale detection of anti-ASFV.

Data availability statement

The datasets presented in this study can be found in online repositories. The names of the repository/repositories and accession number(s) can be found in the article/Supplementary material.

Author contributions

YY: formal analysis, investigation, and validation. QX: formal analysis. QS: methodology and writing–review and editing. YZ: formal analysis and investigation. YL, ZG, and JZ: investigation and validation. XM: validation. BL and YQ: validation and writing–review and editing. KL: validation. DS: methodology. ZM: conceptualization, funding acquisition, and project administration. JW: conceptualization, formal analysis, funding acquisition, investigation, methodology, and writing–original draft. All authors contributed to the article and approved the submitted version.

Funding

The work was supported by grants from the National Key Research and Development Program of China (Nos. 2021YFD1801300 and 2021YFD1801401 awarded to JW and YQ, respectively), the National Natural Science foundation of China (No. 31941012 awarded to JW), the Project of Shanghai Science and Technology Commission (No. 20392002400 awarded to JW), and the Agricultural Science and Technology Innovation Program (CAAS-ZDRW202203 awarded to ZM). The funders had no role in the study design, data collection and analysis, the decision to publish, or preparation of the manuscript.

Conflict of interest

The authors declare that the research was conducted in the absence of any commercial or financial relationships that could be construed as a potential conflict of interest.

Publisher's note

All claims expressed in this article are solely those of the authors and do not necessarily represent those of their affiliated organizations, or those of the publisher, the editors and the reviewers. Any product that may be evaluated in this article, or claim that may be made by its manufacturer, is not guaranteed or endorsed by the publisher.

Supplementary material

The Supplementary Material for this article can be found online at: https://www.frontiersin.org/articles/10.3389/fvets.2022.971841/full#supplementary-material

References

1. Sang H, Miller G, Lokhandwala S, Sangewar N, Waghela SD, Bishop RP, et al. Progress toward development of effective and safe african swine fever virus Vaccines. *Front Vet Sci.* (2020) 7:84. doi: 10.3389/fvets.2020.00084

2. Nix RJ, Gallardo C, Hutchings G, Blanco E, Dixon LK. Molecular epidemiology of African swine fever virus studied by analysis of four variable genome regions. *Arch Virol.* (2006) 151:2475–94. doi: 10.1007/s00705-006-0794-z

3. Costard S, Mur L, Lubroth J, Sanchez-Vizcaino JM, Pfeiffer DU. Epidemiology of African swine fever virus. *Virus Res.* (2012) 173:191–7. doi: 10.1016/j.virusres.10030

4. Zhou X, Li N, Luo Y, Liu Y, Miao F, Chen T, et al. Emergence of African swine fever in China, 2018. *Transbound Emerg Dis.* (2018) 65:1482–4. doi: 10.1111/tbed.12989

5. Wang T, Sun Y, Qiu HJ. African swine fever: an unprecedented disaster and challenge to China. *Infect Dis Poverty.* (2018) 7:111. doi: 10.1186/s40249-018-0495-3

6. Teklue T, Sun Y, Abid M, Luo Y, Qiu HJ. Current status and evolving approaches to African swine fever vaccine development. *Transbound Emerg Dis.* (2020) 67:529–42. doi: 10.1111/tbed.13364

7. Wang D, Yu J, Wang Y, Zhang M, Li P, Liu M, et al. Development of a real-time loop-mediated isothermal amplification (LAMP) assay and visual LAMP assay for detection of African swine fever virus (ASFV). *J Virol Methods.* (2020) 276:113775. doi: 10.1016/j.jviromet.2019.113775

8. Wang T, Sun Y, Huang S, Qiu HJ. Multifaceted immune responses to African swine fever virus: implications for vaccine development. *Vet Microbiol.* (2020) 249:108832. doi: 10.1016/j.vetmic.2020.108832

9. Ward MP, Tian K, Nowotny N. African swine fever, the forgotten pandemic. *Transbound Emerg Dis.* (2021) 68:2637–9. doi: 10.1111/tbed.14245

10. Miao F, Zhang J, Li N, Chen T, Wang L, Zhang F, et al. Rapid and sensitive recombinase polymerase amplification combined with lateral flow strip for detecting african swine fever virus. *Front Microbiol.* (2019) 10:1004. doi: 10.3389/fmicb.2019.01004

11. Alonso C, Borca M, Dixon L, Revilla Y, Rodriguez F, Escribano JM, et al. ICTV virus taxonomy profile: asfarviridae. *J Gen Virol.* (2018) 99:613–4. doi: 10.1099/jgv.0.001049

12. Wang F, Zhang H, Hou L, Yang C, Wen Y. Advance of African swine fever virus in recent years. *Res Vet Sci.* (2021) 136:535–9. doi: 10.1016/j.rvsc.2021.04.004

13. Awosanya EJ, Olugasa BO, Gimba FI, Sabri MY, Ogundipe GA. Detection of African swine fever virus in pigs in Southwest Nigeria. *Vet World.* (2021) 14:1840–5. doi: 10.14202/vetworld.2021.1840-1845

14. Jacobs, S. C., Dixon, L. K., Brookes, S. M., and Smith, GL. Expression of African swine fever virus envelope protein j13L inhibits vaccinia virus morphogenesis. *J Gen Virol.* (1998) 79(Pt 5):1169–78. doi: 10.1099./0022-1317-79-5-1169

15. Salas ML, Andres G. African swine fever virus morphogenesis. *Virus Res.* (2012) 173:29–41. doi: 10.1016/j.virusres.2012.09.016

16. Wang P, Liu C, Wang S, Wen L, Shi Z, Chi Y, et al. Production and application of mouse monoclonal antibodies targeting linear epitopes in pB602L of African swine fever virus. *Arch Virol.* (2022) 167:415–424. doi: 10.1007/s00705-021-05335-0

17. Gutierrez-Castaneda B, Reis AL, Corteyn A, Parkhouse RM, Kollnberger S. Expression, cellular localization and antibody responses of the African swine fever virus genes B602L and K205R. *Arch Virol.* (2008) 153:2303–6. doi: 10.1007/s00705-008-0246-z

18. Simulundu E, Sinkala Y, Chambaro HM, Chinyemba A, Banda F, Mooya L, et al. Genetic characterisation of African swine fever virus from 2017 outbreaks in Zambia: Identification of p72 genotype II variants in domestic pigs. *Onderstepoort J Vet Res.* (2018) 85:e1–5. doi: 10.4102/ojvr.v85i1.1562

19. Zhang S, Wang D, Jiang Y, Li Z, Zou Y, Li M, et al. Development and application of a baculovirus-expressed capsid protein-based indirect ELISA for detection of porcine circovirus 3 IgG antibodies. *BMC Vet Res.* (2019) 15:79. doi: 10.1186/s12917-019-1810-3

20. Zhong K, Zhu M, Yuan Q, Deng Z, Feng S, Liu D, et al. Development of an indirect ELISA to detect african swine fever virus pp62 protein-specific antibodies. *Front Vet Sci.* (2021) 8:798559. doi: 10.3389/fvets.2021.798559

21. Liu Y, Zhang X, Qi W, Yang Y, Liu Z. An T, et al. Prevention and Control Strategies of African Swine Fever and Progress on Pig Farm Repopulation in China. *Viruses.* (2021) 13:2552. doi: 10.3390./v13122552

22. Arias M, Jurado C, Gallardo C, Fernandez-Pinero J, Sanchez-Vizcaino JM. Gaps in African swine fever: analysis and priorities. *Transbound Emerg Dis.* (2018) 65 Suppl 1:235–47. doi: 10.1111/tbed.12695

23. Gaudreault NN, Madden DW, Wilson WC, Trujillo JD, Richt JA. African swine fever virus: an emerging DNA arbovirus. *Front Vet Sci.* (2020) 7:215. doi: 10.3389/fvets.2020.00215

24. Fernandez-Pinero J, Gallardo C, Elizalde M, Robles A, Gomez C, Bishop R, et al. Molecular diagnosis of african swine fever by a new real-time PCR using universal probe library. *Transbound Emerg Dis.* (2013) 60:48–58. doi: 10.1111/j.1865-201201317.x

25. Petrovan V, Yuan F, Li Y, Shang P, Murgia MV, Misra S, et al. Development and characterization of monoclonal antibodies against p30 protein of African swine fever virus. *Virus Res.* (2019) 269:197632. doi: 10.1016/j.virusres.05010

26. Owolodun OA, Bastos AD, Antiabong JF, Ogedengbe ME, Ekong PS, Yakubu B, et al. Molecular characterisation of African swine fever viruses from Nigeria (2003–2006) recovers multiple virus variants and reaffirms CVR epidemiological utility. *Virus Genes.* (2010) 41:361–8. doi: 10.1007/s11262-009-0444-0

27. Gallardo C, Mwaengo DM, Macharia JM, Arias M, Taracha EA, Soler A, et al. Enhanced discrimination of African swine fever virus isolates through nucleotide sequencing of the p54, 72. and pB602L (CVR) genes. *Virus Genes.* (2009) 38:85–95. doi: 10.1007/s11262-008-0293-2

28. Lokhandwala S, Waghela SD, Bray J, Sangewar N, Charendoff C, Martin C, et al. Adenovirus-vectored novel African swine fever virus antigens elicit robust immune responses in swine. *PLoS ONE.* (2017) 12:e0177007. doi: 10.1371/journal.pone.0177007

29. Minoungou GL, Diop M, Dakouo M, Ouattara AK, Settypalli TBK, Lo M, et al. Molecular characterization of African swine fever viruses in Burkina Faso, Mali, and Senegal 1989-2016: genetic diversity of ASFV in West Africa. *Transbound Emerg Dis.* (2021) 68:2842–52. doi: 10.1111/tbed.14240

30. Onzere CK, Bastos AD, Okoth EA, Lichoti JK, Bochere EN, Owido M, et al. Multi-locus sequence typing of African swine fever viruses from endemic regions of Kenya and Eastern Uganda (2011–2013) reveals rapid B602L central variable region evolution. *Virus Genes.* (2018) 54:111–23. doi: 10.1007/s11262-017-1521-4

31. Laage R, Langosch D. Strategies for prokaryotic expression of eukaryotic membrane proteins. *Traffic.* (2001) 2:99–104. doi: 10.1034/j.1600-0854.2001.020204.x

32. Porowinska D, Wujak M, Roszek K, Komoszynski M. Prokaryotic expression systems. *Postepy Hig Med Dosw.* (2013) 67:119–29. doi: 10.5604/17322693.1038351

frontiers | Frontiers in Veterinary Science

TYPE Brief Research Report
PUBLISHED 28 September 2022
DOI 10.3389/fvets.2022.1000969

OPEN ACCESS

EDITED BY
Wentao Li,
Huazhong Agricultural University, China

REVIEWED BY
Ndawula Charles,
National Livestock Resources Research Institute, Uganda
Sylvester Ochwo,
Makerere University, Uganda

*CORRESPONDENCE
Xinglong Wang
wxlong@nwsuaf.edu.cn
Zhichun Yan
Jasonynh@126.com

†These authors have contributed equally to this work and share first authorship

SPECIALTY SECTION
This article was submitted to Veterinary Experimental and Diagnostic Pathology, a section of the journal Frontiers in Veterinary Science

RECEIVED 22 July 2022
ACCEPTED 30 August 2022
PUBLISHED 28 September 2022

CITATION
Li X, Li Y, Fan M, Fan S, Gao W, Ren J, Liu Q, Li J, Wu W, Li J, Yu Q, Wang X and Yan Z (2022) Inguinal lymph node sample collected by minimally invasive sampler helps to accurately diagnose ASF in dead pigs without necropsy. *Front. Vet. Sci.* 9:1000969. doi: 10.3389/fvets.2022.1000969

Inguinal lymph node sample collected by minimally invasive sampler helps to accurately diagnose ASF in dead pigs without necropsy

Xiaowen Li[1,2,3†], Yang Li[1,4†], Mingyu Fan[2], Shiran Fan[4], Wenchao Gao[1], Jing Ren[5], Qingyuan Liu[1,3], Jingtao Li[4], Weisheng Wu[4], Junxian Li[4], Qiannan Yu[2], Xinglong Wang[3*] and Zhichun Yan[4*]

[1]Shandong New Hope Liuhe Agriculture and Animal Husbandry Technology Co., Ltd., (NHLH Academy Swine Research), Dezhou, China, [2]Xiajin New Hope Liuhe Agriculture and Animal Husbandry Co., Ltd., Dezhou, China, [3]College of Veterinary Medicine, Northwest A&F University, Yangling, China, [4]New Hope Liuhe Co., Ltd., Chengdu, China, [5]Swine Health Data and Intelligent Monitoring Project Laboratory, Dezhou University, Dezhou, China

African swine fever (ASF) is a highly contagious hemorrhagic and transboundary animal disease, and it threatens global food security. A full necropsy to harvest the sample matrices for diagnosis in the farm may lead to contamination of the premises and directly threaten to the herds. In the present study, we compared the ASFV loads of the common samples that can be collected without necropsy. The unmatched nasal, throat, rectal samples were randomly taken using cotton swabs, and inguinal lymph node samples were collected by the minimally invasive samplers from the dead pigs of an ASF field outbreak farm. The ASFV loads of the samples were detected by qPCR and the results suggested that the overall ASFV nucleic acids levels of inguinal lymph node samples were higher than the swabs. What's more, sets of matched nasal swabs, rectal swabs, throat swabs, inguinal lymph nodes, serums, spleens and lungs samples were collected from 15 dead ASFV naturally infected pigs. Similarly, the results showed that inguinal lymph node samples, together with serum, spleen and lungs samples, contained more ASFV nucleic acids than the swabs. Our findings demonstrated that the inguinal lymph node collected by minimally invasive sampler is an ideal tissue for diagnosing ASFV infection in dead pigs without necropsy.

KEYWORDS

African swine fever, inguinal lymph node, minimally invasive sampler, qPCR, diagnosis

Introduction

African swine fever (ASF) is a devastating swine viral disease that is reportable to the World Organization for Animal Health (WOAH). It causes high fever, severe depression, ataxia and hemorrhages in domestic swine and results in a mortality rate approaching 100% (1). Since its emergence in Kenya in the 1920's, ASF remains endemic

in sub-Saharan Africa, the Indian Ocean region and Eastern Europe (2–4). In 2007, ASF was confirmed in Georgia and Russia, posing the risk of further dissemination into neighboring countries (5). Since August 2018, ASF has spread to China, the world's largest pork producer and a leading pork importer (6). Ongoing outbreaks of ASF afflicted the livestock industry and wiped out 40% of the nation's pigs, leading to severe socioeconomic losses (7–9).

The causative agent of the disease, ASF virus (ASFV), belongs to the genus *Asfivirus* within the *Asfarviridae* family (10). ASFV is a complex enveloped virus containing a large double-stranded DNA genome that ranges in length from 170 to 193 kbp (11, 12). Although scientists worldwide have made great efforts to study the etiology and immunology of ASFV, no prophylactic vaccine or treatment option is widely accepted and used. Clinical diagnosis is impractical for the similar classic symptoms of ASF and classic swine fever, swine erysipelas and highly pathogenic porcine reproductive and respiratory syndrome. Laboratory diagnosis is indispensable to make a definite diagnosis for the dead ASF suspected pigs. WOAH recommends two types of laboratory diagnosis, including etiological diagnosis and serological diagnosis. To date, qPCR has been widely used to detect ASFV nucleic acids due to its simple, rapid, highly sensitive and specific features. Nevertheless, the quantity and quality of conventional samples, such as oral, nasal and rectal swabs vary from pig to pig. False-negative results pose a concerning threat to herds. High ASFV loads was found in organs, including brain, heart, spleen, tonsil, bone marrow, lung, liver, kidney and lymph node (10, 13–15). However, opening up the carcasses is time-consuming and skilled, which often leads to contamination of the premises and increases the risk of ASFV infection in the herds (16). Researchers reported that the average viral loads of lymph nodes were comparable with internal organs (14, 15). The purpose of this study was to compare the ASFV loads of inguinal lymph nodes and the common swabs that can be collected without a full necropsy.

Method

This study was performed in line with the principles of the Declaration of Helsinki. Approval was granted by the Technology Ethics Committee of the Dezhou University (DZU/IACUC_2022-2-18-1). The unmatched inguinal lymph node samples, throat swabs, nasal swabs and rectal swabs were collected randomly from the dead-ASFV positive pigs of a naturally infected 1–2-year-old Landrace-Duroc-Large white crossbred swine herd in Xiajin County, Shandong Province, China (116°16′67″E, 37°13′17″N). For inguinal lymph node samples, the minimally invasive sampler was used which consists of a needle, a syringe, a handle and a connection rod inside the needle (Figure 1A). The needle contains a barb, which can remove the lymphoid tissue from the muscle. The connection rod can be inserted into the needle to extrude the tissue. As shown in Figure 1B, the skin was punctured vertically with the sampler to ensure that the barb entirely entered the tissue. The sampler was pulled out, and the handle was pressed to push the tissue out of the needle. The tissue was placed into a centrifuge tube and submerged in 0.5 mL saline solution. For throat swab sample, a long swab was inserted into the throat and moved back and forth for five times. The mucus was eluted with 1 mL saline solution in a sealing bag and the eluate was transferred into a centrifuge tube (Figure 1C). The nasal swabs (Figure 1D) and rectal swabs (Figure 1E) were collected using the short swabs and eluted with 0.5 mL saline solution. The matched inguinal lymph node samples, throat swabs, nasal swabs and rectal swabs were collected from 15 naturally infected dead-ASFV positive pigs using the same methods. Blood in thorax were centrifuged at 3,000 g for 2 min to separate serum. Sliced spleen and lung samples were collected from a full necropsy in a slaughterhouse.

To determine the viral loads in each sample, the following primers specific for ASFV B646L gene were designed based on the ASFV isolate Pig/HLJ/18 (GenBank: MK333180.1) (10) and used for qPCR: 5'-AAAATGATACGCAGCGAAC-3' (forward), 5'-TTGTTTACCAGCTGTTTGGAT-3' (reverse), 5'-FAM-TTCACAGCATTTTCCCGAGAACT-BHQ1-3' (probe). The qPCR was carried out in a Step One Plus instrument (ABI) with PerfectStart® II Probe qPCR SuperMix (TransGen Biotech, China) according to the manufacturer's instructions. To process the samples, homogenates of lymph nodes, spleens and lungs were prepared using Precellys lysing kits with the Precellys tissue homogenizer (Bertin, France). Swab samples were oscillated and then centrifuged at 8,000 g for 2 min. The total DNA of each sample (200 μL) was extracted by Virus DNA Extraction Kit II (Geneaid, Taiwan) as described in the handbooks without modification. Five microliters of extracting solution was taken for qPCR detection. Results of qPCR were initially recorded as quantification cycle values.

Partial sequences of ASFV B646L were cloned into the pMD18-T vector (Takara) to construct the ASFV DNA standard plasmids (Supplementary material 1). Briefly, B646L gene partial sequences were amplified using the following primers: 5'-TACGAATTCGTTGGCCAGGAGGTATCGGT-3' (forward), 5'-AGAGGATCCAAGAGGGGGCTGATAGTATT-3' (reverse). Amplification was carried out using a pre-mixed PCR solution (P111-01, Vazyme) according to the instructions. As a standard procedure, 40 consecutive cycles of thermal denaturation at 95°C (15 s), primer annealing at 60°C (15 s) and primer extension at 72°C (30 s) were carried out in a PCR thermocycler (C1000, Bio-Rad). PCR products and pMD18-T plasmids were digested with same restriction enzymes (EcoR I and BamH I, Takara). Fragments were purified by agarose gel electrophoresis and linked by DNA ligases (C301-01, Vazyme) according to the standard procedure. Positive clones were screened out with Ampicillin culture dish and identified by sequencing. The standard curve was obtained using a known concentration of the recombinant T vector, which was serially diluted from

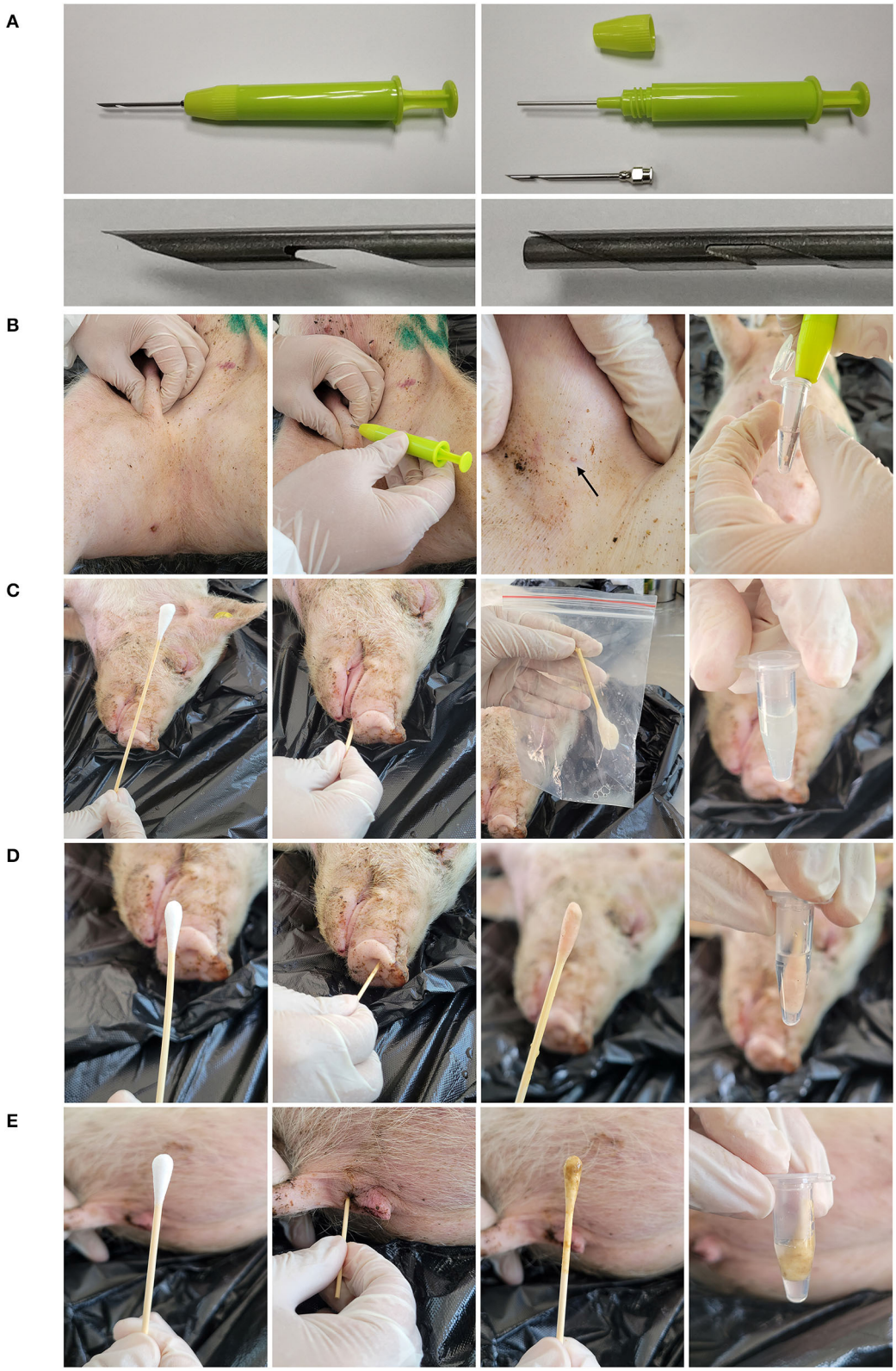

FIGURE 1
Sampling tools and methods. **(A)** The structure of minimally invasive sampler. The sample contains three parts: the needle, the body and the screw cap. The connection rod can insert into the needle to extrude the tissue. **(B)** Collect the inguinal lymph node sample with the minimally invasive sampler. First, fix the inguinal lymph node and puncture the skin with the sampler. Then pull out the sampler and extrude the tissue into

(Continued)

FIGURE 1 (Continued)
0.5 mL saline solution. **(C)** Collect the throat sample with a long swab. Insert the swab into the throat and moved back and forth for five times. The swab was then eluted in 1 mL saline solution in a sealing bag. The eluate was stored in the centrifuge tube. Collect the nasal swab sample **(D)** and rectal swab sample **(E)** with short swabs. The swabs were inserted into the nostril or anus and moved back and forth for five times. The swabs were then eluted in 0.5 mL saline solution.

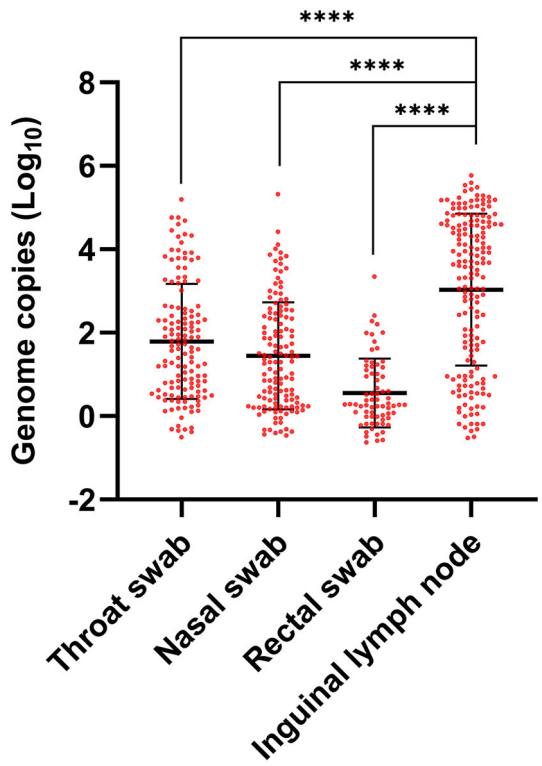

FIGURE 2
ASFV contents in lymph nodes and swabs. Throat, nasal and rectal samples were randomly collected by swabs and inguinal lymph nodes were collected by minimally invasive sampler from the dead pigs of an ASF field outbreak. ASFV contents were detected by qPCR using specific primers and probes targeting B646L gene. Individual CT values were converted to viral genomic $\log_{10}$ copy numbers based on an established standard curve. The difference analysis was carried out by GraphPad Prism v8.3.0 using unpaired *t*-test. ****p value < 0.0001.

10^8 to 10^3 copies/μL. The detection limit of qPCR assay is 2.5 copies/μL of the ASFV genome. The sample CT values were converted to ASFV copy numbers based on the standard curve. GraphPad Prism v8.3.0 was used to make graphs and analyze the data by *t*-test.

Results

A total of 175 lymph node samples, 137 throat swab, 134 nasal swab, 71 rectal swab samples randomly collected from the ASFV infected dead pigs were tested to determine the copy numbers of ASFV by qPCR. The overall highest copy numbers of ASFV were found in the inguinal lymph node samples ($p < 0.0001$, unpaired *t*-test) compared with the swab samples, and the lowest copy numbers were found in the rectal samples (Figure 2). The nasal and throat swab samples had almost the same ASFV copies, which were relatively lower than the lymph node samples and higher than the rectal samples. These data suggested that the overall ASFV loads of inguinal lymph node were higher than the unmatched swab samples in the field.

To compare the ASFV loads in different samples more directly, we collected the throat swab, nasal swab, rectal swab samples and inguinal lymph node sample from the single dead pig ($n = 15$). Pigs were then dissected to collect the matched serum, lung and spleen samples. All samples were tested for ASFV contents by qPCR. As is shown in Figure 3A, viral loads of lymph node samples were comparable with serums, spleens and lungs. All of the 15 inguinal lymph node samples had higher ASFV copies than the swab samples. Over all, the ASFV copies of the throat swabs were parallel with the nasal swabs, and 12 of 15 rectal swabs had the lowest ASFV copies. These data demonstrated that inguinal lymph nodes contain higher ASFV loads than the swab samples.

When the ASFV genome copy numbers in the inguinal lymph node samples were compared with those of the throat swabs, nasal swabs and rectal swabs, there was a weakly positive correlation ($r = 0.12$, 0.39, and 0.12, respectively). Though all of lymph nodes, spleens and lungs samples contain high ASFV copies, there was no strong correlativity. However, strong positive correlation was found between the viral contents of serum and inguinal lymph node samples ($r = 0.78$). Interestingly, strong positive correlation ($r = 0.89$) also existed between the respiratory and alimentary samples, including rectal swabs, throat swabs, nasal swabs and lungs (Figure 3B). These results indicated that even though ASFV genomic copy numbers of throat swabs, nasal swabs and rectal swabs were relative, but they were less than the inguinal lymph node samples as well as the serum and internal organs.

Discussion

ASF is an acute viral infection that has a major impact on global pig production. The availability of effective and safe ASFV vaccines would support and enforce control–eradication strategies. Therefore, work leading to the rational development of protective ASF vaccines is a high priority (17–20). It

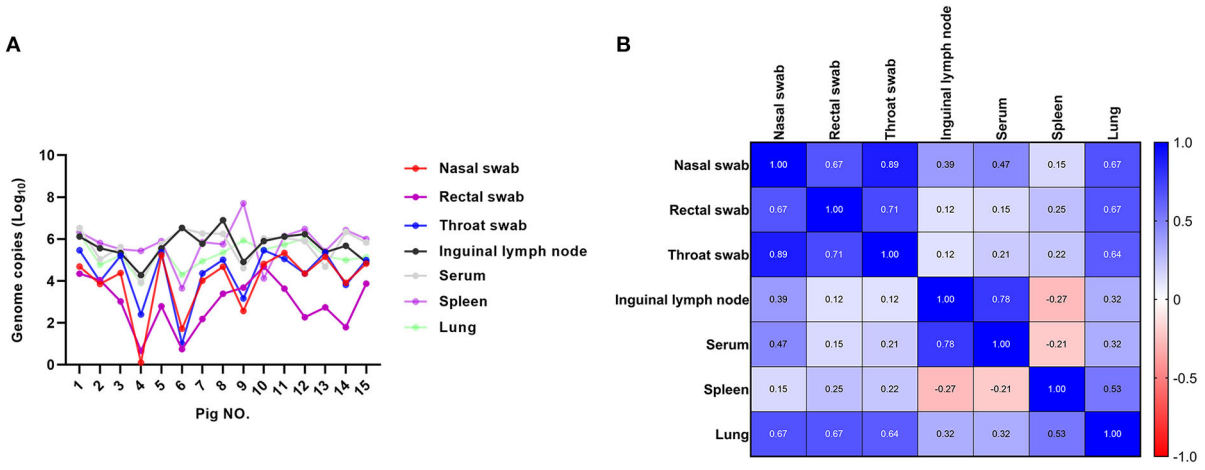

FIGURE 3
The comparison of ASFV contents of different sample types from the single pig. Sets of matched nasal swabs, rectal swabs, throat swabs, inguinal lymph nodes, serums, spleens and lungs of 15 pigs were collected and the ASFV contents were detected by qPCR. **(A)** Individual CT values were converted to viral genomic $\log_{10}$ copy numbers. **(B)** The correlation values of ASFV genome copies between different types of samples were calculated using GraphPad Prism v8.3.0. Deeper blue means there are stronger positive correlation between the viral contents of different kinds of samples. Similarly, red color indicates the negative correlation.

was recently reported that a promising recombinant vaccine candidate, ASFV-G-ΔI177L, was developed by deleting the I177L gene from the genome of the highly virulent ASFV strain Georgia (21–24). However, the presence of efficacy, residual virulence and the possibility of reversion to virulence must be evaluated in the field, which will need much further research before commercialization. Due to the lack of vaccine or effective treatments, prevention, control and eradication measures are mainly based on enhanced biosecurity and early detection by efficient laboratory diagnosis (18).

qPCR assays have many advantages compared with immunology methods, such as simple operation processes, high sensitivity, high specificity and excellent repeatability. Thus, qPCR is the most commonly used laboratory test method to diagnose ASFV at present. The low viral load, of course, also means infection, as long as the test results are indeed positive. However, in fact, weakly positive results always puzzle the experimenter because of the possible reagents contamination and aerosol contamination. The most challenging thing of qPCR is how to get the samples with higher viral loads. The internal organs such as spleen, lymph nodes, bone marrow, lung, tonsil and kidney contain high viral loads and are WOAH-recommended samples for ASF dead pigs, however, opening up the carcass is inevitable and risky (25). A robust viremia generally occurs within 2 days post ASFV infection and serum was an usual sample to diagnose the disease (26, 27). However, blood clotting happens within hours after the death, which means serum is always unavailable in dead pigs. ASFV spreads through the lymph and blood to secondary lymphoid organs within 2–3 days, thus the lymphoid grans were thought be an ideal tissue type for early detection of ASFV (28). It's interesting to note that viral content of inguinal lymph node sample has strong positive correlation with that of serum (Figure 3B), suggesting that inguinal lymph node sample can replace serum to detect ASFV in dead pigs. Actually, lymph nodes were used for viral loads measurements in many studies (29–31). Among the superficial lymph nodes, inguinal lymph node is the largest and the most accessible one. ASFV genome copy numbers in superficial inguinal lymph nodes highly correlate with those in the spleen and its sensitivity to diagnose ASF oro-nasally infection is 100% (16).

For the absolute avoidance of environmental contamination, the minimally invasive sampler instead of surgical operation was utilized to puncture the skin in a minimally invasive manner to obtain lymph node tissue in the present study. As a result, 10 of 15 inguinal lymph node samples showed much higher ASFV genomic copy numbers than the swabs, while the other five contains similar but no less viral loads compared with the throat swabs and nasal swabs. This possibly due to the sampling errors caused by the sampling position deviation, reminding us that the operating personnel should be well-trained to puncture the lymph node accurately with the minimally invasive sampler.

The needle of the minimally invasive sampler costs a bit more than a normal steel syringe needle. The sampler body and the needle can be recycled after cleaning and disinfection, which helps to keep costs down. What's more, the sampler helps to increase the confirmed diagnostic rate and avoid the risk of ASFV spread, which may sometimes save the whole herd in the ASFV epidemic area. We believe that the costs of minimally invasive sampler are acceptable to most ASF-disturbed breeders.

In conclusion, the ASFV viral loads was proved to be higher in the inguinal lymph nodes than the throat, nasal and rectal swabs samples. Considering the threaten of ASFV contamination to the herds, the lymph node samples collected by minimally invasive sampler can be an optional alternative of a full necropsy or a surgical operation to diagnose ASF in dead pigs.

Data availability statement

The datasets generated during the current study are available from the corresponding author on reasonable request.

Ethics statement

The animal study was reviewed and approved by Technology Ethics Committee of the Dezhou University. Written informed consent was obtained from the owners for the participation of their animals in this study.

Author contributions

ZY and XL contributed to the study conception and design. SF, WG, QL, JiL, WW, JuL, and QY performed the material preparation and data collection. JR, MF, XW, and YL performed the analysis. YL and XW wrote the draft of the manuscript. All authors read and approved the final manuscript.

Funding

This work was supported by the Integration and Demonstration of Comprehensive Prevention and Control of ASFV by the Ministry of Science and Technology of the People's Republic of China (No. 2018YFC0840405), the Scientific and Technological Innovation 2030 Program of Ministry of Science and Technology of the People's Republic of China (No. 2021ZD0113803), and the National Natural Science Foundation of China (No. 31701424).

Conflict of interest

Authors XL, YL, MF, SF, WG, QL, JiL, WW, JuL, QY, and ZY were employed by New Hope Liuhe Co., Ltd., China, Xiajin New Hope Liuhe Agriculture and Animal Husbandry Co., Ltd., Dezhou, China, and/or Shandong New Hope Liuhe Agriculture and Animal Husbandry Technology Co., Ltd., China.

The remaining authors declare that the research was conducted in the absence of any commercial or financial relationships that could be construed as a potential conflict of interest.

Publisher's note

All claims expressed in this article are solely those of the authors and do not necessarily represent those of their affiliated organizations, or those of the publisher, the editors and the reviewers. Any product that may be evaluated in this article, or claim that may be made by its manufacturer, is not guaranteed or endorsed by the publisher.

Supplementary material

The Supplementary Material for this article can be found online at: https://www.frontiersin.org/articles/10.3389/fvets.2022.1000969/full#supplementary-material

References

1. Ge S, Li J, Fan X, Liu F, Li L, Wang Q, et al. Molecular characterization of African swine fever virus, China, 2018. *Emerg Infect Dis.* (2018) 24:2131–3. doi: 10.3201/eid2411.181274

2. Costard S, Wieland B, de Glanville W, Jori F, Rowlands R, Vosloo W, et al. African swine fever: how can global spread be prevented? *Philos Trans R Soc Lond B Biol Sci.* (2009) 364:2683–96. doi: 10.1098/rstb.2009.0098

3. Gallardo C, Fernandez-Pinero J, Pelayo V, Gazaev I, Markowska-Daniel I, Pridotkas G, et al. Genetic variation among African swine fever genotype II viruses, Eastern and Central Europe. *Emerg Infect Dis.* (2014) 20:1544–7. doi: 10.3201/eid2009.140554

4. Oganesyan AS, Petrova ON, Korennoy FI, Bardina NS, Gogin AE, Dudnikov SA. African swine fever in the Russian Federation: spatio-temporal analysis and epidemiological overview. *Virus Res.* (2013) 173:204–11. doi: 10.1016/j.virusres.2012.12.009

5. Chapman DA, Darby AC, Da Silva M, Upton C, Radford AD, Dixon LK. Genomic analysis of highly virulent Georgia 2007/1 isolate of African swine fever virus. *Emerg Infect Dis.* (2011) 17:599–605. doi: 10.3201/eid1704.101283

6. Ma J, Chen H, Gao X, Xiao J, Wang H. African swine fever emerging in China: distribution characteristics and high-risk areas. *Prev Vet Med.* (2020) 175:104861. doi: 10.1016/j.prevetmed.2019.104861

7. Li X, Tian K. African swine fever in China. *Vet Rec.* (2018) 183:300–1. doi: 10.1136/vr.k3774

8. Lu G, Pan J, Zhang G. African swine fever virus in Asia: Its rapid spread and potential threat to unaffected countries. *J Infect.* (2020) 80:350–71. doi: 10.1016/j.jinf.2019.11.011

9. Zhou X, Li N, Luo Y, Liu Y, Miao F, Chen T, et al. Emergence of African swine fever in China, 2018. *Transbound Emerg Dis.* (2018) 65:1482–4. doi: 10.1111/tbed.12989

10. Zhao D, Liu R, Zhang X, Li F, Wang J, Zhang J, et al. Replication and virulence in pigs of the first African swine fever virus isolated in China. *Emerg Microbes Infect*. (2019) 8:438–47. doi: 10.1080/22221751.2019.1590128

11. Dixon LK, Chapman DA, Netherton CL, Upton C. African swine fever virus replication and genomics. *Virus Res*. (2013) 173:3–14. doi: 10.1016/j.virusres.2012.10.020

12. Tulman ER, Delhon GA, Ku BK, Rock DL. African swine fever virus. *Curr Top Microbiol Immunol*. (2009) 328:43–87. doi: 10.1007/978-3-540-68618-7_2

13. Olesen AS, Lohse L, Boklund A, Halasa T, Gallardo C, Pejsak Z, et al. Transmission of African swine fever virus from infected pigs by direct contact and aerosol routes. *Vet Microbiol*. (2017) 211:92–102. doi: 10.1016/j.vetmic.2017.10.004

14. Pikalo J, Deutschmann P, Fischer M, Roszyk H, Beer M, Blome S. African swine fever laboratory diagnosis-lessons learned from recent animal trials. *Pathogens*. (2021) 10:20177. doi: 10.3390/pathogens10020177

15. Walczak M, Zmudzki J, Mazur-Panasiuk N, Juszkiewicz M, Wozniakowski G. Analysis of the clinical course of experimental infection with highly pathogenic african swine fever strain, isolated from an outbreak in poland. aspects related to the disease suspicion at the farm level. *Pathogens*. (2020) 9:30237. doi: 10.3390/pathogens9030237

16. Goonewardene KB, Onyilagha C, Goolia M, Le VP, Blome S, Ambagala A. Superficial inguinal lymph nodes for screening dead pigs for african swine fever. *Viruses*. (2022) 14:83. doi: 10.3390/v14010083

17. Sánchez EG, Pérez-Núñez D, Revilla Y. Development of vaccines against African swine fever virus. *Virus Res*. (2019) 265:150–5. doi: 10.1016/j.virusres.2019.03.022

18. Arias M, de la Torre A, Dixon L, Gallardo C, Jori F, Laddomada A, et al. Approaches and perspectives for development of African swine fever virus vaccines. *Vaccines (Basel)*. (2017) 5:35. doi: 10.3390/vaccines5040035

19. Bosch-Camós L, López E, Rodriguez F. African swine fever vaccines: a promising work still in progress. *Porcine Health Manag*. (2020) 6:17. doi: 10.1186/s40813-020-00154-2

20. Karger A, Pérez-Núñez D, Urquiza J, Hinojar P, Alonso C, Freitas FB, et al. An update on african swine fever virology. *Viruses*. (2019) 11:864. doi: 10.3390/v11090864

21. Borca MV, Ramirez-Medina E, Silva E, Vuono E, Rai A, Pruitt S, et al. Development of a highly effective African swine fever virus vaccine by deletion of the I177L gene results in sterile immunity against the current epidemic Eurasia strain. *J Virol*. (2020) 5:19. doi: 10.1128/jvi.02017-19

22. Tran XH, Le TTP, Nguyen QH, Do TT, Nguyen VD, Gay CG, et al. African swine fever virus vaccine candidate ASFV-G-ΔI177L efficiently protects European and native pig breeds against circulating Vietnamese field strain. *Transbound Emerg Dis*. (2021) 24:14329. doi: 10.1111/tbed.14329

23. Borca MV, Ramirez-Medina E, Silva E, Vuono E, Rai A, Pruitt S, et al. ASFV-G-ΔI177L as an effective oral nasal vaccine against the Eurasia Strain of Africa swine fever. *Viruses*. (2021) 13:765. doi: 10.3390/v13050765

24. Tran XH, Phuong LTT, Huy NQ, Thuy DT, Nguyen VD, Quang PH, et al. Evaluation of the safety profile of the ASFV vaccine candidate ASFV-G-ΔI177L. *Viruses*. (2022) 14:896. doi: 10.3390/v14050896

25. Lacasta A, Monteagudo PL, Jimenez-Marin A, Accensi F, Ballester M, Argilaguet J, et al. Live attenuated African swine fever viruses as ideal tools to dissect the mechanisms involved in viral pathogenesis and immune protection. *Vet Res*. (2015) 46:135. doi: 10.1186/s13567-015-0275-z

26. Penrith ML, Vosloo W. Review of African swine fever: transmission, spread and control. *J S Afr Vet Assoc*. (2009) 80:58–62. doi: 10.4102/jsava.v80i2.172

27. Neilan JG, Zsak L, Lu Z, Burrage TG, Kutish GF, Rock DL. Neutralizing antibodies to African swine fever virus proteins p30, p54, and p72 are not sufficient for antibody-mediated protection. *Virology*. (2004) 319:337–42. doi: 10.1016/j.virol.2003.11.011

28. Blome S, Gabriel C, Beer M. Pathogenesis of African swine fever in domestic pigs and European wild boar. *Virus Res*. (2013) 173:122–30. doi: 10.1016/j.virusres.2012.10.026

29. Senthilkumar D, Rajukumar K, Sen A, Kumar M, Shrivastava D, Kalaiyarasu S, et al. Pathogenic characterization of porcine reproductive and respiratory syndrome virus of Indian origin in experimentally infected piglets. *Transbound Emerg Dis*. (2018) 65:1522–36. doi: 10.1111/tbed.12893

30. Liu J, Li Z, Ren X, Li H, Lu R, Zhang Y, et al. Viral load and histological distribution of atypical porcine pestivirus in different tissues of naturally infected piglets. *Arch Virol*. (2019) 164:2519-2523. doi: 10.1007/s00705-019-04345-3

31. Palya V, Homonnay ZG, Mato T, Kiss I. Characterization of a PCV2d-2 isolate by experimental infection of pigs. *Virol J*. (2018) 15:185. doi: 10.1186/s12985-018-1098-0

frontiers | Frontiers in Veterinary Science

TYPE Original Research
PUBLISHED 29 November 2022
DOI 10.3389/fvets.2022.1036744

OPEN ACCESS

EDITED BY
Yongtao Li,
Henan Agricultural University, China

REVIEWED BY
Chao Zhang,
Henan Agricultural University, China
Fei Liu,
Nanjing Agricultural University, China

*CORRESPONDENCE
Zili Li
lizili@mail.hzau.edu.cn

SPECIALTY SECTION
This article was submitted to Veterinary Experimental and Diagnostic Pathology, a section of the journal Frontiers in Veterinary Science

RECEIVED 05 September 2022
ACCEPTED 07 November 2022
PUBLISHED 29 November 2022

CITATION
Wang Y, Li R, Zhang Y, Zhang W, Hu S and Li Z (2022) Visual and label-free ASFV and PCV2 detection by CRISPR-Cas12a combined with G-quadruplex.
Front. Vet. Sci. 9:1036744.
doi: 10.3389/fvets.2022.1036744

Visual and label-free ASFV and PCV2 detection by CRISPR-Cas12a combined with G-quadruplex

Ying Wang[1,2], Rong Li[1], Yang Zhang[1], Weida Zhang[1], Sishun Hu[1,3,4] and Zili Li[1,3,4]*

[1]State Key Laboratory of Agricultural Microbiology, College of Veterinary Medicine, Huazhong Agricultural University, Wuhan, China, [2]College of Veterinary Medicine, Shanxi Agricultural University, Jinzhong, China, [3]Key Laboratory of Preventive Veterinary Medicine in Hubei Province, Wuhan, China, [4]Key Laboratory of Development of Veterinary Diagnostic Products, Ministry of Agriculture of the People's Republic of China, Wuhan, China

African swine fever (ASF) and postweaning multisystemic wasting syndrome (PMWS) are acute infectious diseases caused by the African swine fever virus (ASFV) and porcine circovirus type 2 (PCV2). At present, there are no effective vaccines for the prevention of ASFV. PMWS, which is harmful to the domestic and even the world pig industry, is difficult to cure and has a high mortality. So, developing simple, inexpensive, and accurate analytical methods to detect and effectively diagnose ASFV and PCV2 can be conducive to avoid ASFV and PCV2 infection. CRISPR has become a potentially rapid diagnostic tool due to recent discoveries of the trans-cleavage properties of CRISPR type V effectors. Herein, we report the visual detection based on CRISPR-Cas12a (cpf1), which is more convenient than fluorescence detection. Through *in vitro* cleavage target DNA activation, Cas12a can trans-cleavage ssDNA G-quadruplex. TMB/H_2O_2 and Hemin cannot be catalyzed by cleavaged G-DNA to produce green color products. This protocol is useful for the detection of ASFV and PCV2 with high sensitivity. This method can enable the development of visual and label-free ASFV and PCV2 detection and can be carried out in the field without relying on instruments or power. This method can complete nucleic acid detection at 37 °C without using other instruments or energy. Our research has expanded the application of Cas12a and laid the foundation for the field's rapid detection of viral nucleic acid in future.

KEYWORDS

ASFV, PCV2, detection, Cas12a, G-quadruplex

Introduction

African swine fever (ASF) and porcine circovirus-associated diseases are infectious diseases caused by the African swine fever virus (ASFV) and porcine circovirus. ASFV's clinical symptoms vary from acute and subacute to chronic.

It is characterized by high fever, cyanosis, widespread internal organ bleeding, respiratory disorder, and neurological symptoms. It is incidence and mortality rate are nearly 100% (1). ASF has broken out in Europe, Africa, and Asia and brought huge economic losses to the pig industry (2, 3). ASF was first reported in China in 2018 and has caused huge social and economic losses (4, 5). Recently, the low pathogenicity of ASFV non-hemadsorbing isolates has been reported (6), which makes the prevention and control of ASF more and more difficult. Real-time polymerase chain reaction (PCR) assay and chemiluminescence immunoassay have been reported for the detection of ASFV (7, 8).

Porcine circovirus type 2 (PCV2) is classified in the circoviridae family and ssDNA animal virus (9) and is associated with postweaning multisystemic wasting syndrome (PMWS) in the pig. PCV2 has caused severe losses in the global swine industry in recent decades (10). Although the PCV2 vaccine is available because of the short protection period and mixed infection of different genotypes, it is not easy to eliminate PCV2 from pigs by vaccination alone (11, 12). Loop-mediated isothermal amplification (LAMP) and multiplex real-time PCR assay have been used for PCV2 detection (13, 14).

Developing simple, inexpensive, and accurate analytical methods to detect and effectively diagnose ASFV and PCV2 is conducive to avoid ASFV and PCV2 infection. The diagnosis of virus infection generally includes virus isolation and identification, the detection of virus nucleic acid, antigen, and the specific antibody, which not only takes a long time but also requires high standards of medical equipment and operators. Ideal diagnostic tests should deliver results quickly and be enabled for instant use on a variety of sample types without excessive reliance on a technician or an auxiliary device (15).

At the University of California, Jennifer Doudna, Alexandra East-Seletsky, and their colleagues used Cas13a incidental cleavage activity to detect RNA (16). Zhang Feng has demonstrated that Cas13-based Specific High Sensitivity

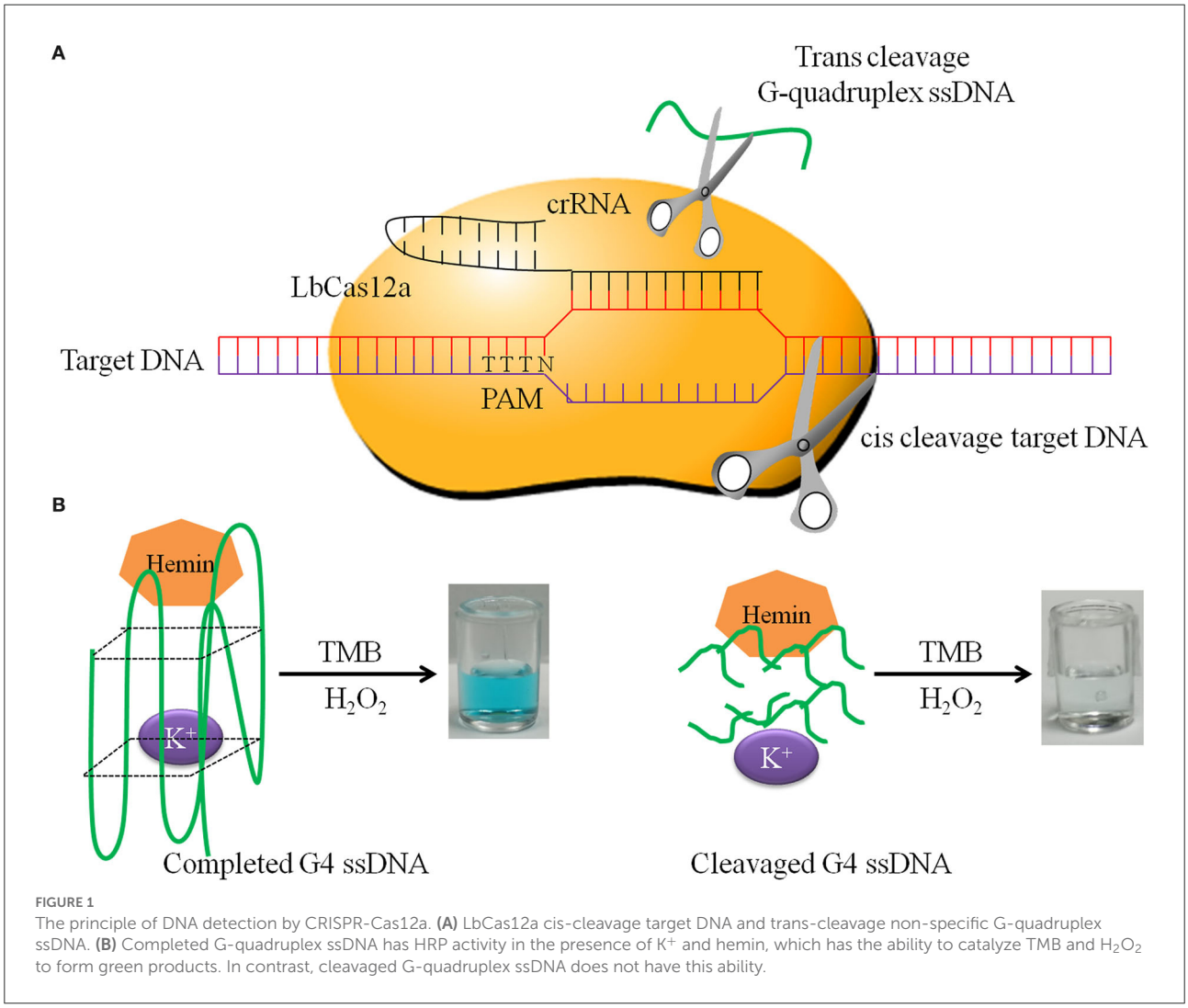

FIGURE 1
The principle of DNA detection by CRISPR-Cas12a. **(A)** LbCas12a cis-cleavage target DNA and trans-cleavage non-specific G-quadruplex ssDNA. **(B)** Completed G-quadruplex ssDNA has HRP activity in the presence of K^+ and hemin, which has the ability to catalyze TMB and H_2O_2 to form green products. In contrast, cleavaged G-quadruplex ssDNA does not have this ability.

Enzymatic Reporter UnLOCKing (SHERLOCK) can be applied for detecting Zika virus (ZIKV) and Dengue virus (DENV) in patient's samples (17). When Cas13a detects the target RNA sequence, its indistinguishable RNAase activity (incidental cleavage activity) also cleaves the RNA reporter molecule and releases detectable fluorescent signals.

When Cas13a binds to crRNA and identifies the corresponding RNA sequence, Cas13a RNAase activity is activated, and the activity of Cas13a also cuts other untargeted RNA. This phenomenon is called the "collateral effect." At the same time, Chinese and American researchers proposed that FnCpf1 and LbCpf1 proteins (also known as FnCas12a and LbCas12a) also have the "collateral effect" (18). These gene detection techniques based on LbCas12a are named DETECTR (DNA Endonuclease Targeted CRISPR Trans Reporter). The principle of DETECTR is similar to SHERLOCK. Cas13a recognizes target RNA and is activated for untargeted RNA cleavage, while Cas12a recognizes target DNA and is activated for untargeted ssDNA cleavage. F-Q label RNA/ssDNA cleavage by Cas13a/12a is confirmed by fluorescence detection.

DNAzymes possess practical advantages (19), DNA hybridization assays, and catalytic beacons for the detection of DNA and telomerase activity (20). As for metal ion detection, K(+) sensitive G-quadruplex DNA PS5.M as a sensitive element has promoted the development of K(+) detection (21). Aptasensors for small molecules and proteins, utilizing the bioelectrocatalytic function of hemin/G-quadruplex DNase activity to develop glucose oxidation and biosensors detection methods also can be used to detect DNA or low-molecular-weight substrates (22). For example, visual detection of single-nucleotide polymorphisms (SNP) (23). Therefore, they can be promising candidates for practical applications.

Herein, we report the visual detection based on CRISPR-Cas12a (cpf1), which is more convenient than fluorescence detection. Through *in vitro* cleavage target DNA activation Cas12a trans-cleavage ssDNA G-quadruplex. TMB/H_2O_2 and Hemin cannot be catalyzed by cleavage G-DNA to produce green color products. This protocol is useful for the detection of ASFV and PCV2 nucleic acid with high sensitivity. As demonstrated, our research could enable the development of visual and label-free ASFV detection and can be carried out in the field without relying on instruments or power.

Materials and methods

The short G-rich DNA sequence (GDS) PW17 5' GGGTAGGGCGGGTTGGG 3' and primers used in this study were synthesized and provided by Tsingke Biotech Co. (Beijing, China) (Supplementary Table S1). Hemin, Tris–HCl, DMSO (Dimethyl Sulfoxide), and KCl were purchased from Sigma-Aldrich (Shanghai, China). TwistAmp® Basic recombinase polymerase amplification (RPA) was used to amplify clinical samples. LbCas12a was purchased from NEB (M0653T, Beijing, NEB). T7 high-yield RNA transcription kit was purchased from Vazyme (Nanjing, China). 10 × reaction buffer prepared with 100 mM Tris–HCl, 150 mM NaCl, 12 mM $MgCl_2$, and 12 mM KCl.

Determination of the optimum hemin and G-quadruplex concentration

PW17 is a nucleic acid sequence often used to form G-quadruplex monomer. Synthetic PW17 was dissolved in 100 μM DNA stock solution by ddH_2O. PW17 was diluted before use. Hemin was dissolved with DMSO to 50 mM, stored at 4 °C, and diluted before use. In order to determine the optimum hemin concentration, 1.0 μM G-quadruplex and different concentrations of hemin were mixed, respectively, with reaction buffer at a total volume of 50 μL at 37 °C for 60 min. For checking the optimum G-quadruplex concentration, 2.0 μM hemin was mixed with different G-quadruplex concentrations, respectively. The reaction system is the same as above. The optimal reaction time was measured to determine the best detection time. We mixed 2.0 μM hemin with 0.4 μM G-quadruplex at 37 °C, observed the color, and determined the OD_{450} at different times.

ASFV and PCV2 target DNA selected and crRNA designed

The African swine fever virus VP72 protein gene and PCV2 capsid protein (Cap protein) gene are the conserved gene sequences selected as target DNAs. The target DNAs were cloned by PCR with primer pairs ASFV VP72 F/R and PCV2 Cap F/R (Supplementary Table S1).

CRISPR-DT online design website was used for crRNA prediction (24). crRNA F and PCV2 crRNA R primers were used for synthesizing crRNA, which targets PCV2. crRNA F and ASFV crRNA R primers were used for synthesizing crRNA, which targets ASFV. The T7 high-yield RNA transcription kit for RNA synthesis *in vitro*.

Analysis of crRNA cleavage efficiency and optimal cleavage time

LbCas12a and crRNA cleaving target DNA activity *in vitro* were verified by the following reaction system: 500 ng DNA fragment, reaction buffer (10×) 2.5 μL, crRNA 1 μL (40 ng/μL final), 1 μM LbCas12a (Cpf1) 2.5 μL (100 nM final), total reaction volume 25 μL at 37°C for 60 min, and 72°C for 10 min

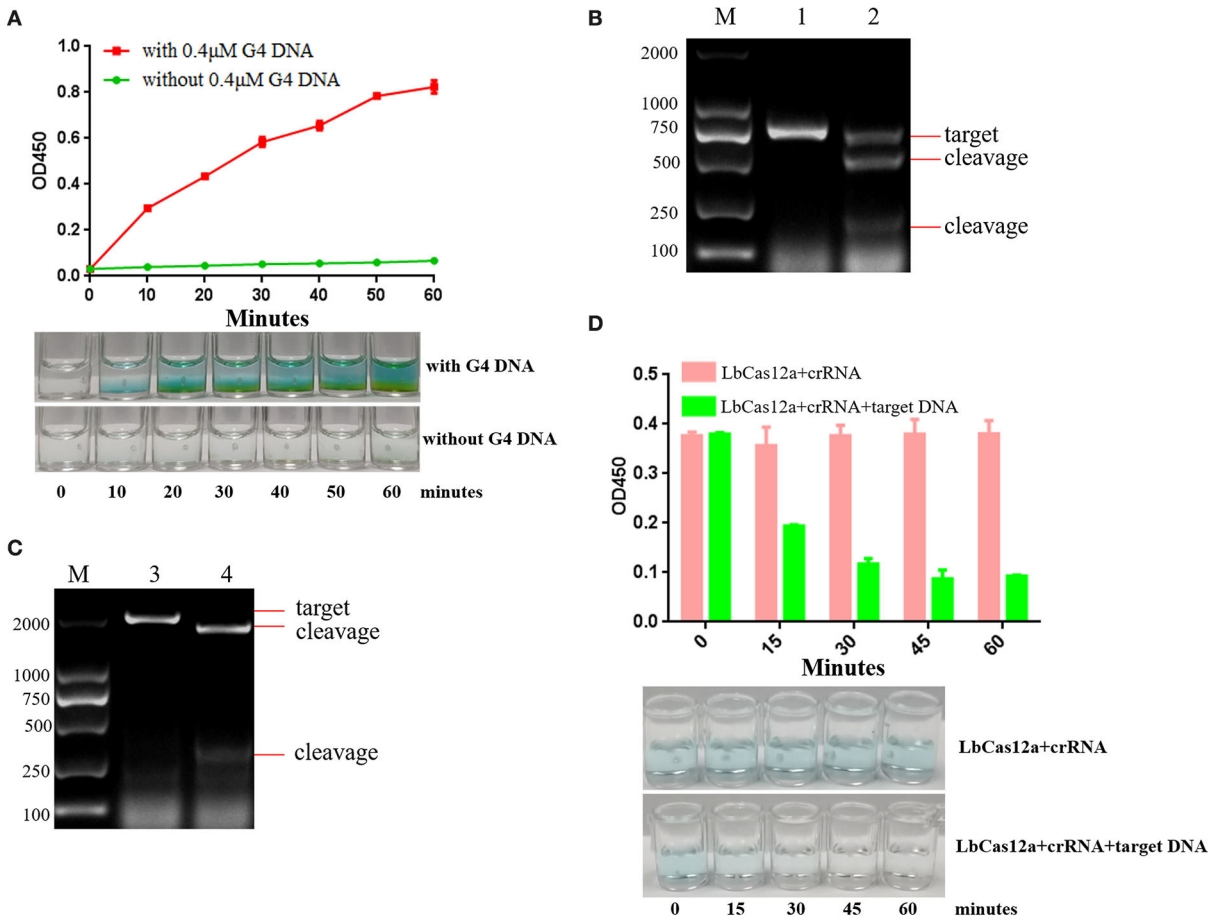

FIGURE 2
The analysis of optimal reaction time and target DNA sequence. **(A)** TMB is catalyzed by 0.4 μM G-quadruplex and 2 μM hemin. The color gradually deepened with the increase of time, and the green color could be observed after incubation at 37 °C for 20 min. **(B)** crRNAs were designed and synthesized according to the PCV2 Cap protein gene, and the cleavage efficiency of crRNA targeting PCV2 Cap was analyzed. Lane M: 2000 DNA ladder; Lane 1: negative control, PCV2 Cap gene was cut by ASFV crRNA and Lbcas12a; Lane 2: PCV2 Cap gene was cut by PCV2 crRNA and Lbcas12a. **(C)** crRNA was designed and synthesized according to ASFV VP72 protein gene, and the cleavage efficiency of crRNA targeting ASFV VP72 was analyzed. Lane M: 2000 DNA ladder; Lane 3: negative control, ASFV VP72 gene was cut by PCV2 crRNA and Lbcas12a; Lane 4: ASFV VP72 gene was cut by ASFV crRNA and Lbcas12a. **(D)** Evaluation of the efficiency of trans-cleavage G-quadruplex ssDNA by LbCas12a with crRNA over time.

inactivation. Gel electrophoresis is used for the analysis of cleaving efficiency.

A concentration of 50 nM ASFV VP72 DNA fragment, 2.5 μL of cleavage buffer (10×), 1 μL of crRNA at a final concentration of 40 ng/μL, 2.5 μL of 1 μM LbCas12a (Cpf1) at a final concentration of 100 nM, and 1 μL of G-quadruplex and added up to 25 μL by H_2O at 37 °C for different time periods. Analysis of cutting efficiency is determined by adding 2 μM of hemin, reaction buffer, and 100 μL of TMB/H_2O_2. The reaction solution was incubated at 37 °C for 20 min. The color and OD_{450} were observed and determined at different times.

RPA amplification and nucleic acid extraction

Recombinase polymerase amplification was used to amplify clinical samples *in vitro* (25). TwistAmp® Basic was applied for amplification. PCV2 RPA F/R and ASFV RPA F/R primer pairs were used for RPA. PCV2 Cap and ASFV VP72 DNA templates were adjusted to 1.0×10^3, 1.0×10^2, and 1.0×10^1 copies, and 2 μL of DNA template was added for RPA amplification. MagBead DNA Purification Kit was applied for the purification of the DNA fragments, which were resuspended and recovered with 20 μL of ddH_2O.

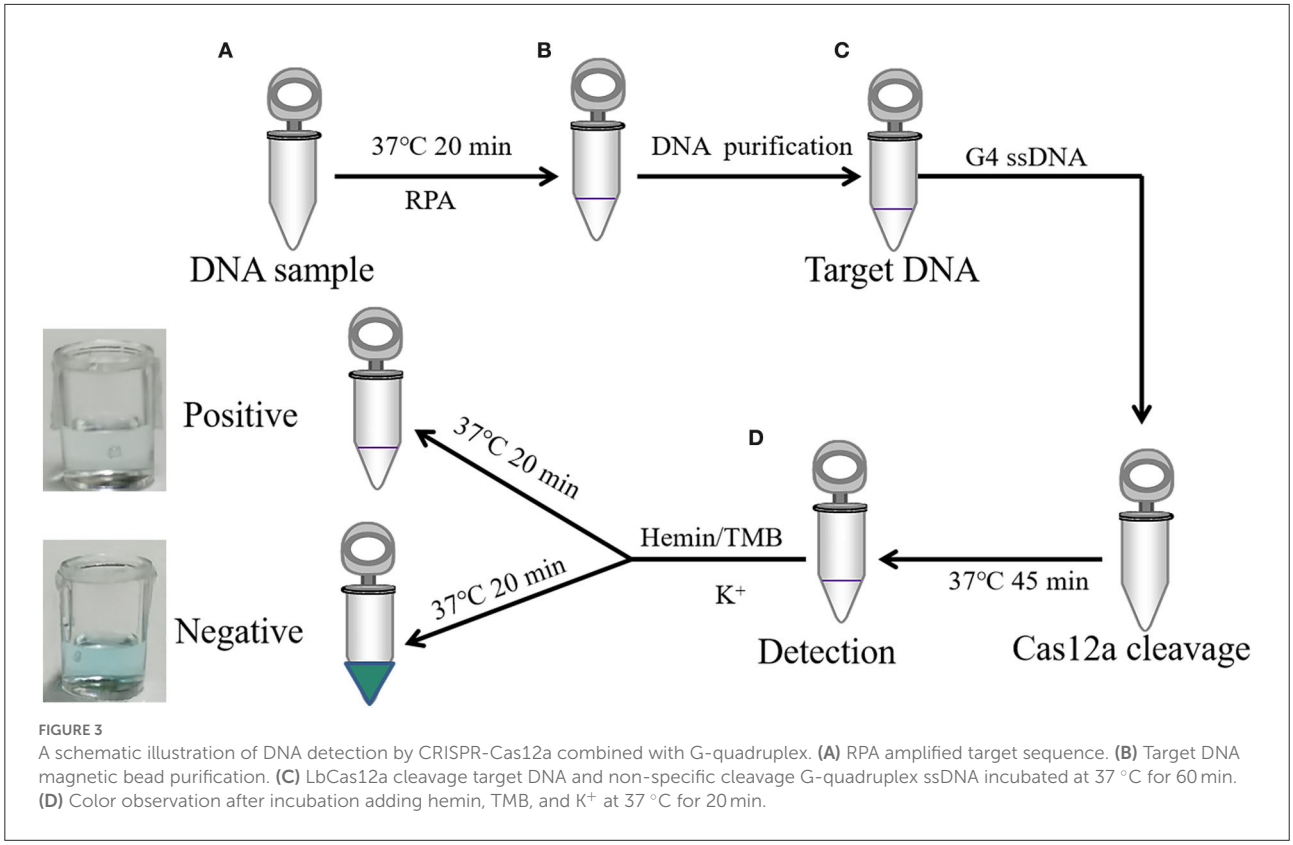

FIGURE 3
A schematic illustration of DNA detection by CRISPR-Cas12a combined with G-quadruplex. **(A)** RPA amplified target sequence. **(B)** Target DNA magnetic bead purification. **(C)** LbCas12a cleavage target DNA and non-specific cleavage G-quadruplex ssDNA incubated at 37 °C for 60 min. **(D)** Color observation after incubation adding hemin, TMB, and K^+ at 37 °C for 20 min.

Sensitivity of PCV2 and ASFV DNA detection by CRISPR-Cas12a combined with G-quadruplex

Porcine circovirus type 2 capsid and ASFV VP72 DNA templates were adjusted to 1.0×10^3, 1.0×10^2, and 1.0×10^1 copies, and 2 μL of DNA template was added for RPA amplification. DNA fragments were purified by resuspending and recovering by 20 μL H_2O. The 18 μL of RPA reaction product was added with 2.5 μL of reaction buffer (10×), 1 μL of crRNA at a concentration of 40 ng/μL, 2.5 μL of LbCas12a (Cpf1) at a concentration of 100 nM, and 1 μL of G-quadruplex and incubated at 37 °C for 45 min. 2.0 μM hemin, reaction buffer, and 100 μL TMB were added and incubated for 20 min. The observation of green-colored oxidized products determined DNA detection.

Gel electrophoresis

Gel electrophoresis was to confirm the PCR and RPA amplification and DNA cleavage. The 40 mL agarose gel contains 1.2% agarose and 1×TBE at pH 8.0. The electrophoresis was run with a voltage of 120 V for 30 min.

Results

Determination of the optimum hemin and G-quadruplex concentration

Cas12a, upon cleaving the target dsDNA, will proceed to cleave ssDNA in a nonspecific manner, the so-called "trans-cleavage." Using this principle, the target sequence, amplificated by RPA, is cut by Cas12a and crRNA, activating the trans-cleavage activities of Cas12a. The G-quadruplex ssDNA is cut by activated Cas12a, so it cannot form a spatial structure and loses the oxidase activity. If there is no target sequence, the G-quadruplex ssDNA is not cut by Cas12a. Then G-quadruplex forms a spatial structure and has oxidase activity. The complete G-quadruplex and hemin combine to catalyze TMB to show blue. In this study, the positive reaction is colorless, and the negative reaction is blue. The principle of DNA detection by CRISPR-Cas12a and the research scheme of this study is shown in Figure 1. When the OD_{450} was close to 1.0, the minimum hemin concentration was the best dosage. We determined that the optimal hemin concentration was 2.0 μM (Supplementary Figure S1). When the reaction was obviously green, the minimum G-quadruplex concentration was selected as the best dosage. The optimal G-quadruplex concentration was 0.4 μM (Supplementary Figure S2). With the prolongation of reaction time, the color green gradually deepened, and OD

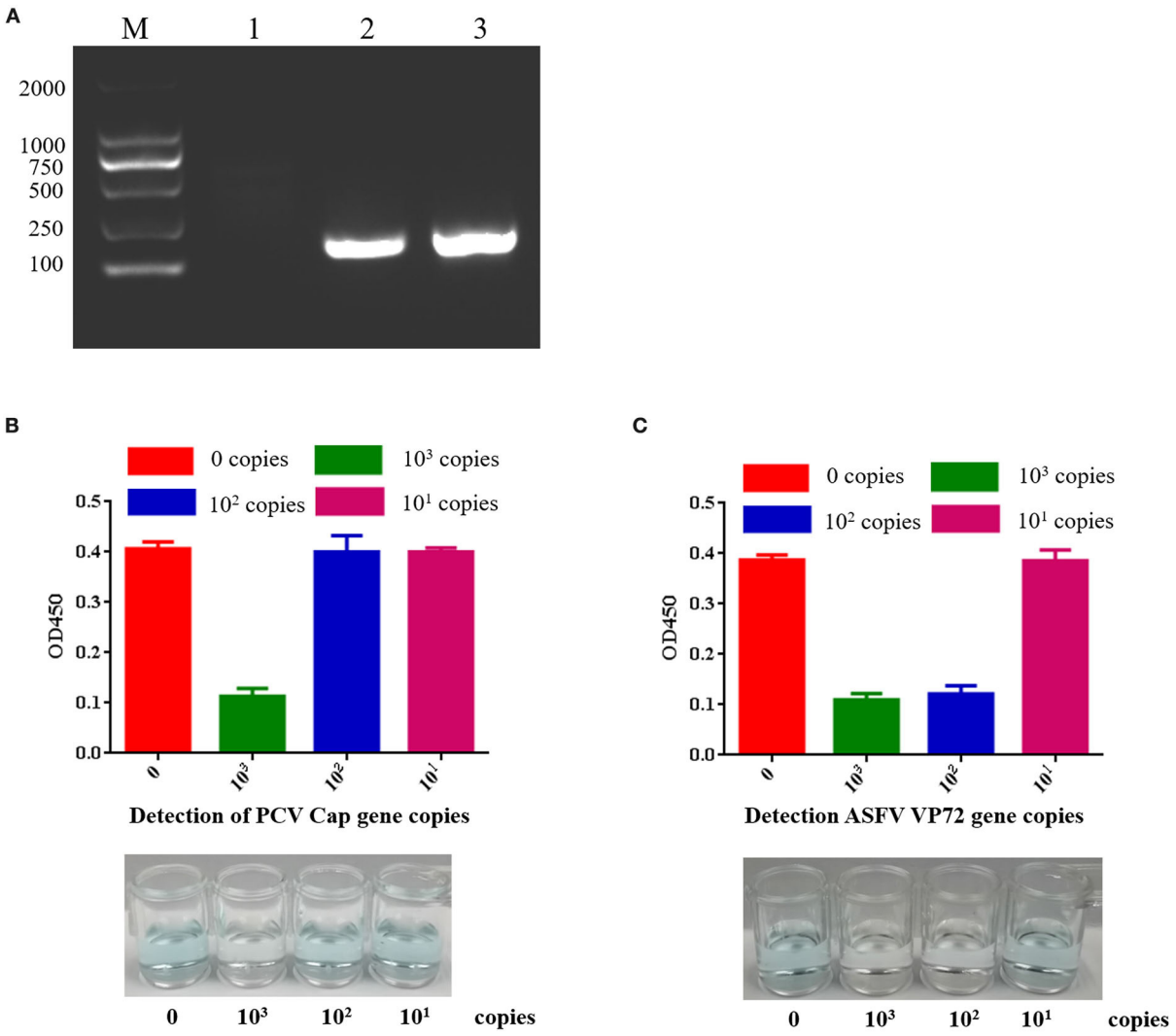

FIGURE 4
Sensitivity of PCV2 and ASFV DNA detection by CRISPR-Cas12a combined with G-quadruplex. **(A)** RPA amplified target DNA. Lane M: 2000 DNA ladder; Lane 1: negative control; Lane 2: RPA amplification of PCV2 target sequence; Lane 3: RPA amplified ASFV target sequence. **(B)** PCV2 DNA detection by CRISPR-Cas12a combined with G-quadruplex. The least copies of this method were 10^3 copies. **(C)** ASFV DNA detection by CRISPR-Cas12a combined with G-quadruplex. The least copies of this method were 10^2 copies.

increased; the figure shows the color development over the time period of 60 min (Figure 2A).

ASFV VP72 protein gene and PCV2 cap protein gene as the target DNAs

VP72 and Cap are the conserved genes of ASFV and PCV2. To investigate the DNA cleavage feature of Cas12a, we employed LbCas12a to cleave target DNA *in vitro*. ASFV VP72 protein gene and PCV2 Cap protein gene are the target DNAs and were cloned (Supplementary Figure S3) by PCR with primer pairs PCV2 Cap F/R and ASFV VP72 F/R.

crRNA cutting efficiency and optimal cleavage time

CRISPR-DT online design website was used for crRNA prediction. Two crRNAs were designed (Supplementary Figures S4, S5) and synthesized, respectively, in each target DNA with primer crRNA F and PCV2 crRNA R/ASFV crRNA R by T7 high-yield RNA transcription kit. The activity of LbCas12a and crRNA cleaving target DNA *in vitro* was verified. The results are presented in Figures 2B,C. In the presence of LbCas12a and crRNA, the PCV2 Cap gene and ASFV VP72 gene target sequences were cut and generated short products. The results indicated that target DNAs were recognized by designing crRNA efficiently.

Single-stranded DNA can be degraded by activated Cas12a non-specifically. LbCas12a and crRNA cutting PW17 G-quadruplex ssDNA activity *in vitro* was verified. The results indicated that G-quadruplex DNA was cut by activated LbCas12a. Once generated cleavage G-quadruplex, the green color will not be observed. The best cleavage efficiency can be achieved in 45 min (Figure 2D). Over time, the green color could not be observed. In order to ensure the completion of G-quadruplex cleavage, 45 min had been selected as the reaction cleavage time.

Sensitivity of PCV2 and ASFV DNA detection by CRISPR-Cas12a combined with G-quadruplex

LbCas12a is a fluorescence analyzer for gene detection, so it is important to develop a detection method for LbCas12a nucleic acid without power or instruments. Activated Cas12a can cut G-quadruplex and make the color reaction disappear. It can be used for unmarked naked-eye detection.

Cas12a nucleic acid detection scheme is shown in Figure 3. RPA was used to amplify clinical samples *in vitro* (25). TwistAmp® Basic was applied for amplification. PCV2 Cap gene and ASFV VP72 gene were amplified by RPA (Figure 4A). PCV2 Cap and ASFV VP72 DNA template were adjustment to 1.0×10^3, 1.0×10^2, and 1.0×10^1 copies, and 2 μL of DNA template was added for RPA amplification. The RPA maximum amplification is 1.0×10^3 copies for the PCV2 Cap gene (Supplementary Figure S6), and 1.0×10^2 copies for the ASFV VP72 gene (Supplementary Figure S7).

MagBead DNA Purification Kit is used for purifying DNA fragments, 20 μL of ddH_2O resuspend and recover DNA fragments. The 18 μL RPA reaction product was added with 2.5 μL of reaction buffer (10×), 1 μL of crRNA at a final concentration of 40 ng/μL, 2.5 μL of 1 μM LbCas12a (Cpf1) at a final concentration of 100nM, and 1 μL of G-quadruplex and incubated in 37 °C 45 min. 2.0 μM hemin and 100 μL TMB were added and incubated for 20 min. Green-colored oxidized product was used for DNA detection (Figures 4B,C). If the reaction fluid is green, it indicates no target DNA, while colorless indicates target DNA. The results showed that the least copies of PCV2 DNA detected by CRISPR-Cas12a combined with G-quadruplex was 10^3 copies, and the least copies number of ASFV DNA detected by CRISPR-Cas12a combined with G-quadruplex was 10^2 copies. Our results indicated that G-quadruplex could be used as a substrate for color reaction, nucleic acid could be detected without an instrument, and the reaction could be carried out at room temperature. This method can be used for field diagnosis with high detection speed and accuracy in poor conditions.

Discussion

The African swine fever virus, a double-stranded DNA virus with a genome size of 170–193 kb, belongs to the ASF family (26). The virus has five unique structural features, including an outer membrane, capsid, double inner membrane, core–shell, and genome. The virus particle contains more than 30,000 protein subunits and is assembled into spherical particles with a diameter of about 260 nm. Most of the virus surface is composed of the main capsid protein VP72 (27). At present, there are no effective vaccines for the prevention of ASF, so a rapid detection for effective diagnoses of ASFV is conducive to the purification of ASF.

At present, there are no specific treatments for PCV2. It is easy for it to be coinfected with other viruses, such as classical swine fever virus (CSFV), porcine reproductive and respiratory syndrome virus (PRRSV), and porcine pseudorabies virus (PRV), thus brings great difficulties to the diagnosis (28). The virus was detected according to clinical symptoms, and mixed infection was easy to lead to missed detection of the PCV2 virus. Some methods have been developed for PCV2 detection. An isothermal RPA assay has been established (29). In addition, the droplet digital polymerase chain reaction (30) and TB green II-based duplex real-time fluorescence quantitative PCR assay (31) were applied to detect PCV2 and PCV3.

African swine fever continues to mutate in China, and there is no effective vaccine yet. Therefore, the farms need to find it early and report it to the authorities as soon as possible, to kill and disinfect the pigs in the epidemic area, and to better limit the spread of the virus. As an immunosuppressive disease, PCV2 needs to be isolated and eliminated from infected pigs. This method can promote the diagnosis of infected pigs and assist the management of pig farms.

At present, the detection of ASFV and PCV2 has been reported in many methods and with high sensitivity. The detection sensitivity of DNA extraction-free qPCR, visual LAMP, and fluorescent LAMP assays for the detection of ASFV could detect 5.8 copies/μL, the same as qPCR (32). The RPA-Cas12a-fluorescence assay can be detected with as few as two copies of ASFV (33). The One-pot platform for rapid detecting viruses utilizing RAA and CRISPR/Cas12a could detect 3.07 copies/μL (34). The detection sensitivity of EvaGreen real-time PCR combined with melting curve analysis could detect 5.0 copies/μL (35). LAMP-coupled CRISPR-Cas12a can be detected with a low detectable limit of 1 copy/μL of PCV2 (36). In this study, the detection sensitivity of ASFV and PCV2 was 10^2 copies and 10^3 copies, respectively, which are lower than the above detection methods. The above methods, especially the qPCR method, which is the gold method for virus detection, require instruments and are not conducive to field detection. Our method can well avoid this problem. It does not rely on instruments but only on reaction in tubes. Our method

can directly observe the results with naked eyes, which is not available in the above methods.

The HlyA gene is by hemin/G-quadruplex DNAzyme and hybridization chain reaction signal amplification (37). G-quadruplex-based biosensors have a particular focus on SARS-CoV-2 detection (38). The detection of patulin toxin is by using DNA G-quadruplex with aggregation-induced emission (39).

African swine fever and porcine circovirus are two infectious diseases that China's breeding industry pays more attention. The rapid detection of ASF is helpful for the farms to report the epidemic situation to the authorities. After the official diagnosis, the pigs in the farms will be harmlessly treated as soon as possible to limit the spread of ASFV. Porcine circovirus infection leads to the decline of pig immunity, and it is easy to infect other bacterial or viral infectious diseases. The method we studied can quickly detect ASF and circovirus type 2 without relevant instruments. At present, this method is aimed at DNA viruses and mainly relies on the DNA amplification of RPA. It cannot detect RNA vaccines. Therefore, it is necessary to develop further the RNA virus detection method based on this study.

Conclusion

At present, ASF is spreading in China and European countries, and farms need to find and report quickly to better limit the spread of the virus. PCV2 is an immunosuppressive disease. This method can speed up the diagnosis of infected pigs and isolate and eliminate infected pigs. In this study, effective detection of ASFV and PCV2 nucleic acid as the target gene is achieved. In addition, this method can complete nucleic acid detection at 37 °C without using other instruments or energy. Our research has expanded the application of Cas12a and laid the foundation for the field rapid detection of viral nucleic acid in future.

Data availability statement

The original contributions presented in the study are included in the article/Supplementary material, further inquiries can be directed to the corresponding author.

Author contributions

YW contributed to the investigation, visualization, and writing of original draft. YW, RL, and YZ contributed to the methodology. YW, WZ, and SH contributed to the project administration. ZL contributed to the resources, supervision, validation, and writing of review's editing. All authors contributed to the article and approved the submitted version.

Funding

This work was funded by the Key Science and Technology Project of Guangxi (Gui Ke AA18118051 to ZL) and the National Key Research and Development Program of China (2018YFD0500800 to ZL).

Conflict of interest

The authors declare that the research was conducted in the absence of any commercial or financial relationships that could be construed as a potential conflict of interest.

Publisher's note

All claims expressed in this article are solely those of the authors and do not necessarily represent those of their affiliated organizations, or those of the publisher, the editors and the reviewers. Any product that may be evaluated in this article, or claim that may be made by its manufacturer, is not guaranteed or endorsed by the publisher.

Supplementary material

The Supplementary Material for this article can be found online at: https://www.frontiersin.org/articles/10.3389/fvets.2022.1036744/full#supplementary-material

SUPPLEMENTARY FIGURE S1
Determination of the optimum hemin concentration. Red curve with 1mM G4; Green curve without G4.

SUPPLEMENTARY FIGURE S2
Determination of the optimum G-quadruplex concentration. Red curve with 2 μM hemin; Green curve without hemin.

SUPPLEMENTARY FIGURE S3
Target gene amplification. Lane M: 2000 DNA marker; Lane 1: negative control; Lane 2: PCV2 Cap protein gene PCR amplification; Lane 3: ASFV VP72 protein gene PCR amplification.

SUPPLEMENTARY FIGURE S4
RPA primers and crRNA design of PCV2 Cap gene.

SUPPLEMENTARY FIGURE S5
RPA primers and crRNA design of ASFV VP72 gene.

SUPPLEMENTARY FIGURE S6
Sensitivity of RPA for PCV2. Different copies of PCV2 DNA were used as template for RPA. The PCV2 lowest copies that could be determined by RPA was 10^3 copies. Lane M: 2000 DNA marker; Lane 1: Negative control; Lane 2: 10^3 copies; Lane 3: 10^2 copies; Lane 4: 10^1 copies.

SUPPLEMENTARY FIGURE S7
Sensitivity of RPA for ASFV. Different copies of ASFV DNA were used as template for RPA. The ASFV lowest copies that could be determined by RPA was 10^2 copies. Lane M: 2000 DNA marker; Lane 1: Negative control; Lane 2: 10^3 copies; Lane 3: 10^2 copies; Lane 4: 10^1 copies.

SUPPLEMENTARY TABLE S1
Sequence information for primers.

References

1. Lokhandwala S, Petrovan V, Popescu L, Sangewar N, Elijah C, Stoian A, et al. Adenovirus-vectored African swine fever virus antigen cocktails are immunogenic but not protective against intranasal challenge with Georgia 2007/1 isolate. *Vet Microbiol.* (2019) 235:10–20. doi: 10.1016/j.vetmic.2019.06.006

2. Galindo I, Alonso C. African swine fever virus: a review. *Viruses.* (2017) 9:103. doi: 10.3390/v9050103

3. Sanchez-Cordon PJ, Montoya M, Reis AL, Dixon LK. African swine fever: a re-emerging viral disease threatening the global pig industry. *Vet J.* (2018) 233:41–8. doi: 10.1016/j.tvjl.2017.12.025

4. Ge S, Li J, Fan X, Liu F, Li L, Wang Q, et al. Molecular characterization of African swine fever virus, China, 2018. *Emerg Infect Dis.* (2018) 24:2131–3. doi: 10.3201/eid2411.181274

5. Zhao D, Liu R, Zhang X, Li F, Wang J, Zhang J, et al. Replication and virulence in pigs of the first African swine fever virus isolated in China. *Emerg Microbes Infect.* (2019) 8:438–47. doi: 10.1080/22221751.2019.1590128

6. Sun E, Zhang Z, Wang Z, He X, Zhang X, Wang L, et al. Emergence and prevalence of naturally occurring lower virulent African swine fever viruses in domestic pigs in China in 2020. *Sci China Life Sci.* (2021) 64:752–65. doi: 10.1007/s11427-021-1904-4

7. Trinh TBN, Truong T, Nguyen VT, Vu XD, Dao LA, Nguyen TL, et al. Development of a novel real-time PCR assay targeting p54 gene for rapid detection of African swine fever virus (ASFV) strains circulating in Vietnam. *Vet Med Sci.* (2021) 7:2268–72. doi: 10.1002/vms3.605

8. Yang Y, Lv C, Fan J, Zhao Y, Jiang L, Sun X, et al. Development of a chemiluminescence immunoassay to accurately detect African swine fever virus antibodies in serum. *J Virol Methods.* (2021) 298:114269. doi: 10.1016/j.jviromet.2021.114269

9. Tischer I, Gelderblom H, Vettermann W, Koch MAA. Very small porcine virus with circular single-stranded DNA. *Nature.* (1982) 295:64–6. doi: 10.1038/295064a0

10. Segalés J, Allan GM, Domingo M. Porcine circovirus diseases. *Anim Health Res Rev.* (2005) 6:119–42. doi: 10.1079/AHR2005106

11. Beach NM, Meng XJ. Efficacy and future prospects of commerciallyavailable and experimental vaccines against porcine circovirus type 2 (PCV2). *Virus Res.* (2012) 164:33–42. doi: 10.1016/j.virusres.2011.09.041

12. Zhai SL, Chen SN, Xu ZH, Tang MH, Wang FG, Li XJ, et al. Porcine circovirus type 2 in China: an update on and insights to its prevalence and control. *Virol J.* (2014) 11:88. doi: 10.1186/1743-422X-11-88

13. Zhao K, Shi W, Han F, Xu Y, Zhu L, Zou Y, et al. Specific, simple and rapid detection of porcine circovirus type 2 using the loop-mediated isothermal amplification method. *Virol J.* (2011) 8:126. doi: 10.1186/1743-422X-8-126

14. Wang Y, Noll L, Porter E, Stoy C, Dong J, Anderson J, et al. Development of a differential multiplex real-time PCR assay for porcine circovirus type 2 (PCV2) genotypes PCV2a, PCV2b and PCV2d. *J Virol Methods.* (2020) 286:113971. doi: 10.1016/j.jviromet.2020.113971

15. Chertow DS. Next-generation diagnostics with CRISPR. *Science.* (2018) 360:381–2. doi: 10.1126/science.aat4982

16. East-Seletsky A, O'Connell MR, Knight SC, Burstein D, Cate JH, Tjian R, et al. Two distinct RNase activities of CRISPR-C2c2 enable guide-RNA processing and RNA detection. *Nature.* (2016) 538:270–73. doi: 10.1038/nature 19802

17. Gootenberg JS, Abudayyeh OO, Lee JW, Essletzbichler P, Dy AJ, Joung J, et al. Nucleic acid detection with CRISPR-Cas13a/C2c2. *Science.* (2017) 356:438–42. doi: 10.1126/science.aam9321

18. Chen JS, Ma E, Harrington LB, Da Costa M, Tian X, Palefsky JM. M. CRISPR-Cas12a target binding unleashes indiscriminate single-stranded DNase activity. *Science.* (2018) 360:436–39. doi: 10.1126/science.aar6245

19. Kosman J, Juskowiak B. Peroxidase-mimicking DNAzymes for biosensing applications: a review. *Anal Chim Acta.* (2011) 707:7–17. doi: 10.1016/j.aca.2011.08.050

20. Xiao Y, Pavlov V, Niazov T, Dishon A, Kotler M, Willner I, et al. Catalytic beacons for the detection of DNA and telomerase activity. *J Am Chem Soc.* (2004) 126:7430–1. doi: 10.1021/ja031875r

21. Yang X, Li T, Li B, Wang E. Potassium-sensitive G-quadruplex DNA for sensitive visible potassium detection. *Analyst.* (2010) 135:71–5. doi: 10.1039/B913036E

22. Niazov A, Freeman R, Girsh J, Willner I. Following glucose oxidase activity by chemiluminescence and chemiluminescence resonance energy transfer (CRET) processes involving enzyme-DNAzyme conjugates. *Sensors (Basel).* (2011) 11:10388–97. doi: 10.3390/s111110388

23. Kolpashchikov DM. Split DNA enzyme for visual single nucleotide polymorphism typing. *J Am Chem Soc.* (2008) 130:2934–5. doi: 10.1021/ja711192e

24. Zhu H, Liang C. CRISPR-DT: designing gRNAs for the CRISPR-Cpf1 system with improved target efficiency and specificity. *Bioinformatics.* (2019) 35:2783–9. doi: 10.1093/bioinformatics/bty1061

25. Piepenburg O, Williams CH, Stemple DL, Armes NADNA. detection using recombination proteins. *PLoS Biol.* (2006) 4:e204. doi: 10.1371/journal.pbio.0040204

26. de Villiers EP, Gallardo C, Arias M, da Silva M, Upton C, Martin R, et al. Phylogenomic analysis of 11 complete African swine fever virus genome sequences. *Virology.* (2010) 400:128–36. doi: 10.1016/j.virol.2010.01.019

27. Wang N, Zhao D, Wang J, Zhang Y, Wang M, Gao Y, et al. Architecture of African swine fever virus and implications for viral assembly. *Science.* (2019) 366:640–4. doi: 10.1126/science.aaz1439

28. Chen N, Huang Y, Ye M, Li S, Xiao Y, Cui B, et al. Co-infection status of classical swine fever virus (CSFV), porcine reproductive and respiratory syndrome virus (PRRSV) and porcine circoviruses (PCV2 and PCV3) in eight regions of China from 2016 to 2018. *Infect Genet Evol.* (2019) 68:127–35. doi: 10.1016/j.meegid.2018.12.011

29. Yang Y, Qin X, Sun Y, Cong G, Li Y, Zhang Z, et al. Development of isothermal recombinase polymerase amplification assay for rapid detection of porcine circovirus type 2. *Biomed Res Int.* (2017) 2017:8403642. doi: 10.1155/2017/8403642

30. Liu Y, Meng H, Shi L, Li L. Development of a droplet digital polymerase chain reaction for sensitive and simultaneous identification of porcine circovirus type 2 and 3. *J Virol Methods.* (2019) 270:34–7. doi: 10.1016/j.jviromet.2019.04.021

31. Zhao Y, Han HY, Fan L, Tian RB, Cui JT, Li JY, et al. Development of a TB green II-based duplex real-time fluorescence quantitative PCR assay for the simultaneous detection of porcine circovirus 2 and 3. *Mol Cell Probes.* (2019) 45:31–6. doi: 10.1016/j.mcp.2019.04.001

32. Yang L, Wang L, Lv M, Sun Y, Cao J. Clinical validation of DNA extraction-free qPCR, visual LAMP, and fluorescent LAMP assays for the rapid detection of African swine fever virus. *Life (Basel).* (2022) 12. doi: 10.3390/life12071067

33. Fu J, Zhang Y, Cai G, Meng G, Shi S. Rapid and sensitive RPA-Cas12a-fluorescence assay for point-of-care detection of African swine fever virus. *PLoS ONE.* (2021) 16:e0254815. doi: 10.1371/journal.pone.0254815

34. Xiong Y, Cao G, Chen X, Yang J, Shi M, Wang Y, et al. One-pot platform for rapid detecting virus utilizing recombinase polymerase amplification and CRISPR/Cas12a. *Appl Microbiol Biotechnol.* (2022) 106:4607–16. doi: 10.1007/s00253-022-12015-9

35. Wen D, Liu G, Opriessnig T, Yang Z, Jiang Y. Simultaneous detection of five pig viruses associated with enteric disease in pigs using EvaGreen real-time PCR combined with melting curve analysis. *J Virol Methods.* (2019) 268:1–8. doi: 10.1016/j.jviromet.2019.03.001

36. Lei L, Liao F, Tan L, Duan D, Zhan Y, Wang N, et al. LAMP Coupled CRISPR-Cas12a Module for Rapid, Sensitive and Visual Detection of Porcine Circovirus 2. *Animals (Basel).* (2022) 12:413. doi: 10.3390/ani12182413

37. Shang Q, Su Y, Liang Y, Lai W, Jiang J, Wu H, et al. Ultrasensitive cloth-based microfluidic chemiluminescence detection of Listeria monocytogenes hlyA gene by hemin/G-quadruplex DNAzyme and hybridization chain reaction signal amplification. *Anal Bioanal Chem.* (2020) 412:3787–97. doi: 10.1007/s00216-020-02633-5

38. Xi H, Juhas M, Zhang Y. G-quadruplex based biosensor: a potential tool for SARS-CoV-2 detection. *Biosens Bioelectron.* (2020) 167:112494. doi: 10.1016/j.bios.2020.112494

39. Zhang M, Wang Y, Sun X, Bai J, Peng Y, Ning B, et al. Ultrasensitive competitive detection of patulin toxin by using strand displacement amplification and DNA G-quadruplex with aggregation-induced emission. *Anal Chim Acta.* (2020) 1106:161–7. doi: 10.1016/j.aca.2020.01.064

frontiers | Frontiers in Veterinary Science

TYPE Original Research
PUBLISHED 23 December 2022
DOI 10.3389/fvets.2022.1045190

OPEN ACCESS

EDITED BY
Bui Thi To Nga,
Vietnam National University of Agriculture, Vietnam

REVIEWED BY
Kohtaro Miyazawa,
National Agriculture and Food Research Organization, Japan
Aruna Ambagala,
National Centre for Foreign Animal Disease (NCFAD), Canada

*CORRESPONDENCE
Qigai He
✉ he628@mail.hzau.edu.cn

SPECIALTY SECTION
This article was submitted to Veterinary Experimental and Diagnostic Pathology, a section of the journal Frontiers in Veterinary Science

RECEIVED 15 September 2022
ACCEPTED 05 December 2022
PUBLISHED 23 December 2022

CITATION
Wu H, Tian Z, Yao L, Ghonaim AH, Chen X, Ruan S, Li H, Li W and He Q (2022) Combination of $Fe(OH)_3$ modified diatomaceous earth and qPCR for the enrichment and detection of African swine fever virus in water. *Front. Vet. Sci.* 9:1045190. doi: 10.3389/fvets.2022.1045190

Combination of $Fe(OH)_3$ modified diatomaceous earth and qPCR for the enrichment and detection of African swine fever virus in water

Hao Wu[1,2], Zihan Tian[1,2], Lun Yao[1,2], Ahmed H. Ghonaim[1,2,3], Xiaoyu Chen[1,2], Shengnan Ruan[1,2], Huimin Li[1,2], Wentao Li[1,2] and Qigai He[1,2]*

[1]State Key Laboratory of Agricultural Microbiology, College of Veterinary Medicine, Huazhong Agricultural University, Wuhan, China, [2]The Cooperative Innovation Center for Sustainable Pig Production, Huazhong Agricultural University, Wuhan, China, [3]Desert Research Center, Cairo, Egypt

Water is one of the primary vectors for African swine fever virus (ASFV) transmission among swine herds. However, the low concentrations of ASFV in water represent a challenge for the detection of the virus by conventional PCR methods, and enrichment of the virus would increase the test sensitivity. In this study, aiming to enrich ASFV in water quickly and efficiently, a rapid and efficient water-borne virus enrichment system (MDEF, modified diatomaceous earth by ferric hydroxide colloid) was used to enrich ASFV in water. After enrichment by MDEF, conventional real-time PCR (qPCR) was used for ASFV detection. ASFV were inactivated and diluted in 10 L of water, of which 4 mL were collected after 60 min treatment using the MDEF system. Two thousand five hundred times reduction of the sample volume was achieved after enrichment. A high adsorption rate of about 99.99 (±0.01)% and a high recovery rate of 64.01 (±10.20)% to 179.65 (±25.53)% was achieved by using 1g modified diatomaceous earth for 10 L ASFV contaminated water. The limit of qPCR detection of ASFV decreased to $1 \times 10^{-1.11}$ GU ml^{-1} (genomic units per milliliter) from $1 \times 10^{2.71}$ GU ml^{-1} after concentrating the spiked water from 10 L to 4 ml. Preliminary application of MDEF allowed successful detection of African swine fever virus (ASFV), porcine circovirus type 2 (PCV2), and pseudorabies virus (PRV) in sewage. Thus, the combination of modified diatomaceous earth and real-time PCR is a promising strategy for the detection of viruses in water.

KEYWORDS

modified diatomaceous earth, $Fe(OH)_3$ colloid, virus enrichment, African swine fever virus, waterborne viruses

1. Introduction

Pathogens in drinking water cause significant hazards to both human and animal health. The causative agents of waterborne disease fall into three major categories, namely, bacteria, viruses, and parasites (1). In 1993, Charles N. Haas estimated that

human have a 5% lifetime risk of death from exposure to waterborne viruses (2) and these risks have not changed significantly over time (3). Most pathogens spread through media contaminated by infected animals' body fluids, exhaled aerosols, and fecal or urinary excretions. Many viruses are detected in water, including environmental waters, bath water, river, and seawater (4). The use of sedimentation, filtration, and other sanitization methods have decreased the risk of infection by pathogens in human drinking water (5). However, relatively little research has focused on the risk assessment of pathogens present in water used for animal production. Most livestock farms use untreated or inadequately treated river- or groundwater, posing a high risk of diseases to livestock and threatening food safety. P.F.M. Teunis reported that traditional water treatment methods, such as long-term storage, flocculation/precipitation, filtration, and ozone disinfection, cannot fully disinfect water, and the low concentration of pathogens in post-treatment samples frequently result in zero counts during measurement (6).

Most current assessment procedures for water quality and disease risk focus of the water's bacterial CFU index. However, there is no association between bacterial indicators and the type and number of waterborne viruses, and consequently, waterborne viruses are often ignored (7). Hence, efficient and cost-effective enrichment methods are urgently needed for the detection of waterborne viruses. Such procedures would allow the assessment of the biosafety risk of water.

Pork is a leading source of high-quality protein in many people's diets and, thus, its supply and safety have significant implications for human health. The emergence of several swine viral diseases can potentially cause pork supply shortages and international trade restrictions. In particular, an acute and highly contagious viral disease (mortality rate exceeding 90%), African swine fever (ASF), is currently causing severe economic losses to the swine industry. It is especially serious since ASF was reported to spread in China in 2018, which has half of the world's swine population. ASF has been listed as one of the notable diseases by the World Organization for Animal Health (WOAH) because of its significant economic, trade, and food-security implications (8).

ASF, belonging to the genus *Asfivirus* of the family *Asfarviridae* is a large, enveloped, double-stranded DNA virus. It can be transmitted through different routes, such as direct or indirect contact with infected pigs and their secretions, excretions, blood, tissues, pork, and pork products, as well as being transported in contaminated water, vehicles, feed, personnel, and other approaches (9). Strong biosecurity measurements have been applied on swine farms in ASF-affected areas to prevent the spread of the disease. Even though personnel, vehicles, and goods can be managed, it is difficult to avoid the spread of ASFV to a pig farm if flooding with ASFV-contaminated water occurs. Within a farm, ASFV is spread primarily through virus-infected saliva or feces. Sewage from washing pens, water trough residues (10), and other manufacturing activity could easily lead to ASFV pollution in affected pig farms. ASFV can infect pigs at a dose as low as 1 $TCID_{50}$; therefore, pigs can be easily infected by ASFV-contaminated water (11). As the detection of ASFV at low concentrations is challenging, an extra enrichment step is required to increase the template concentration before virus detection. Pei and colleagues reported that the number of pathogens in river water, well water, and other water sources are extremely low and often more than 10 L of water is required for enrichment for pathogen detection (12).

Viruses and other bio-colloids have a pH-dependent surface charge in polar media such as water. This electrostatic charge determines the mobility of the soft particle in an electric field, governing its colloidal behavior, which in turn plays a key role in viral adsorption processes. The isoelectric points (IEPs) of viruses range from 1.9 to 8.4, with most in the region of 3.5 to 7.0 (13). Viruses can be adsorbed on a solid matrix by electrostatic attraction or hydrophobic interaction at a defined pH value. Because of this electrochemical property, charged filter material can be used for adsorption of viruses in water. The adsorbed virus can then be eluted from the membrane for detection. Two types of filters are used to concentrate viruses, namely, electro-positively charged filters to concentrate viruses at around pH 7.0 (14–16) and electronegatively charged filters to concentrate viruses at lower pH (17). The adsorption efficiency can be further enhanced by modifying the surface charge of the filter with divalent and trivalent cations such as aluminum (Al^{3+}), magnesium (Mg^{2+}), ferric iron (Fe^{3+}), and other ions (18). A combination of charged membrane filters and microfluidic filtration techniques have also been used to process large volumes of water. These methods are particularly useful when processing large sample volumes and can be used on a scale of liters. However, the miniaturization of filtration techniques into microfluidic devices may result in clogging, limiting their applications to clinical samples (1). Since water in natural environments, such as rivers and wells, is usually weakly alkaline (pH $>$ 7), and viruses carry a negative charge on their surfaces (IEP $<$ pH), positively charged filter media are extremely efficient for capturing viruses (15, 16, 19, 20). Seeley and Primrose coated microporous filters with aluminum hydroxide. The filters tended to be clogged, reducing their filtration of water, and thus reduced their application efficacy. Michen et al. reported that modified diatomaceous earth allowed better water flow due to its larger pore size and the fact that viruses may be retained by adsorption mechanisms resulting from intermolecular and surface forces (21). Emerging water treatment technologies using ferrous and zero-valent iron have shown the potential of reducing viral contamination using both inactivation and adsorption. Iron electrocoagulation was investigated for virus mitigation in drinking water using laboratory experiments (22).

Methods such as ultracentrifugation, immuno-filtration (23), immunomagnetic separation (24), precipitation, and organic flocculation (25) have also been used for virus enrichment. According to the recommendations by the manual of Diagnostic Tests and Vaccines for Terrestrial Animals (World Organization for Animal Health, WOAH), real-time PCR is widely used for ASFV detection. A promising method for detecting ASFV in farms could be the combination of an enrichment system and real-time PCR.

2. Materials and methods

2.1. Preparation of MDEF filter and EGM filter

The MDEF system's filter material was diatomaceous earth (Qingdao Ocean Chemical Co., Ltd., Qingdao, China) with $Fe(OH)_3$ colloids attached to the surface (Supplementary Figure S1). A saturated solution of $FeCl_3$ was prepared by dissolving 1.6 g of ferric chloride hexahydrate (Sinopharm Chemical Reagent Company Limited, Shanghai, China) in 1 ml of distilled water at room temperature (25°C). Next, 0.5 ml of saturated $FeCl_3$ solution was added dropwise to 100 ml boiling distilled water. The heating equipment was turned off when the solution turned a burgundy color. After standing for 1 h, the Tyndall effect was applied to assess the development of $Fe(OH)_3$ colloids (there is a distinct light channel when the colloid is illuminated by a laser pointer). The pellets should not be visible in this solution (Figure 1A). One hundred grams of diatomaceous earth with a size range of 0.12–0.16 mm were then mixed with 100 ml of the $Fe(OH)_3$ colloids, and the mixture was dried at 50°C for more than 24 h. One gram of the dried modified diatomaceous earth was then applied to a polypropylene column (JinYang Filter Equipment, Hebei, China) with an inside diameter of 1.5 cm and a height of 7.5 cm pre-packed with a filter pad (JinYang Filter Equipment, Hebei, China).

The polypropylene filter cartridges and $Al(OH)_3$ precipitates were prepared for filter cartridge systems with electropositive granule media (EGM) as previously described (26). First, 1.26 g $AlCl_3$ and 8.55 ml of 2 mol L^{-1} Na_2CO_3 were used to create an $Al(OH)_3$ precipitate. This was mixed well with 80 g silica gel (Marine Chemical Co., Qingdao, China) and dried at 50°C for over 24 h, resulting in the EGM. Lastly, 1 g of the EGM was gently added to a polypropylene filter cartridge containing sterile water (26, 27).

2.2. Description of the MDEF system

The MDEF system comprised two water containers, two PVC (polyvinylchloride) pipes with inner diameters of 4.8 mm, an MDEF filter, and one peristaltic pump (Figures 1B, C). Water samples flowed into the collection barrel after passing through the filter column and peristaltic pump (maximum pumping speed of 250 ml min^{-1}). After filtration, the ASFV on the MDEF were eluted using elution buffer. Three types of elution buffer (the details are listed in Table 1), including 10× nutrient broth medium (10×NB), 1M NaCl, and 1.5% beef extract with 0.05 M glycine (1.5% GBE), were tested to compare their efficiency for virus elution. Four milliliters of elution buffer were added to the filtration column with the virus for MDEF suspension in the added buffer. The suspension was transferred to 10 ml Eppendorf (EP) tubes, placed on a horizontal shaker, and shaken for 1 h to ensure that the MDEF could release the ASFV into the elution buffer. After 1 h of shaking, the suspension was allowed to precipitate, and 1 ml of the supernatant was used for qPCR analysis.

2.3. Preparation of spiked water sample

ASFV was inactivated at 60°C for 60 min in a Class II biosafety cabinet in an ABSL-3 laboratory (8). Inactivation was confirmed by inoculation into porcine alveolar macrophages (PAM) cells resulting in no virus growth. Samples were then transferred to a BSL-2 laboratory for follow-up testing. Briefly, inactive anticoagulated blood was subjected to three freeze-thaw cycles and centrifuged at 12,000 rpm to remove cell debris. Varying dilutions of the supernatant were then added to water, resulting in spiked water samples.

2.4. Nucleic acid extraction

ASFV DNA was extracted using the TIANamp Genomic DNA Kit (DP304) (TianGen Biotech (Beijing) CO., TD., Beijing, China) according to the manufacturer's instructions. DNA and RNA in clinically samples were extracted simultaneously using the TIANamp Virus DNA/RNA Kit (DP315) (TianGen Biotech (Beijing) CO., TD., Beijing, China). Two hundred microliter samples were used for one extraction. Nucleic acid negative controls were prepared at this stage for each treated and negative control sample by running parallel extractions of nuclease-free water with the kit. The extracted DNA and controls were stored at −20°C until TaqMan® PCR amplification.

2.5. TaqMan® PCR amplification

The detection and quantification of 250 bp of the ASFV B646L genes were performed as previously described by King and colleagues (28). This method is recommended by the WOAH. Nuclease-free qPCR Reaction Master Mix (2×) (Takara Bio (China) Co., Ltd.) was prepared in

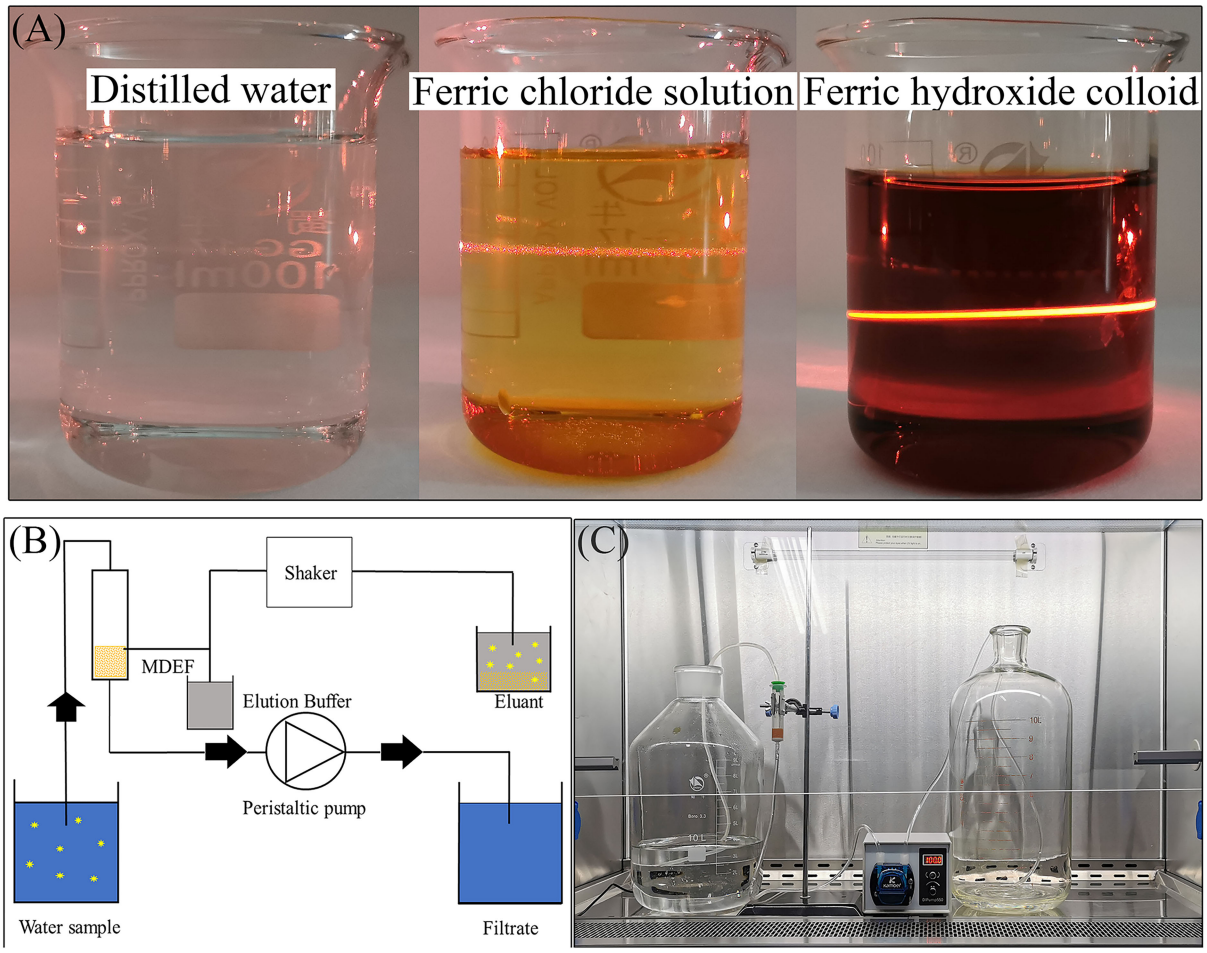

FIGURE 1
A laser pen was used to irradiate three types of liquid from the side of the beaker, with the appearance of an obvious optical path in the $Fe(OH)_3$ colloid which was not apparent in neither the ferric chloride solution nor the distilled water **(A)**, schematic diagram showing the MDEF enrichment and elution procedures **(B)**, and the actual MDEF system **(C)**.

TABLE 1 Recovery efficiency of three elution buffers at different pH values.

Elution buffer	Ingredients (m/v)	ASFV in spiked water (log GU/μL)	% Recovered ± SD			
			pH 3.0	pH 5.0	pH 7.0	pH 9.5
1M NaCl	1 mol/L NaCl	5.97	0.18 ± 0.00	0.18 ± 0.00	0.18 ± 0.00	0.18 ± 0.00
1.5% GBE	1.5% beef extract with 0.05m glycine		0.18 ± 0.00	1.42 ± 0.97	2.40 ± 3.14	3.93 ± 5.30
10×NB	10% Peptone 3% Beef Extract and 5% NaCl		2.31 ± 1.61	40.01 ± 2.45	71.64 ± 5.23	82.76 ± 3.55

advance. Primers (Sangon Biotech, China) were prepared at a concentration of 10 pmol/μl. Primer F sequence 5′-CTGCTCATGGTATCAATCTTATCGA-3′; Primer R sequence 5′-GATACCACAAGATC(AG)GCCGT-3′. Fluorescent-labeled hydrolysis probe (5′-FAM-CCACGGGAGGAATACCAACCCAGTG-3′-TAMRA, Sangon Biotech, China) was used at a

concentration of 10 pmol/μl. The PCR reaction mixture was prepared in sterile 1.5-ml microcentrifuge tubes, as described. The reaction mixture contained: nuclease-free water (5 μl); (2 conc.) 2× PCR reaction master mix (10 μl); primer F (10 pmol, 0.4 μl), primer R (10 pmol, 0.4 μl), fluorescent-labeled probe (10 pmol, 0.4 μl). A further 16.2 μl of PCR reaction mixture was added to each well of an optical reaction plate for the assay and 3.8 μl of the extracted DNA template or blank extraction control was added to each well and covered with a cap. The plate was centrifuged for 1 min in a suitable centrifuge to mix the contents, and PCR amplification was performed on CFX Touch 96-well Real-Time PCR Detection Systems (Bio-Rad, Hercules, CA, USA) with the following parameters: one cycle at 50°C for 2 min; one cycle at 95°C for 10 min; 40 cycles at 95°C for 15 s; 58°C for 1 min (28).

2.6. Adsorption experiments

In these experiments, 40 ml of distilled water ($n = 12$, $m = 3$) was spiked with inactivated ASFV to final concentrations of $1 \times 10^{3.61\pm0.06}$ GU ml^{-1} (genomic units per milliliter), $1 \times 10^{4.78\pm0.05}$ GU ml^{-1}, $1 \times 10^{6.10\pm0.07}$ GU ml^{-1}, and $1 \times 10^{7.73\pm0.05}$ GU ml^{-1}. The spiked water samples were mixed in 50-ml centrifuge tubes with the three types of filter materials [aluminum hydroxide ($Al(OH)_3$) colloid modified-diatomite, $Fe(OH)_3$ colloid modified-diatomite and unmodified diatomite] and placed on a shaker for 1 h. After shaking for 1 h, the filtered material was allowed to settle to the bottom of the flask for 5 min before 2 ml of the supernatant were transferred to a new centrifuge tube for subsequent experiments. Triplication of 0.2 ml aliquots were removed from the supernatants for detection of the remaining ASFV.

2.7. Elution experiment

Previous studies have reported electrostatic interactions between proteins and filter surfaces (29). Three strategies were investigated in this study. The first involved the use of an organic buffer containing a high protein concentration, i.e., 10 times the concentration of the nutrient broth medium (10×NB) for detaching the bound virus on the filter. The second option was the use of chloride ions (1M NaCl solution) to neutralize the charge on the surface of modified diatomite, disrupting the electrostatic attraction between the virus and the filter (18). Beef extract (1.5%) with 0.05 m glycine (1.5% GBE, pH = 9.5) has been frequently used for elution, for instance, for the 1MDS cartridge filters recommended by United States EPA (17). The recovery efficiencies of the three different elutes, i.e., 10×NB buffer, 1M NaCl solution, and 1.5% GBE buffer, were compared. The elution buffers were adjusted to specific pH values (3.0, 5.0, 7.0, or 9.5).

2.8. Determination of the detection limit of the MDEF/qPCR combination

The MDEF system enriched the inactivated ASFV in the water. Serial dilutions of ASFV standard plasmid DNA were prepared and used to develop a standard curve for quantification of ASFV by qPCR (Supplementary Figure S2). It was observed that when a low amount virus was added into a large volume of water, the detection limit was lower than the theoretical concentration due to Brownian motion. For example, addition of 1 ml of inactivated ASFV ($1 \times 10^{8.39\pm0.03}$ GU ml^{-1}) to 10 L water would result in a detectable ASFV genome of $1 \times 10^{3.87\pm0.29}$ GU ml^{-1}, indicating that if the volume increased by $1 \times 10^{4.00}$ times, the concentration could be reduced by $1 \times 10^{4.52}$ times. Hence, the amount of ASFV genome added into the water was used to calculate the recovery rate instead of the amount detected in the spiked water. In practice, this phenomenon hardly ever occurs in spiked water with high viral concentrations.

After calculating the amount of virus input, different amounts of virus were added to 10 L of water to model the different virus concentrations in spiked water. Six final concentrations in spiked water ($1 \times 10^{-0.33\pm0.06}$ GU ml^{-1}, $1 \times 10^{0.93\pm0.06}$ GU ml^{-1}, $1 \times 10^{2.14\pm0.01}$ GU ml^{-1}, $1 \times 10^{3.24\pm0.04}$ GU ml^{-1}, $1 \times 10^{4.41\pm0.04}$ GU ml^{-1}, $1 \times 10^{5.35\pm0.07}$ GU ml^{-1}) were prepared in 18 barrels. All the spiked water was filtered and eluted. The viral concentration in the eluents was determined, and the limitations of detection (LOD) of the combined MDEF system and qPCR method were calculated.

2.9. PEG precipitation

Polyethylene glycol (PEG) is frequently used to enrich viruses. The capacity of PEG-6000 to precipitate viruses was also evaluated in this study. Different concentrations of PEG-6000 were mixed with 10 × NB elution buffer to prepare 10 ml mixtures with $10^{4.17\pm0.01}$GU of inactivated ASFV. The solutions were placed in 15-ml centrifuge tubes, mixed well, and incubated at 4°C for 12 h. After centrifugation for 1 h, 9.6 ml of the supernatant was removed, and the precipitate was rinsed with the the remaining 0.4 ml of the supernatant and analyzed by qPCR.

2.10. Statistical analysis

Each experiment was performed at least three times. The results were statistically analyzed, and the significance of the differences was determined with a one-way analysis of variance (ANOVA) and Tukey's multiple comparison tests. In all cases, a value of $p < 0.05$ was deemed a significant difference. The adsorption rate was determined by dividing the total number

of ASFV genomes in the filtered water by that in the spiked water. The recovery rate was calculated by dividing the total number of ASFV genomes in the eluates by that in the spiked water. The quantitative detection of ASFV nucleotide acid in water samples and eluted solutions was done by qPCR (the standard curve for ASFV B646L gene plasmids was shown in Supplementary Figure S2). The following formulas were used to calculate the adsorption and recovery rates:

$$\text{Adsorption rate (\%)}^{1*} = (1 - \frac{C_1}{C_0}) \times 100$$

$$\text{Adsorption rate (\%)}^{2*} = (1 - 2^{CT^{*}before\ absorbed - CT\ after\ absorbed}) \times 100$$

Where, C_1 represents the concentration of the ASFV genome left in the water after being absorbed, and C_0 represents the concentration of the ASFV genome in water before being absorbed. CT represents the cycle threshold value determined by qPCR. The adsorption rate was calculated using two formulae. Formula 1* (which was used in this study) could be applied regardless of the quantitative method used. Formula 2* (which is more convenient) can be used when with qPCR quantification and its amplification efficiency was 100% (±5%). The calculated adsorption rates did not differ between the two formulae.

$$\text{Recovery rate (\%)} = \frac{Q_1}{Q_0} \times 100$$

Here, Q_1 and Q_0 represent the quantity of ASFV genome measured in the final eluate after concentration and the quantity of ASFV genome seeded into the spiked water samples before concentration, respectively.

3. Results

3.1. Adsorption of metal hydroxide colloid modified diatomaceous earth

Modification with different salts led to an increase in the zeta potential of the diatomaceous earth (30). The activity of $Al(OH)_3$ colloid and $Fe(OH)_3$ colloid modified-diatomite were compared with unmodified diatomite to examine their ASFV adsorption capabilities. Each combination was set up with three duplicates to calculate the standard deviation. Figure 2 demonstrates the filter media's adsorption efficiency at various viral concentrations. No genome was detected in the samples with low ASFV concentration ($1 \times 10^{3.61\pm0.06}$ GU ml^{-1}) treated by $Al(OH)_3$ colloid modified-diatomite and $Fe(OH)_3$ colloid modified-diatomite. The CT values of samples that could not be detected (no CT value) were determined as 40 cycles (CT = 40) for calculation. Due to the constraint in the calculation method, the real adsorption rate was higher than the calculated value of 91.93 (±0.003)%.

ASFV nucleic acids were detected at a concentration of $1 \times 10^{3.28\pm0.04}$ GU ml^{-1}, with only a 52.89 (±4.61)% adsorption rate in the unmodified diatomite. The adsorption rates were 6.71 (±1.86) and 11.29 (±12.64)% in the ASFV genome-concentrated spiked water. The $Al(OH)_3$ colloid-modified diatomite showed adsorption rates in the range of 91.93 (±0.00) to 40.19 (±1.87)%. The adsorption efficiency of the $Fe(OH)_3$ modified diatomite was almost 100%, and no ASFV genome was detected in water after adsorption, even at the highest concentration of ASFV in the spiked water. In general, 1 g of $Fe(OH)_3$ colloid-modified diatomite could completely absorb the ASFV in 40 ml water with a concentration $<1 \times 10^{7.73\pm0.05}$ GU ml^{-1}. This result is consistent with the findings of Farrah and colleagues (30).

The results indicated that the adsorption efficiency of diatomite modified by $Fe(OH)_3$ colloid was much higher than that of the other filter media ($p < 0.01$). Thus, the $Fe(OH)_3$ colloid was used as the filter material in the MDEF system.

3.2. The recovery efficiency of eluents at different pH conditions

It was found that ASFV absorbed by modified diatomite were effectively eluted using 10× NB (Table 1). The recovery efficiency of the alkaline medium (82.76 ± 3.55% at pH 9.5, 71.64 ± 5.32% at pH 7.0) was much higher than that of the acidic medium (40.01 ± 2.45% at pH 5, 2.31 ± 1.61% at pH 3). However, there was no significant difference in recovery efficiency between pH 7.0 and 9.5. To avoid adjustment of the pH, 10 × NB of pH 7.0 was used in subsequent experiments. A non-significant elution of ASFV (0.00 ± 0.00% to 3.93 ± 5.30%) was observed using 1M NaCl and 1.5% GBE as eluents.

3.3. Comparison of virus-enrichment methods

$Al(OH)_3$ is commonly used for virus enrichment from water (31–33). Recovery of the MDEF was compared to that of the $Al(OH)_3$-modified EGM filter cartridge system. The preparation of $Al(OH)_3$ colloid-modified diatomite and filtration procedure were based a previously published protocol (26). The recovery of the MDEF system (112.46 ± 16.10%) was significantly higher than that of the EGM (14.71 ± 1.36%) in the recovery of ASFV genomes from 10 L of spiked water ($1 \times 10^{4.93}$ GU) with 1 g of filter material. The recoveries of the MDEF and EGM systems declined as the concentration of ASFV genome increased. However, at all concentrations of spiked water, the recovery of the MDEF system was significantly more efficient ($p < 0.01$) than that of the EGM system (Figure 3).

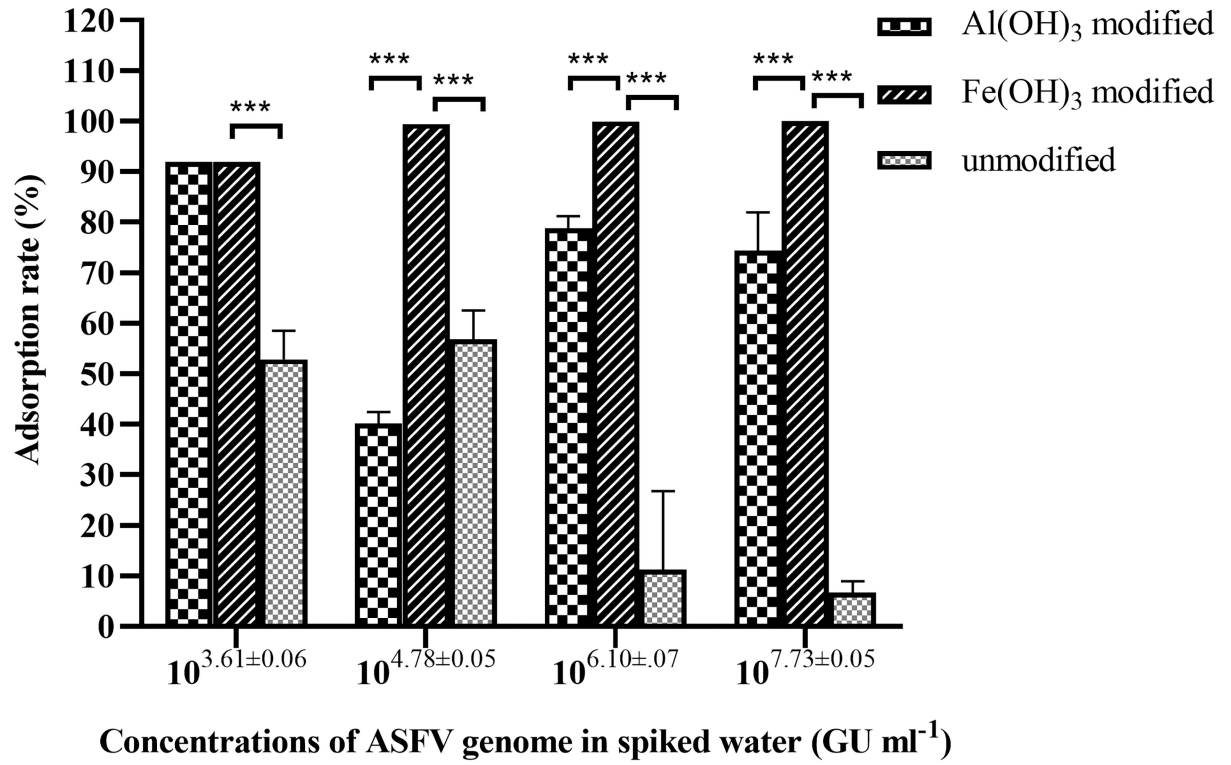

FIGURE 2
Adsorption of ASFV by $Al(OH)_3$-modified, $Fe(OH)_3$-modified, and unmodified diatomaceous earth from 40 ml of spiked water containing different concentrations of virus. The adsorption efficiency of the $Fe(OH)_3$-modified diatomaceous earth was significantly higher than that of the other two materials. ***Significant difference between groups ($p < 0.01$).

3.4. Detection limit of the MDEF/qPCR combination

The limitations of detection (LODs) of the individual ASFV qPCR and the combined method were used to determine the efficiency of the combined MDEF/qPCR system (Figure 4). The lowest detectable concentrations were $1 \times 10^{3.67\pm0.27}$ GU ml^{-1}(spiked water) and $1 \times 10^{4.00\pm0.06}$ GU ml^{-1} (eluant). 179.65 (±25.53)% ASFV genome was recovered from the spiked water ($1 \times 10^{-0.33\pm0.27}$ GU ml^{-1}) by eluting ($1 \times 10^{4.00\pm0.06}$ GU ml^{-1}) after concentrating 2,500 times of the volume of them. These performances demonstrated the efficiency of the system's recovery capacity. The ASFV genome could not be detected in a series of spiked water samples $<10^{3.67\pm0.27}$ GU ml^{-1}. However, after enrichment, ASFV genome concentrations were detected in eluants as $1 \times 10^{8.55\pm0.07}$ GU ml^{-1} (64.01 ± 10.20%), $1 \times 10^{7.67\pm0.04}$ GU ml^{-1} (76.85 ± 6.60%), $1 \times 10^{6.55\pm0.04}$ GU ml^{-1} (81.84 ± 6.60%), $1 \times 10^{5.50\pm0.01}$ GU ml^{-1} (91.12 ± 2.31%), $1 \times 10^{4.41\pm0.06}$ GU ml^{-1} (112.46 ± 16.10%), and $1 \times 10^{3.40\pm0.06}$ GU ml^{-1} (179.65 ± 25.53%). Their corresponding final concentrations in spiked water were $1 \times 10^{5.35\pm0.07}$ GU ml^{-1}, $1 \times 10^{4.41\pm0.04}$ GU ml^{-1}, $1 \times 10^{3.24\pm0.04}$ GU ml^{-1}, $1 \times 10^{2.14\pm0.01}$ GU ml^{-1},$1 \times 10^{0.93\pm0.06}$ GU ml^{-1}, and $1 \times 10^{-0.33\pm0.06}$ GU ml^{-1}.

These results indicate that the LOD in 10 L of ASFV-contaminated water increased by $1 \times 10^{4.0}$ times (from $1 \times 10^{3.67\pm0.27}$ GU ml^{-1} to $1 \times 10^{-0.33\pm0.27}$ GU ml^{-1}) using the combined MDEF and qPCR method.

3.5. Additional experiments

Over 50.42 (±4.53)% of the virus ($1 \times 10^{3.93\pm3.93}$ GU) was recovered using 20% PEG-6000 solution (Figure 5). Although the concentration was 10 times higher than non-PEG-6000 precipitation protocol, this required more than 13 h of treatment and the use of a high-speed centrifuge. Hence, extra treatment was only recommended in well-equipped laboratories.

3.6. Natural water experiments

The MDEF system was used to measure a total of 59 samples of natural water and sewage to determine its clinical applications

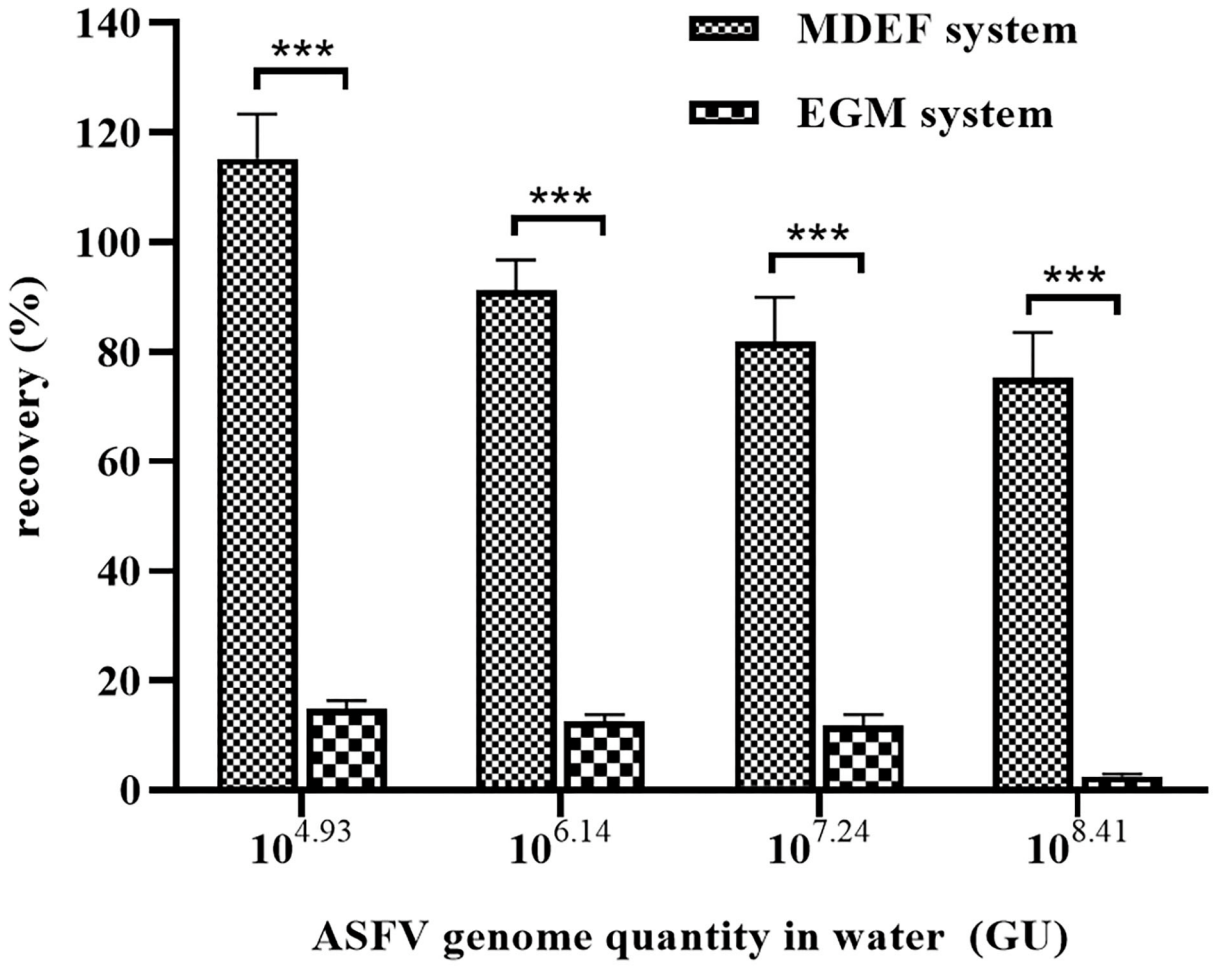

FIGURE 3
The EGM and MDEF systems were used to recover viruses from spiked water (10 L) containing different ASFV genome concentrations. The recovery rates of the MDEF system were significantly higher than those of the EGM system for all four types of spiked water. ***Significant difference between groups ($p < 0.01$).

(Table 2). The 59 samples consisted of 10 fecal sewage samples (No. 1–4) from the ASFV animal infection experiments, eight samples from washed pigsties in ASFV-infected farms (No. 5 to 10) where the pigsties had had an ASF outbreak but had since been cleaned and dried and five liters of water were used for sample collection on equipment surfaces through repeated washing of the surfaces, nine samples from unwashed pigsties (No. 11–19) on ASFV-positive farms where the pigsties were undisinfected or disinfected with NaOH and contained lots of sewage, two water samples from a slaughterhouse depilation tank (No. 20 and 21), and 14 samples from well water obtained from five pig farms well water samples from 5 pig farms (No. 31). ASFV was detected in several of these samples. It was notable that some of these samples were diagnosed as ASFV-positive after processing with the MDEF system, whereas they were misdiagnosed as ASFV-negative when only using qPCR for detection.

In addition, the MDEF system was used in the flood-affected pig farms (No. 22–30, Henan province, July 2021), Yezi Lake (No. 32), and Yangtze River (No. 33, Hubei Province, February 2022). Despite the use of small volumes of water, PCV2 and PRV were successfully detected.

4. Discussion

Methods for the concentration and enrichment of waterborne viruses have been studied for a while, and many adsorbent materials have been developed. Negatively charged filters require the addition of multivalent salts and acidification of the water sample for efficient virus adsorption, making large-volume sampling difficult; these filters include the Millipore membrane filter (cellulose nitrate) (34) and the Filterite pleated cartridge filter (epoxy-fiberglass) (35). In contrast, positively

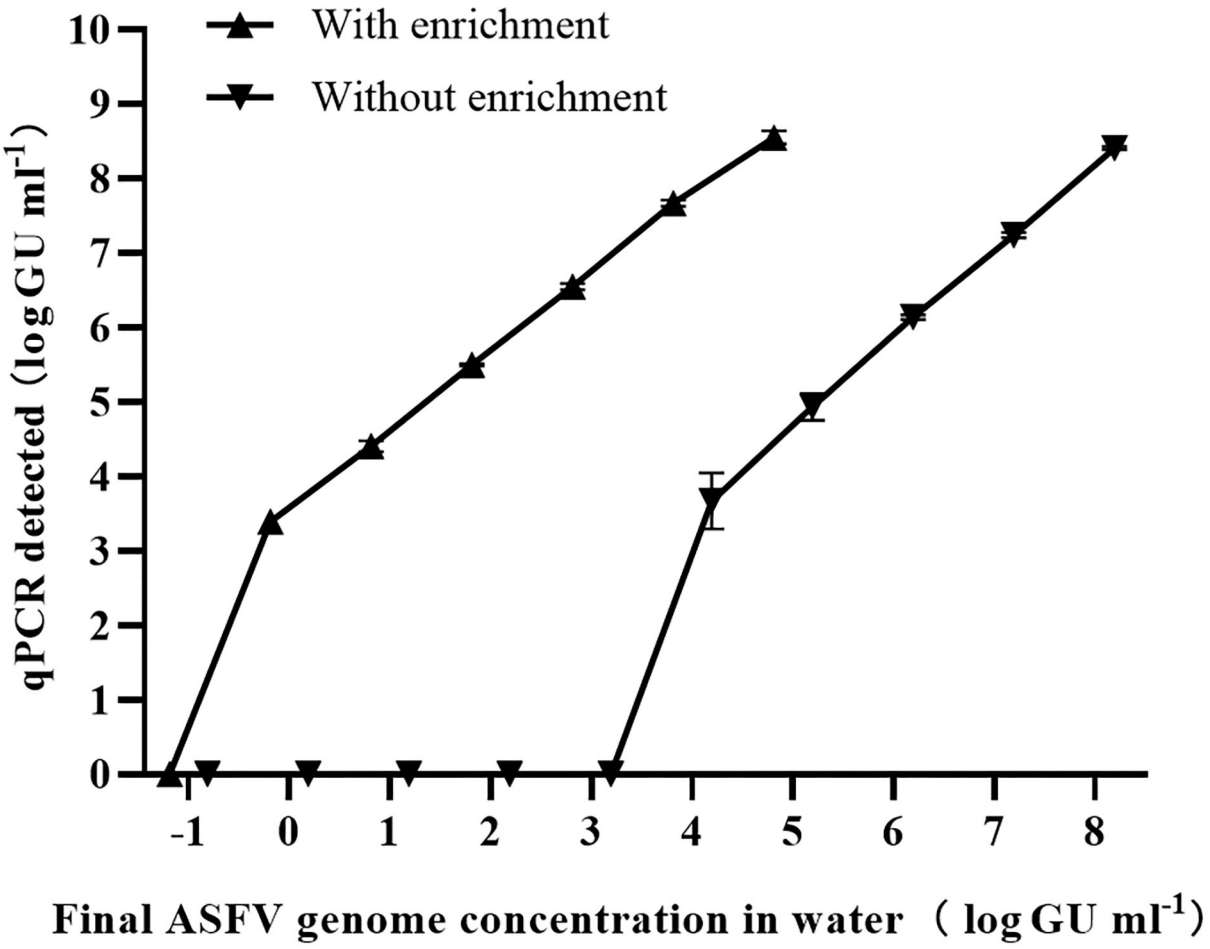

FIGURE 4
Eighteen barrels of spiked water with six final concentrations of ASFV (10 L per barrel) were enriched using the MDEF system, and the presence of the ASFV genome in both spiked water (without enrichment) and eluates (with enrichment) was measured by qPCR. The LODs were determined for both conditions with the LOD of the 10-L ASFV-contaminated increasing $1 \times 10^{4.0}$ times (from $1 \times 10^{3.67\pm0.27}$ GU ml^{-1} to $1 \times 10^{-0.33\pm0.27}$ GU ml^{-1}) after enrichment.

charged filters require no preconditioning of samples and can concentrate viruses from water over a wider pH range than electronegative filters (18). These materials, however, cannot be widely used in veterinary diagnosis due to the need for expensive equipment, inefficient adsorption rates, and differences in virus species. Metal-based adsorption materials have been extensively investigated, especially positively charged filters (15, 18, 24, 27, 36–39). In this study, $Fe(OH)_3$-modified diatomaceous earth was found to possess superior adsorption and recovery efficiency than $Al(OH)_3$-modified diatomite in the ASFV enrichment experiments. This result can be attributed to the chemical characteristics of these two metal sorbents. According to Luo M, Al^{3+} hydrolysates differed at different pH levels: $[Al(OH)_n]^{(n-3)-}$ (n = 6, 7, 8, 9, or 10) at pH < 4; $[Al_6(OH)_{15}]^{3+}$, $[Al_7(OH)_{17}]^{4+}$, $[Al_8(OH)_{20}]^{4+}$ and $[Al_{13}(OH)_{34}]^{5+}$ at 4 < pH < 6; $[Al(OH)_3]$ at 6 < pH < 8; $[Al(OH)_4]^-$, $[Al_8(OH)_{26}]^{2-}$ at 8 < pH (40, 41). Different hydrolysates exhibit different electrical properties, and $Al(OH)_3$ is not positively charged in natural water as a result of its hydrolysates at 7 < pH. Thus, water samples require adjustment to pH ≤6.0 before concentration with an aluminum-based method (31, 33). Previous studies have shown that phosphate removal by aluminum-loaded shirasu-zeolite was 80–40% at pH values from 2 to 11 (42). These studies confirmed that poor adsorption effects of aluminum-based methods in neutral or alkaline media. Similar to Al^{3+} hydrolysates, Fe^{3+} hydrolysates also differed at different pH values: Fe^{3+} at pH < 2; $FeOH^{2+}$, $Fe(OH)^+$, $Fe_2(OH)_2^{4+}$, $Fe_3(OH)_4^{5+}$ and other polymers at 2 < pH < 8.1; $Fe(OH)_3$ at 8.1 < pH < 12; and $Fe(OH)_4^-$ at 12 < pH. Thus, ferric-based materials are positively charged in solutions with pH < 8.1 (40).

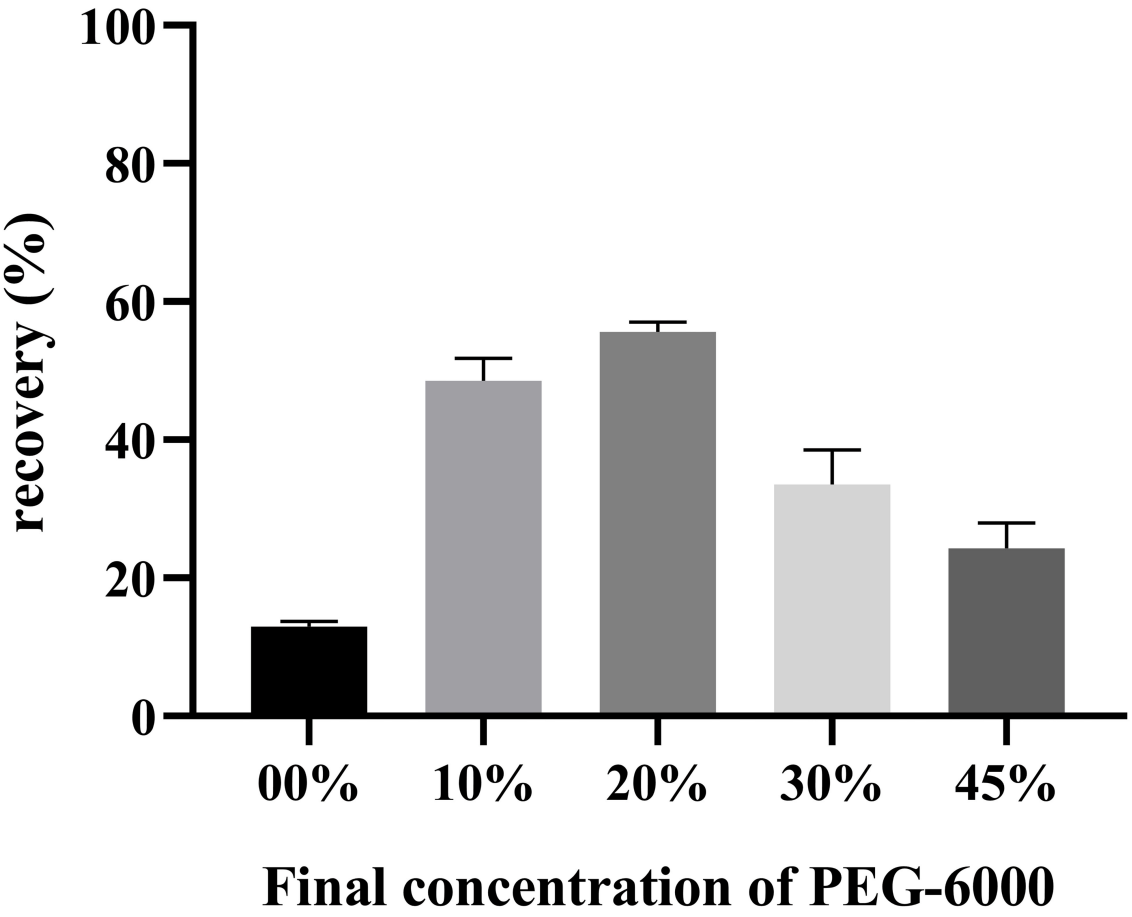

FIGURE 5
Different final concentrations of PEG-6000 was added to the ASFV-containing eluate for determination viral recovery. After precipitation and centrifugation, the volume of liquid was reduced from 10 ml to 0.4 ml. More than 50.42 (±4.53)% of the virus was recovered using the 20% PEG-6000 solution.

The findings of this study indicated that the use of ferric-based materials for the adsorption of negatively charged groups in natural water have stronger electrostatic attraction than aluminum-based materials. Our findings are consistent with previous studies reporting that ferric hydroxide outperforms aluminum hydroxide in the removal of negatively charged groups such as arsenate (43, 44).

We found that the recoveries using the MDEF and EGM systems declined as the ASFV genome concentration increased. A previous study by Armanious et al. investigated the mechanism by which viruses bind to adsorbents (29). These authors found that virus-sorbent interactions were governed by long-ranged electrostatic forces together with contributions from the hydrophobic effect, while the shorter-range van der Waals interactions were of secondary importance. The topographic irregularities on both the virus and sorbent surfaces influenced steric effects. In our study, the long-range electrostatic interactions on MDEF gradually decreased as the amount of adsorbed virus increased, leading to reduced virus adsorption. At the same time, the adsorption of more virus to the MDEF surface leads to steric effects, further weakening the interaction between the MDEF and virus. Thus, the MDEF recovery rate gradually decreased as the virus load increased. Increasing the weight of the filter media could be a solution, but it can only be considered when the volume of water exceeds 10 L.

CD2v (encoded by pE402R) and p12 (encoded by ORF 061R) are the primary adhesion proteins present on the ASFV external envelope membrane (45), and their isoelectric points have been predicted to be 6.21 and 7.63, respectively (https://web.expasy.org/compute_pi). Based on these values, the surface of ASFV was predicted to be negatively charged at pH > 6.21. A critical characteristic of the adsorbents is surface charge, which is expressed as the zeta potential of the adsorbent

10.3389/fvets.2022.1045190

TABLE 2 The MDEF system was applied to 59 samples of natural water or sewage.

Sources	No.	Numbers	Volume	Virus species	CT value	
					Without MDEF	With MDEF
Fecal sewage from animal infection assay	1	1	500 ml	ASFV	NT*[1]	36.56
	2	1	200 ml	ASFV	38.62	35.75
	3	1	1 L	ASFV	33.78	30.4
	4	7	500 ml−1 L	-	NT	NT
Water from the clean-washed pigsties	5	1	5 L	ASFV	NT	36.90
	6	1	5 L	ASFV	NT	37.49
	7	1	5 L	ASFV	NT	35.98
	8	1	5 L	ASFV	NT	34.24
	9	1	5 L	ASFV	NT	36.60
	10	3	5 L	–	NT	NT
Water from the unwashed pigsties	11	1	450 ml	ASFV	36.90	36.94
	12	1	400 ml	ASFV	37.22	34.84
	13	1	500 ml	ASFV	39.84	35.45
	14	1	400 ml	ASFV	37.04	36.85
	15	1	1 L	–	NT	32.67
	16	1	450 ml	–	NT	35.38
	17	1	900 ml	ASFV	37.99	31.71
	18	1	900 ml	ASFV	37.06	30.92
	19	1	350 ml	–	NT	NT
Water from slaughterhouse depilation tanks	20	1	5 L	ASFV	NT	35.28
	21	1	600 ml	–	NT	NT
Drinking water from pig farms	22	1	400 ml	PCV2	NT	37.39
Fecal sewage from pig farms	23	1	400 ml	PCV2e*[2]	33.78	29.54
	24	1	400 ml	PRV	NT	38.29
				PCV2d*[3]	30.75	27.78
	25	1	400 ml	–	NT	NT
Sewer ditch from pig farms	26	1	500 ml	PCV2	NT	38.42
	27	1	500 ml	PCV2	NT	35.05
	28	1	500 ml	PCV2	NT	35.51
	29	1	250 ml	PCV2	NT	38.07
	30	2	500 ml	–	NT	NT
Well water from 5 pig farms	31	14	500 ml−5 L	–	NT	NT
Lake water	32	3	10 L	–	NT	NT
Yangtze water	33	3	10 L	–	NT	NT

*[1] No positive result.
*[2,*3] Sequencing confirmed that these porcine circoviruses were gene types 2e and 2d.

surface (46). Although the electrostatic force constitutes one of the mechanisms involved in metal-based adsorption, the mechanism of MS2 virus removal by iron coagulation involves the adsorption of negatively charged virus particles onto the positively charged iron oxyhydroxide, FeOOH(s), floc particles, similar to the mechanism proposed for virus removal by the precipitation of aluminum hydroxide in the Standard Methods virus concentration procedure (47–49). The results of a study by Sobsey and Jones (50) supported the idea that electrostatic forces were instrumental in virus–filter interactions due to the correlation between zeta potential (i.e., electrokinetic potential) measured for the electronegative and positively charged adsorptive materials, and the retention efficiencies were measured for each filter. These reports explained the mechanism by which the MDEF system was superior to the EGM system in the process of concentrating ASFV in natural water.

The low recovery of 1.5% GBE in this study can be explained by the strong electrostatic force of the iron hydroxide colloid compared to other filter media, such as nitrocellulose membranes, 1MDS Cartridge filters, and $Al(OH)_3$ colloids. The elution buffer (10× NB) had a high protein concentration to dislodge the bound virus from the modified diatomite through competitive binding. While previous studies have demonstrated the use of ferric-based materials in adsorption, these were rarely used in enrichment and recovery, probably due to the use of ineffective eluents (51). Here, the 10×NB buffer was shown to elute viruses from the materials more efficiently compared to other eluents.

Electronegative filters require acidification or the addition of polyvalent salts to water samples before use, which makes large-volume sample processing difficult. Thus, positively charged filter media present an alternative to electronegative adsorbents. Although Virosorb 1MDS demonstrated efficient virus adsorption from various water quality types for both small and large volumes, its high cost reduced the affordability of large-scale applications. Thus, the MDEF system is promising as an inexpensive and effective methodology for monitoring the presence of viruses in water. Also, compared with the commonly used ultracentrifugation-based methods, the MDEF system can be used in smaller and less well-equipped laboratories due to its capacity for large-volume processing without the need for ultracentrifugation.

5. Conclusion

Although there are a number of viral enrichment methods, many show poor reproducibility and low recovery and are thus limited in their clinical use. Others are limited by complex procedures and high cost. The MDEF system is the first method used to enrich ASFV in water by modify diatomaceous earth with $Fe(OH)_3$ colloid, resulting in an efficient and stable enrichment capacity. Viruses were found to be efficiently eluted from the modified diatomaceous earth using a nutritious broth. This system efficiently enriched ASFV in water. It also showed the following advantages for efficient ASFV detection in water: (1) rapid enrichment of ASFV in more than 10 liters of water from various sources; (2) increased viral concentrations at least 1 × 104 times after enrichment; (3) easy operation; (4) portable and outdoor-friendly; (5) low cost and widely use.

Data availability statement

The original contributions presented in the study are included in the article/Supplementary material, further inquiries can be directed to the corresponding author/s.

Ethics statement

The animal study was reviewed and approved by Laboratory Animal Ethics Committee of Huazhong Agriculture University (HZAUSW-2022-0017).

Author contributions

HW and ZT contributed to the conception or design of the work, and the acquisition of data. HW and LY completed the data analysis. XC, AG, HL, SR, and WL drafted the manuscript and revised it for important intellectual content. QH provided the samples and helped to design the experiments. All authors have read and edited the manuscript.

Funding

This study was funded by the National Key Research and Development Program of China (2021YFD1800101-2) and the Hubei Agricultural Research System (HBHZD-ZB-2020-005).

Conflict of interest

The authors declare that the research was conducted in the absence of any commercial or financial relationships that could be construed as a potential conflict of interest.

Publisher's note

All claims expressed in this article are solely those of the authors and do not necessarily represent those of their affiliated organizations, or those of the publisher, the editors and the reviewers. Any product that may be evaluated in this article, or

claim that may be made by its manufacturer, is not guaranteed or endorsed by the publisher.

Supplementary material

The Supplementary Material for this article can be found online at: https://www.frontiersin.org/articles/10.3389/fvets.2022.1045190/full#supplementary-material

SUPPLEMENTARY FIGURE 1
Scanning electron micrographs of the surface structure of the diatomaceous earth: **(A–C)** modified diatomaceous earth without $Fe(OH)_3$, showing a flat clean surface; **(D–F)** modified diatomaceous earth with $Fe(OH)_3$, showing coarsening of the diatomaceous earth surface resulting from attachment of the $Fe(OH)_3$ colloids.

SUPPLEMENTARY FIGURE 2
Standard curve for B646L gene plasmids.

References

1. Connelly JT, Baeumner AJ. Biosensors for the detection of waterborne pathogens. *Anal Bioanal Chem.* (2012) 402:117–27. doi: 10.1007/s00216-011-5407-3

2. Haas CN, Rose JB, Gerba C, Regli S. Risk assessment of virus in drinking-water. *Risk Anal.* (1993) 13:545–52. doi: 10.1111/j.1539-6924.1993.tb00013.x

3. Masciopinto C, De Giglio O, Scrascia M, Fortunato F, La Rosa G, Suffredini E, et al. Human health risk assessment for the occurrence of enteric viruses in drinking water from wells: role of flood runoff injections. *Sci Total Environ.* (2019) 666:559–71. doi: 10.1016/j.scitotenv.2019.02.107

4. Fernandez-Cassi X, Timoneda N, Martínez-Puchol S, Rusiñol M, Rodriguez-Manzano J, Figuerola N, et al. Metagenomics for the study of viruses in urban sewage as a tool for public health surveillance. *Sci Total Environ.* (2018) 618:870–80. doi: 10.1016/j.scitotenv.2017.08.249

5. Chen L, Deng Y, Dong S, Wang H, Li P, Zhang H, et al. The occurrence and control of waterborne viruses in drinking water treatment: a review. *Chemosphere.* (2021) 281:130728. doi: 10.1016/j.chemosphere.2021.130728

6. Teunis PF, Rutjes SA, Westrell T, de Roda Husman AM. Characterization of Drinking Water treatment for virus risk assessment. *Water Res.* (2009) 43:395–404. doi: 10.1016/j.watres.2008.10.049

7. Griffin DW, Donaldson KA, Paul JH, Rose JB. Pathogenic human viruses in coastal waters. *Clin Microbiol Rev.* (2003) 16:129–43. doi: 10.1128/CMR.16.1.129-143.2003

8. WOAH. *World Organisation for Animal Health, Terrestrial manual, Paris*. Available online at: https://www.woah.org/fileadmin/Home/eng/Health_standards/tahm/3.08.01_ASF.pdf (accessed on January 23, 2022).

9. Dixon LK, Stahl K, Jori F, Vial L, Pfeiffer DU. African swine fever epidemiology and control. *Annu Rev Anim Biosci.* (2020) 8:221–46. doi: 10.1146/annurev-animal-021419-083741

10. Murase K, Watanabe T, Arai S, Kim H, Tohya M, Ishida-Kuroki K, et al. Characterization of pig saliva as the major natural habitat of streptococcus suis by analyzing oral, fecal, vaginal, and environmental microbiota. *PLoS ONE.* (2019) 14:e0215983. doi: 10.1371/journal.pone.0215983

11. Niederwerder MC, Stoian AMM, Rowland RRR, Dritz SS, Petrovan V, Constance LA, et al. Infectious dose of african swine fever virus when consumed naturally in liquid or feed. *Emerg Infect Dis.* (2019) 25:891–7. doi: 10.3201/eid2505.181495

12. Pei L, Rieger M, Lengger S, Ott S, Zawadsky C, Hartmann NM, et al. Combination of crossflow ultrafiltration, monolithic affinity filtration, and quantitative reverse transcriptase Pcr for rapid concentration and quantification of model viruses in water. *Environ Sci Technol.* (2012) 46:10073–80. doi: 10.1021/es302304t

13. Michen B, Graule T. Isoelectric points of viruses. *J Appl Microbiol.* (2010) 109:388–97. doi: 10.1111/j.1365-2672.2010.04663.x

14. Wang XW Li JS, Guo TK, Zhen B, Kong QX Yi B, et al. Concentration and detection of sars coronavirus in sewage from Xiao Tang Shan Hospital and the 309th hospital. *J Virol Methods.* (2005) 128:156–61. doi: 10.1016/j.jviromet.2005.03.022

15. Cashdollar JL, Dahling DR. Evaluation of a method to re-use electropositive cartridge filters for concentrating viruses from tap and river water. *J Virol Methods.* (2006) 132:13–7. doi: 10.1016/j.jviromet.2005.08.016

16. Hess S, Niessner R, Seidel M. Quantitative detection of human adenovirus from river water by monolithic adsorption filtration and quantitative Pcr. *J Virol Methods.* (2021) 292:114128. doi: 10.1016/j.jviromet.2021.114128

17. USEPA. *Usepa Manual of Methods for Virology. Chapter 14: Concentration and processing of waterborne viruses by positive charge 1MDS cartridge filters and organic flocculation.* Cincinnati, OH: Environmental Monitoring and Support Laboratory Office of Research and Development (2001).

18. Ikner LA, Gerba CP, Bright KR. Concentration and recovery of viruses from water: a comprehensive review. *Food Environ Virol.* (2012) 4:41–67. doi: 10.1007/s12560-012-9080-2

19. Zhang B, Song X, Zhang Y, Han D, Tang C, Yu Y, et al. Hydrochemical characteristics and water quality assessment of surface water and groundwater in Songnen Plain, Northeast China. *Water Res.* (2012) 46:2737–48. doi: 10.1016/j.watres.2012.02.033

20. Xiao J, Wang L, Deng L, Jin Z. Characteristics, sources, water quality and health risk assessment of trace elements in river water and well water in the Chinese Loess Plateau. *Sci Total Environ.* (2019) 650:2004–12. doi: 10.1016/j.scitotenv.2018.09.322

21. Michen B, Meder F, Rust A, Fritsch J, Aneziris C, Graule T. Virus removal in ceramic depth filters based on diatomaceous earth. *Environ Sci Technol.* (2012) 46:1170–7. doi: 10.1021/es2030565

22. Heffron J, McDermid B, Maher E, McNamara PJ, Mayer BK. Mechanisms of virus mitigation and suitability of bacteriophages as surrogates in drinking water treatment by iron electrocoagulation. *Water Res.* (2019) 163. doi: 10.1016/j.watres.2019.114877

23. Lucht A, Formenty P, Feldmann H, Gotz M, Leroy E, Bataboukila P, et al. Development of an immunofiltration-based antigen-detection assay for rapid diagnosis of ebola virus infection. *J Infect Dis.* (2007) 196:S184–92. doi: 10.1086/520593

24. Bidawid S, Farber JM, Sattar SA. Rapid concentration and detection of hepatitis a virus from lettuce and strawberries. *J Virol Methods.* (2000) 88:175–85. doi: 10.1016/S0166-0934(00)00186-5

25. Enriquez CE, Gerba CP. Concentration of enteric adenovirus-40 from tap, sea and waste-water. *Water Res.* (1995) 29:2554–60. doi: 10.1016/0043-1354(95)00099-7

26. Miao J, Jiang HJ, Yang ZW, Shi DY, Yang D, Shen ZQ, et al. Assessment of an electropositive granule media filter for concentrating viruses from large volumes of coastal water. *Environ Sci-Wat Res.* (2019) 5:325–33. doi: 10.1039/C8EW00699G

27. Jin M, Guo X, Wang XW, Yang D, Shen ZQ, Qiu ZG, et al. Development of a novel filter cartridge system with electropositive granule media to concentrate viruses from large volumes of natural surface water. *Environ Sci Technol.* (2014) 48:6947–56. doi: 10.1021/es501415m

28. King DP, Reid SM, Hutchings GH, Grierson SS, Wilkinson PJ, Dixon LK, et al. Development of a Taqman (R) Pcr assay with internal amplification control for the detection of african swine fever virus. *J Virol Methods.* (2003) 107:53–61. doi: 10.1016/S0166-0934(02)00189-1

29. Armanious A, Aeppli M, Jacak R, Refardt D, Sigstam T, Kohn T, et al. Viruses at solid-water interfaces: a systematic assessment of interactions driving adsorption. *Environ Sci Technol.* (2016) 50:732–43. doi: 10.1021/acs.est.5b04644

30. Farrah SR, Preston DR, Toranzos GA, Girard M, Erdos GA, Vasuhdivan V. Use of modified diatomaceous-earth for removal and recovery of viruses in water. *Appl Environ Microb.* (1991) 57:2502–6. doi: 10.1128/Aem.57.9.2502-2506.1991

31. Cuevas-Ferrando E, Randazzo W, Perez-Cataluna A, Sanchez G. Hev occurrence in waste and drinking water treatment plants. *Front Microbiol.* (2020) 10:2937. doi: 10.3389/fmicb.2019.02937

32. Randazzo W, Truchado P, Cuevas-Ferrando E, Simon P, Allende A, Sanchez G. SARS-CoV-2 Rna in Wastewater Anticipated Covid-19 Occurrence in a Low Prevalence Area. *Water Res.* (2020) 181:115942. doi: 10.1016/j.watres.2020.115942

33. Randazzo W, Piqueras J, Evtoski Z, Sastre G, Sancho R, Gonzalez C, et al. Interlaboratory comparative study to detect potentially infectious human enteric viruses in influent and effluent waters. *Food Environ Virol.* (2019) 11:350–63. doi: 10.1007/s12560-019-09392-2

34. Hsu BM, Chen CH, Kung CM, Wan MT, Shen SM. Evaluation of enterovirus recovery in surface water by different adsorption and elution procedures. *Chemosphere.* (2007) 66:964–9. doi: 10.1016/j.chemosphere.2006.06.054

35. Lukasik J, Scott TM, Andryshak D, Farrah SR. Influence of salts on virus adsorption to microporous filters. *Appl Environ Microb.* (2000) 66:2914–20. doi: 10.1128/AEM.66.7.2914-2920.2000

36. Jothikumar N, Khanna P, Paulmurugan R, Kamatchiammal S, Padmanabhan P, A. Simple device for the concentration and detection of enterovirus, hepatitis E virus and rotavirus from water samples by reverse transcription-polymerase chain reaction. *J Virol Methods.* (1995) 55:401–15. doi: 10.1016/0166-0934(95)00089-9

37. Xu WX, Xu N, Zhang MY, Wang Y, Ling GX, Yuan Y, et al. Nanotraps based on multifunctional materials for trapping and enrichment. *Acta Biomater.* (2022) 138:57–72. doi: 10.1016/j.actbio.2021.08.047

38. Cashdollar JL, Wymer L. Methods for primary concentration of viruses from water samples: a review and meta-analysis of recent studies. *J Appl Microbiol.* (2013) 115:1–11. doi: 10.1111/jam.12143

39. Pawar SD, Keng SS, Tare DS, Thormothe AL, Sapkal GN, Anukumar B, et al. A Virus precipitation method for concentration & detection of avian influenza viruses from environmental water resources & its possible application in outbreak investigations. *Indian J Med Res.* (2019) 150:612–9. doi: 10.4103/ijmr.IJMR_1697_18

40. Luo M. *Study on the Novel Regeneration Technology of the Weakly Basic Anion-Exchange Resin [master]*. Dalian JiiaoTong University (2004).

41. Deschaume O, Shafran KL, Perry CC. Interactions of bovine serum albumin with aluminum polyoxocations and aluminum hydroxide. *Langmuir.* (2006) 22:10078–88. doi: 10.1021/la061285h

42. Xu YH, Shigeru AO, Maeda. Removal of arsenate, phosphate, and fluoride ions by aluminium-loaded shirasu-zeolite. *Toxicol Environ Chem.* (2000) 76: 111–24. doi: 10.1080/02772240009358921

43. Lakshmanan D, Clifford D, Samanta G. Arsenic removal by coagulation with aluminum, iron, titanium, and zirconium. *J AWWA.* (2008) 100:76–88. doi: 10.1002/j.1551-8833.2008.tb08144.x

44. Gulledge JH, O'Connor JT. Removal of arsenic (V) from water by adsorption on aluminum and ferric hydroxides. *J AWWA.* (1973) 65:548–52. doi: 10.1002/j.1551-8833.1973.tb01893.x

45. Wang GG, Xie MJ, Wu W, Chen ZZ. Structures and functional diversities of Asfv proteins. *Viruses-Basel.* (2021) 13:2124. doi: 10.3390/v13112124

46. Kazantsev SO, Lozhkomoev AS, Rodkevich NG. Preparation and adsorption properties of nanostructured composites derived from Al/Fe nanoparticles with respect to arsenic. *Nanomaterials-Basel.* (2022) 12:3177. doi: 10.3390/nano12183177

47. Rezwan K, Studart AR, Voros J, Gauckler LJ. Change of zeta potential of biocompatible colloidal oxide particles upon adsorption of bovine serum albumin and lysozyme. *J Phys Chem B.* (2005) 109:14469–74. doi: 10.1021/jp050528w

48. Rezwan K, Meier LP, Gauckler LJ. Lysozyme and bovine serum albumin adsorption on uncoated silica and alooh-coated silica particles: the influence of positively and negatively charged oxide surface coatings. *Biomaterials.* (2005) 26:4351–7. doi: 10.1016/j.biomaterials.2004.11.017

49. Zhu B, Clifford DA, Chellam S. Virus removal by iron coagulation-microfiltration. *Water Res.* (2005) 39:5153–61. doi: 10.1016/j.watres.2005.09.035

50. Sobsey MD, Jones BL. Concentration of poliovirus from tap water using positively charged microporous filters. *Appl Environ Microb.* (1979) 37:588–95. doi: 10.1128/Aem.37.3.588-595.1979

51. Liu S. The *Research of Arsenic Removal by Ferric Chloride and the Mechanism [master].* Xi'an University of Architecture and Technology (2013).

frontiers | Frontiers in Veterinary Science

TYPE Original Research
PUBLISHED 04 January 2023
DOI 10.3389/fvets.2022.1037728

OPEN ACCESS

EDITED BY
Wentao Li,
Huazhong Agricultural University, China

REVIEWED BY
Fernando Costa Ferreira,
University of Lisbon, Portugal
Tereza Cristina Cardoso,
Universidade Estadual de São Paulo, Brazil

*CORRESPONDENCE
Jeong Hee Kim
jhkimh@khu.ac.kr

SPECIALTY SECTION
This article was submitted to Veterinary Experimental and Diagnostic Pathology, a section of the journal Frontiers in Veterinary Science

RECEIVED 06 September 2022
ACCEPTED 04 October 2022
PUBLISHED 04 January 2023

CITATION
Hwang HJ, Choi YS, Song K, Frant M and Kim JH (2023) Development and validation of a fast quantitative real-time PCR assay for the detection of African swine fever virus. *Front. Vet. Sci.* 9:1037728. doi: 10.3389/fvets.2022.1037728

Development and validation of a fast quantitative real-time PCR assay for the detection of African swine fever virus

Hyun Jin Hwang[1], Yun Seong Choi[1], Kyungyoung Song[1], Maciej Frant[2] and Jeong Hee Kim [3,4]*

[1]R&D Center, Ahram Biosystems Inc., Seoul, South Korea, [2]Department of Swine Diseases, National Veterinary Research Institute, Puławy, Poland, [3]Department of Oral Biochemistry and Molecular Biology, School of Dentistry, Kyung Hee University, Seoul, South Korea, [4]Department of KHU-KIST Converging Science and Technology, Graduate School, Kyung Hee University, Seoul, South Korea

African swine fever virus (ASFV) is a double-stranded DNA virus that causes African swine fever (ASF), a lethal hemorrhagic fever that is highly contagious among domestic pigs and wild boars. Due to the high mortality rates and highly contagious nature of the ASF, it is important to develop a fast detection method for ASFV with high sensitivity and specificity to take an immediate action to stop wide spread of the virulent disease. Therefore, a fast and quantitative molecular detection method of ASFV is presented in this study. A total of 24 genotypes of ASFV have been identified based on nucleic acid sequences of the major capsid protein p72. The primers and probe of the present assay was designed to detect all of the p72-based genotypes of ASFV. The turnaround time for PCR detection was within 50 min which is at least about two-times faster compared to other PCR assays. Limit of detection (LoD) was 6.91 genomic copies/reaction for the most virulent genotype II. LoD values for other genotypes were within 10–20 copies/reaction. Cross-reactivity of the assay was validated using a panel of pathogens related to swine disease, and no cross-reactivity was observed. Positive and negative clinical samples (50 samples each) obtained from sick and healthy animals, were used to validate the assay. The results showed that 100% agreement for both positive and negative samples. In summary, the assay described in this study offers the advantage of rapid detection of all genotypes of ASFV with high sensitivity and specificity. The assay is a valuable tool both in clinical and laboratory uses for sensitive and fast detection of ASFV.

KEYWORDS

African swine fever virus, real-time PCR, fast, quantitative, diagnostics

Introduction

African swine fever (ASF) is a highly contagious viral disease caused by ASF virus (ASFV), an enveloped virus with a large, double-stranded DNA which belongs to the *Asfarviridae* family (1, 2). The clinical symptoms include high fever, anorexia, vomiting, diarrhea, and hemorrhage. These clinical symptoms and post-mortem findings are difficult to distinguish from those of classical swine fever (CSF).

ASFV is highly contagious and causes high mortality rates: close to 100% in domestic pigs and approximately 95% in wild bores. Therefore, it is under strict surveillance under Office International des Épizooties (OIE, World Organization of Animal Health). ASF is a serious threat for pork production industry and causes a significant economic impact globally (2–4).

Total of 24 distinct genotypes of ASFV have been identified based on sequences of the gene encoding the major capsid protein p72. Eight serotypes are also known based on viral hemagglutinin CD2-like protein (CD2v) and C-type lectin (2, 5, 6). Among these, genotype II stain is highly virulent and is prevalent in Europe, Russia, China, and Southeast Asia (7–12).

Currently, no vaccine or treatment is available for ASF. Therefore, development of fast and reliable molecular diagnostics method is critical to timely apply the control measures and to prevent wide spread among domestic and wild pigs. In addition, since there are similarities in clinical symptoms between ASF and other swine diseases, it is important to have rapid and specific diagnosis for timely implementation of follow-up measures.

The traditional methods for diagnosis of viral diseases were generally based on virus isolation. However, this process is labor-intensive and time-consuming (13, 14). And not all viruses can be isolated from the samples. Conventional Polymerase chain reaction (PCR)-based technology have been used for the detection of infectious diseases including ASF. PCR technology can be applicable for samples that are not suitable for virus isolation. However, detection of ASFV with conventional PCR involves extra post-PCR steps such as electrophoresis, and the sensitivity was generally much lower than the real-time PCR method (15–17).

An alternative technology for ASFV detection is loop-mediated isothermal amplification (LAMP) (18, 19). Recently, application of CRSPR-Cas12a coupled with LAMP was shown to give an enhanced fluorescence assay sensitivity (20, 21). Recombinase polymerase amplification (RPA) combined with a lateral flow strip for ASF detection was also introduced (22, 23). However, the drawback of these methods is that they require a larger number of primers with more complicated primer design. Moreover, LAMP and RPA showed lower sensitivity compared to PCR assays (24). Real-time PCR technology has been most widely used for the detection of infectious diseases including ASFV because of its high sensitivity and specificity (14, 25–29). However, the reported studies of real-time PCR detection of ASFV involved relatively long reaction times, approximately from 1 and half hours to 2 h (14, 25, 29).

In this study, we developed and validated a fast and quantitative real-time PCR test that can detect all currently known 24 genotypes of ASFV utilizing a new chemistry including a fast Taq polymerase. ASFV detection can be completed within 50 min without losing its sensitivity and specificity.

TABLE 1 Classification of 24 genotypes of the genes for ASFV p72 protein.

Group name	Representative p72 genotype	p72 genotypes
GT2	II	I, II, XVII, XVIII
GT3	III	III, IV, V, VI, XIX, XX, XXI, XXII, XXIV
GT7	VII	VII
GT8	VIII	VIII, XI, XII, XIII, XIV, XV, XVI
GT9	IX	IX
GT10	X	X
GT23	XXIII	XXIII

Materials and methods

Synthetic double stranded DNA template

Synthetic double-stranded DNAs for different genotypes of ASFV p72 gene were used for analytical performance tests of the assay. Twenty-four genotypes of ASFV p72 gene were classified into seven genotype groups based on nucleic acid sequences of the p72 target region (Table 1). The seven genotype groups were designated as GT2, GT3, GT7, GT8, GT9, GT10 and GT23, referring to the representative genotype of each group. A double-stranded DNA of the p72 conservative region with a size of about 400 bp (gBlocks, IDT, Singapore) was synthesized for each genotype group and used as a standard sample. The synthesized DNAs were dissolved in nuclease-free water (Molecular Biology grade, Sigma-Aldrich, USA) to the concentration of 1×10^9 copies/μL, aliquoted and stored at −70°C.

Primer and probe design

The sequences of the seven known groups of ASFV within the conserved region of ASFV major capsid protein p72 were searched. Primers and TaqMan probe were designed to target the conserved region and also to match all 7 genotype groups of ASFV listed in Table 1. The sequences of forward and reverse primers and probes (from LGC Biosearch Technologies, USA) are listed in Table 2. A 1:1 mixture of two forward primers, ASFV-F1 and ASFV-F2, were used for PCR. For internal PCR control (IPC), primers and probe were designed to target human tubulin alpha 1a gene (NCBI Reference Sequence: NG_008966.1).

DNA isolation and optimization of real-time PCR assay

For optimization of the PCR conditions, GT2 synthetic DNA was used as a template. To mimic clinical samples, 30

TABLE 2 Sequence of primers and probes used in this study.

Target	Name	Sequence (5' to 3')	Tm (°C)	GC (%)	Amplicon size (bp)
ASFV	ASFV-F1	ACGTAATCCGTGTCCCAACTAA	55.9	45.5	217
	ASFV-F2	ACATAATCTGTGTCCCAGCTAA	53.5	40.9	
	ASFV-R	CTGCTCATGGTATCAATCTTATCGA	54.4	40.0	
	ASFV-Probe-FAM	CTGGGTTGGTATTCCTCCCGTGGCT	64.4	60.0	
Internal PCR Control (IPC)*	IPC-F	CCAGGTTTCCACAGCTGTAGT	57.0	52.5	219
	IPC-R	GGGCTCCATCAAATCTCAGG	55.5	55.0	
	IPC-Probe-HEX	AGCCCTACAACTCCATCCTCACC	60.5	56.5	

*Tubulin alpha a1 gene.

ng of swine genomic DNA was included in each of the PCR mixture as a background genomic DNA. Swine genomic DNA was purified from pork meat using a DNeasy Blood and Tissue Kit (Qiagen, Germany), according to the protocol provided by the supplier. Concentrations of primers, probe and $MgCl_2$ were optimized to achieve maximum amplification efficiency and minimal threshold cycle (Ct). The reaction mixture contained 5 μL of DNA extracts, 5.0 mM of $MgCl_2$, 1.6 units of *Taq* DNA polymerase and 8×10^4 copies of a plasmid DNA encoding the IPC target in 50 mM TE, pH8.5 buffer (10 mM Tris and 0.5 mM EDTA, pH 8.5). Concentrations of the primers and probes were as follows: 500 nM of ASFV-F1, 500 nM of ASFV-F2, 500 nM of ASFV-R and 200 nM of ASFV-probe-FAM for ASFV, and 150 nM of IPC-F, 150 nM of IPC-R and 180 nM of IPC-Probe-HEX for IPC.

PCR amplification and real-time detection was performed on Bio-Rad CFX96 real-time PCR Detection System (Biorad, USA). The PCR protocol consists of a hot-start of 95°C for 2 min, followed by 45 cycles of 95°C for 5 s and 56°C for 10 s. Upon completion, amplification graphs and Ct values were recorded. All experiments were performed at least in triplicate.

Analytical sensitivity

To determine the limit of detection (LoD), serial dilutions the standard template, ASFV DNA GT2 were prepared in TE, pH 9.0 buffer for 5 different concentrations (20, 2, 1, 0.6 and 0.2 copies/μL). For each template concentration, PCR assay was performed in 96-replicates and the positive hit rate with $Ct \leq 40$ was determined. The serially diluted standard samples were assayed in triplicate to determine the LoD of the assay by adding 5 μL of each diluted standard sample to the PCR mixture. The resulting concentrations per each PCR mixture were 100, 10, 5, 3 and 1 copies/reaction. In the PCR mixture of 20 μL, 2 μL of porcine genomic DNA (15 ng/μL) was also added to mimic the clinical specimens. The PCR conditions used were described above. The results were analyzed using PROBIT regression analysis.

We also evaluated analytical sensitivity of the assay using serial dilutions of a known viral titer. Viral titer was defined as the amount of virus causing hemadsorption in 50% of infected cultures (HAD_{50}/mL). The titer used for serial dilution was $10^{5.36}$ HAD_{50}/mL.

Cross-reactivity test

Viruses and bacterium used for cross-reactivity test are: Classical swine fever virus (CSFV), *Erysipelothrix rhusiopathiae*, Aujeszky's disease virus (ADV), *Actinobacillus Pleuropneumonia*, *Salmonella Typhimurium* and *Pasteurella multocida*. DNAs were isolated using QIAamp DNA Mini Kit (Qiagen, Germany) according to the protocol provided by the supplier. Isolated DNA samples were tested to confirm the cross-reactivity of the fast ASFV PCR assay.

Clinical performance test

Panels of ASFV positive and negative clinical samples of blood and tissues from domestic pigs and wild bores were used for the clinical performance test. The clinical samples consist of fifty positive samples of varying virulence and fifty negative samples that were collected from domestic pigs and wild boars during the year of 2018 to 2019 by National Veterinary Research Institute in Puławy, Poland. The positive samples consisted of 9 blood samples and 41 tissue samples, and the negative samples consisted of 14 blood samples and 36 tissue samples. The tissue samples were from various organs consisting of tonsil, spleen, kidney, lymph node and bone marrow. DNAs from the clinical samples were extracted using QIAamp DNA Mini Kit (Qiagen, Germany) according to the protocol provided by the

supplier. Isolated DNA samples were tested to check the clinical performance of the fast ASFV PCR assay.

Results

Selection of primers, probes, and optimized parameters for detection of ASFV

The primers and probe for detection of ASFV were designed based on the nucleic acid sequences of all genotypes of the ASFV p72 gene. The gene sequences were acquired from GenBank data base. Several candidate sequences were tried for the primers and probe, and the best results were obtained with ASFV-F1 and ASFV-R1 primers for the genotype group GT2 (data not shown). To cover all 7 groups of ASFV genotypes (24 genotypes), a modified forward primer, ASFV-F2 was included. The sequences of the primers and probe used in this study are listed in Table 2. Equal amounts of ASFV-F1 and ASFV-F2 primers were mixed and used as forward primers. Human tubulin alpha a1 sequence, that is also present in the swine genome, was used as an internal PCR control (IPC), and the primer and probe sequences for detection of IPC are also listed in Table 2.

Annealing temperature and concentrations of primers and probes were optimized for real-time PCR. Optimum annealing temperature was 56°C, and optimum concentrations of primers and probe were 500 nM and 200 nM, respectively, for ASFV and 150 nM and 180 nM, respectively, for IPC. The optimum PCR protocol was as follows: one cycle at 95°C for 2 min, 45 cycles at 95°C for 5 s, then at 56°C for 10 s. Total PCR running time was about 50 min on the Bio-Rad CFX96.

Limit of detection

The limit of detection (LoD) of the optimized assay was determined by testing serial dilutions of the standard sample template, ASFV DNA GT2. Ct values and hit rates were measured for 6 different template concentrations (100, 10, 5, 3, 1 and 0 copies/reaction), and the results are listed in Table 3. The test results were analyzed using the PROBIT regression method as shown in Figure 1. The LoD was determined to be 6.91 copies/reaction (5.40 ∼ 9.85 copies/reaction at 95% confidence interval).

The LoD values of the DNA standards for other 6 genotype groups (GT3, GT7, GT8, GT9, GT10 and GT 23) were tested in comparison with the standard sample template, ASFV DNA GT2, and the results are listed in Table 4. GT3, GT8, GT10 and GT23 which include 18 genotypes showed hit rates of > 95% at the concentration of 10 copies/reaction. These values are similar to the value determined for the ASFV DNA GT2 which include 4 genotypes (genotypes I, II, XVII and XVIII). ASFV DNA GT7 and GT9 which include 2 genotypes (genotypes VII and IX) showed a hit rate of 89.6% for 10 copies/reaction, and 95.8 and 100%, respectively, for 20 copies/reaction. The data suggested that LoD of other genotypes is 10∼20 copies/reaction or better at ≥95% hit rate.

TABLE 3 Threshold cycle (Ct) values and hit rates of serially diluted samples.

Concentration (copies/reaction)	Number of samples	Ct		Hit rate (%)
		Average	SD	
100	96	32.45	1.04	100
10	96	36.34	1.70	97.9
5	96	38.06	2.68	92.7
3	96	38.73	3.22	77.1
1	96	37.69	3.54	44.8
0	48	ND	-	0

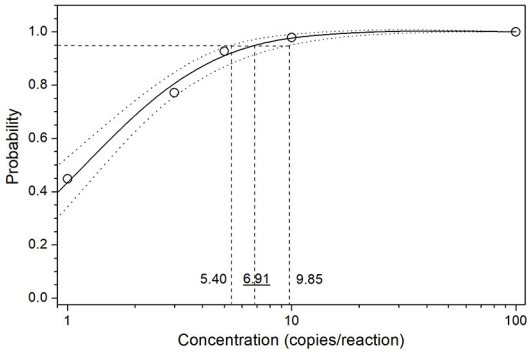

FIGURE 1
PROBIT regression result for determination of the analytical sensitivity. Serial dilutions of the standard sample template GT2 were used to measure the Ct values and hit rates. The limit of detection (LoD) at 95% hit rate was determined to be 6.91 copies/reaction (5.40∼9.85 copies/reaction at 95% confidence interval).

Analytical sensitivity of the assay was also determined by testing serial dilutions of a known viral titer ($10^{5.36}$ HAD_{50}/mL). The last detectable dilution was 10^4 as shown in Table 5, corresponding to the analytical sensitivity of $10^{1.36}$ HAD_{50}/mL.

Standard curve

The analytical sensitivity was further studied by testing triplicate of 9-fold serial dilutions of the standard sample template, ASFV DNA GT2. The experiments were performed in the presence of 30 ng of porcine genomic DNA to mimic the clinical test condition. A standard curve was generated by plotting the mean Ct value of the three replicates against the template concentration (10–10^9 copies/reaction).

TABLE 4 Threshold cycle (Ct) values and hit rates of 7 standard genotype groups.

ASFV group	Concentration (copies/reaction)	Number of samples	Positive	Ct		Hit rate (%)
				Mean	SD	
GT2	10	72	72	35.02	1.28	100.0
GT3	10	48	47	37.86	1.88	97.9
GT7	20	48	46	37.78	2.51	95.8
	10	48	43	38.73	2.85	89.6
GT8	10	48	48	37.67	1.53	100
GT9	20	48	48	35.19	1.43	100
	10	48	43	38.13	4.07	89.6
GT10	10	48	48	36.77	2.05	100
GT23	10	48	48	36.92	1.66	100

TABLE 5 Analytical sensitivity measured with a known viral titer.

Virus	Genotype	Virus titer (HAD_{50}/mL)	Dilution	Ct (ASFV)	Ct (IPC)	Results
ASFV	II	$10^{5.36}$	1	24.25	26.11	Positive
		$10^{4.36}$	10	27.85	24.80	Positive
		$10^{3.36}$	10^2	31.77	26.15	Positive
		$10^{2.36}$	10^3	34.76	25.91	Positive
		$10^{1.36}$	10^4	39.16	26.20	Positive
		$10^{0.36}$	10^5	No Ct	26.01	Negative

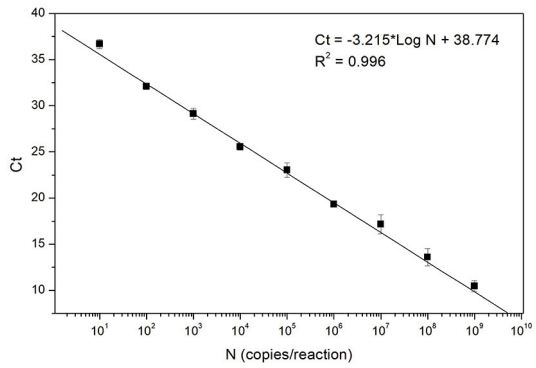

FIGURE 2
Standard curve of the fast ASFV PCR assay. The curve was generated by analyzing triplicate of 9-fold serial dilutions of the standard sample template, ASFV DNA GT2. Each data point (filled square) corresponds to the mean Ct value of the three replicates at each concentration.

As shown in Figure 2, a linear regression analysis represents a high coefficient of determination (0.996), demonstrating a linear dynamic range across the 9 orders of magnitude tested, ranging from 10^9 to the 10 copies/reaction. This standard curve result confirms that the fast ASFV PCR assay developed in this study can be used for quantitative determination of the template concentration. The analytical sensitivity estimated from the standard curve (down to 10 copies/reaction) is also in agreement with the result of the LoD study described above.

TABLE 6 Cross- reactivity of the ASFV assay kit.

No.	Sample	Ct	
		ASFV	IPC*
1	Classical swine fever virus (CSFV)	No Ct	23.98
2	*Erysipelothrix rhusiopathiae*	No Ct	25.38
3	Aujeszky's disease virus (ADV)	No Ct	24.66
4	*Actinobacillus Pleuropneumonia*	No Ct	24.62
5	*Salmonella Typhimurium*	No Ct	27.83
6	*Pasteurella multocida*	No Ct	24.82

*IPC, internal PCR control.

Cross-reactivity of the assay

The cross-reactivity was tested for Classical swine fever virus (CSFV), *Erysipelothrix rhusiopathiae*, Aujeszky's disease

virus (ADV), *Actinobacillus Pleuropneumonia*, *Salmonella Typhimurium* and *Pasteurella multocida*. DNAs were extracted from each microorganism and tested for cross-reactivity. As shown in Table 6, none of the pathogens showed positive results with the assay developed, while positive Ct values were observed for all of the pathogens, confirming no cross-reactivity for the pathogens tested.

Clinical performance test

Clinical performance of the assay was tested with ASFV clinical samples which consist of 50 positive and 50 negative clinical samples of blood and tissues collected from domestic pigs and wild bores during the year of 2018 to 2019. The samples were previously tested and confirmed by National Veterinary Research Institute in Pulawy, Poland. For the test, DNAs were extracted from the clinical samples and used for the PCR assay.

The results of the clinical performance test are listed in Table 7. The results of the fast ASFV PCR assay of this study show 100% agreement with the original diagnosis results: All 50 positive samples were detected to be positive and all 50 negative samples were detected to be negative. Therefore, it is confirmed that both sensitivity and specificity are 100%.

Agreement with the standard real-time PCR method [Fernández-Pinero method using UPL-162 probe (26)] recommended by European Union Reference Laboratory (EURL) in Valdeolmos, Spain and by the International Animal Health Organization (OIE), was also tested. As shown in Table 8, the results of the fast ASFV PCR assay of this study are in 100% agreement for both positive and negative samples with those of the Fernández-Pinero method.

Discussion

The average time of ASF symptom onset after exposure to ASFV was about 5 to 13 days and death of the infected pigs began to occur at 8–15 days after exposure (11, 22). The time period from the onset of the disease to death of the animal is relatively short and the morbidity and mortality rate is almost 100% (2–4). Moreover, due to the recent increase in the international trade, animal transport and human travel, the risk of transboundary spreading of infectious diseases became significantly higher. Therefore, fast and timely diagnosis and treatment of suspected pigs became more important. In other aspect, infections with different viruses cause similar clinical signs in swine which makes it difficult to diagnosis (17, 30, 31). Therefore, highly specific identification of syndromic pathogens is also required.

Currently, PCR is the most widely used diagnostic techniques for detecting ASF because of its high sensitivity and specificity. Both conventional and real-time PCR assays have

TABLE 7 Clinical sensitivity and specificity.

			Results of original diagnosis		Total
			Positive	Negative	
Fast ASFV PCR assay of this study	Positive	Blood	9	0	50
		Tissue	41	0	
	Negative	Blood	0	14	50
		Tissue	0	36	
Total			50	50	100

Clinical sensitivity: 100% (92.9%–100% at 95% confidence interval).
Clinical specificity: 100% (92.9%–100% at 95% confidence interval).

TABLE 8 Agreement with Fernández-Pinero method (UPL-162 probe).

			Fernadez-Pinero method (UPL-162 probe)		Total
			Positive	Negative	
Fast ASFV PCR assay of this study	Positive	Blood	9	0	50
		Tissue	41	0	
	Negative	Blood	0	14	50
		Tissue	0	36	
Total			50	50	100

Positive Percent Agreement (PPA): 100% (92.9–100% at 95% confidence interval).
Negative Percent Agreement (NPA): 100% (92.9–100% at 95% confidence interval).
Overall Percent Agreement (OPA): 100% (96.3–100% at 95% confidence interval).

been recommended for diagnosis of ASF by OIE. Although these two PCR methods have been used widely, they are either not fast enough or not sufficiently sensitive. In the present study, a highly sensitive, time-saving quantitative real-time PCR technique was developed. The LoD of the assay was 6.91 copies/reaction which is much lower than those of the previously reported values ranging from several 100 and several tens of copies/ reaction (14, 27, 28). The LoD measured with known viral titer was $10^{1.36}$ HAD_{50}/mL that is at least two-times lower than other PCR methods. One study showed a similar LoD of 6 copies/reaction which is comparable with the data presented in this study (29). The LoD value achieved with the assay developed was much lower than those of the conventional PCR Assay (15–17), LAMP assay (18, 19), and RPA assay (22, 23).

When designing primers and probes for molecular diagnostic assays, it is important to select highly conserved regions of viral genome to ensure the assay can detect all known variants or genotypes of the virus. We designed the primers to detect all 24 genotypes of ASFV that are currently identified, and confirmed that all 24 genotypes can be detected with sufficient analytical sensitivity. No cross-reactivity was observed with other swine pathogens and the pathogens of related diseases. It was also demonstrated that the linear dynamic range of this assay is 9-log orders of concentration, sufficient for quantitative determination of ASFV DNA.

The clinical performance was evaluated with 50 positive and 50 negative clinical samples of blood and tissues collected from domestic pigs and wild bores. The test results obtained with clinical samples revealed that the assay has 100% sensitivity and 100% specificity, and also 100% PPA and 100% NPA when compared with the standard Fernández-Pinero method. The whole PCR process to results can be completed in about 50 min which is at least about two-times shorter than the 90∼120 min running time of other real-time PCR assays (14, 25, 28, 29).

In summary, a real-time PCR assay has been developed that is faster, more sensitive than currently available PCR methods and can detect all 24 genotypes of ASF. The results of the analytical and clinical performance tests revealed that the assay is much faster and more sensitive than other PCR methods and represents high specificity with no cross-reactivity. The assay developed in this study can be a useful molecular diagnostic tool for the prompt control and prevention of ASF.

Data availability statement

The original contributions presented in the study are included in the article/supplementary materials, further inquiries can be directed to the corresponding author.

Ethics statement

The animal study was reviewed and approved by National Veterinary Research Institute, Al. Partyzantów 57, 24-100 Puławy, Poland.

Author contributions

HJH contributed to the idea conception. YSC and KS performed the analytical data collection and analysis. MF performed the clinical data collection and analysis. JHK and HJH contributed to design of the study and analysis of the data. JHK supervised the experiments. HJH and JHK prepared the manuscript. All authors contributed to the article and approved the submitted version.

Funding

This work was supported by Korea Evaluation Institute of Industrial Technology and funded by the Ministry of Trade, Industry and Energy, Korea (Grant 10080151).

Conflict of interest

Authors HJH, YSC, and KS were employed by Ahram Biosystems, Inc.

The remaining authors declare that the research was conducted in the absence of any commercial or financial relationships that could be construed as a potential conflict of interest.

Publisher's note

References

1. Cackett G, Matelska D, Sýkora M, Portugal R, Malecki M, Bähler J, et al. The African swine fever virus transcriptome. *J Virol.* (2020) 94:e00119–20. doi: 10.1128/JVI.00119-20

2. Gaudreault NN, Madden DW, Wilson WC, Trujillo JD, Richt JA. African swine fever virus: an emerging DNA arbovirus. *Front Vet Sci.* (2020) 7:215. doi: 10.3389/fvets.2020.00215

3. Galindo I, Alonso C. African swine fever virus: a review. *Viruses.* (2017) 9:103. doi: 10.3390/v9050103

4. Urbano AC, Ferreira F. African swine fever control and prevention: an update on vaccine development. *Emerg Microbes Infect.* (2022) 11:2021–33. doi: 10.1080/22221751.2022.2108342

5. Malogolovkin A, Burmakina G, Tulman ER, Delhon G, Diel DG, Salnikov N, et al. African swine fever virus CD2v and C-type lectin gene loci mediate serological specificity. *J General Virol.* (2015) 96:866–73. doi: 10.1099/jgv.0.000024

6. Gaudreault NN, Richt JA. Subunit vaccine approaches for African swine fever virus. *Vaccines.* (2019) 7:56. doi: 10.3390/vaccines7020056

7. Chapman DA, Darby AC, Da Silva M, Upton C, Radford AD, Dixon LK. Genomic analysis of highly virulent Georgia 2007/1 isolate of African swine fever virus. *Emerg Infect Dis.* (2011) 17:599. doi: 10.3201/eid1704.101283

8. Gallardo C, Fernández-Pinero J, Pelayo V, Gazaev I, Markowska-Daniel I, Pridotkas G, et al. Genetic variation among African swine fever genotype II viruses, eastern and central Europe. *Emerg Infect Dis.* (2014) 20:1544. doi: 10.3201/eid2009.140554

9. Ge S, Li J, Fan X, Liu F, Li L, Wang Q, et al. Molecular characterization of African swine fever virus, China, 2018. *Emerg Infect Dis.* (2018) 24:2131. doi: 10.3201/eid2411.181274

10. Garigliany M, Desmecht D, Tignon M, Cassart D, Lesenfant C, Paternostre J, et al. Phylogeographic analysis of African swine fever virus, Western Europe, 2018. *Emerg Infect Dis.* (2019) 25:184. doi: 10.3201/eid2501.181535

11. Gallardo C, Soler A, Nurmoja I, Cano-Gómez C, Cvetkova S, Frant M, et al. Dynamics of African swine fever virus (ASFV) infection in domestic pigs infected with virulent, moderate virulent and attenuated genotype II ASFV European isolates. *Transbound Emerg Dis.* (2021) 68:2826–41. doi: 10.1111/tbed.14222

12. Denstedt E, Porco A, Hwang J, Nga NTT, Ngoc PTB, Chea S, et al. Detection of African swine fever virus in free-ranging wild boar in Southeast Asia. *Transbound Emerg Dis.* (2021) 68:2669–75. doi: 10.1111/tbed.13964

13. Oura CAL, Edwards L, Batten CA. Virological diagnosis of African swine fever—comparative study of available tests. *Virus Res.* (2013) 173:150–8. doi: 10.1016/j.virusres.2012.10.022

14. Luo Y, Atim SA, Shao L, Ayebazibwe C, Sun Y, Liu Y, et al. Development of an updated PCR assay for detection of African swine fever virus. *Arch Virol.* (2017) 162:191–9. doi: 10.1007/s00705-016-3069-3

15. Agüero M, Fernández J, Romero L, Sánchez Mascaraque C, Arias M, Sánchez-Vizcaíno JM. Highly sensitive PCR assay for routine diagnosis of African swine fever virus in clinical samples. *J Clin Microbiol.* (2003) 41:4431–4. doi: 10.1128/JCM.41.9.4431-4434.2003

16. Cao S, Chen H, Zhao J, Lü J, Xiao S, Jin M, et al. Detection of porcine circovirus type 2, porcine parvovirus and porcine pseudorabies virus from pigs with postweaning multisystemic wasting syndrome by multiplex PCR. *Vet Res Commun.* (2005) 29:263–9. doi: 10.1023/B:VERC.0000047501.78615.0b

17. Giammarioli M, Pellegrini C, Casciari C, De Mia GM. Development of a novel hot-start multiplex PCR for simultaneous detection of classical swine fever virus, African swine fever virus, porcine circovirus type 2, porcine reproductive and respiratory syndrome virus and porcine parvovirus. *Vet Res Comm.* (2008) 32:255–62. doi: 10.1007/s11259-007-9026-6

18. James HE, Ebert K, McGonigle R, Reid SM, Boonham N, Tomlinson JA, et al. Detection of African swine fever virus by loop-mediated isothermal amplification. *J Virol Methods.* (2010) 164:68–74. doi: 10.1016/j.jviromet.2009.11.034

19. Wang D, Yu J, Wang Y, Zhang M, Li P, Liu M, et al. Development of a real-time loop-mediated isothermal amplification (LAMP) assay and visual LAMP assay for detection of African swine fever virus (ASFV). *J Virol Methods.* (2020) 276:113775. doi: 10.1016/j.jviromet.2019.113775

20. Tao D, Liu J, Nie X, Xu B, Tran Thi TN, Niu L, et al. Application of CRISPR-Cas12a enhanced fluorescence assay coupled with nucleic acid amplification for the sensitive detection of African swine fever virus. *ACS Synth Biol.* (2020) 9:2339–50. doi: 10.1021/acssynbio.0c00057

21. Wang X, Ji P, Fan H, Dang L, Wan W, Liu S, et al. CRISPR/Cas12a technology combined with immunochromatographic strips for portable detection of African swine fever virus. *Communications Biology.* (2020) 3:1–8. doi: 10.1038/s42003-020-0796-5

22. Miao F, Zhang J, Li N, Chen T, Wang L, Zhang F, et al. Rapid and sensitive recombinase polymerase amplification combined with lateral flow strip for detecting African swine fever virus. *Front Microbiol.* (2019) 10:1004. doi: 10.3389/fmicb.2019.01004

23. Fan X, Li L, Zhao Y, Liu Y, Liu C, Wang Q, et al. Clinical validation of two recombinase-based isothermal amplification assays (RPA/RAA) for the rapid detection of African swine fever virus. *Front Microbiol.* (2020) 11:1696. doi: 10.3389/fmicb.2020.01696

24. Flannery J, Ashby M, Moore R, Wells S, Rajko-Nenow P, Netherton CL, et al. Identification of novel testing matrices for African swine fever surveillance. *J Vet Diagn Invest.* (2020) 32:961–3. doi: 10.1177/1040638720954888

25. King DP, Reid SM, Hutchings GH, Grierson SS, Wilkinson PJ, Dixon LK, et al. Development of a TaqMan® PCR assay with internal amplification control for the detection of African swine fever virus. *J Virol Methods.* (2003) 107:53–61. doi: 10.1016/S0166-0934(02)00189-1

26. Fernández-Pinero J, Gallardo C, Elizalde M, Robles A, Gómez C, Bishop R, et al. Molecular Diagnosis of African Swine Fever by a New Real-Time PCR Using Universal Probe Library. *Transbound Emerg Dis.* (2013) 60:48–58. doi: 10.1111/j.1865-1682.2012.01317.x

27. Haines FJ, Hofmann MA, King DP, Drew TW, Crooke HR. Development and validation of a multiplex, real-time RT PCR assay for the simultaneous detection of classical and African swine fever viruses. *PLoS ONE.* (2013) 8:e71019. doi: 10.1371/journal.pone.0071019

28. Wang A, Jia R, Liu Y, Zhou J, Qi Y, Chen Y, et al. Development of a novel quantitative real-time PCR assay with lyophilized powder reagent to detect African swine fever virus in blood samples of domestic pigs in China. *Transbound Emerg Dis.* (2020) 67:284–97. doi: 10.1111/tbed.13350

29. Wang Y, Xu L, Noll L, Stoy C, Porter E, Fu J, et al. Development of a real-time PCR assay for detection of African swine fever virus with an endogenous internal control. *Transbound Emerg Dis.* (2020) 67:2446–54. doi: 10.1111/tbed.13582

30. Wernike K, Hoffmann B, Beer M. Single-tube multiplexed molecular detection of endemic porcine viruses in combination with background screening for transboundary diseases. *J Clin Microbiol.* (2013) 51:938–44. doi: 10.1128/JCM.02947-12

31. Shi X, Liu X, Wang Q, Das A, Ma G, Xu L, et al. A multiplex real-time PCR panel assay for simultaneous detection and differentiation of 12 common swine viruses. *J Virol Methods.* (2016) 236:258–65. doi: 10.1016/j.jviromet.2016.08.005

frontiers | Frontiers in Veterinary Science

TYPE Original Research
PUBLISHED 10 February 2023
DOI 10.3389/fvets.2023.1093440

OPEN ACCESS

EDITED BY
Bin Li,
Jiangsu Academy of Agricultural Sciences (JAAS), China

REVIEWED BY
Sonalika Mahajan,
Indian Veterinary Research Institute (IVRI), India
Dongming Zhao,
Harbin Veterinary Research Institute (CAAS), China

*CORRESPONDENCE
Jiaqiang Wu
✉ wujiaqiang2000@sina.com
Jiang Yu
✉ yujiang_2213@163.com

†These authors have contributed equally to this work

SPECIALTY SECTION
This article was submitted to Veterinary Experimental and Diagnostic Pathology, a section of the journal Frontiers in Veterinary Science

RECEIVED 09 November 2022
ACCEPTED 27 January 2023
PUBLISHED 10 February 2023

CITATION
Li J, Jiao J, Liu N, Ren S, Zeng H, Peng J, Zhang Y, Guo L, Liu F, Lv T, Chen Z, Sun W, Hrabchenko N, Yu J and Wu J (2023) Novel p22 and p30 dual-proteins combination based indirect ELISA for detecting antibodies against African swine fever virus.
Front. Vet. Sci. 10:1093440.
doi: 10.3389/fvets.2023.1093440

Novel p22 and p30 dual-proteins combination based indirect ELISA for detecting antibodies against African swine fever virus

Jianda Li[1†], Jian Jiao[1,2†], Na Liu[1,3†], Sufang Ren[1], Hao Zeng[1], Jun Peng[4], Yuyu Zhang[1,3], Lihui Guo[1], Fei Liu[1], Tingting Lv[1,3], Zhi Chen[1], Wenbo Sun[1], Nataliia Hrabchenko[1], Jiang Yu[1,2*] and Jiaqiang Wu[1,2,3*]

[1]Shandong Key Laboratory of Animal Disease Control and Breeding, Institute of Animal Science and Veterinary Medicine, Shandong Academy of Agricultural Sciences, Jinan, China, [2]School of Veterinary Medicine, Qingdao Agricultural University, Qingdao, China, [3]School of Life Sciences, Shandong Normal University, Jinan, China, [4]College of Animal Science and Technology, Shandong Agricultural University, Tai'an, China

Introduction: African swine fever virus (ASFV) infection is one of the most complex and fatal hemorrhagic viral diseases, causing a devastating loss to the swine industry. Since no effective vaccine is available, prevention and control of ASFV heavily depends on early diagnostic detection.

Methods: In this study, a novel indirect ELISA was established for detecting antibodies against ASFV using dual-proteins, p22 and p30. Recombinants p22 and p30 were expressed and purified from *E.coli* vector system by recombined plasmids pET-KP177R and pET-CP204L. p22 and p30 were mixed as antigens for developing the indirect ELISA.

Results: Through optimizing coating concentrations of p30 and p22, coating ratio (p30: p22 = 1:3), and serum dilution (as 1:600), the established ELISA performed higher specificity, sensitivity, and repeatability against ASFV-positive serum. Furthermore, 184 clinical serum samples from suspected diseased pigs were verified the established ELISA in clinical diagnosis. The results showed that compared with two commercial ELISA kits, the established ELISA possessed higher sensitivity and almost uniform coincidence rate.

Conclusion: The novel indirect ELISA based on dual-proteins p30 and p22 performed a valuable role in diagnostic detection of ASFV, providing a broad insight into serological diagnostic methods of ASFV.

KEYWORDS

African swine fever virus, indirect ELISA, p22, p30, serological diagnosis

1. Introduction

African swine fever (ASF) is an acute and highly contact infectious disease, caused by African swine fever virus (ASFV). ASFV infection induced high fever, lethargy, and death in pigs, causing a devastating loss to the swine industry. ASF was firstly found in Kenya in 1909 and reported in 1921 (1). Subsequently, ASFV spread to Central and Eastern Europe (2). In China, ASFV infection first occurred in Liaoning Province in August 2018, and subsequently spread to all provinces of China (3). Moreover, genotype I ASFVs and low virulent genotype II ASFVs occurred in China (4, 5). Since no commercial vaccine is available, the emergence of ASFVs presents new challenges for the early diagnosis and control of ASF.

As the only member of the family *Asfarviridae*, ASFV is an enveloped virus containing 170–190 kb double-stranded DNA. The ASFV genome includes more than 150 open reading frames, encoding 54 structural proteins and more than 100 nonstructural proteins (6). Among these proteins, p22, encoded by KP177R gene, is a structural protein located at the inner envelope of ASFV virion (7). Recently, a function genomics has shown that p22 protein interacts with host proteins involved in several cellular function, including cell signaling transduction, cell structure, and virus binding (8). Although a recombinant ASFV lacking p22 has no effect on pathogenicity and virulence of ASFV, immunization with p22 could induce a higher antibody titer, indicating that p22 has potential as a target for serological diagnosis (9, 10). p30 protein is one of the most immunogenic structural proteins in the ASFV virion, which is encoded by CP204L gene (11). During ASFV infection of macrophage, the expression of p30 is detected at 2–4 h post-infection and then persists throughout the infection cycle (12). Thus, p30 is considered to be an ideal diagnostic protein using for diagnosis of ASFV in the early state of infection.

Since no commercial vaccines against this disease currently, early detection and diagnosis play a vital role in the prevention and control of ASFV. In addition to molecular diagnostic method, serological detection is another method for virus infection, which is conducive to identify infected animals and eradicate the potential risk (13, 14). Although molecular diagnostic methods are very important for the early diagnosis and prevention of ASF, the characteristics of low cost and convenience of serological methods are more suitable for large-scale field epidemiological investigation (14–16). The establishment of reliable serological diagnostic methods is closely related to the antigenicity of the selected antigens (17, 18). Enzyme-linked immunosorbent assay (ELISA) is a designated experiment specified by OIE (World Organization for Animal Health) for international trade to detect specific antibodies to ASFV. Screening several viral proteins with higher reactivity is very important for establishing reliable serological diagnostic methods and avoiding unnecessary biosafety problems (19, 20). In this study, we expressed and purified ASFV p22 and p30 proteins, and established an indirect ELISA method for detecting antibodies against ASFV.

2. Materials and methods

2.1. Serum samples

ASFV-positive serum was purchased from China Institute of Veterinary Drug Control. All clinical swine sera were donated from Vland Biotech (China). The negative sera against ASFV, and the positive sera against porcine circovirus type 2 (PCV2), porcine pseudorabies virus (PRV), classical swine fever virus (CSFV), porcine reproductive and respiratory syndrome virus (PRRSV), and *Haemophilus parasuis* (HPS) were stored in our lab.

2.2. Sequence analysis and optimization

The amino acid sequences of p22 and p30 were analyzed for immunogenicity, hydrophilicity and transmembrane region by IEDB database (http://tools.immuneepitope.org/bcell/). According to *Escherichia coli* (*E.coli*) expression systems, the sequences of KP177R gene and CP204L gene were optimized and synthesized based on ASFV HLJ/18 strain (Accession number MK333180.1). Subsequently, the synthesized sequences were cloned into pEASY-Blunt vector by gene synthesis corporation.

TABLE 1 The sequences of primers.

Primers name	Primers sequences
CP204L-R	*GGATCC*ATGGATTTCATCCTGAATATC
CP204L-F	*CTCGAG*TTTTTTTTTCAGCAGTTTAA
KP177R-R	*GGATCC*AAAAAACAGCAGCCGCCGA
KP177R-F	*CTCGAG*TTATGCGTGTTTATGATTAC

2.3. Expression of p22 and p30

To construct the expression plasmids of p22 and p30, the sequences of CP204L and KP177R were amplified by PCR using the primers containing *BamHI* and *XhoI* restriction enzyme sites (Table 1). After verification by sequencing, the sequences of CP204L and KP177R were inserted into pET-32a vector. The plasmids recombinants pET-KP177R and pET-CP204L were transformed into *E.coli* BL21(DE3) cells. The recombinants *E.coli* were cultured in LB medium and the condition of proteins expression were optimized, such as culture time, temperature, IPTG concentration. The immunogenicity evaluation was performed with standard ASFV-positive serum (China Institute for Veterinary Drug Control) and His-Tag monoclonal antibody (Proteintech).

2.4. Purification of p22 and p30

After optimizing the culture conditions, the *E.coli* were centrifuged to get the pellets (4,000 rpm, 30 min, 4°C) and then resuspended in pre-cold PBS on ice for ultrasonication. According the manufacturer's protocol, the supernatants were collected and filtered through a 0.22 μm filter and purified using a Ni-NTA resin-based column (GE Healthcare) following centrifuging at 12,000 rpm for 30 min. After eluting with elution buffer, the fractions were dissolved in PBS containing 5% glycerol and concentrated by ultrafiltration. The protein concentration was determined by a BCA Protein Assay Kit (Thermo Fisher). The purified p22 and p30 proteins were verified using sodium dodecyl sulfate-polyacrylamide gel electrophoresis (SDS-PAGE) and Coomassie blue staining.

2.5. Western blot

Following separation by SDS-PAGE, proteins were transferred onto PVDF membrane. After blocking with 5% skim milk for 2 h, the membrane was incubated with standard ASFV-positive serum (1:1,000) overnight at 4°C. Then, the membrane was incubated with HRP-conjugated goat anti-pig secondary antibodies (1:8,000, Abcam). Finally, the membrane was visualized in Bioanalytical imaging system.

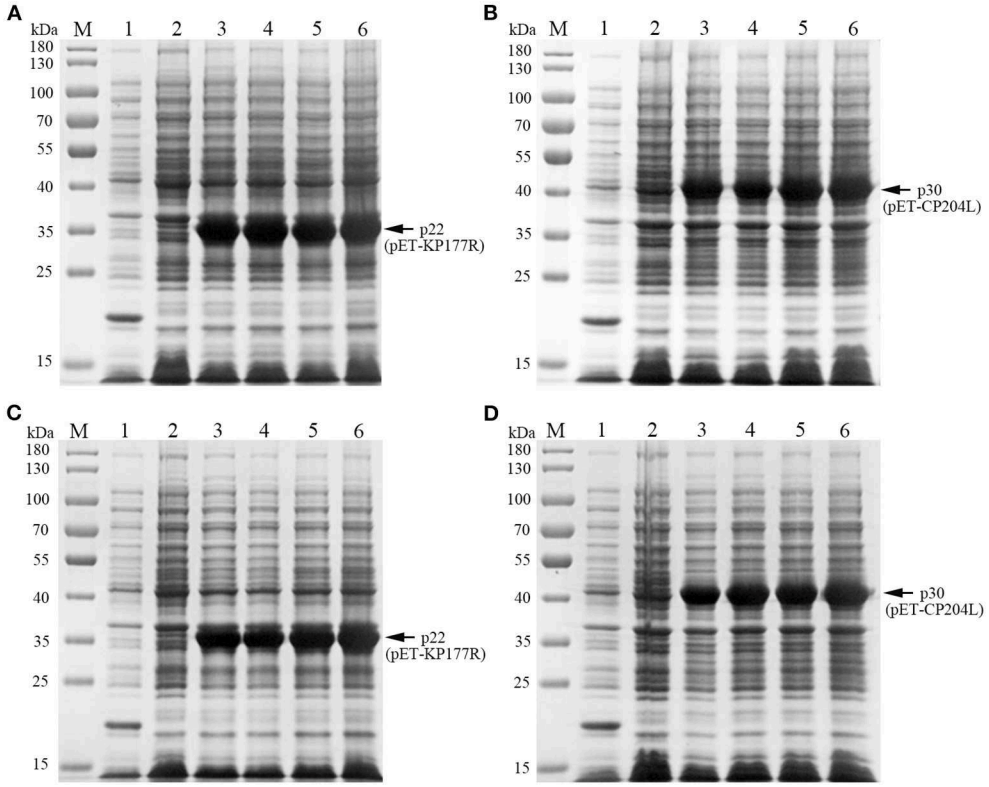

FIGURE 1
Exploration of p22 and p30 proteins induction conditions. **(A, B)** Determination of optimal IPTG concentration of p22 **(A)** and p30 **(B)**. M, Marker; (1) pET-32a empty carrier; (2) Before induction; (3–6) IPTG concentration at 0.1, 0.4, 0.7, and 1.0 mM. **(C, D)** Determination of the best OD_{600} of p22 **(C)** and p30 **(D)**. M, Marker; (1) pET-32a empty carrier; (2) Before induction; (3–6) OD_{600} at 0.4, 0.6, 0.8, 1.

2.6. Establishment of indirect ELISA

2.6.1. Determination of coating concentration and serum concentration

The coating concentration and serum concentration were optimized by checkerboard titration (21). Briefly, p22 and p30 were diluted (1:20–1:400) and coated on 96-well microtitration plates. ASFV-positive and ASFV-negative sera with different dilutions were incubated. After incubating with HRP-conjugated goat anti-swine IgG (H+L) antibody and stopping with stop solution, the plates were quantified using a microplate reader at 450 nm. Coating concentration and serum concentration were developed the best reaction condition by determining the negative sample (N) value, positive sample (P) value, and P/N ratio. Based this condition, the optimal dilution of horseradish peroxidase-conjugated secondary antibodies was further determined.

2.6.2. Determination of cut-off value, specificity, sensitivity, and repeatability

To determine the cutoff vale of the established ELISA, 50 ASFV-negative serum samples were evaluated. The competitive ELISA based on p32 (produced by ID.vet) was used as a reference. The mean value (X) and standard deviation (SD) of 50 samples were calculated. Negative $\leq X + 2\times SD$. Positive $\geq X + 3\times SD$. The middle is considered as the suspicious range.

For verifying the specificity of the established indirect ELISA, pig serums positive against other pig pathogens were tested, including pseudorabies virus (PRV), porcine reproductive and respiratory syndrome virus (PRRSV), porcine circovirus 2 (PCV2), classical swine fever virus (CSFV), *Haemophilus parasuis* (HPS). The ASFV-positive serum and the serum from specific pathogen-free (SPF) pig was used as positive and negative control, respectively.

According to the optimized condition, the sensitivity was carried out by testing the serial dilution multiple of ASFV-positive serum (1:200–1:15,000).

To assess the repeatability of the indirect ELISA, ASFV-positive blood samples (determined by ID.vet competitive ELISA) were selected for intra-assay and inter-assay repeatability experiments. For inter-assay variability, each sample was retested three times on plates of different batches. For intra-assay variability, each sample was repeated 3 times on the same plate at the same time. The results are expressed as the coefficient of variation (CV), that is, the ratio of the SD of each group of samples to the average OD_{450} value.

2.7. Detection of clinical samples

A total of 184 serum samples from suspected diseased pigs was blinded by the established indirect ELISA and two commercial ELISA kits (ID.vet and JUNO). All the serum samples were detected by p22 and p30 dual-proteins combination based indirect ELISA method in this study. The coincidence was calculated.

10.3389/fvets.2023.1093440

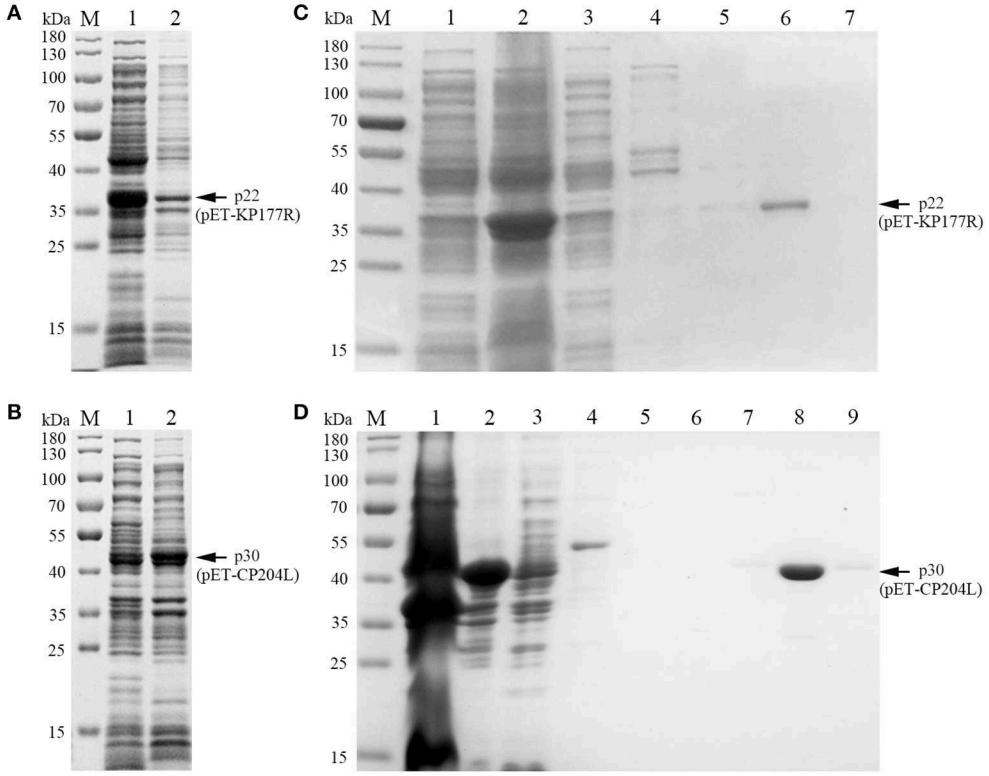

FIGURE 2
Soluble analysis and purification of p22 and p30 proteins. **(A, B)** Soluble analysis of p22 protein **(A)** and p30 protein **(B)**. M, Marker; (1) Supernatant after ultrasound; (2) Precipitation after ultrasound. **(C, D)** The purification results of p22 protein **(C)** and p30 protein **(D)**. **(C)** M, Marker; (1–7) Flow through fluid, supernatant after ultrasound, 20, 40, 50, 100, and 200 mM imidazole. **(D)** M, Marker; (1–9) Precipitation after ultrasound, supernatant after ultrasound, flow through fluid, 20, 40, 50, 100, 200, and 200 mM imidazole.

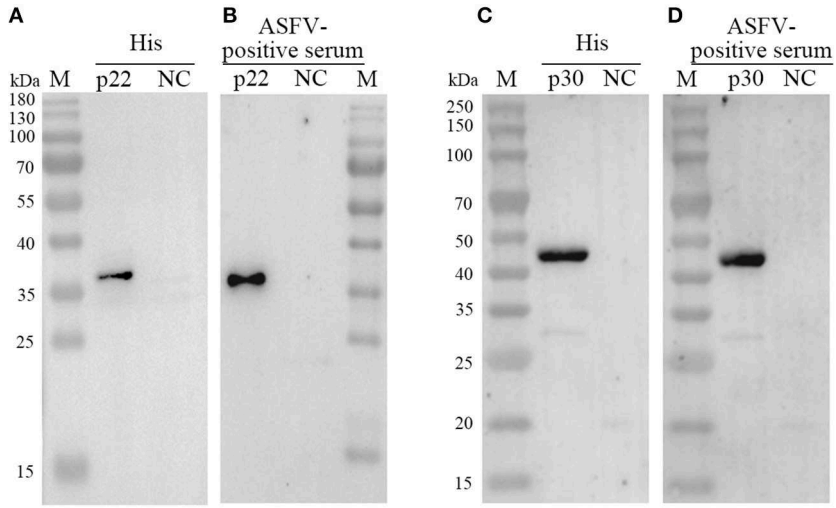

FIGURE 3
Determination the expression of p22 and p30. **(A, C)** The expression of p22 protein **(A)** and p30 protein **(C)** was determined by anti-His antibody. **(B, D)** The expression of p22 protein **(B)** and p30 protein **(D)** was immunoreactive with ASFV-positive serum.

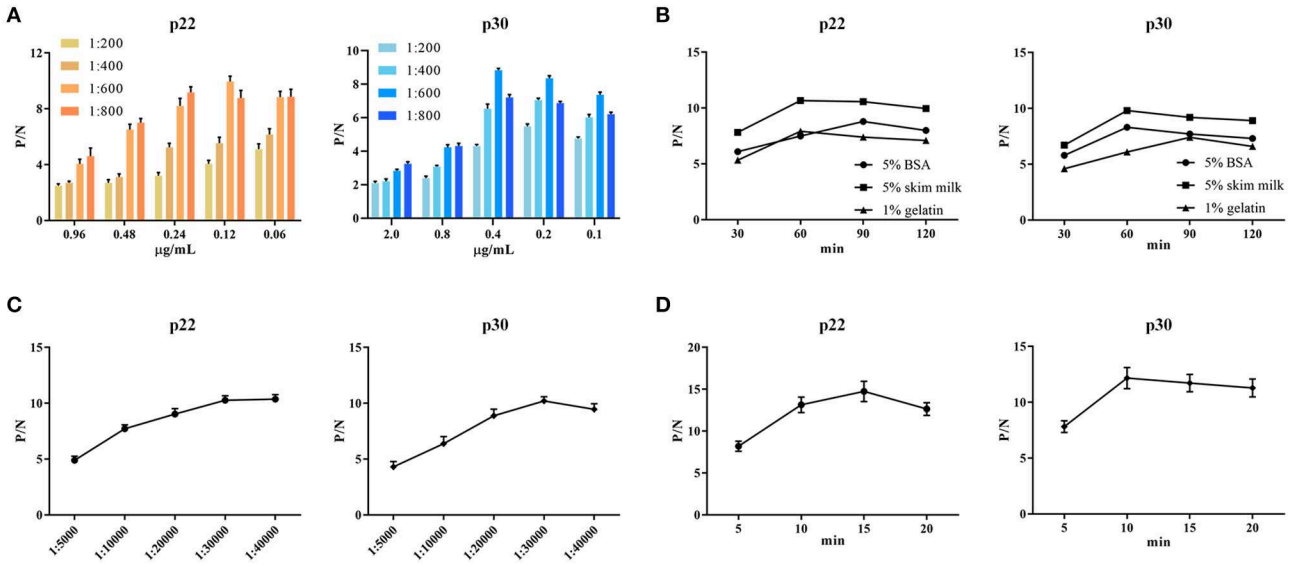

FIGURE 4
Optimal conditions of ELISA. **(A)** Optimal concentration of coating protein and serum dilution. **(B)** Optimal blocking solution and best blocking time. **(C)** Determination of the optimum dilution of enzyme-labeled secondary antibody. **(D)** Optimum substrate-enzyme interaction time.

TABLE 2 Coating volume ratio of p30 and p22.

Volume ratio of p30 to p22	p30	p22	1:1	2:1	1:2	3:1	1:3
ASFV-positive sera	2.920	1.394	1.537	1.672	1.261	1.502	0.835
ASFV-negative sera	0.474	0.195	0.244	0.219	0.164	0.186	0.101
P/N	6.2	7.2	6.3	7.6	7.7	8.1	8.3

3. Results

3.1. Expression and purification of p22 and p30

To explore the optimal conditions for the expression of p22 and p30, the recombinants *E.coli* (containing pET-KP177R or pET-CP204L) was cultivated with different concentrations of IPTG for 4 h at 37°C. The results showed induction expression using 0.1–1.0 mM IPTG had no effect on the expression of p22 and p30 (Figures 1A, B). When the OD_{600} value reach 0.8–1.0, the recombinants *E.coli* were more conducive to induction expression (Figures 1C, D). We further found that p22 was mainly expressed in the supernatant, while p30 was expressed both in the supernatant and precipitation (Figures 2A, B). The soluble protein fraction was purified with Ni-NTA Sepharose, and the result showed that 100 mM imidazole was more conducive to elution of p22 protein and 200 mM imidazole was beneficial to elute p30 protein (Figures 2C, D).

3.2. Immunogenicity of recombinant protein p22 and p30

Both of purified p22 and p30 were primarily verified by Western blot and performed a strong immunoreactivity with anti-His antibody (Figures 3A, C). Furthermore, the results of Western blot showed that the purified p22 and p30 protein specifically reacted with ASFV-positive serum (Figures 3B, D). Taken together, the purified p22 and p30 exhibited higher immunogenicity.

3.3. Optimization of experimental conditions for ELISA

To determine the optimal conditions, the checkerboard titrations were performed. The results showed that the optimum coated concentration of p22 and p30 was determined at 0.12 and 0.4 μg/mL, and the optimum dilution ratio of serum as primary antibody was 1:600 (Figure 4A). For blocking conditions, we found compared with 5% BSA and 1% gelatin, using 5% skim milk for 60 min exhibited higher performed a higher blocking effect (Figure 4B). Moreover, the dilution ratio of secondary antibody and the reaction time of substrate-enzyme were explored. The result showed for p22, the optimum dilution of secondary antibody reached 1:40,000 (Figure 4C) and the optimum reaction time is 15 min (Figure 4D); for p30, the optimum dilution of secondary antibody was 1:30,000 and the reaction time of substrate-enzyme is 10 min (Figures 4C, D). To develop the indirect ELISA based p22 and p30, the coating ratio of both proteins were evaluated. Based on calculating P/N value, we found that the optimum volume ratio of p30 to p22 reached 1:3 (Table 2).

3.4. Determination of cut-off value, sensitivity, repeatability, and specificity

Fifty ASFV-negative serum samples (determined by ID.vet competitive ELISA) were used to determine the cut-off value of the established ELISA. As shown in Figure 5A, the mean value of ASFV-negative serum was 0.174, and the cut-off value was determined to be 0.34. For assessing the sensitivity of this ELISA, ASFV-positive serums were diluted to detect. The results showed compared with ID.vet ELISA kit, the established ELISA performed higher sensitivity (Table 3). To determine the repeatability of this ELISA, 4 selected ASFV-positive serums were performed by intra-assay and inter-assay. We found the intra-assay coefficients of variation (CV) ranged from 2.0 to 4.5% And the inter-assay CV ranged from 2.5 to 5.5% (Table 4), indicating that the indirect ELISA exhibited higher repeatability. To assess the specificity of this ELISA, the positive serums against PCV2, PRV, PRRSV, CSFV, and HPS were detected. The results showed that all these serums were negative (Figure 5B), indicating the established ELISA possessed high specificity.

3.5. Clinical samples detection

Total 184 pig blood samples were detected by the above established indirect ELISA, and 99 positive samples and 83 negative samples were detected by ID.vet competitive ELISA kit. Among 184 samples, the results of 174 samples detected by the established ELISA were consistent with that of ID.vet ELISA, the coincidence rate of the established ELISA arrived at 94.6% (compared with ID.vet ELISA) (Table 5). Moreover, the sensitivity of the established ELISA was higher than that of other ELISA kits (Table 5). Several negative samples determined by ID.vet ELISA were identified as positive samples and suspicious samples by the established ELISA. Taken together, the indirect ELISA based on p22 and p30 could be adapted to clinical serological diagnosis.

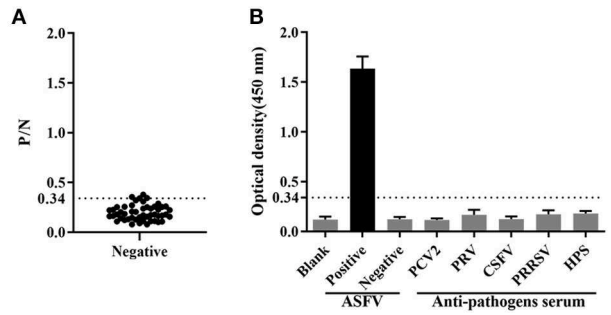

FIGURE 5
Determination of sensitivity and specificity. **(A)** The cut-off value of the established ELISA. **(B)** The specificity was determined using positive serums against PCV2, PRV, CSFV, PRRSV and HPS.

4. Discussion

ASF is a global epidemic disease with high mortality, causing a serious impact on the global swine industry. Considering that there is no effective vaccine to prevent and control ASFV, the only effective measure is to diagnostic analysis and eliminate infected animals. Thus, highly sensitive and specific diagnostic analysis performed an important role in rapid detection of ASFV. Due to the advantages of low cost, high sensitivity, and strong specificity, ELSIA is recommended as the primary method for detecting ASFV antibody (22).

ASFV encodes more than 50 structural proteins. It is necessary to develop ELISA based on the viral proteins expressed in different stages of viral infection. At present, several commercial ELISA kits were effective and available for detecting ASFV antibodies. For example, the multi-antigen indirect ELISA kit based on the mixture of three recombinant proteins p32, p62 and p72 produced by ID.vet in France. Besides, several studies have used p30, p54, p72, and other viral proteins as coating proteins for establishing ELISA to detect ASFV antibodies. p72 is a late structural protein of ASFV, which is located in the middle or surface layer of viral particles (23). ASFV p72 gene possesses highly conserved sequence, inducing a strong immune response (24). Moreover, a recent study has used p72 protein expressed by eukaryotic system as coating antigen to establish an blocking ELISA (25). p54 protein is an early structural protein in ASFV infection, which involves in viral replication, transfection, and maintenance of structural stability (23). An indirect ELISA detection method based on the p54 protein produced by baculovirus expression system was developed and performed higher coincidence rate compared with the commercial kits (26). pp62 is an important structural protein of ASFV, cleaved into p35, p15 and p8 proteins by s273r protease during maturation of viral particle (7). The recombinant pp62 protein using baculovirus expression system

TABLE 4 Determination of repeatability by inter-assay and intra-assay.

Sample no.	Intra-assay		Inter-assay	
	Results	CV%	Results	CV%
1	2.513±0.072	2.86	2.525±0.135	5.34
2	1.404 ± 0.045	3.21	1.372 ± 0.025	2.55
3	1.64 ± 0.033	2.01	1.684 ± 0.054	3.21
4	0.835 ± 0.034	4.07	0.821 ± 0.39	4.75

TABLE 3 Determination of sensitivity.

Test kit	Dilution ratios	1:200	1:400	1:800	1:1,600	1:3,200	1:6,400	1:12,800	1:25,600
p22 and p30	OD_{450}	2.387	2.105	1.791	1.379	1.086	0.732	0.435	0.216
	P/N	+	+	+	+	+	+	+	-
ID.vet	OD_{450}	0.172	0.285	0.397	0.511	0.654	/	/	/
	P/N	+	+	+	+	-	-	-	-

TABLE 5 Coincidence rate of clinical samples.

ELISA kit	Sample numbers	Positive samples		Negative samples		Suspicious samples	Samples with different results	Coincidence rate (Compared with ID.vet)
		Numbers	Positive detection rate	Numbers	Negative detection rate			
p22 and p30	184	101	54.9%	79	42.9%	4	10	94.6%
ID.vet	184	99	53.8%	83	45.1%	2	/	/
JUNO	184	96	52.2%	87	47.3%	1	7	96.2%

has been used as coating protein for establishing ELISA, which is recommended by OIE resulting its sensitivity and specificity (27). CD2v is a membrane protein embedded in the outer surface of the virus capsule and a late expression protein of ASFV (28), which can lead to the adsorption of erythrocytes on the surface of virus infected cells and contribute to their diffusion in the host (29). ASFV CD2v protein was expressed in CHO-K1 cells and established an indirect ELISA method with good specificity and sensitivity (21).

Since ELISA based on different ASFV proteins has different characteristics, it is necessary to continuously explore other viral proteins of ASFV that can be used for specific antibody detection, and select different antigen combinations to further improve ELISA detection methods. p22 is an early transcribed, structural protein localized at the inner envelope of ASFV particle. Although recent study has confirmed p22 protein did not seem to be involved in viral replication or virulence in pigs by developing a recombinant ASFV lacking the KP177R gene, p22 protein could interact with cellular proteins to participate in viral binding, signal transduction, and cell adhesion (8). Recently, a blocking ELISA based on p22-monoclonal antibody showed higher s sensitivity and specificity for detecting ASFV antibodies (30). p30, a membrane phosphorylated protein, is expressed in the early stage of ASFV infection and plays a significant role in virus internalization (31, 32). Recent research has showed p30 could interact with 7 cellular proteins to involve in viral internalization mediated by clathrin and micropinocytosis, and might regulate innate immunity by interacting with innate immune regulators (33). Furthermore, an indirect ELISA based on p30 expressed by prokaryotic expression system has been established and showed higher specificity (34). In this study, based on the recombinant proteins p22 and p30 were expressed in prokaryotic expression system, an indirect ELISA was developed and showed higher sensitivity and specificity.

5. Conclusion

An indirect ELISA based on p30 and p22 protein was established. Through detection of standard ASFV-positive serums, positive serums against other virus, and negative serums, the sensitivity and specificity of this ELISA was determined. Our study provides a broad insight into serological diagnostic methods of ASFV antibodies, but it still needs to be further verified by more pig serums from different sources to expand the experimental data and improve the detection method.

Data availability statement

The raw data supporting the conclusions of this article will be made available by the authors, without undue reservation.

Ethics statement

The animal study was reviewed and approved by Shandong Province Animal Ethics Committee.

Author contributions

JL, JJ, and NL performed the experiments and wrote the manuscript. SR, HZ, LG, JP, and TL were responsible for samples collection. YZ, FL, ZC, WS, and NH corrected the manuscript. JW and JY initiated the study, designed the experiments, and supplied the manuscript. All authors reviewed the manuscript. All authors contributed to the article and approved the submitted version.

Funding

This study was supported by the National Natural Science Funds (32070178), Shandong Provincial Modern Agricultural Industry and Technology System (SDAIT-08-01), Key Research and Development Program of Shandong Province (Major Technological Innovation Project) (2020CXGC010801), General Project of Shandong Provincial Natural Science Foundation (ZR2020MC177), Agricultural Science and Technology Innovation Project of Shandong Academy of Agricultural Sciences (CXGC2022A17), and Collaborative Promotion Plan of Major Agricultural Technologies in Shandong Province (SDNYXTTG-2022-02).

Conflict of interest

The authors declare that the research was conducted in the absence of any commercial or financial relationships that could be construed as a potential conflict of interest.

Publisher's note

References

1. Blasco R, Agüero M, Almendral JM, Viñuela E. Variable and constant regions in African swine fever virus DNA. *Virology.* (1989) 168:330–8. doi: 10.1016/0042-6822(89)90273-0

2. Costard S, Wieland B, de Glanville W, Jori F, Rowlands R, Vosloo W, et al. African swine fever: how can global spread be prevented? *Philos Trans R Soc Lond B Biol Sci.* (2009) 364:2683–96. doi: 10.1098/rstb.2009.0098

3. Ge S, Li J, Fan X, Liu F, Li L, Wang Q, et al. Molecular characterization of african swine fever virus, China, 2018. *Emerg Infect Dis.* (2018) 24:2131–3. doi: 10.3201/eid2411.181274

4. Sun E, Huang L, Zhang X, Zhang J, Shen D, Zhang Z, et al. Genotype I African swine fever viruses emerged in domestic pigs in China and caused chronic infection. *Emerg Microbes Infect.* (2021) 10:2183–93. doi: 10.1080/22221751.2021.1999779

5. Sun E, Zhang Z, Wang Z, He X, Zhang X, Wang L, et al. Emergence and prevalence of naturally occurring lower virulent African swine fever viruses in domestic pigs in China in 2020. *Sci China Life Sci.* (2021) 64:752–65. doi: 10.1007/s11427-021-1904-4

6. Duan X, Ru Y, Yang W, Ren J, Hao R, Qin X, et al. Research progress on the proteins involved in African swine fever virus infection and replication. *Front Immunol.* (2022) 13:947180. doi: 10.3389/fimmu.2022.947180

7. Alejo A, Matamoros T, Guerra M, Andrés G. A proteomic atlas of the African swine fever virus particle. *J Virol.* (2018) 92:e01293-18. doi: 10.1128/JVI.01293-18

8. Zhu X, Fan B, Zhou J, Wang D, Fan H, Li B, et al. High-throughput method to analyze the interaction proteins with p22 protein of african swine fever virus *in vitro*. *Front Vet Sci.* (2021) 8:719859. doi: 10.3389/fvets.2021.719859

9. Vuono EA, Ramirez-Medina E, Pruitt S, Rai A, Espinoza N, Velazquez-Salinas L, et al. Evaluation of the function of the ASFV KP177R gene, encoding for structural protein p22, in the process of virus replication and in swine virulence. *Viruses.* (2021) 13:986. doi: 10.3390/v13060986

10. Díaz C, Salát J, Kolarová DB, Celer V, Frébort I. Examination of immunogenic properties of recombinant antigens based on p22 protein from African swine fever virus. *J Vet Res.* (2022) 66:297–304. doi: 10.2478/jvetres-2022-0043

11. Petrovan V, Yuan F, Li Y, Shang P, Murgia MV, Misra S, et al. Development and characterization of monoclonal antibodies against p30 protein of African swine fever virus. *Virus Res.* (2019) 269:197632. doi: 10.1016/j.virusres.2019.05.010

12. Lithgow P, Takamatsu H, Werling D, Dixon L, Chapman D. Correlation of cell surface marker expression with African swine fever virus infection. *Vet Microbiol.* (2014) 168:413–9. doi: 10.1016/j.vetmic.2013.12.001

13. Arias M, Jurado C, Gallardo C, Fernández-Pinero J, Sánchez-Vizcaíno JM. Gaps in African swine fever: analysis and priorities. *Transbound Emerg Dis.* (2018) 65 Suppl 1:235–47. doi: 10.1111/tbed.12695

14. Zsak L, Borca MV, Risatti GR, Zsak A, French RA, Lu Z, et al. Preclinical diagnosis of African swine fever in contact-exposed swine by a real-time PCR assay. *J Clin Microbiol.* (2005) 43:112–9. doi: 10.1128/JCM.43.1.112-119.2005

15. Gallardo C, Fernández-Pinero J, Arias M. African swine fever (ASF) diagnosis, an essential tool in the epidemiological investigation. *Virus Res.* (2019) 271:197676. doi: 10.1016/j.virusres.2019.197676

16. Dixon LK, Chapman DA, Netherton CL, Upton C. African swine fever virus replication and genomics. *Virus Res.* (2013) 173:3–14. doi: 10.1016/j.virusres.2012.10.020

17. Gallardo C, Reis AL, Kalema-Zikusoka G, Malta J, Soler A, Blanco E, et al. Recombinant antigen targets for serodiagnosis of African swine fever. *Clin Vaccine Immunol.* (2009) 16:1012–20. doi: 10.1128/CVI.00408-08

18. Pérez-Filgueira DM, González-Camacho F, Gallardo C, Resino-Talaván P, Blanco E, Gómez-Casado E, et al. Optimization and validation of recombinant serological tests for African Swine Fever diagnosis based on detection of the p30 protein produced in Trichoplusia ni larvae. *J Clin Microbiol.* (2006) 44:3114–21. doi: 10.1128/JCM.00406-06

19. Ward MP, Tian K, Nowotny N. African Swine Fever, the forgotten pandemic. *Transbound Emerg Dis.* (2021) 68:2637–9. doi: 10.1111/tbed.14245

20. Galindo I, Alonso C. African swine fever virus: a review. *Viruses.* (2017) 9:103. doi: 10.3390/v9050103

21. Jiang W, Jiang D, Li L, Wan B, Wang J, Wang P, et al. Development of an indirect ELISA for the identification of African swine fever virus wild-type strains and CD2v-deleted strains. *Front Vet Sci.* (2022) 9:1006895. doi: 10.3389/fvets.2022.1006895

22. Gallardo C, Nieto R, Soler A, Pelayo V, Fernández-Pinero J, Markowska-Daniel I, et al. Assessment of African swine fever diagnostic techniques as a response to the epidemic outbreaks in eastern european union countries: How to improve surveillance and control programs. *J Clin Microbiol.* (2015) 53:2555–65. doi: 10.1128/JCM.00857-15

23. Wang Y, Kang W, Yang W, Zhang J, Li D, Zheng H. Structure of African swine fever virus and associated molecular mechanisms underlying infection and immunosuppression: a review. *Front Immunol.* (2021) 12:715582. doi: 10.3389/fimmu.2021.715582

24. Kaneko H, Iida T, Aoki K, Ohno S, Suzutani T. Sensitive and rapid detection of herpes simplex virus and varicella-zoster virus DNA by loop-mediated isothermal amplification. *J Clin Microbiol.* (2005) 43:3290–6. doi: 10.1128/JCM.43.7.3290-3296.2005

25. Caixia W, Songyin Q, Ying X, Haoyang Y, Haoxuan L, Shaoqiang W, et al. Development of a blocking ELISA Kit for Detection of ASFV antibody based on a monoclonal antibody against full-length p72. *J AOAC Int.* (2022) 105:1428–36. doi: 10.1093/jaoacint/qsac050

26. Liang Y, Cao C, Tao H, Tang Y. Eukaryotic expression of African swine fever virus P54 protein and development of an indirect ELISA for detection of antibody against ASFV. *Vet Sci China.* (2014) 44:373–8. doi: 10.16656/j.issn.1673-4696.2014.04.006

27. Gallardo C, Blanco E, Rodríguez JM, Carrascosa AL, Sanchez-Vizcaino JM. Antigenic properties and diagnostic potential of African swine fever virus protein pp62 expressed in insect cells. *J Clin Microbiol.* (2006) 44:950–6. doi: 10.1128/JCM.44.3.950-956.2006

28. Goatley LC, Dixon LK. Processing and localization of the African swine fever virus CD2v transmembrane protein. *J Virol.* (2011) 85:3294–305. doi: 10.1128/JVI.01994-10

29. Wang F, Zhang H, Hou L, Yang C, Wen Y. Advance of African swine fever virus in recent years. *Res Vet Sci.* (2021) 136:535–9. doi: 10.1016/j.rvsc.2021.04.004

30. Tsegay G, Tesfagaber W, Zhu Y, He X, Wang W, Zhang Z, et al. Novel P22-monoclonal antibody based blocking ELISA for the detection of African swine fever virus antibodies in serum. *Biosaf Health.* (2022) 4:234–43. doi: 10.1016/j.bsheal.2022.04.002

31. Wu P, Lowe AD, Rodríguez YY, Murgia MV, Dodd KA, Rowland RR, et al. Antigenic regions of African swine fever virus phosphoprotein P30. *Transbound Emerg Dis.* (2020) 67:1942–53. doi: 10.1111/tbed.13533

32. Gaudreault NN, Madden DW, Wilson WC, Trujillo JD, Richt JA. African Swine Fever Virus: An Emerging DNA Arbovirus. *Front Vet Sci.* (2020) 7:215. doi: 10.3389/fvets.2020.00215

33. Chen X, Chen X, Liang Y, Xu S, Weng Z, Gao Q, et al. Interaction network of African swine fever virus structural protein p30 with host proteins. *Front Microbiol.* (2022) 13:971888. doi: 10.3389/fmicb.2022.971888

34. Giménez-Lirola LG, Mur L, Rivera B, Mogler M, Sun Y, Lizano S, et al. Detection of African swine fever virus antibodies in serum and oral fluid specimens using a recombinant protein 30 (p30) dual matrix indirect ELISA. *PLoS ONE.* (2016) 11:e0161230. doi: 10.1371/journal.pone.0161230

frontiers | Frontiers in Veterinary Science

TYPE Original Research
PUBLISHED 23 February 2023
DOI 10.3389/fvets.2023.1079918

OPEN ACCESS

EDITED BY
Sonja Hartnack,
University of Zurich, Switzerland

REVIEWED BY
Chaidate Inchaisri,
Chulalongkorn University, Thailand
Eleftherios Meletis,
University of Thessaly, Greece

*CORRESPONDENCE
Rachel Schambow
✉ scham083@umn.edu

SPECIALTY SECTION
This article was submitted to Veterinary Epidemiology and Economics, a section of the journal Frontiers in Veterinary Science

RECEIVED 25 October 2022
ACCEPTED 06 February 2023
PUBLISHED 23 February 2023

CITATION
Schambow R, Giménez-Lirola LG, Hanh VD, Huong LTL, Lan NT, Trang PH, Luc DD, Bo HX, Chuong VD, Rauh R, Nelson W, Mora-Díaz JC, Rovira A, Culhane MR and Perez AM (2023) Modeling the accuracy of a novel PCR and antibody ELISA for African swine fever virus detection using Bayesian latent class analysis. *Front. Vet. Sci.* 10:1079918. doi: 10.3389/fvets.2023.1079918

Modeling the accuracy of a novel PCR and antibody ELISA for African swine fever virus detection using Bayesian latent class analysis

Rachel Schambow[1,2]*, Luis G. Giménez-Lirola[3], Vu Duc Hanh[4], Lai Thi Lan Huong[4], Nguyen Thi Lan[4], Pham Hong Trang[4], Do Duc Luc[5], Ha Xuan Bo[5], Vo Dinh Chuong[6], Rolf Rauh[7], William Nelson[7], Juan Carlos Mora-Díaz[8], Albert Rovira[2,9], Marie R. Culhane[2,10] and Andres M. Perez[1,2]

[1]Center for Animal Health and Food Safety, University of Minnesota, St. Paul, MN, United States, [2]Department of Veterinary Population Medicine, College of Veterinary Medicine, University of Minnesota, St. Paul, MN, United States, [3]Innoceleris LLC., Ames, IA, United States, [4]Faculty of Veterinary Medicine, Vietnam National University of Agriculture, Hanoi, Vietnam, [5]Faculty of Animal Science, Vietnam National University of Agriculture, Hanoi, Vietnam, [6]Vietnam Department of Animal Health, Ministry of Agriculture and Rural Development, Hanoi, Vietnam, [7]Tetracore, Inc., Rockville, MD, United States, [8]Department of Veterinary Diagnostic and Production Animal Medicine, College of Veterinary Medicine, Iowa State University, Ames, IA, United States, [9]Veterinary Diagnostic Laboratory, College of Veterinary Medicine, University of Minnesota, St. Paul, MN, United States, [10]Secure Food Systems Team, University of Minnesota, St. Paul, MN, United States

Introduction: Diagnostic test evaluation for African swine fever (ASF) in field settings like Vietnam is critical to understanding test application in intended populations for surveillance and control strategies. Bayesian latent class analysis (BLCA) uses the results of multiple imperfect tests applied to an individual of unknown disease status to estimate the diagnostic sensitivity and specificity of each test, forgoing the need for a reference test.

Methods: Here, we estimated and compared the diagnostic sensitivity and specificity of a novel indirect ELISA (iELISA) for ASF virus p30 antibody (Innoceleris LLC.) and the VetAlert™ ASF virus DNA Test Kit (qPCR, Tetracore Inc.) in field samples from Vietnam by assuming that disease status 1) is known and 2) is unknown using a BLCA model. In this cross-sectional study, 398 paired, individual swine serum/oral fluid (OF) samples were collected from 30 acutely ASF-affected farms, 37 chronically ASF-affected farms, and 20 ASF-unaffected farms in Vietnam. Samples were tested using both diagnostic assays. Diagnostic sensitivity was calculated assuming samples from ASF-affected farms were true positives and diagnostic sensitivity by assuming samples from unaffected farms were true negatives. ROC curves were plotted and AUC calculated for each test/sample combination. For comparison, a conditionally dependent, four test/sample combination, three population BLCA model was fit.

Results: When considering all assumed ASF-affected samples, qPCR sensitivity was higher for serum (65.2%, 95% Confidence Interval [CI] 58.1–71.8) and OF (52%, 95%CI 44.8–59.2) compared to the iELISA (serum: 42.9%, 95%CI 35.9–50.1; OF: 33.3%, 95%CI 26.8–40.4). qPCR-serum had the highest AUC (0.895, 95%CI 0.863–0.928). BLCA estimates were nearly identical to those obtained when assuming disease status and were robust to changes in priors. qPCR sensitivity was considerably higher than ELISA in the acutely-affected population, while ELISA sensitivity was higher in the chronically-affected population. Specificity was nearly perfect for all test/sample types.

Discussion: The effect of disease chronicity on sensitivity and specificity could not be well characterized here due to limited data, but future studies should aim to elucidate these trends to understand the best use of virus and antibody detection methods for ASF. Results presented here will help the design of surveillance and control strategies in Vietnam and other countries affected by ASF.

KEYWORDS

Bayesian latent class analysis, ELISA, PCR, African swine fever, diagnostic test, evaluation, Vietnam

1. Introduction

African Swine Fever (ASF) is arguably one of the most significant animal disease threats currently facing global pork production. ASF is a notifiable disease of swine caused by the ASF virus (ASFV), a large (175–215 nm), icosahedral, enveloped, double-stranded DNA arbovirus (1). ASFV only infects members of the *Suidae* family including domestic pigs and wild boar, and it is not a threat to human health. ASF was first reported in Kenya in 1921 and now is globally widespread throughout Eastern Europe, Asia, and Africa (2, 3). Notably, it was detected in the Dominican Republic and Haiti in 2021 (4). No effective treatments exist for ASF, and even though promising vaccine candidates have been developed, their safety is still under evaluation, and it may be some time until they are regularly available for widespread use (5, 6). ASF disease control relies on preventing introduction with effective biosecurity, passive and active surveillance, and early detection of potential outbreaks followed by quarantine and eradication through mass depopulation to avoid disease spread (7).

Successful ASF surveillance and control strategies rely on timely and accurate ASF diagnosis to prevent disease spread and avoid false-positive ASF misdiagnosis that can lead to unnecessary culling of pigs and disruption to industry. Diagnostic assays based on virus and antibody detection are useful for surveillance, provided their intended use is appropriately defined and their diagnostic performance evaluated prior to deployment. Evaluation of the diagnostic sensitivity (DSe) and specificity (DSp) is part of the World Organization for Animal Health (WOAH)'s pathway for test validation, with various methodologies approved for analysis (8). In initial assessments of DSe and DSp, ideally samples from positive and negative reference populations that are representative of the intended target population should be used (8). Estimation of DSe and DSp would then involve the use of a gold standard reference test to which the new test is compared to. Although this method may be acceptable in circumstances where reference tests with high accuracy are available, the use of samples of known infection status is ideal for precise and unbiased evaluation of the diagnostic performance of a test. However, when animals or samples of unknown status are used or when no suitable reference test is available, considerable bias may be introduced. This is often the case in field studies, where it may be possible to determine the status of the herd or farm but impossible to ascertain the true disease status at animal level. However, field samples may best represent the intended use of these diagnostic tests and provide a more accurate evaluation of their performance, and they are important in monitoring assay performance after initial validation (8). To address these concerns, latent class models were developed to provide a flexible alternative for diagnostic test evaluation (9, 10).

Latent class models use multiple imperfect reference tests applied simultaneously to one or more populations to estimate the DSp and DSe of each test (9). These models allow for uncertainty about the samples' true status, making them an appropriate fit for analysis of field samples. They also can address the potential conditional dependence between tests that have similar biological basis, providing a more accurate estimate of DSe and DSp (11, 12). Bayesian latent class models (BLCA) use a Bayesian framework to formally incorporate prior knowledge to estimate the posterior probability of each tests' DSe and DSp. The prior represents how likely one believes the hypothesis to be true before data has been collected. In BLCA models of diagnostic test accuracy, priors can be provided for estimates of the DSe and DSp of each test and the disease prevalence in each sampled population (13). The use of these models is supported by the WOAH, and their implementation has become more common in veterinary medicine over the past 20 years (14–16).

For tests that provide a continuous outcome, results can be dichotomized into "positive" and "negative" categories (8). Additional categories, such as "intermediate" or "suspect", are sometimes used as well. These categorical designations are made by specifying cut-off points. DSe and DSp of a diagnostic test can be increased or decreased by modifying its cut-off points, but their relationship is inversely related. Thus, test developers must choose a cut-off point that balances the desired DSe and DSp of the diagnostic test for its intended purpose. Receiver operating characteristic (ROC) curves can be a useful analysis to compare DSe and DSp over different cut-off points (17). Additionally, the area under the ROC curve (AUC) provides an estimate of the diagnostic test's global accuracy across all assay values and can be used to compare different assays.

Typically, ASF test assessment and validation have been performed on experimental samples. However, ongoing ASF outbreaks in Southeast Asia provide a unique opportunity for field testing of novel diagnostic tests. Particularly, Vietnam confirmed its first outbreak of ASF in February 2019 on a backyard pig farm in Hung Yen Province (18). Since then, ASF spread to all 63 provinces in Vietnam and resulted in an estimated nearly 6 million pigs lost in 2019 (19). Despite continuous efforts from private and public stakeholders to control the disease, since 2020 up to the present day, new ASF outbreaks continue to be reported (20, 21). The objective of the this study was to estimate and

compare the diagnostic performance of a novel indirect enzyme-linked immunosorbent assay (iELISA) for ASF serum antibodies (iELISA), developed by Innoceleris Ames, IA, USA and produced and commercialized by Tetracore (Rockville, MD, USA), and the VetAlert™ ASFV DNA Test Kit (qPCR, Tetracore) in both serum and oral fluid (OF) samples collected on farms in Vietnam. Because no gold standard reference test was assumed and true disease status of sampled individuals was unknown, we also aimed to compare estimates from BLCA modeling to those produced when assuming disease status is known based on history, location, clinical signs, and duration of the ASF outbreak in Vietnam.

2. Materials and methods

2.1. Study design—Sampling, populations

The study was a prospective, cross-sectional field study to evaluate the performance of the two diagnostic assays, qPCR and iELISA, on serum and OF samples in Vietnam. Samples were collected from dates 2019 to 2021. Selection of farms was not researcher-driven, but part of ongoing ASFV regulatory activities by the Vietnamese veterinary services. Farms were from 17 provinces (Bac Giang, Bac Ninh, Dong Nai, Ha Nam, Ha Noi, Ha Tay, Hai Duong, Hoa Binh, Hung Yen, Nam Dinh, Nghe An, Phu Tho, Son La, Thai Binh, Thai Nguyen, Vinh Phuc, and Yen Bai). Sample collection was performed on farms throughout Vietnam using outbreaks detected/reported by the farm's veterinarian and farm owner. ASF-acutely affected, chronically affected, and unaffected herds were targeted. Acutely affected farms were defined as those with pigs with severe clinical symptoms of ASF, chronically affected farms as those with pigs which had developed mild clinical symptoms of ASF for a period of time (~6 weeks−2 months), and unaffected farms as those with no clinical or laboratory history of ASF at the farm level. On farm, pigs were selected by the farm's veterinarian, and on ASF-affected farms specifically, animals exhibiting clinical signs consistent with ASF were targeted for sampling. All pigs on farms were eligible for sampling. Paired individual serum and OF samples were collected from 100 pigs on 30 acutely ASF-affected farms, 98 pigs on 37 chronically affected farms, and 200 pigs on 20 non-affected farms, for a total of 398 paired samples from 87 farms. The number of samples taken per acute or chronic farm ranged from 1 to 10, while 10 samples were consistently collected on each unaffected farm. Farm information was recorded at the time of sampling including the farm's province, farm type, animals per barn and pen, brief history of ASF on the farm, overall health status of the pigs, and general vaccination status. Each sampled pig's age group category was also recorded.

2.2. Sample collection and processing, ELISA, and PCR protocols

2.2.1. Sample collection and processing

All animal sampling and activities were performed in accordance with guidelines of the animal ethics committee of Vietnam National University of Agriculture. Blood was collected *via* right jugular vein venipuncture using a 20 gauge or smaller needle and syringe, with needle size adjusted per pig age. The 8–10 mL of blood collected was placed into a glass vial sans anticoagulant. The blood was allowed to clot at room temperature. Clotted blood was transferred to the laboratory under refrigerated conditions by placing the vials on ice gel packs in a transport container for serum extraction at the laboratory. Clotted blood was centrifuged for 10 min at 1,000 × *g* (Allegra™64R Centrifuge, Beckman Coulter), the sera were separated and aliquoted into 2 mL cryogenic vials, then stored at −80°C until further use.

Pig OF samples were collected using dry cotton swabs (prepared on 25 cm wooden stick). The cotton swab was used to rub inside the oral cavity, tonsils and pharynx of pigs 5–6 times so that the fluid was absorbed. Afterwards, the cotton swabs were transferred into a tube with 1.5 mL of phosphate-buffered saline (PBS—Tablets, USA) pH 7.4 and transported to the lab in an ice box. In the lab, the wooden stick was removed, and the cotton tip submerged in PBS was transferred into a zip bag. The fluid was collected by compressing the cotton swab in the bag. Aliquots of OF were placed into 2 mL cryogenic vials and stored at −80°C until tested.

2.2.2. qPCR for ASFV DNA detection

Viral DNA extractions from serum and OF samples were performed using a MagMAX-96 viral kit (Thermo Fisher Scientific) with KingFisher Flex 96 Deep-Well Magnetic Particle Processor (Thermo Fisher Scientific). For the specific detection of ASFV DNA, the ASF 2.0 PCR dry assay (Tetracore, Inc., Rockville, MD, United States) was used. The assay, including ready-to-use reagents, was provided in a dried-down format, which can be stored and shipped at room temperature. The reagents were rehydrated by adding 20 μL of the rehydration buffer (TC-9094-064, Tetracore) to each ASFV reaction tube. The tube was then kept at room temperature for 5 min to allow for rehydration of the dry reagents. After this step, the tube was briefly vortexed (Cleaver, Scientific Ltd., Rugby, United Kingdom) for 10 s to fully dissolve the dry reagents. The rehydrated reagents were then transferred to the reaction tube and 5 μL of the extracted sample was then added to the reaction tube and loaded on the real-time PCR Instrument (CFX96™Real-Time System, Bio-Rad). Each sample was tested following these thermal cycling conditions: 95°C for 2 min, 45 cycles of, 95°C for 15 s, 60°C for 60 s (Collecting Optical data in channel FAM). Serum and OF samples with Ct values < 38 were considered as positive and containing ASFV DNA. Samples with Ct values ≥ 38 were considered as negative and not containing ASFV DNA (manufacturer-specified).

2.2.3. ASFV iELISA for antibody detection

In the present study, an ASFV VP30-based iELISA was used that was originally designed by Innoceleris LLC. and produced and commercialized by Tetracore Inc. Samples were tested according to manufacturer's instructions. With the exception of the wash solution (provided 20X), all iELISA reagents and controls were provided ready-to-use. In brief, 100 μL (reaction volume) of pre-diluted serum (1:100) or OF (1:2) samples were transferred to the pre-coated iELISA plate. After 45 min incubation (19–22°C), plates were washed 5 times using 300 μL of 1X wash solution, then 100 μL of enzyme conjugate was added to each well and the plates incubated (19–22°C) for 30 min. Then, after another washing step,

the reaction was visualized by adding 100 μL of TMB substrate to each well and the plates incubated for 10 min at 19–22°C. Thereafter, 100 μL of stop solution was added to stop the reaction and the plates were read (450 nm) with a spectrophotometer (Epoch2, BioTek). The optical density (OD) response was expressed as sample to positive (S/P) ratios using the equation below.

$$S/P = \frac{\text{Sample OD} - \text{Average Negative Control OD}}{\text{Average Positive Control OD.} - \text{Average Negative Control OD}}$$

Serum samples with S/P $<$ 1 considered as negative and not having ASFV antibodies, while samples with S/P $\geq$ 1 were considered as positive and having ASFV-specific antibodies (manufacturer-specified). OF samples with S/P $<$ 0.5 considered as not having ASFV antibodies, while samples with S/P $\geq$ 0.5 were considered as having ASFV-specific antibodies.

2.3. Statistical models

Two methods were used to evaluate the DSe and DSp of each test and sample type: (1) calculation assuming disease status in reference populations; and (2) Bayesian latent class analysis assuming imperfect tests and unknown disease status. For the first approach, it was assumed that all samples from the ASF-acute and ASF-chronic populations were disease-positive and that all samples from the unaffected farms were disease-negative. The continuous test values for each subject were dichotomized into positive and negative categories using the cut-offs described in Sections 2.2.2 and 2.2.3. The tests' DSe using serum or OF were estimated using the ASF-affected populations, and DSp were estimated using the unaffected population, by placing the data in a 2 × 2 table of disease and test status. DSe was calculated as the proportion of disease-positive samples that tested positive, while DSp was calculated as the proportion of disease-negative samples that tested negative (Table 1). Ninety-five percent confidence intervals were calculated using the specified Clopper-Pearson exact method. The tests' DSe was calculated individually for the acute and chronic populations, and then for both populations combined.

2.3.1. Bayesian latent class model

The Bayesian latent class analysis approach to evaluate DSe and DSp followed that of Dendukuri and Joseph (11) and Branscum et al. (13). A three population, four tests model with pairwise dependency was fit using the acute, chronic, and unaffected populations and each test-sample type combination (Figure 1). The full model is available in Supplementary material 1. Guidelines for reporting studies of diagnostic test accuracy using BLCMs were followed (16) (Supplementary material 2). Because both antibody and virus detection methods were modeled together, the latent class here represents infection where viral DNA is present yet is prolonged enough for antibodies to have been produced.

Covariance was modeled between samples tested by the same diagnostic test (i.e., between serum and OF samples tested by iELISA for ASFV antibodies and between serum and OF samples tested by qPCR for viral DNA, Figure 1), resulting in four pairwise comparisons. This accounts for the expectation that tests that use similar biological basis (e.g., detection of ASFV antibody) may be correlated, meaning the event that they classify individuals of infected or uninfected status the same will occur more than by chance. The covariance structure was parameterized using the approach described by (11) between the DSe or DSp for each pair of tests, where a Beta (1,1) prior was used to constrain the covariance estimates to positive values. The overall correlation of test outcome between pairs of tests for infected (rhoD) and uninfected (rhoDc) was calculated as described in Branscum et al. (13).

Prior values for each tests' DSe and DSp using serum and OF were estimated using previously published reports of the tests' performance, experimental studies, and through consultation with test designers and experts where data was limited (Table 2). In published reports, the VetAlert™ qPCR has consistently demonstrated high or perfect DSe and DSp across many different sample types (23, 24), however OF were not tested. Based on studies where other ASF DNA PCRs were evaluated using OFs, it was assumed that DSe of the VetAlert™ qPCR using OF would still be high but reduced compared to sample types such as whole blood (25, 26). The iELISA used here was recently evaluated in experimentally ASF-infected pigs in Russia using both serum and OF samples across 14 weeks (22). Raw data from those experiments were used directly to estimate priors by estimating an average DSe and DSp across timepoints and calculating 95% Clopper-Pearson exact confidence intervals. Additional results from samples collected through regulatory veterinary diagnostic laboratory testing in the United States, currently free of ASF, were also used to support the assumption of high DSp of the iELISA in serum and OF (Gimenez-Lirola, unpublished data). Because each population (acute, chronic, unaffected) was created by sampling a few pigs from many farms of a known ASF-status, it was assumed that the disease status of individuals within each sample population was likely very uniform; i.e., near certain high prevalence in the acute and chronic populations, and near certain freedom in the unaffected population. Due to this sampling strategy, reports of ASF-prevalence in herds in Vietnam were not chosen for informing the prevalence priors, and subjective estimates from the experts and authors were used instead (Table 2). No data was available to estimate correlation between tests, so vague Beta (1,1) priors were used for all covariance parameters. Using the most likely value for each estimate and its 95% confidence interval, BetaBuster (1.0) software was used to obtain the α and β parameters of the beta distributions for each prior (27). Some of the initial prior distributions for DSe and DSp were very narrow and resulted in non-convergence of the model, so the lower 95% confidence value was decreased by 10% for DSe and DSp estimates when obtaining the beta parameters in BetaBuster. A hyperprior of the form Bernoulli (0.001) was used to inform the prior value of the ASF-unaffected population.

The dichotomized test results were cross-classified in a contingency table (Table 3) representing all the possible combinations of test results from the four tests ($2^4 = 16$ possible test combinations). The data was modeled multinomial with respect to p (the probability of an individual having a particular combination of test results, i.e., the probability of each cell in the contingency table) and n (the size of each population sampled). The probability of a given combination of test results p was

TABLE 1 Number of correctly classified test results using iELISA serum and oral fluid (OF) antibody tests and qPCR serum and OF DNA tests under the assumption that all samples from acute and chronically affected farms are ASF-positive and all samples from unaffected farms are ASF-negative.

Population	iELISA, serum Ab	qPCR, serum DNA	iELISA, oral fluid Ab	qPCR, oral fluid DNA
Number of test positive samples				
Acute ($n = 100$)	16	74	11	69
Chronic ($n = 98$)	69	55	55	34
Acute and Chronic Combined ASF-affected ($n = 198$)	85	129	66	103
Number of test negative samples				
ASF-unaffected ($n = 200$)	200	200	198	200

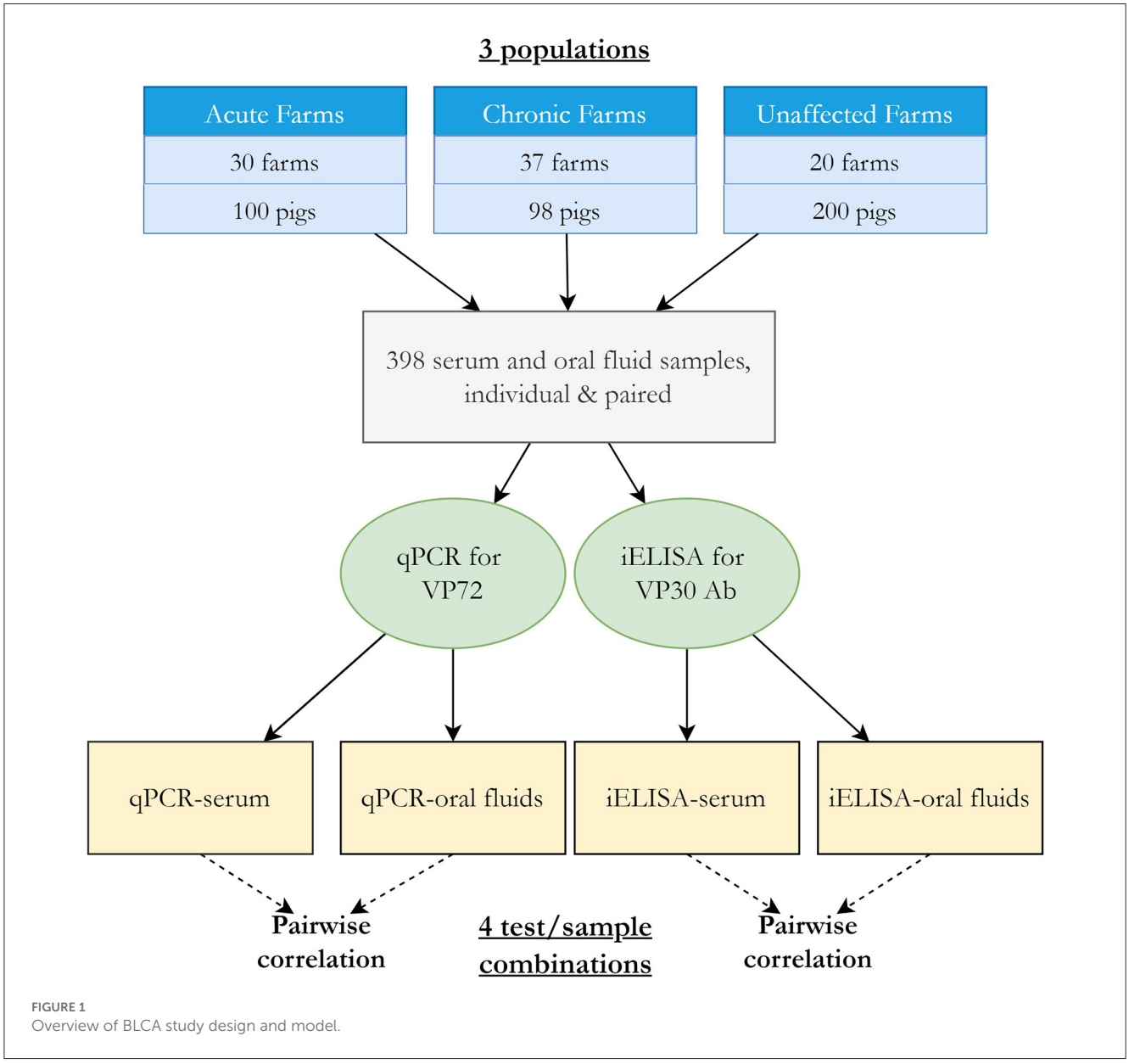

FIGURE 1
Overview of BLCA study design and model.

modeled using the prevalence of each population and each tests' DSe and DSp and pairwise covariances. Five parallel DSe and DSp schemes (only serum, only OF, only PCR, only iELISA, or all four tests/samples) were also calculated within the model. Parallel testing here referred to the interpretation of test results whereby an animal is considered positive if any of the simultaneously

TABLE 2 Values and sources of priors used for BLCA model.

Test and sample type	DSe/DSp	Most likely	95% CI	α, β parameters	References
iELISA, serum Ab	DSe	0.82	0.55, 0.99	9.20, 2.80	(22), Gimenez-Lirola, unpublished data
	DSp	0.99	0.89–1	30.29, 1.30	
qPCR, serum	DSe	1	0.88–1	23.43, 1	(23, 24)
	DSp	1	0.78–1	12.06, 1	
iELISA, oral fluid Ab	DSe	0.48	0.25–62.6	5.45, 5.82	(22), Gimenez-Lirola, unpublished data
	DSp	0.99	0.89-1	30.29, 1.30	
qPCR, oral fluids	DSe	0.95	0.5–1	4.77, 1.20	(23–25)
	DSp	1	0.79–1	12.71, 1	
ASF-acute population		1	0.1–1	1.30, 1	
ASF-chronic population		1	0.1–1	1.30, 1	
ASF-uninfected population		0.01	0.002–0.058	1.88, 88.28	
Covariance between iELISA serum and oral fluid, infected subjects				1, 1	
Covariance between qPCR serum and oral fluid, infected subjects				1, 1	
Covariance between iELISA serum and oral fluid, uninfected subjects				1, 1	
Covariance between qPCR serum and oral fluid, uninfected subjects				1, 1	

95% CI for diagnostic Se/Sp (DSe/DSp) estimates represents relaxed lower CI values.

applied tests are positive and can only be considered negative if all simultaneously applied tests are negative. Parallel DSe and DSp were calculated for pairwise parallel testing schemes and for all four test/sample combinations, adjusting for correlation for test pairs that were considered dependent (iELISA serum and iELISA OF; qPCR serum and qPCR OF) following that of Branscum et al. (13) and Bates et al. (28).

The Bayesian latent class analysis was performed using the freely available software WinBUGS v1.4.3 within R using the R2WinBUGS package (29, 30). WinBUGS (Bayesian inference Using Gibbs Sampling) is a program that allows for Bayesian inference using Markov chain Monte Carlo (MCMC) methods. The model was performed using three MCMC chains over 50,000 iterations with an initial burn-in of 5,000 iterations to obtain an effective sample size of at least 10,000 for the parameters. To eliminate potential autocorrelation, thinning was applied where 1 in every 10 consecutive samples were selected. Each parameter in each MCMC chain had a different starting input to ensure full exploration of the probability space. Convergence was visually confirmed by examining traceplots and obtaining a Gelmin-Rubin statistic for each parameter (31). Autocorrelation was assessed by examining autocorrelation plots. Summary statistics were generated for the parameters from the posterior density plots, where the median value represented the 50th percentile and the 95% credibility intervals represented the 2.5th and 97.5th percentile values.

2.3.2. Sensitivity analysis

Other model structures and prior distributions were explored to assess the robustness of the BLCA model (Supplementary material 3). To assess the effect of the priors on the posterior distributions, two alternative sets of priors were used: vague Beta (1,1) distributions or changing by 25% of their original value. Alternative covariance structures were also explored. Pairwise dependence was modeled between iELISA and PCR samples of the same type, i.e., between PCR-serum/iELISA-serum and PCR-OF/iELISA-OF. Additionally, the original model was modified by parameterizing the covariance distributions as uniform using their natural minimum and maximum (11), allowing covariance take negative values. Due to constraints imposed on the MCMC sampler by the hyperprior for the unaffected population's prevalence, the effects of removing this hyperprior on convergence and parameter estimates were also explored.

An assumption of BLCA is equal performance of diagnostics tests across populations (9, 10). Because there was evidence that this assumption was potentially not met due to different performance in the acutely and chronically affected populations, a four test, two population model was fit where population one used the combined acute and chronic population data and population two used the unaffected population data. Two additional two-population models were fit where only the acute or chronic population data were used for population one, and the unaffected population data was used for population two. Results from these two models were compared to the DSe and DSp estimates when assuming infection status in acute and chronic populations only, respectively. For all the alternative analytical approximations, formulations, and parameterizations assessed in the sensitivity analysis here, variations of $<10\%$ in the point estimates and overlapping Bayesian credibility intervals (BCI) for the posterior values of the assessed parameters were considered evidence of robustness of the initial modeling approach.

TABLE 3 Cross-classified results of iELISA serum (iELISA-S) and OF (iELISA-OF) antibody (Ab) tests and qPCR serum (qPCR-S) and oral fluids (qPCR-OF) tests used in BLCA representing all 16 possible test combinations, for acute, chronic, and unaffected populations.

Population	iELISA-OF Ab	iELISA-S Ab	qPCR-OF +		qPCR-OF -	
			qPCR-S +	qPCR-S –	qPCR-S +	qPCR-S –
ASF-affected, acute ($n = 100$)	+	+	4	0	4	0
		–	2	0	1	0
	–	+	4	1	3	0
		–	33	25	23	0
ASF-affected, chronic ($n = 98$)	+	+	9	8	21	17
		–	0	0	0	0
	–	+	5	2	6	1
		–	6	4	8	11
ASF-unaffected ($n = 200$)	+	+	0	0	0	0
		–	0	0	0	2
	–	+	0	0	0	0
		–	0	0	0	198

2.4. ROC curves/AUC calculation

To understand how changes in cut-off values may affect DSe and DSp, ROC curves were produced and AUC calculated for each test-sample type combination using the package ROCR in R (17, 32). ASF-acute and -chronic population data were combined into one ASF-affected population, where all samples were assumed to be disease-positive. All ASF-unaffected farm samples were assumed to be disease-negative.

3. Results

3.1. Population and sample characteristics

Farms were distributed across 17 provinces mainly in Northcentral Vietnam and few in southern Vietnam. Most farms were located in Hung Yen ($n = 22$ farms) and Dong Nai ($n = 8$). In the acute population, 13 farms were classified as intensive and 17 as small holders, while in the chronic population, 14 farms were considered intensive and 22 as small holders. All ASF-unaffected farms were considered as industrial farms. As described in Vietnamese regulations, small holders contain from 10 to 29 animals, intensive farms contain from 30 to 299 animals, and industrial farms contain 300 or more animals (33). The age category of sampled pigs varied by population and farm. Of samples from acutely affected farms, 45 were grower pigs, 44 from sows, and 11 from weaned pigs. Samples from chronically affected farms were comprised of 28 growers, 6 finishers, 13 mature, 47 sows, and 4 weaned pigs. On ASF unaffected farms, 90 samples came from sows and 110 samples from weaned pigs. Sampled weaned pigs across farm types were of 3–5 weeks of age. Overall, no farms reported any type of ASF-vaccine usage. Other vaccine usage varied between farms, with many vaccinating for some combination of circovirus, parvovirus, foot-and-mouth disease (FMD) virus and/or classical swine fever (CSF) virus. Few farms also vaccinated for Porcine Reproductive and Respiratory Syndrome (PRRS).

3.2. Estimates under assumption of true disease status in populations

The qPCR had greatly increased DSe (serum: 74%, 95% CI 64.3–82.3; OF: 69%, 95% CI 58.97–77.9) compared to the iELISA (serum: 16%, 95% CI 9.43–24.7; OF: 11%, 95% CI 5.62–18.8) for both sample types in the acutely affected population and moderately increased DSe (serum: 65.2%, 95% CI 58.1–71.8; OF: 52%, 95% CI 44.8–59.2) compared to iELISA (serum: 42.9%, 95% CI 35.9–50.1; OF: 33.3%, 95% CI 26.8–40.4) in the combined populations (Table 4). The iELISA had higher DSe (serum: 70.4%, 95% CI 60.3–79.2; OF: 56.1%, 95% CI 45.7–66.1) compared to qPCR (serum: 56.1%, 95% CI 45.7–66.1; OF: 34.7%, 95% CI 25.4–44.98) with both sample types when considering only the chronically affected population. DSp was high for all test-sample combinations for all assays, with a minimal decrease in DSp for OF tested for antibodies by iELISA (99%, 95% CI 96.4–99.9).

3.3. BLCA model

The BLCA model converged well for all parameters with minimal autocorrelation. Posterior prevalence estimates were high for the acutely and chronically affected populations and near zero for the unaffected population (Table 5). The model provided higher posterior median estimates of DSe for all four test-sample types (Table 5; iELISA-serum: 46.2%, 95% BCI 39.4–52.9; iELISA-OF: 36.0%, 95% BCI 29.7–42.9; qPCR-serum: 70.0% 95% BCI 63.6–76.0; qPCR-OF: 53.9%, 95% BCI 46.7–61.0) compared to the values calculated from the combined, acutely, and chronically affected populations assuming positive disease status (Table 4),

TABLE 4 Estimates of diagnostic sensitivity (DSe) of ASFV iELISA and qPCR ASFV DNA assay for serum and oral fluid samples in acute, chronic, and combined-ASF-affected populations assuming true disease status, and diagnostic specificity (DSp) estimates in free-population, with 95% Clopper-Pearson confidence intervals.

Test	Sample	Sensitivity, acutely affected	Sensitivity, chronically affected	Sensitivity, combined affected	Specificity, negative, i.e., unaffected
iELISA for ASFV Ab	Serum	16 (9.43–24.7)	70.4 (60.3–79.2)	42.9 (35.9–50.1)	100 (98.2–100)
	Oral fluids	11 (5.62–18.8)	56.1 (45.7–66.1)	33.3 (26.8–40.4)	99 (96.4–99.9)
qPCR for ASFV DNA	Serum	74 (64.3–82.3)	56.1 (45.7–66.1)	65.2 (58.1–71.8)	100 (98.2–100)
	Oral fluids	69 (58.97–77.9)	34.7 (25.4–44.98)	52.0 (44.8–59.2)	100 (98.2–100)

though the overall trends of test performance were identical. Posterior DSp estimates were nearly identical between the two evaluation methods, and overall, 95% BCI were of similar width to the estimated 95% confidence intervals (Tables 4, 5). Pairwise correlation for infected subjects (rhoD13) was high between the iELISA using serum and OF and low-moderate for uninfected subjects (rhoDc13) though the latter had a very wide 95% BCI. RhoD24 was low between qPCR serum and OF samples, while RhoDc24 was low-moderate and, similarly to the iELISA pairwise correlation, had a very wide 95% BCI. Of the five parallel testing schemes assessed, using all four test and sample combinations resulted in the highest parallel DSe with only a small decrease in DSp. The parallel DSe and DSp of using only qPCR samples or using only serum samples were similar with overlapping 95% BCI. The use of only iELISA samples had the lowest parallel DSe.

3.4. Sensitivity analysis

The sensitivity analysis showed that parameter estimates were robust to changes in priors, hyperpriors, and model structure across the additional six different four test, three or two population models that were explored (Supplementary material 3). Removing the hyperprior allowed for better convergence of the parameter for the unaffected population prevalence, but with similar final results. The two population model where acute and chronic population data were combined also provided similar posterior medians and overlapping 95% BCI as the three population model (Supplementary material 3). The two population models where acute and chronic data were modeled separately showed small increased estimates for some DSe parameters compared to those when assuming disease status, but 95% confidence intervals and 95% BCI overlapped.

3.5. ROC curve analysis

The best performing test according to its AUC value was the qPCR to detect ASF viral DNA in serum samples (Table 6). The remaining tests, i.e., qPCR to detect ASF viral DNA in OF and iELISA to detect ASFV antibodies in serum or OF, had similar AUC values with overlapping 95% confidence intervals. According to the ROC plots (Figure 2), decreasing iELISA cut-off or increasing PCR cut-off points to improve DSe would lead to substantial decreases in DSp with minimal gain in DSe.

4. Discussion

The ever-growing spread of ASF globally makes accurate and early ASFV detection critical to identify infected populations and successfully control disease outbreaks. Having reliable and accurate diagnostic assays not only improves detection but also reduces false positives, which is also an important component of an efficient disease response. ASF lacks any pathognomonic clinical signs and can present indistinguishably from diseases such as classical swine fever (CSF) or PRRS, among other systemic and hemorrhagic diseases, making confirmation of infection by diagnostic tests vitally important (34, 35). Here, we aimed to evaluate the DSe and DSp of two novel diagnostic tests, iELISA for ASFV antibody detection and qPCR for ASFV DNA detection, in both serum and OF samples from pigs under field conditions in Vietnam.

Overall, when population data was combined, qPCR had higher DSe than iELISA for both serum and OF samples. However, when considering acute or chronic populations separately, qPCR had higher DSe in the acute samples, while iELISA had higher DSe in chronic samples. The dynamics of ASFV viremia and the host's antibody response may explain in part the observed difference in DSe depending on infection stage. ASFV causes an initial viremia detectable by PCR within days after infection and is sustained for ~1 month. In pigs surviving the initial stages of infection, viremia decreases, and the amount of viral DNA present in the pig blood or sera may become too low to be reliably detected *via* viral DNA detection assays, but antibody testing allows for detection of the infection during and after cessation of viremia. ASFV antibodies become detectable ~7 days post-infection (dpi), per different antibody detection methods, including indirect immunoperoxidase, indirect immunofluorescence, and some ELISA (22, 36, 37). Furthermore, antibodies formed as a result of moderately virulent ASFV infections and/or in pigs that are in the chronic stage of ASFV infection are more reliably detected 13–14 days dpi. For example, in experimentally infected pigs, peak Cq values by qPCR were obtained by 18–19 dpi, with decreasing amounts of ASFV DNA in blood from 29 dpi onward until only 52% of pigs were qPCR-positive at 91 dpi (38). In contrast, in the same group of pigs, the percentage of ASFV-Ab positive animals and blocking values using the INGEZIM PPA COMPAC ELISA (Ingenasa) steadily increased from 10 dpi until reaching 99–100% by 63 dpi. In another study, pigs infected with ASFV through direct contact displayed a relatively steady decline in Ct values of a qPCR viral DNA tests of whole blood and oropharyngeal swabs from day 13 onward (39). In two surviving pigs, a strong antibody response

TABLE 5 BLCA posterior estimates of iELISA and qPCR diagnostic sensitivity and specificity (%) in serum and oral fluid samples with 95% Bayesian credibility intervals (BCI).

Parameter		Posterior estimates and 95% BCI	
Test	Sample	Sensitivity	Specificity
ELISA for ASFV Ab	Serum	46.2 (39.4–52.9)	99.6 (98.1–99.97)
	OF	36.0 (29.7–42.9)	98.5 (96.5–99.6)
	rhoD13, serum and OF	73.0 (63.9–81.2)	
	rhoDc13, serum and OF	24.3 (1.23–70.0)	
PCR for ASFV DNA	Serum	70.0 (63.6–76.0)	99.6 (98.0–99.99)
	OF	53.9 (46.7–61.0)	99.6 (98.1–99.99)
	rhoD24, serum and OF	2.14 (0.09–9.78)	
	rhoDc24, serum and OF	29.2 (1.18–84.56)	
Prevalence ASF-affected, acute		99.3 (96.2–99.9)	
Prevalence ASF-affected, chronic		95.1 (87.6–99.6)	
Prevalence ASF-unaffected		0 (0–0)	
Parallel testing scheme		**Parallel sensitivity**	**Parallel specificity**
All test/samples		92.7 (90.0–94.6)	97.3 (94.7–98.9)
iELISA-serum and iELISA-OF		48.2 (41.3–54.8)	98.2 (95.9–99.4)
PCR-serum and PCR-OF		85.6 (81.2–89.1)	99.2 (97.4–99.9)
iELISA-serum and PCR-serum		83.9 (79.8–87.7)	99.0 (97.0–99.8)
iELISA-OF and PCR-OF		70.1 (64.7–76.1)	98.0 (95.6–99.3)

RhoD and RhoDc are the overall correlation between tests within the infected and uninfected subjects, respectively.

was detected by blocking ELISA and IPT from 16 to 76 dpi. For PCR detection of ASF viral DNA, these dynamics may be further complicated by infections with moderate and low virulence ASFV strains, which may induce lower or inconsistent levels of viremia compared to highly virulent ASFV strains (39). These and the current results highlight the importance of using both virus and antibody detection methods in surveillance strategies to increase the probability of detection, as one method alone may fail to identify all infected pigs.

Another important characteristic of ASFV infection is its relatively slow within-herd spread. Though ASFV is sometimes considered to be highly contagious due to its high lethality, the initial number of infected pigs is low, and the transmission between infected and susceptible pigs is gradual compared to other high-consequence pathogens of swine like foot-and-mouth disease virus and CSF virus (40). For example, models of ASFV within-herd transmission have estimated delays in detection of weeks to months if only using mortality triggers, i.e., having a herd-level mortality that is higher than baseline, to initiate diagnostic investigation (41, 42). By this time, the infected population of pigs will be comprised of pigs at different time points of infection and various disease state durations. Thus, a limitation of the present study was the low number of pigs sampled per ASF-affected farms (<10), which definitively impacted the estimated DSe of the tests. The use of both virus and antibody detection diagnostic assay, along with an increased sample size will provide a higher probability of disease detection and confirmation. Again, this is of considerable importance in outbreaks caused by ASF strains of low or moderate virulence where pigs are more likely to survive the initial infection (39). Antibody-detection methods may be particularly useful and important in countries such as Vietnam, where partial culling methods are allowed (43). Using this approach, generally, farms are allowed to cull only ASF-affected animals and units rather than total depopulation. When unsuccessful, this technique can lead to farms being chronically affected with ASF, where antibody-detection would presumably be useful for herd-level surveillance.

TABLE 6 AUC and associated 95% confidence intervals for each test-sample type.

Test	Sample	AUC (95% CI)
ELISA for ASFV antibodies	Serum	0.712 (0.659–0.766)
	Oral fluids	0.778 (0.733–0.823)
PCR for ASFV DNA	Serum	0.895 (0.863–0.928)
	Oral fluids	0.742 (0.693–0.79)

The BLCA model's high correlation for test outcome in infected subjects between iELISA serum and OF antibodies is both expected and highlights the importance of incorporating test dependency in diagnostic test evaluation models. OF is made of components produced in buccal-associated tissues and from continuous exchange between the circulatory system and the buccal cavity through both passive and active processes (e.g., ultrafiltration, transudation, selective, and/or receptor mediated transport) (44). Consequently, what is detected in serum can often

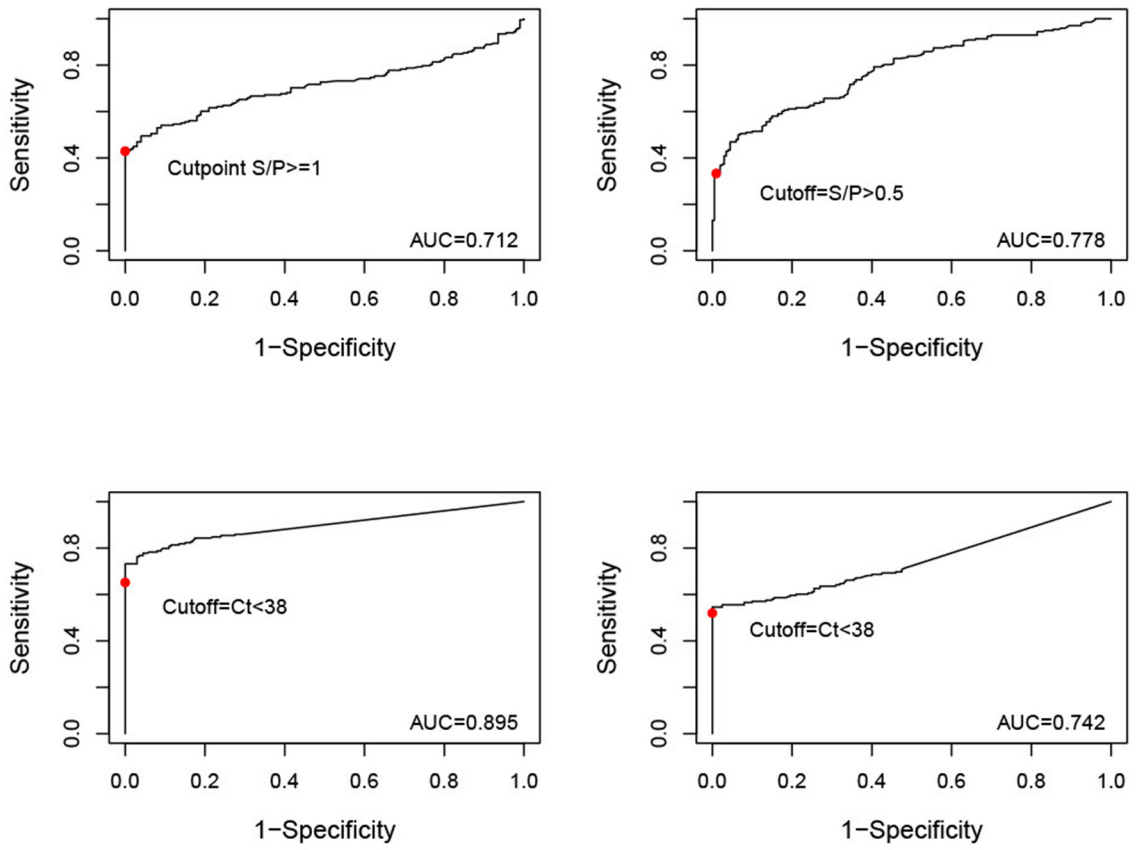

FIGURE 2
ROC curves (y = sensitivity, x = 1-specificity) for serum samples tested by iELISA, oral fluid (OF) samples tested by iELISA, serum samples tested by qPCR, and OF samples tested by qPCR. The solid red dot indicates the cut-off value used for analysis (iELISA serum positive = S/P ≥ 1, iELISA OF positive = S/P ≥ 0.5, qPCR serum and OF positive = Ct < 38).

also be detected in OF. It is somewhat unexpected that the model estimated minimal correlation between PCR of detecting ASF viral DNA in serum and OF samples, and the reason behind this is unclear. This may be due to the method used to estimate the upper and lower boundaries for the correlation term, whereby high performing tests, such as the PCR-serum, result in low upper boundary values.

The similar AUC estimates and their overlapping CIs for samples tested by iELISA and OF tested by qPCR likely reflects their similar performance, depending on the tested population (e.g., acutely vs. chronically infected). AUC also indicated that serum samples tested by PCR performed the best overall. Long-lasting viremia may favor ASFV DNA detection across acute and chronic disease timepoints in serum compared to OF or antibody detection. Another consideration is that whole blood is the preferred diagnostic sample for PCR, having demonstrated a lower limit-of-detection compared to serum (45). This is likely because in blood ASFV is mostly associated with red blood cells (46). Detection *via* the PCR evaluated here may be improved when using whole blood samples. The ROC curves themselves indicate that the current cut-off values for test status established by the manufacturers are likely appropriate. For example, decreasing the cut-off value for iELISA in serum samples to 0.46 would achieve a modest increase in DSe to 56% in the current observed population, but at the cost of a decrease in DSp to 95%. It seems unlikely given the high consequences of a false positive for ASF that such a decrease in DSp would be acceptable for only minor improvements in Dse.

Based on our results and the particular experimental design of the present study, ELISA and qPCR diagnostic assays are best suited for herd-level surveillance. The high DSp of the tests presented here lends them to have few false positives, a critical need when performing surveillance in low-prevalence or disease-free regions to avoid extra unneeded, costly disease investigations. Field surveillance requires near-perfect DSp because any false positive results could cause significant disruptions to production (e.g., quarantines and no animal movements during the disease investigation) and financial consequences not only to the pork production system under investigation but to the whole swine industry if it resulted in a loss of ASF-free status, falling market prices, trade embargoes, or loss of consumer confidence and negative reactions to control measures (47, 48). This emphasizes the importance of establishing cut-off values that maximize DSp with minimal impact on DSe. Since DSe "evolves" dynamically during the course of infection (i.e., viremia decreases over time while antibodies increase over time) continuous active surveillance may reveal the true status at the next sampling time point.

When antibody- and virus-detection assays are combined in parallel testing schemes, these diagnostic assays may provide suitable herd-level DSe for surveillance strategies. Here, five parallel testing schemes were considered, varying from only serum, only OF, only PCR, only iELISA, or all four tests/samples being used. While the use of all four tests/samples resulted in an acceptable DSe (92.7%) for herd-level surveillance, it seems unlikely that this testing scheme would be realistic due to the costs of running multiple tests. It is likely more convenient to run both assays on the same sample type, as this would streamline sample collection, with the added benefit of assessing for presence of both virus and antibodies simultaneously. Using the values estimated in our BLCA model, parallel DSe using either serum (83.9%) or OF samples (70.1%) would likely be acceptable for herd-level testing with minimal loss in DSp. Another important consideration is that while in the present study OF were collected individually to correlate results with pig serum, typically OF samples are collected *via* pen-level sampling tools such as cotton ropes (49). This aggregate sample can be used to detect and monitor pathogens even at low prevalence, reducing both labor and cost associated with individual sampling. Future studies should consider evaluating aggregate OF samples as well to understand their potential for increasing the probability of ASF detection. Overall, animal health officials and producers would need to decide acceptable frequencies of false alarms and how to manage them before deploying any of these testing schemes. Future studies that incorporate test performance into disease transmission models could help to elucidate their potential use in surveillance and reduce uncertainty about their benefits and drawbacks.

The BCLA provided similar DSe and DSp estimates to those of the combined population data assuming true disease status. This may in part be due to the sampling methods used for selecting farms and individual animals. Only farms with unequivocal histories of ASF-status were chosen for sampling, and within ASFV-infected farms, animals with clinical signs were targeted. This created study populations for which we could be quite certain of the true disease status, although by all accounts the disease status was indeed assumed. BLCA models would likely more applicable for studies that can only be conducted on pigs of unclear/uncertain disease status or in herds with variable within-herd ASF prevalence.

Some assumptions of BLCA modeling may limit its use here. For example, BLCA assumes equal performance of tests across multiple populations (14). Based on our results, the tests had high variability of performance depending on the potential time point in disease. To understand how this and the prior choice may affect the model estimates, six other model structures and/or prior specifications were explored. Sensitivity analysis results were robust to these changes (Supplementary material 3), indicated by a $<$10% change in the posterior point estimates and overlapping BCI. Two additional two population, four test models were evaluated where the acute or chronic populations were included one at a time alongside the ASF-unaffected populations. These models were compared to the estimates from the ASF-acute or ASF-chronic specific DSe and DSp estimates when assuming disease status is known. Results showed minimal variability and overlapping BCI with the 95% confidence intervals (Table 4, ASF-acute and ASF-chronic). In future works, more complex analyses with detailed data that incorporate timepoint as a covariate into the model might help address this concern. Also, BLCA tends to be more difficult to apply to study designs using tests with different definitions of true disease status (e.g., presence of viral DNA vs. presence of antibodies) (14). Here, the tests' characterization of disease status varies considerably over time due to differing presence of viremia and antibodies. Despite these limitations, the ability to incorporate imperfect reference tests and correlation between tests likely has created less biased estimates of disease Se and Sp in the present study and is a strength of BLCA.

We acknowledge that there were some limitations in data collection that prevented further analyses. The sample collection did not follow a predefined scientific approach, but instead was a part of ongoing ASF regulatory activities. Consequently, the samples come with the limitations of field data, and ASF-status was assumed based on farm history. BLCA was used here to help obtain accurate DSe and DSp estimates despite these limitations. To obtain a suitable number of samples for analysis, many Vietnam farms were sampled ($n = 87$), but for many acutely and chronically affected farms, as few as 1–3 animals sampled per farm. This was most likely due to low within-herd prevalence of sick pigs to sample, the slow within-farm spread of ASFV, and the need to adequately represent differential stages of the infection across individual animals. The exact time point of infection for sampled pigs from acute and chronic farms was unknown, so it was difficult to assess the true impact of infection time point on test performance. It is unclear how much further in disease progression all chronic farms were compared to acute farms. As this is clearly an important factor to ASF test performance, future longitudinal studies with repeated sampling of individuals over time would be highly beneficial to understand these dynamics. Additionally, other important covariates of test status were not collected and could not be included in the analysis. Factors such as breed, presence of individual clinical signs, and accurate pig age all might be important for test performance but could not be considered in the present study. Finally, it is unknown how well these results may generalize to pigs of European or American origin; thus these tests may perform differently in other swine populations.

In summary, these results are an important evaluation of novel ASF diagnostic tests in field settings that provides real-world context about their performance. Animal health officials and epidemiologists can use these results to appropriately apply these diagnostic tests in surveillance and control strategies in Vietnam and other ASF-affected countries.

Data availability statement

The original contributions presented in the study are included in the article/Supplementary material, further inquiries can be directed to the corresponding author.

Ethics statement

Ethical review and approval was not required for the animal study because ASF continues to be a regulated and reportable disease in Vietnam. This study was IACUC exempted as it did not involve special sampling procedures that require ethical approval.

Written informed consent for participation was not obtained from the owners because ASFV continues to be a regulated and reportable disease in Vietnam and sampling was conducted as a part of regular reporting and ASFV testing procedures.

Author contributions

LG-L and AP designed the study. VC, NL, LH, VH, PT, DL, and HB coordinated sample collection, field testing, and laboratory analysis. LG-L assembled the data. LG-L, AP, MC, and AR helped in interpretation of the results. RS ran the statistical analyses and drafted the manuscript. All authors contributed to the article and approved the submitted version.

Funding

This research was funded by the Swine Health Information Center (20-080).

Acknowledgments

The authors thank the experts who provided insight for the prior distributions and to the farmers and veterinarians who participated in farm sampling in Vietnam.

Conflict of interest

RR and WN work for the company Tetracore Inc. LG-L is Associate Professor in the Department of Veterinary Diagnostic and Production Animal Medicine at Iowa State University and founder of Innoceleris LLC.

The remaining authors declare that the research was conducted in the absence of any commercial or financial relationships that could be construed as a potential conflict of interest.

Publisher's note

All claims expressed in this article are solely those of the authors and do not necessarily represent those of their affiliated organizations, or those of the publisher, the editors and the reviewers. Any product that may be evaluated in this article, or claim that may be made by its manufacturer, is not guaranteed or endorsed by the publisher.

Supplementary material

The Supplementary Material for this article can be found online at: https://www.frontiersin.org/articles/10.3389/fvets.2023.1079918/full#supplementary-material

References

1. Dixon LK, Sun H, Roberts H. African swine fever. *Antiviral Res.* (2019) 165:34–41. doi: 10.1016/j.antiviral.2019.02.018

2. Montgomery, Eustace R. On a form of swine fever occurring in British East Africa (Kenya Colony). *J Comp Pathol Ther.* (1921) 34:159–91. doi: 10.1016/S0368-1742(21)80031-4

3. World Organization for Animal Health. *African Swine Fever (ASF) – Situation Report 12.* OIE - World Organ Anim Health (2022). Available online at: https://www.oie.int/en/document/african-swine-fever-asf-situation-report-12/ (accessed May 18, 2022).

4. USDA APHIS. *USDA Statement on Confirmation of African Swine Fever in the Dominican Republic.* (2021). Available online at: https://www.aphis.usda.gov/aphis/newsroom/news/sa_by_date/sa-2021/asf-confirm (accessed February 28, 2022).

5. Tran XH, Phuong LTT, Huy NQ, Thuy DT, Nguyen VD, Quang PH, et al. Evaluation of the safety profile of the ASFV vaccine candidate ASFV-G-ΔI177L. *Viruses.* (2022) 14:896. doi: 10.3390/v14050896

6. Borca MV, Ramirez-Medina E, Silva E, Vuono E, Rai A, Pruitt S, et al. Development of a highly effective African swine fever virus vaccine by deletion of the I177L gene results in sterile immunity against the current epidemic Eurasia strain. *J Virol.* (2020) 94:e02017–19. doi: 10.1128/JVI.02017-19

7. Dixon LK, Stahl K, Jori F, Vial L, Pfeiffer DU. African swine fever epidemiology and control. *Annu Rev Anim Biosci.* (2020) 8:221–46. doi: 10.1146/annurev-animal-021419-083741

8. World Organization for Animal Health. *Principles and Methods of Validation of Diagnostic Assays for Infectious Diseases. Man Diagn Tests Vaccines Terr Anim.* (2021). Available online at: https://www.oie.int/fileadmin/Home/eng/Health_standards/aahm/current/chapitre_validation_diagnostics_assays.pdf (accessed May 18, 2022).

9. Hui SL, Zhou XH. Evaluation of diagnostic tests without gold standards. *Stat Methods Med Res.* (1998) 7:354–70. doi: 10.1191/096228098671192352

10. Hui SL, Walter SD. Estimating the error rates of diagnostic tests. *Biometrics.* (1980) 36:167–71. doi: 10.2307/2530508

11. Dendukuri N, Joseph L. Bayesian approaches to modeling the conditional dependence between multiple diagnostic tests. *Biometrics.* (2001) 57:158–67. doi: 10.1111/j.0006-341X.2001.00158.x

12. Gardner IA, Stryhn H, Lind P, Collins MT. Conditional dependence between tests affects the diagnosis and surveillance of animal diseases. *Prev Vet Med.* (2000) 45:107–22. doi: 10.1016/S0167-5877(00)00119-7

13. Branscum AJ, Gardner IA, Johnson WO. Estimation of diagnostic-test sensitivity and specificity through Bayesian modeling. *Prev Vet Med.* (2005) 68:145–63. doi: 10.1016/j.prevetmed.2004.12.005

14. Cheung A, Dufour S, Jones G, Kostoulas P, Stevenson MA, Singanallur NB, et al. Bayesian latent class analysis when the reference test is imperfect: -EN- -FR- Analyse bayésienne à classes latentes dans les situations où le test de référence est imparfait -ES- Análisis bayesiano de clases latentes cuando la prueba de referencia es imperfecta. *Rev Sci Tech OIE.* (2021) 40:3224. doi: 10.20506/rst.40.1.3224

15. World Organization for Animal Health. *Statistical Approaches to Validation.* (2014). Available online at: https://www.oie.int/fileadmin/Home/eng/Health_standards/aahm/current/3.6.05_STATISTICAL_VALIDATION.pdf (accessed February 14, 2022).

16. Kostoulas P, Nielsen SS, Branscum AJ, Johnson WO, Dendukuri N, Dhand NK, et al. Standards for the reporting of diagnostic accuracy studies that use bayesian latent class models. *Prev Vet Med.* (2017) 138:37–47. doi: 10.1016/j.prevetmed.2017.01.006

17. Greiner M, Pfeiffer D, Smith RD. Principles and practical application of the receiver-operating characteristic analysis for diagnostic tests. *Prev Vet Med.* (2000) 45:23–41. doi: 10.1016/S0167-5877(00)00115-X

18. Le VP, Jeong DG, Yoon S-W, Kwon H-M, Trinh TBN, Nguyen TL, et al. Outbreak of African swine fever, Vietnam, 2019. *Emerg Infect Dis.* (2019) 25:1433–5. doi: 10.3201/eid2507.190303

19. Bui N, Gilleski S. *Vietnam: Vietnam African Swine Fever Update.* Hanoi, Vietnam: USDA Foreign Agricultural Service (2019). Available online at: https://www.fas.usda.gov/data/vietnam-vietnam-african-swine-fever-update (accessed June 9, 2022).

20. Bui N. *Vietnam African Swine Fever Update.* USDA Foreign Agricultural Service (2021). Available online at: https://apps.fas.usda.gov/newgainapi/api/Report/DownloadReportByFileName?fileName=Vietnam%20African%20Swine%20Fever%20Update_Hanoi_Vietnam_05-08-2021.pdf (accessed June 9, 2022).

21. Food and Agriculture Organization of the United Nations. *ASF Situation in Asia & Pacific Update*. (2022). Available online at: https://www.fao.org/ag/againfo/programmes/en/empres/ASF/situation_update.html (accessed August 16, 2022).

22. Havas KA, Gogin AE, Basalaeva JV, Sindryakova IP, Kolbasova OL, Titov IA, et al. An assessment of diagnostic assays and sample types in the detection of an attenuated genotype 5 African swine fever virus in European pigs over a 3-month period. *Pathog Basel Switz.* (2022) 11:404. doi: 10.3390/pathogens11040404

23. Pikalo J, Carrau T, Deutschmann P, Fischer M, Schlottau K, Beer M, et al. Performance characteristics of real-time PCRs for African swine fever virus genome detection-comparison of twelve kits to an OIE-recommended method. *Viruses.* (2022) 14:220. doi: 10.3390/v14020220

24. Schoder M-E, Tignon M, Linden A, Vervaeke M, Cay AB. Evaluation of seven commercial African swine fever virus detection kits and three Taq polymerases on 300 well-characterized field samples. *J Virol Methods.* (2020) 280:113874. doi: 10.1016/j.jviromet.2020.113874

25. Grau FR, Schroeder ME, Mulhern EL, McIntosh MT, Bounpheng MA. Detection of African swine fever, classical swine fever, and foot-and-mouth disease viruses in swine oral fluids by multiplex reverse transcription real-time polymerase chain reaction. *J Vet Diagn Invest.* (2015) 27:140–9. doi: 10.1177/1040638715574768

26. Goonewardene KB, Chung CJ, Goolia M, Blakemore L, Fabian A, Mohamed F, et al. Evaluation of oral fluid as an aggregate sample for early detection of African swine fever virus using four independent pen-based experimental studies. *Transbound Emerg Dis.* (2021) 68:2867–77. doi: 10.1111/tbed.14175

27. Gardiner J. *Software. Cent Anim Dis Model Surveill CADMS*. (2018). Available online at: https://cadms.vetmed.ucdavis.edu/diagnostic/software (accessed March 15, 2022).

28. Bates A, Laven R, O'Brien R, Liggett S, Griffin F. Estimation of the sensitivity and specificity of four serum ELISA and one fecal PCR for diagnosis of paratuberculosis in adult dairy cattle in New Zealand using Bayesian latent class analysis. *Prev Vet Med.* (2020) 185:105199. doi: 10.1016/j.prevetmed.2020.105199

29. Sturtz S, Ligges U, Gelman A. R2WinBUGS: a package for running WinBUGS from R. *J Stat Softw.* (2005) 12:1–16. doi: 10.18637/jss.v012.i03

30. Lunn DJ, Thomas A, Best N, Spiegelhalter D. WinBUGS — a Bayesian modelling framework: concepts, structure, and extensibility. *Stat Comput.* (2000) 10:325–37. doi: 10.1023/A:1008929526011

31. Gelman A, Rubin DB. Inference from iterative simulation using multiple sequences. *Stat Sci.* (1992) 7:457–72. doi: 10.1214/ss/1177011136

32. Sing T, Sander O, Beerenwinkel N, Lengauer T, Unterthiner T, Ernst FGM. *Package "ROCR"*. (2020). Available online at: https://cran.r-project.org/web/packages/ROCR/ROCR.pdf (accessed June 23, 2022).

33. Vietnam Ministry of Agriculture and Rural Development. *Decree 13/2020/ND-CP Elaboration the Law on Animal Husbandry*. (2020). Available online at: https://vanbanphapluat.co/decree-13-2020-nd-cp-elaboration-the-law-on-animal-husbandry (accessed September 13, 2022).

34. Schulz K, Staubach C, Blome S. African and classical swine fever: similarities, differences and epidemiological consequences. *Vet Res.* (2017) 48:84. doi: 10.1186/s13567-017-0490-x

35. World Organization for Animal Health. *African Swine Fever*. OIE Tech Dis Card (2019). p. 5.

36. Giménez-Lirola LG, Mur L, Rivera B, Mogler M, Sun Y, Lizano S, et al. Detection of African swine fever virus antibodies in serum and oral fluid specimens using a recombinant protein 30 (p30) dual matrix indirect ELISA. *PLoS ONE.* (2016) 11:e0161230. doi: 10.1371/journal.pone.0161230

37. Gallardo C, Fernández-Pinero J, Arias M. African swine fever (ASF) diagnosis, an essential tool in the epidemiological investigation. *Virus Res.* (2019) 271:197676. doi: 10.1016/j.virusres.2019.197676

38. Petrov A, Forth JH, Zani L, Beer M, Blome S. No evidence for long-term carrier status of pigs after African swine fever virus infection. *Transbound Emerg Dis.* (2018) 65:1318–28. doi: 10.1111/tbed.12881

39. Gallardo C, Soler A, Nurmoja I, Cano-Gómez C, Cvetkova S, Frant M, et al. Dynamics of African swine fever virus (ASFV) infection in domestic pigs infected with virulent, moderate virulent and attenuated genotype II ASFV European isolates. *Transbound Emerg Dis.* (2021) 68:2826–41. doi: 10.1111/tbed.14222

40. Schulz K, Conraths FJ, Blome S, Staubach C, Sauter-Louis C. African swine fever: fast and furious or slow and steady? *Viruses.* (2019) 11:866. doi: 10.3390/v11090866

41. Ssematimba A, Malladi S, Bonney PJ, St Charles KM, Boyer TC, Goldsmith T, et al. African swine fever detection and transmission estimates using homogeneous versus heterogeneous model formulation in stochastic simulations within pig premises. *Open Vet J.* (2022) 12:787–96. doi: 10.5455/ovj.2022.v12.i6.2

42. Malladi S, Ssematimba A, Bonney PJ, St Charles KM, Boyer T, Goldsmith T, et al. Predicting the time to detect moderately virulent African swine fever virus in finisher swine herds using a stochastic disease transmission model. *BMC Vet Res.* (2022) 18:84. doi: 10.1186/s12917-022-03188-6

43. Anonymous. *Vietnam Laws: About the Approval of the "National Plan for Prevention and Control of African Swine Fever, Period 2020 - 2025"*. (2020). Available online at: https://thuvienphapluat.vn/van-ban/The-thao-Y-te/Quyet-dinh-972-QD-TTg-2020-Ke-hoach-quoc-gia-phong-chong-benh-Dich-ta-lon-Chau-Phi-446925.aspx (accessed January 3, 2023).

44. Azevedo LR, De Lima AAS, Machado MÂN, Grégio AMT, de Almeida PDV. Saliva composition and functions: a comprehensive review. *J Contemp Dent Pract.* (2008) 9:72–80. doi: 10.5005/jcdp-9-3-72

45. Pikalo J, Deutschmann P, Fischer M, Roszyk H, Beer M, Blome S. African swine fever laboratory diagnosis—lessons learned from recent animal trials. *Pathogens.* (2021) 10:177. doi: 10.3390/pathogens10020177

46. Wardley RC, Wilkinson PJ. The association of African swine fever virus with blood components of infected pigs. *Arch Virol.* (1977) 55:327–34. doi: 10.1007/BF01315054

47. FAO. *Risk-Based Disease Surveillance: A Manual for Veterinarians on the Design and Analysis of Surveillance for Demonstration of Freedom from Disease*. Rome: FAO (2014). p. 215. Available online at: https://www.fao.org/publications/card/en/c/1440fee4-be47-4d38-8571-4dad3f3036d6/ (accessed February 28, 2022).

48. Elbers ARW, Gorgievski-Duijvesteijn MJ, Zarafshani K, Koch G. To report or not to report: a psychosocial investigation aimed at improving early detection of avian influenza outbreaks. *Rev Sci Tech Int Off Epizoot.* (2010) 29:435–49. doi: 10.20506/rst.29.3.1988

49. Ramirez A, Wang C, Prickett JR, Pogranichniy R, Yoon K-J, Main R, et al. Efficient surveillance of pig populations using oral fluids. *Prev Vet Med.* (2012) 104:292–300. doi: 10.1016/j.prevetmed.2011.11.008

frontiers | Frontiers in Veterinary Science

TYPE Brief Research Report
PUBLISHED 04 April 2023
DOI 10.3389/fvets.2023.1093733

OPEN ACCESS

EDITED BY
Wentao Li,
Huazhong Agricultural University, China

REVIEWED BY
Yang Zhan,
Hunan Agricultural University, China
Meishen Ren,
Sichuan Agricultural University, China

*CORRESPONDENCE
Xiaodong Wu
✉ wuxiaodong@cahec.cn
Zhiliang Wang
✉ wangzhiliang@cahec.cn

†These authors have contributed equally to this work

SPECIALTY SECTION
This article was submitted to Veterinary Experimental and Diagnostic Pathology, a section of the journal Frontiers in Veterinary Science

RECEIVED 09 November 2022
ACCEPTED 02 March 2023
PUBLISHED 04 April 2023

CITATION
Qi C, Zhang Y, Wang Z, Li J, Hu Y, Li L, Ge S, Wang Q, Wang Y, Wu X and Wang Z (2023) Development and application of a TaqMan-based real-time PCR method for the detection of the ASFV MGF505-7R gene. *Front. Vet. Sci.* 10:1093733. doi: 10.3389/fvets.2023.1093733

Development and application of a TaqMan-based real-time PCR method for the detection of the ASFV MGF505-7R gene

Chuanxiang Qi[1,2†], Yongqiang Zhang[1†], Zhenzhong Wang[1,2], Jinming Li[1], Yongxin Hu[1], Lin Li[1], Shengqiang Ge[1], Qinghua Wang[1], Yingli Wang[1], Xiaodong Wu[1*] and Zhiliang Wang[1*]

[1]China Animal Health and Epidemiology Center, Qingdao, Shandong, China, [2]MOE Joint International Research Laboratory of Animal Health and Food Safety, MOA Key Laboratory of Animal Bacteriology, College of Veterinary Medicine, Nanjing Agricultural University, Nanjing, China

African swine fever virus (ASFV), the etiological agent of African swine fever (ASF), causes deadly hemorrhagic fever in domestic pigs. ASF's high mortality and morbidity have had disastrous effects on the world's swine industry. In recent years, the number of African swine virus strains has increased and presented new challenges for detecting classical ASFV-p72-based viruses. In this study, we observed that the ASFV MGF505-7R gene, a member of the multigene family that can enhance ASFV virulence and pathogenesis, has the potential to be a candidate for vaccine formulations. We also developed a real-time PCR assay based on the ASFV MGF505-7R gene and validated it in multiple aspects. The results indicated that the approach could detect standard plasmids with a sensitivity and a specificity of up to 1×10^1 copies/μL. Moreover, the assay had no cross-reactions with other porcine viruses. In laboratory and clinical settings, the assay can detect ASFV-infected samples at an early stage (4 hpi) and show a consistency of 92.56% when compared with classical ASFV detection in clinically ASFV-infected materials. This study's results also indicated that the TaqMan-based quantitative real-time PCR assay we developed for detecting the ASFV MGF505-7R gene is both sensitive and specific. This assay can provide a quick and accurate method for detecting ASFV and has the potential to be used as an optional tool for screening and monitoring ASF outbreaks.

KEYWORDS

ASFV, MGF505 7R, qPCR, application, diagnosis

1. Introduction

African swine fever virus (ASFV), the etiologic agent of African swine fever (ASF), causes an acute, febrile, and highly contagious disease in domestic pigs and wild boars. Infected pigs exhibit symptoms such as high fever, loss of appetite, nasal discharges, and abortion, with a mortality rate close to 100% (1, 2). ASF can be spread through multiple modes, including a sylvatic cycle between swine and arthropod vectors, direct or indirect contact between the susceptible animal and infected pigs, and contaminated secretions or fomites (3). ASF is statutorily required by the World Organization for Animal Health (OIE) to be reported, and China also classifies ASF as a type I disease that needs to be controlled. Since the first ASF outbreak in China in 2018 (4, 5), nearly 1.2 million live pigs have been slaughtered, leading to significant socioeconomic consequences for the pig

farming industry. To date, no effective vaccine or antiviral compound has been developed for ASF, while quarantine, depopulation, and sanitation strategies remain the common methods to curb the spread of the disease.

As the only member of the family *Asfarviridae*, ASFV has a large double-stranded DNA virus with a linear genome of 173–193 kb, encoding 151–167 open reading frames (ORFs) (6). To date, 24 different genotypes and eight serogroups have been identified based on the ASFV B646L (encoding the capsid protein p72) gene and the EP402R (encoding the serotype-specific protein CD2v) gene, respectively (7, 8). The ASFV multigene families (MGF) are characterized as genes present as repetitive sequences in the highly variable terminal genomic regions. MGF proteins vary widely between ASFV isolates due to frequent duplication, deletion, or inversion of MGF proteins (6). Given the great diversity of MGF, it will be of great interest and challenge to find a suitable target for ASFV diagnosis. At present, the ASFV p72 gene is commonly used for detecting ASFV due to its high conservation (9, 10), but as a late-transcription gene in ASFV (11), p72 shows low expression levels during the early stages of infection, making it difficult to accurately detect and measure viral loads, which may result in the misdiagnosis of some ASFV cases during the incubation period or early stages of infection. In this regard, we found MGF505-7R, a conserved gene from the MGF 505 family. MGF505-7R is located close to the end of the MGF family and thus shows little variation in most ASF strains. A study recently reported that MGF505-7R plays an important role in ASFV infection as it can be recognized by host $CD8^+$ T cells and can potentially be used in vaccine formulations (12).

Additionally, MGF505-7R can enhance ASFV virulence and pathogenesis by inhibiting JAK1- and JAK2-mediated signaling (13) and suppressing the production of IL-1β and type I IFNs (14). The latest piece of research has shown that combinational deletions of MGF360-9L and MGF505-7R can attenuate highly virulent ASFV and provide protection against challenges (15). According to the above review, we believe that MGF505-7R is not only a conserved gene but also has a variety of potential functions that affect viral virulence, making it a promising candidate for detecting ASF.

Currently, there are various detection technologies available for ASFV, including virus isolation based on viral replication in susceptible cells (16, 17), ELISA based on the identification of ASFV antigens (18, 19), recombinase polymerase amplification (RPA) assay for virus gene detection (20, 21), CRISPR-Cas12a and fluorescence-based diagnosis system (22, 23), and loop-mediated isothermal amplification (LAMP) assay for the semi-quantitative analysis of ASFV (24). Despite these detection methods having advantages such as high accuracy, strong operability, and poor temperature requirements, several inconvenient requirements such as high costs, time-consuming nature, and low sensitivity may prevent them from becoming the best identification method (18, 25–27). Currently, the gold standard for ASFV diagnostics in laboratories is polymerase chain reaction (PCR), a viral genome detection technique based on nucleic acid marker amplification, and fluorescent quantitative PCR has become increasingly popular due to its high sensitivity, specificity, less time consumption, and accurate quantification. Fluorescence quantitative PCR mainly includes the SYBR Green method and the TaqMan probe method, and the latter has advantages in terms of specificity and accuracy and is highly applicable as it targets a sequence that is conserved in function, highly expressed during the early stages of infection, and functionally important, making it a valuable complementary target for ASFV diagnosis.

TABLE 1 Primers and probes used in this study.

Name	Primers (5′–3′)	Size (bp)
MGF505-7R-F	TAGGCAACAAATTCAAGGACT	131bp
MGF505-7R-R	CTTTTGTGACAACAGCAATGC	
MGF505-7R-probe	CGGAAGCTTGAGATTCTTACGTGGATGG	

In this study, we developed a highly sensitive and specific TaqMan-based real-time quantitative PCR method for ASFV MGF 505-7R gene detection. The detection limit was low, at 1×10^1 copies/μL, and exhibited good repeatability and specificity. In addition, our methods showed comparable results in laboratory and clinical samples compared to ASFV-p72-based qPCR diagnosis.

The development of the method produced a reliable candidate gene, increased the effectiveness of ASFV detection in the clinic, and may be further used to detect viral loads in various clinical samples from ASFV-infected pigs. The method also served as a technical tool for the pathogenicity study of ASFV, which helped researchers understand the virus better.

2. Materials and methods

2.1. Virus, plasmid, primers and probe

The African swine fever virus (ASFV) China_AnhuiXCGQ_2018 strain used in this study was preserved by the China Animal Health and Epidemiology Center (CAHEC), Shandong province, China (GenBank accession number MK128995.1). The full-length MGF505-7R gene (1584bp) in the p3xFLAG-CMV-7.1 vector, named p3xFLAG-MGF505-7R, was synthesized by Zhiyuan Biotechnology Co. Ltd. (Qingdao, Shandong, China). The recombinant vector was transformed into *E.coli* DH5α competent cells (CWBIO, Beijing, China) and extracted using the QIAGEN Plasmid Plus Maxi Kit. A pair of specific primers, MGF505-7R-F and MGF505-7R-R, and a TaqMan probe targeting MGF505-7R were designed with Oligo7 (Table 1). All primers and probes were also synthesized by Zhiyuan Biotechnology Co. Ltd. DNA and RNA concentrations were quantitated using a NanoDrop ND-1000 spectrophotometer and calculated in copy numbers.

2.2. Sequence analysis of ASFV MGF505-7R

The information of the MGF505-7R gene (QED90472.1, AYW34001.1, AKO62712.1, QBH90517.1, QBH90702.1,

QDL88060.1, SPS73452.1, AJZ77061.1, QEY87835.1, AIY22221.1, AIY22380.1, CAN10378.1, CBW46695.1, QGM12819.1, CAN10129.1, AKO62711.1, CBH29131.1, AXB49776.1, AXB49605.1, AXB49949.1, AXB49433.1, AXB49259.1, and QED21587.1) from 39 different ASFV strains were collected from the GenBank and ASFVdb databases (28). Sequences were aligned using MEGA X software (29) and the clustalW method (30). Homolog analysis of ASFV MGF505-7R nucleotide sequences with multiple sequence alignment results was performed using the DNAMAN 7.0 tool (https://www.lynnon.com/dnaman.html).

2.3. Optimization of qPCR conditions

The qPCR assay was developed and validated using the CFX96Touch (Bio-Rad) and AceQ® qPCR Probe Master Mix (Vazyme, China). The qPCR reaction system was determined as follows: AceQ qPCR Probe Master Mix (2X) of 10/μL, probe (10 pmol/μL) of 0.2 μL, upstream and downstream primers (10 pmol/μL) each of 0.4 μL, DNA of 1 μL, and used dd H_2O to make up to the quantity of 20 μL. According to the designed primer Tm value, six different annealing temperatures were used with three replicates per group: 57, 58, 59, 60, 61, and 62°C, and 10^7 copies/μL p3xFLAG-MGF505-7R plasmid was used as a DNA template, and the optimum annealing temperature was selected based on the measurement results.

2.4. Standard curve

The DNA standard p3xFLAG-MGF505-7R was diluted 10-fold serially and amplified with the optimized qPCR system at a concentration of 1.0×10^7-1.0×10^1 copies/μL. A final standard curve was generated based on the CT value and the logarithm of the standard copy number.

2.5. Sensitivity

To determine the sensitivity of the assay, the p3xFLAG-MGF505-7R plasmid was diluted 10-fold serially with concentrations ranging from 1.0×10^7-1.0×10^0 copies/μL. Prepared standards were amplified with the optimized qPCR system to confirm the detection limit. At the same time, the conventional PCR was performed with the same DNA standard and primers. Amplifications were carried out in a 20 μL reaction system containing 10 μL 2×Taq MasterMix (Vazyme, Nanjing, China), 1 μL of each primer, 2 μL of DNA, and 6 μL of RNase-free dd H_2O. The thermal profile for the PCR was 95°C for 5 min, 35 cycles of amplification (30 s at 95°C, 30 s at 56°C, and 30 s at 72°C), and a final extension step at 72°C for 10 min. The resulting PCR products were analyzed by electrophoresis on an ethidium bromide-stained 1.5% agarose gel. We could compare the sensitivity between qPCR and PCR by observing their detection limits.

2.6. Specificity

The established real-time quantitative PCR method was used to detect common swine infectious viruses, including porcine pseudorabies virus (PRV), porcine reproductive and respiratory syndrome virus (PRRSV), porcine circovirus (PCV2), classical swine fever virus (CSFV), porcine parvovirus (PPV), and swine transmissible gastroenteritis virus (TGEV). A total of six viruses were used for testing the specificity of primers and probes. All viral nucleic acids and negative controls preserved by the laboratory were used as a template for a real-time fluorescence quantitative PCR reaction.

2.7. Repeatability

A repeatability test was carried out with p3xFLAG-MGF505-7R at concentrations of 1.0×10^7-1.0×10^0 copies/μL *via* an optimized protocol three times daily for 3 days to assess the accuracy of the method by calculating intra-assay and inter-assay standard deviations.

2.8. Laboratory samples testing

Porcine alveolar macrophages (PAMs) were used for laboratory sample preparation. To obtain PAMs, Bama pigs were raised for up to 4 weeks in the animal feeding room of the CAHEC. Cells were isolated from the lung lavage fluid (31) with only a slightly modified methodology, as previously described. Briefly, alveolar macrophages were obtained from 40-day-old crossbred piglets confirmed to be free of PCV, PPV, PRRSV, and ASFV by SYBR green-based qPCR and then maintained in RPMI-1640 medium with 10% fetal bovine serum (Hyclone) and 100 U/ml penicillin and 50 mg/ml streptomycin (Hyclone). PAM cells were maintained at 37°C with 5% CO_2 overnight and then infected with 0.5 MOI China_AnhuiXCGQ_2018 at 4, 8, 16, 24, and 32 hpi. Cell samples were extracted for RNA using the FastPure Cell/Tissue Total RNA Isolation Kit V2 and then reverse transcribed into cDNA (Vazyme, Nanjing, China). Prepared templates were used for qPCR with the designed MGF505-7R probe and classic p72 probe (10). To reduce false-negative detections, the porcine housekeeping gene beta-actin (ACTB) was applied as an internal control. The results were analyzed with CFX Manager 3.0 (Bio-Rad) and GraphPad Prism 8 (GraphPad Software, San Diego, CA, USA).

2.9. Clinical samples testing

A total of 94 samples, including domestic pigs' blood, nose swabs, and lymph node tissues, were provided by the National Reference Laboratory for African Swine Fever in the China Animal Health and Epidemiology Center. Total DNA/RNA was extracted automatically from the samples using the Tianlong NP968-C Nucleic Acid Extractor with the GeneRotex96 program (TianLong Medtl, Hangzhou, China). ASFV was inactivated

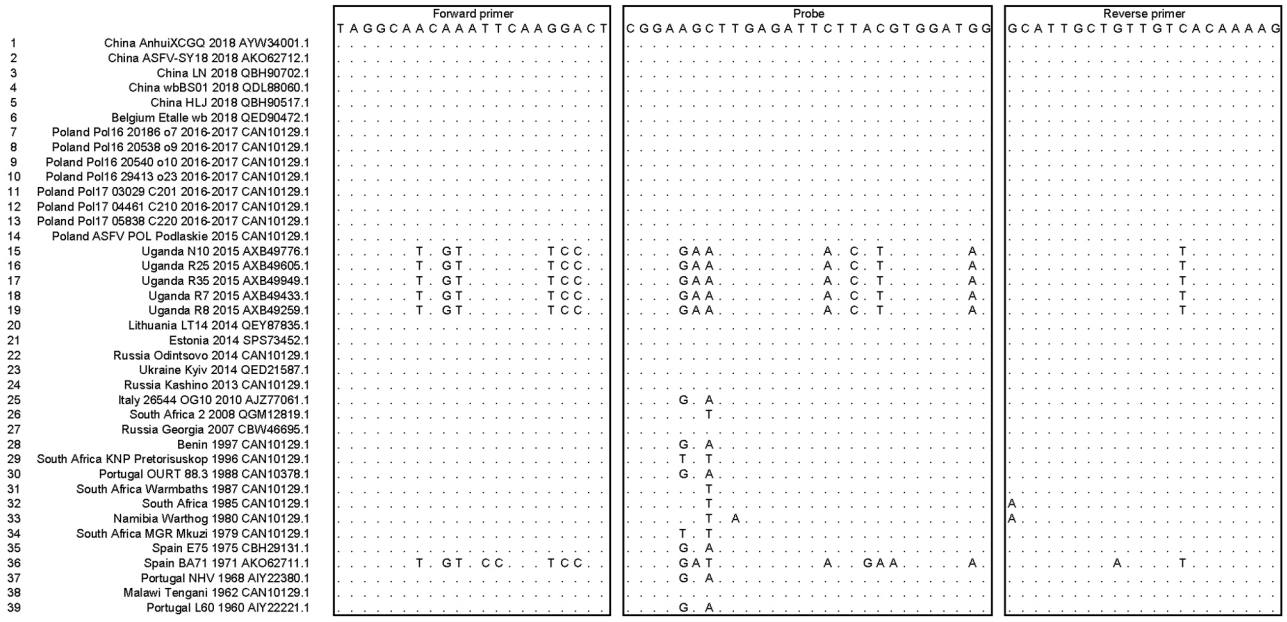

FIGURE 1
Alignment of the primers and probes targeted to the ASFV MGF505-7R genes among multiple ASFV strains. The sequences of the forward primers, probes, and reverse primers (used as an antisense oligonucleotide) were shown in boxes. Dots represented nucleotides identical to the primers and probes.

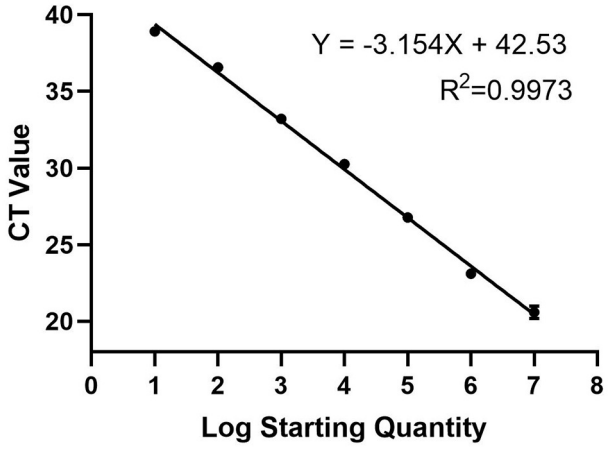

FIGURE 2
Standard curve for qPCR assay of MGF505-7R. A 10-fold serial dilution ranging from 1×10^7 to 1×10^1 copies/μL of the standard DNA was tested in the qPCR. Three replicates were tested for each dilution. The optimal standard formula is $y = -3.154x + 42.53$, and the correlation coefficient is 0.9973.

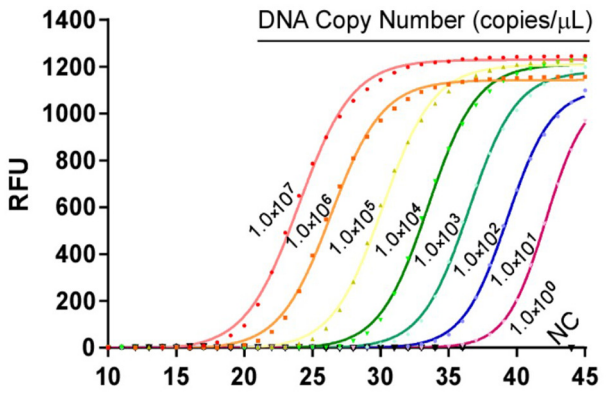

FIGURE 3
Sensitivity tests for qPCR assays based on the MGF505-7R probe. 10-fold serial dilutions of the DNA standard were used to perform the qPCR to obtain the standard curve of the assay. The lowest copy number that could be determined was up to 10 copies/μL.

with 1% (w/v) of NaOH, as previously described in a BSL-3 laboratory (32), and viral DNA/RNA samples were prepared in a BLS-2 laboratory. Nucleic acids were extracted and then stored at −80°C for subsequent use. All these clinical samples were confirmed to be ASFV-positive with a p72-specific primer and probe. They used it for a qPCR assay of MGF505-7R. Samples with CT values below 40 were identified as ASFV-positive.

3. Results

3.1. Sequence analysis of ASFV MGF505-7R

ASFV MGF505-7R nucleotide sequences from 39 different ASFV strains were involved in multiple sequence alignments, mainly including the ASFV genotype II strains epidemic in Asia and Europe in recent years. The homolog identification showed 96.68% identity, indicating that MGF505-7R is a relatively conserved gene. The sequences of the forward primers, probes, and

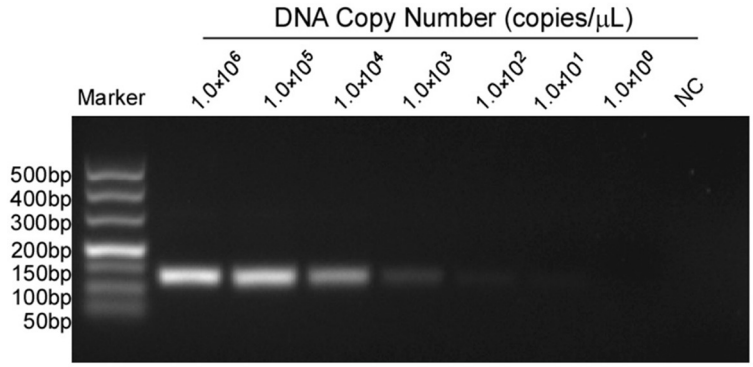

FIGURE 4
Sensitivity tests for conventional PCR of MGF505-7R. Lanes 1 to 7 were the templates, with concentrations ranging from 1×10^6 to 1×10^0 copies/μL. Lane 8 was a negative control. The lowest copy number that could be determined was up to 1.0×10^2 copies/μL.

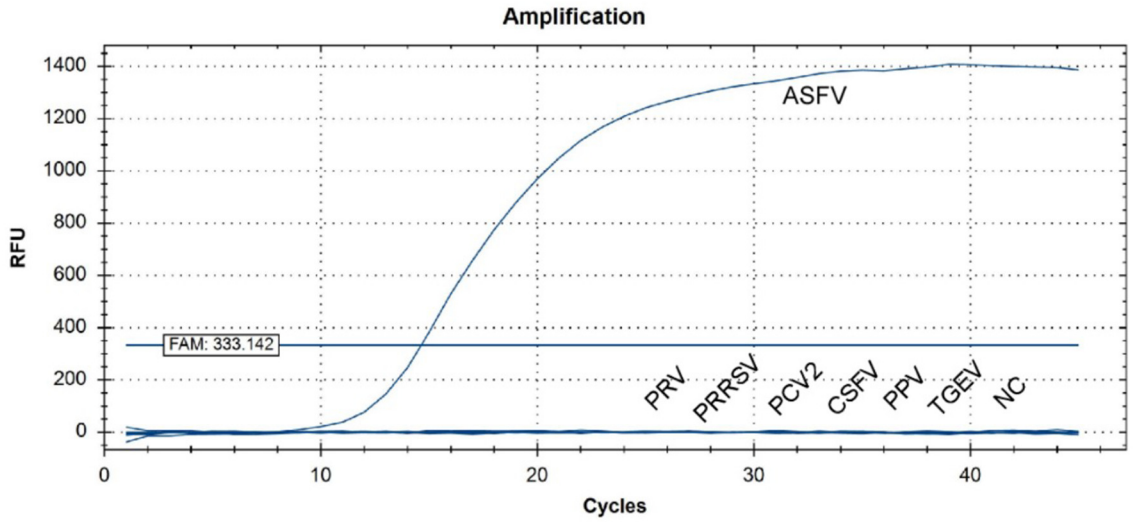

FIGURE 5
QPCR amplification results of the specificity assay. Standard nucleic acid materials, including porcine pseudorabies virus (PRV), porcine reproductive and respiratory syndrome virus (PRRSV), porcine circovirus (PCV2), classical swine fever virus (CSFV), porcine parvovirus (PPV), and swine transmissible gastroenteritis virus (TGEV), were tested together with ASFV nucleic acid. An extra negative control (NC) was set at the same time. qPCR data showed that only ASFV was detected with a positive fluorescence signal, and no other positive signal was observed in the other viruses or the negative control.

reverse primers (used as an antisense oligonucleotide) targeting the ASFV MGF505-7R genes were also aligned, as shown in Figure 1. The mapping results of primers and probes with different strains were also listed. The data showed that the primers and probes we designed mapped well with most epidemic ASFV strains except five Ugandan strains (N10, R7, R8, R25, and R35) and the Spain_BA71 strain, which indicated that the designed assay might be able to detect ASFV MGF505-7R in Asian and European epidemic ASFV strains but not African ones.

3.2. Optimization of qPCR conditions

The p3xFLAG-MGF505-7R plasmid (10^7copies/μL) was amplified by MGF505 7R probe-based qPCR with different annealing temperatures. CT values from different groups were compared. The results showed that, when the annealing temperature was 60°C, the minimum of the average CT values among the six annealing temperatures was 17.776, compared with other groups (57°C−18.185, 58°C−17.914, 59°C−17.890, 61°C−18.376 and 62°C−18.451). Therefore, we used an annealing temperature of 60°C for the real-time fluorescent quantitative PCR. They used a probe qPCR mix (2x) at a concentration of 10/μL, along with a probe (10 pmol/μL) and upstream and downstream primers (10 pmol/μL) at a concentration of 0.4μL and 0.6 μL, respectively. They also used 1μL of DNA and made up the final volume to 20 μL using dd H_2O. The cycling conditions for real-time PCR reactions were 95°C for 1 min, followed by 40 cycles of 95°C for 5 s and 60°C for 60 s.

TABLE 2 The repeatability of the developed qPCR.

Standard Copies/μL	Intra-assay repeatability of CT-value			Inter-assay repeatability of CT-value		
	Mean	SD	CV (%)	Mean	SD	CV (%)
1.0×10^7	19.82	0.15	0.75	20.59	0.04	0.2
1.0×10^6	23.01	0.07	0.28	23.1	0.03	0.15
1.0×10^5	26.13	0.1	0.4	26.78	0.02	0.06
1.0×10^4	29.65	0.14	0.48	30.25	0.02	0.06
1.0×10^3	33.05	0.2	0.62	33.04	0.24	0.72
1.0×10^2	35.7	0.08	0.22	36.23	0.2	0.56
1.0×10^1	38.42	0.24	0.63	38.91	0.4	1.02

3.3. Standard curve

To construct a standard curve with the logarithm of the RNA copy number and the measured Ct value (Figure 2), serial p3xFLAG-MGF505-7R plasmid dilutions at the concentration of 1.0×10^7 to 1.0×10^1 copies/μL were prepared. Three replicates were tested for each dilution. The optimal curve was selected as the standard curve. The development of the MGF505-7R standard curve with the abscissa as the logarithm of copy number and the ordinate as CT value revealed that the correlation coefficient (R2) was 0.9986, the slope was −3.301, and the intercept was 39.416. The standard formula is $y = -3.301x + 39.416$ and $R^2 = 0.9986$.

3.4. Sensitivity

The 10-fold gradient dilution of the standard plasmid was simultaneously detected by the established qPCR and conventional RT-PCR. The minimum detection template concentrations of the established qPCR and conventional RT-PCR were 10 copies/μL and 1.0×10^2copies/μL, respectively (Figures 3, 4), indicating that the qPCR was more sensitive than conventional RT-PCR.

3.5. Specificity

MGF505-7R from the Shandong province was selected for amplifications in a qPCR assay, and strong fluorescent signals were obtained from reactions. However, for other pig viruses such as PRV, PRRSV, CSFV, PPV, PCV2, and TGEV, data showed that the assay gave no signal amplification (Figure 5). Therefore, there is a significant distinction between ASFV and other viruses when comparing the signal strength at different levels.

3.6. Repeatability

The intra-assay repeatability was assessed by testing 10-fold serial dilutions of the standard plasmid ranging from 1×10^7 to 1×10^1 copies/μL in three replicates. The same standard plasmid was analyzed in triplicate on three different days to determine the inter-assay repeatability. As a result, intra-assay standard deviations (SD) ranged from 0.11 to 0.21, and inter-assay standard deviations (SD) ranged from 0.12 to 0.22. The coefficient of variation (CV) values of intra-assay and inter-assay were 0.06% to 1.06% and 0.55 to 0.81%, respectively (Table 2). The results showed that the experiment was repeatable.

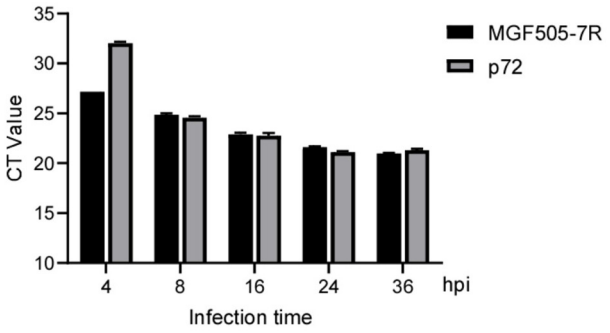

FIGURE 6
Comparison of amplification results between MGF505-7R and p72 in PAM cells at different time points. PAM cells were infected with ASFV (MOI = 0.5), and samples were collected by RNA extraction at indicated time points for qPCR detection with the MGF505-7R probe or the ASFV-p72 probe. The figure shows the CT value with three duplicates at each time point.

3.7. Laboratory samples and clinical samples

For laboratory-made ASFV-infected samples, MGF505-7R probe-based qPCR showed a lower CT value than the p72 probe at 4 hpi. For the remaining 8, 16, 24, and 36 hpi samples, the two groups obtained similar results (Figure 6). For clinical samples, the classical ASFV p72-based detection method showed 100% positives, and 87 out of 94 (92.56%) samples were determined to be MGF505-7R positive by our assay. The data showed that seven samples were diagnosed as ASFV MGF505-7R negative, including six samples showing no signal and one with a CT value higher than 40. Further comparison found that 32 samples showed lower CT values in

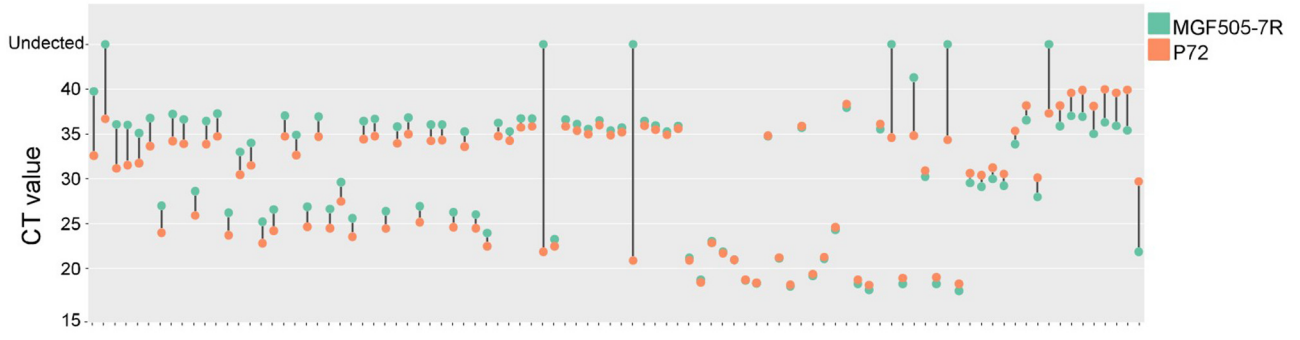

FIGURE 7
Comparison of amplification results between MGF505-7R and P72 in clinical samples. The dumbbell diagram shows the CT value of each clinical sample based on the MGF505-7R probe (blue) and p72 probe (red), respectively.

the MGF505-7R-based group than in the p72-based group. The remaining 55 samples showed higher CT values (Figure 7). The assay based on MGF505-7R showed results close to a classical test method from the preliminary detection results of clinical samples.

4. Discussion

ASF is a highly contagious disease that causes acute hemorrhagic fever in domestic and wild boars, with a fatality rate of up to 100%. After being effectively eradicated from areas outside of Africa and Sardinia in the late 1990s, the "second wave" of ASF that spread cross-continentally to Europe and Asia in 2007 became a major concern for the global pig industry (3). Unfortunately, the cross-regional transport of pigs and pork products, the lack of good farming practices and biosecurity, and the mobility of people and vehicles all contribute to the disease's future spread, which has expensive socioeconomic effects on the affected countries. Given that there is currently no viable vaccine or antiviral agent treatment available, early detection and diagnosis of ASFV in various settings, including farms and slaughterhouses, are urgently required to manage the disease, and are considered the primary method for management.

ASFV is difficult to diagnose, especially outside of a diagnostics laboratory, because it exhibits symptoms similar to those of classical swine fever (CSF) and a number of other swine diseases (33). Therefore, several diagnostic techniques, including ELISA, RPA, and LAMP, have been developed and formally certified for diagnosing ASF. Because of its precision and effectiveness, qPCR stands out among these techniques and is currently widely used despite the limitations of laboratory technology (34). In recent years, classical detection methods have gradually satisfied the increasing number of ASFV strains; therefore, developing candidate detection genes can be of great importance.

In our study, we described a particular real-time quantitative PCR assay based on TaqMan for detecting ASFV MGF505-7R. According to the abovementioned data, qPCR has a detection limit as low as 10 copies/μL, making it 100 times more sensitive than a conventional PCR experiment. Additionally, no signals were detected in the test with any other virus. The intra-assay and inter-assay variances ranged from 0.06 to 1.02%, demonstrating the repeatability of the approach. In conclusion, compared to the traditional RT-PCR method, this study's TaqMan-based real-time qPCR method was quick, sensitive, and specific. The assay was run over a broad dynamic range with little intra- and inter-assay variation, and it revealed no cross-reactivity with many other pig-origin viruses. In an *in vitro* study, MGF505-7R was detected with a lower CT value early in infected PAMs, suggesting that this method can also be applied to laboratory studies. In the results of clinical samples, this assay also showed a similar effect to the standard method for ASFV diagnosis.

The ASFV-p72 protein is highly conserved among different viral strains and has stable antigenicity, which makes it the most common marker for detecting ASFV. In this experiment, we found that the CT value of MGF505-7R became stable and credible as early as 4 hpi, while the expression of p72 tends to be significantly stable at 8 hpi. By comparing the mRNA levels of MGF505-7R and p72 at each stage of ASFV infection, we found similar results to viral gene transcriptome analysis (11), indicating that MGF505-7R has the potential to be a promising candidate for ASFV detection.

Although our method has shown some good characteristics, there is still room for improvement. We observed that the primers and probe in our assay could cover most epidemic ASFV strains from Asia and Europe but not those from Africa (Uganda strains). Therefore, in the future, additional probes and primers may need to be considered for the MGF505-7R gene to supplement this method for better detection.

The development of MGF505-7R-based TaqMan real-time PCR for ASFV diagnosis has shown superior results in identifying the presence of ASFV in the early infection stage compared to the classic method *in vitro*. This method also provides a quantifiable research tool for studying the function of the MGF505-7R gene and investigating the epidemiology of ASFV infections in pigs, which could also facilitate research into the epidemiology of ASFV infections in other animals.

Data availability statement

The original contributions presented in the study are included in the article/supplementary material, further inquiries can be directed to the corresponding authors.

Ethics statement

The animal study was reviewed and approved by the Animal Welfare Committee of the China Animal Health and Epidemiology Center, and written informed consent was obtained from the owners for the participation of their animals in this study.

Author contributions

CQ, YZ, ZheW, ZhiW, and XW conceived and designed the experiments. CQ, YZ, ZheW, and JL performed the experiments. CQ and YZ analyzed the data and wrote the manuscript. YH, LL, QW, and YW contributed reagents/materials/analysis tools. All authors contributed to the article and approved the submitted version.

Funding

This work was supported by the Agricultural Major Applied Technology Innovation Project of Shandong Province (SD2019XM003), Key research and development program (Modern Agriculture) project of Jiangsu Province (BE2020398), and National Project for Prevention and Control of Transboundary Animal Diseases (2022YFD1800500).

Conflict of interest

The authors declare that the research was conducted in the absence of any commercial or financial relationships that could be construed as a potential conflict of interest.

Publisher's note

All claims expressed in this article are solely those of the authors and do not necessarily represent those of their affiliated organizations, or those of the publisher, the editors and the reviewers. Any product that may be evaluated in this article, or claim that may be made by its manufacturer, is not guaranteed or endorsed by the publisher.

References

1. Galindo I, Alonso C. African swine fever virus: a review. *Viruses.* (2017) 9:103. doi: 10.3390/v9050103

2. Sanchez-Cordon PJ, Montoya M, Reis AL, Dixon LK. African swine fever: A re-emerging viral disease threatening the global pig industry. *Vet J.* (2018) 233:41–8. doi: 10.1016/j.tvjl.2017.12.025

3. Dixon LK, Sun H, Roberts H. African swine fever. *Antiviral Res.* (2019) 165:34–41. doi: 10.1016/j.antiviral.2019.02.018

4. Ge S, Li J, Fan X, Liu F, Li L, Wang Q. Molecular characterization of african swine fever virus, China, 2018. *Emerg Infect Dis.* (2018) 24:2131–3. doi: 10.3201/eid2411.181274

5. Zhou X, Li N, Luo Y, Liu Y, Miao F, Chen T. Emergence of African swine fever in China, 2018. *Transbound Emerg Dis.* (2018) 65:1482–4. doi: 10.1111/tbed.12989

6. Dixon LK, Chapman DA, Netherton CL, Upton C. African swine fever virus replication and genomics. *Virus Res.* (2013) 173:3–14. doi: 10.1016/j.virusres.2012.10.020

7. Malogolovkin A, Burmakina G, Titov I, Sereda A, Gogin A, Baryshnikova E. Comparative analysis of African swine fever virus genotypes and serogroups. *Emerg Infect Dis.* (2015) 21:312–5. doi: 10.3201/eid2102.140649

8. Bastos AD, Penrith ML, Cruciere C, Edrich JL, Hutchings G, Roger F. Genotyping field strains of African swine fever virus by partial p72 gene characterisation. *Arch Virol.* (2003) 148:693–706. doi: 10.1007/s00705-002-0946-8

9. Zsak L, Borca MV, Risatti GR, Zsak A, French RA, Lu Z. Preclinical diagnosis of African swine fever in contact-exposed swine by a real-time PCR assay. *J Clin Microbiol.* (2005) 43:112–9. doi: 10.1128/JCM.43.1.112-119.2005

10. King DP, Reid SM, Hutchings GH, Grierson SS, Wilkinson PJ, Dixon LK. Development of a TaqMan PCR assay with internal amplification control for the detection of African swine fever virus. *J Virol Methods.* (2003) 107:53–61. doi: 10.1016/S0166-0934(02)00189-1

11. Zheng Y, Li S, Li SH Yu S, Wang Q, Zhang K, et al. Transcriptome profiling in swine macrophages infected with African swine fever virus at single-cell resolution. *Proc Natl Acad Sci U S A.* (2022) 119:e2201288119. doi: 10.1073/pnas.2201288119

12. Bosch-Camos L, Lopez E, Collado J, Navas MJ, Blanco-Fuertes M, Pina-Pedrero S, et al. M448R and MGF505-7R: two african swine fever virus antigens commonly recognized by ASFV-specific T-cells and with protective potential. *Vaccines.* (2021) 9:508. doi: 10.3390/vaccines9050508

13. Li D, Zhang J, Yang W, Li P, Ru Y, Kang W, et al. African swine fever virus protein MGF-505-7R promotes virulence and pathogenesis by inhibiting JAK1- and JAK2-mediated signaling. *J Biol Chem.* (2021) 297:101190. doi: 10.1016/j.jbc.2021.101190

14. Li J, Song J, Kang L, Huang L, Zhou S, Hu L, et al. pMGF505-7R determines pathogenicity of African swine fever virus infection by inhibiting IL-1beta and type I IFN production. *PLoS Pathog.* (2021) 17:e1009733. doi: 10.1371/journal.ppat.1009733

15. Ding M, Dang W, Liu H, Xu F, Huang H, Sunkang Y, et al. Combinational deletions of MGF360-9L and MGF505-7R attenuated highly virulent african swine fever virus and conferred protection against homologous challenge. *J Virol.* (2022) 96:e0032922. doi: 10.1128/jvi.00329-22

16. Chapman DA, Darby AC, Da Silva M, Upton C, Radford AD, Dixon LK. Genomic analysis of highly virulent Georgia 2007/1 isolate of African swine fever virus. *Emerg Infect Dis.* (2011) 17:599–605. doi: 10.3201/eid1704.101283

17. O'Donnell V, Holinka LG, Sanford B, Krug PW, Carlson J, Pacheco JM, et al. African swine fever virus Georgia isolate harboring deletions of 9GL and MGF360/505 genes is highly attenuated in swine but does not confer protection against parental virus challenge. *Virus Res.* (2016) 221:8–14. doi: 10.1016/j.virusres.2016.05.014

18. Gimenez-Lirola LG, Mur L, Rivera B, Mogler M, Sun Y, Lizano S, et al. Detection of African Swine Fever Virus Antibodies in Serum and Oral Fluid Specimens Using a Recombinant Protein 30 (p30) Dual Matrix Indirect ELISA. *PLoS One.* (2016) 11:e0161230. doi: 10.1371/journal.pone.0161230

19. Cubillos C, Gomez-Sebastian S, Moreno N, Nunez MC, Mulumba-Mfumu LK, Quembo CJ, et al. African swine fever virus serodiagnosis: a general review with a focus on the analyses of African serum samples. *Virus Res.* (2013) 173:159–67. doi: 10.1016/j.virusres.2012.10.021

20. Miao F, Zhang J, Li N, Chen T, Wang L, Zhang F, et al. Rapid and sensitive recombinase polymerase amplification combined with lateral flow strip for detecting African swine fever virus. *Front Microbiol.* (2019) 10:1004. doi: 10.3389/fmicb.2019.01004

21. Wang J, Wang J, Geng Y, Yuan W. A recombinase polymerase amplification-based assay for rapid detection of African swine fever virus. *Can J Vet Res.* (2017) 81:308–12.

22. He Q, Yu D, Bao M, Korensky G, Chen J, Shin M. High-throughput and all-solution phase African Swine Fever Virus (ASFV) detection using CRISPR-Cas12a and fluorescence based point-of-care system. *Biosens Bioelectron.* (2020) 154:112068. doi: 10.1016/j.bios.2020.112068

23. Wang X, Ji P, Fan H, Dang L, Wan W, Liu S, et al. CRISPR/Cas12a technology combined with immunochromatographic strips for portable detection of African swine fever virus. *Commun Biol.* (2020) 3:62. doi: 10.1038/s42003-020-0796-5

24. Yu LS, Chou SY, Wu HY, Chen YC, Chen YH. Rapid and semi-quantitative colorimetric loop-mediated isothermal amplification detection of ASFV via HSV color model transformation. *J Microbiol Immunol Infect.* (2021) 54:963–70. doi: 10.1016/j.jmii.2020.08.003

25. Gallardo C, Nieto R, Soler A, Pelayo V, Fernandez-Pinero J, Markowska-Daniel I, et al. Assessment of African swine fever diagnostic techniques as a response to the epidemic outbreaks in eastern european union Countries: how to improve surveillance and control programs. *J Clin Microbiol.* (2015) 53:2555–65. doi: 10.1128/JCM.00857-15

26. Ikeno S, Suzuki MO, Muhsen M, Ishige M, Kobayashi-Ishihara M, Ohno S, et al. Sensitive detection of measles virus infection in the blood and tissues of humanized mouse by one-step quantitative RT-PCR. *Front Microbiol.* (2013) 4:298. doi: 10.3389/fmicb.2013.00298

27. Khodakov D, Wang C, Zhang DY. Diagnostics based on nucleic acid sequence variant profiling: PCR, hybridization, and NGS approaches. *Adv Drug Deliv Rev.* (2016) 105:3–19. doi: 10.1016/j.addr.2016.04.005

28. Zhu Z, Meng G. ASFVdb: an integrative resource for genomic and proteomic analyses of African swine fever virus. *Database.* (2020) 1:9. doi: 10.1093/database/baaa023

29. Kumar S, Stecher G, Li M, Knyaz C, Tamura K. MEGA X: molecular evolutionary genetics analysis across computing platforms. *Mol Biol Evol.* (2018) 35:1547–9. doi: 10.1093/molbev/msy096

30. Larkin MA, Blackshields G, Brown NP, Chenna R, McGettigan PA, McWilliam H, et al. Clustal W and Clustal X version 2.0. *Bioinformatics.* (2007) 23:2947–8. doi: 10.1093/bioinformatics/btm404

31. Li J, Hu L, Liu Y, Huang L, Mu Y, Cai X. DDX19A Senses Viral RNA and Mediates NLRP3-dependent inflammasome activation. *J Immunol.* (2015) 195:5732–49. doi: 10.4049/jimmunol.1501606

32. Turner C, Williams SM. Laboratory-scale inactivation of African swine fever virus and swine vesicular disease virus in pig slurry. *J Appl Microbiol.* (1999) 87:148–57. doi: 10.1046/j.1365-2672.1999.00802.x

33. Oura CA, Edwards L, Batten CA. Virological diagnosis of African swine fever–comparative study of available tests. *Virus Res.* (2013) 173:150–8. doi: 10.1016/j.virusres.2012.10.022

34. de Leon P, Bustos MJ, Carrascosa AL. Laboratory methods to study African swine fever virus. *Virus Res.* (2013) 173:168–79. doi: 10.1016/j.virusres.2012.09.013

Frontiers in Veterinary Science

Transforms how we investigate and improve animal health

The third most-cited veterinary science journal, bridging animal and human health with a comparative approach to medical challenges. It explores innovative biotechnology and therapy for improved health outcomes.

Discover the latest Research Topics

See more →

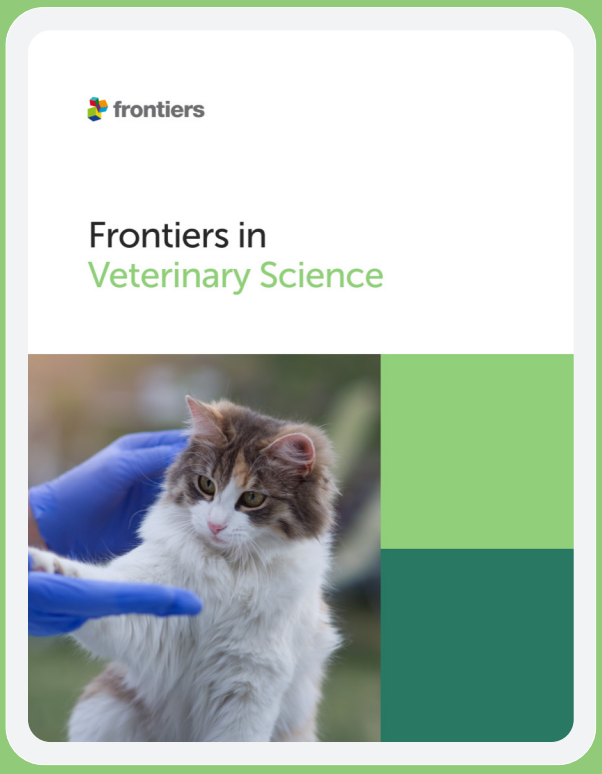

Frontiers

Avenue du Tribunal-Fédéral 34
1005 Lausanne, Switzerland
frontiersin.org

Contact us

+41 (0)21 510 17 00
frontiersin.org/about/contact